THE EFFECT OF GLOBAL CLIMATE CHANGE ON THE RELEASE OF TERRESTRIAL ORGANIC CARBON IN THE ARCTIC REGION

A thesis submitted to The University of Manchester
for the degree of doctor of philosophy
in the Faculty of Engineering and Physical Sciences

2014

AYÇA DOĞRUL SELVER

SCHOOL of EARTH, ATMOSPHERIC and ENVIRONMENTAL SCIENCES

List of Contents

Word count: 46237

List of Figures

List of Tables

The University of Manchester
Ayça Doğrul Selver
PhD

The effect of global climate change on the release of terrestrial carbon in the Arctic Region

2014

Abstract

The Arctic Region is currently experiencing an amplified warming if compared to the rest of the world. The soils in this region store approximately half of the global soil organic carbon (OC), mainly locked in the permanently-frozen ground (permafrost). This carbon sink is sensitive to global warming meaning that the predicted warming will likely increase the thaw-release of this 'old' carbon. However, what happens to this remobilized OC once it is transported to the Arctic Ocean, including the potential conversion to greenhouse gasses causing a positive feedback to climate warming, remains unclear.

In this work, we further investigate the fate of terrestrial derived OC (terrOC) in the Eurasian Arctic Region. The key findings of this work are:

- Glycerol dialkyl glycerol tetraethers (GDGTs) and bacteriohopanepolyols (BHPs) are present in marine sediments of the Eurasian Arctic Region and the associated Branched and Isoprenoidal tetraether (BIT) and R_{soil} indices can be used to trace terrOC in marine realm. However, a slight modification in the R_{soil} index is suggested (R'_{soil}).
- Analyses indicate that the behaviour of BIT is largely controlled by a marine GDGT contribution while the R'_{soil} index is mainly controlled by the removal of soil marker BHPs. Although both indices suggest a non-conservative behavior for the terrOC, this leads to differences in the estimations for the percentage terrOC present. A multi-proxy approach is essential since the use of a single-proxy approach can lead to over/under estimation.
- Comparison of BIT and δ^{13}Csoc indices across the East Siberian Shelf indicates that the BIT index is possibly reflecting a predominantly fluvial input while δ^{13}Csoc represents a mixed fluvial and coastal erosion input.
- The macromolecular terrOC composition varies along a west-east Eurasian Arctic climosequence and is mainly controlled by the river runoff of surface derived terrOC and wetland coverage (sphagnum vs. higher plants) but is not affected by the presence/absence of continuous permafrost.
- The phenols/(phenols+pyridines) ratio was suggested as a proxy to trace terrOC at the macromolecular level along the Kolyma River-East Siberian Sea transect. The results indicate a non-conservative behavior of the macromolecular terrOC comparable to the bulk of the terrOC.

All molecular analyses/based proxies used showed that the remobilized terrOC in the Eurasian Arctic region behaves non-conservatively potentially causing a positive feedback to global climate change.

Declaration

No portion of the work referred to in this thesis has been submitted in support of an application for another degree or qualification of this or any other university or other institute of learning.

Copyright

Acknowledgements

I would like to thank my supervisor Bart van Dongen. I enjoyed working with you and I truly appreciate your support, patience and your open-door policy. You taught me a lot Bart, thank you! To my supervisor Stephen Boult, for your guidance and constructive comments. To our collaborators Helen Talbot and Julianne Bischoff for their help with all the BHPs analyses. To Robert Sparkes, it was nice working with you and thank you for your collaboration and encouragement. To Paul Lythgoe, for invaluable help on LC–MS analyses (…and constantly repairing it), I learned a lot from you!

Martha and Nicola...my wonderful friends, we shared a lot! I will miss all the times we had together… our office, our discussions about life& science, coffee-hours full of chatting, laughing and complaining (..and Martha, thanks for sharing Mexican candies with me! How I am going to live without them now?). Dear Holly, Irma, Stuart and Sharon… I appreciate your friendship and thank you all for being so nice and helpful all the time. This group was the best I can imagine! Alastair, thanks for being such a nice friend, being there and listening to me whenever I need to talk! I fell lucky to have you all as my friend and I wish all the best to all of you.

My amazing parents and sisters, I owe you everything and I love you! My dear husband Erdem, thanks for standing by me through the good times and bad. I am grateful for having such a great family.

Finally, I would like to acknowledge the Ministry of National Education of Turkey for their financial support during this PhD project.

CHAPTER 1

Introduction

1.1. The Arctic Region as a driver of global climate change

Earth's climate is changing in response to anthropogenic perturbations and this climatic change may be one of the biggest challenges of the next 50 years. The Arctic Region is already experiencing amplified warming compared to the rest of the world (IPCC, 2013) and therefore may be the region most affected by global warming in the future. The affects of global warming will be increasing ocean and atmospheric temperatures, permafrost thawing, shrinking of glaciers and ice sheets and decreasing ocean pH (ACIA, 2004; AMAP, 2012; 2013).

Since the industrial revolution, atmospheric greenhouse gas (GHGs) concentrations have increased, altering the capacity of the atmosphere to trap heat and causing warming of the climate (IPCC, 2013). In 2011, the carbon dioxide (CO_2) and methane (CH_4) concentrations exceeded pre-industrial levels by approximately 40% and 150%, respectively (IPCC, 2013). Although human activities are considered as the main source for the increased GHGs, the future trajectory of the atmospheric GHGs pools

also depend on feedback, both positive and negative between temperature and GHG releases from ocean and terrestrial systems (Friedlingstein et al., 2006).

The effects of warming have been observed globally, however predictions and observations show that they will not be spatially uniform (IPCC, 2013) with Polar Regions likely to experience greater changes. Indeed, the observed surface temperature change in parts of Northern Alaska (early 1980s to mid-2000s) was up to 3°C, considerably higher than the global average of 1-1.5°C (IPCC, 2013).

The enhanced early warming of the Polar Regions may interact with its terrestrial carbon sinks, resulting in a local feedback that has global consequences in exacerbating climate change. The Northern latitude soils contain almost half of the global soil organic carbon (OC; 1672 Pg of OC; Schuur et al., 2008), twice as much as currently contained in the atmosphere as CO_2 (Kuhry et al., 2009), mainly stored in the permanently-frozen ground (permafrost) and, therefore, a carbon sink that is sensitive to global warming. Permafrost is defined as a soil or rock body that remains below freezing point for at least two consecutive years and can be classified by its extent, as continuous (90-100%), discontinuous (50-90%), sporadic (10-50%) and isolated patches (0-10%; Figure 1.1). Whilst approximately 25% of land in the Northern Hemisphere and 80% of the Arctic is covered by permafrost (Brown et al., 1998; Zhang et al., 2008), it is not uniformly distributed. Across the Eurasian Arctic, for instance, permafrost characteristics are different in the western part (west of 90°E) if compared to the eastern part (west of 90°E) with discontinuous permafrost underlying the western Great Russian Arctic river watersheds (GRARs; Ob and Yenisey), while continuous permafrost dominates the eastern GRAR basins (Lena, Indigirka and, Kolyma; Figure 1.1).

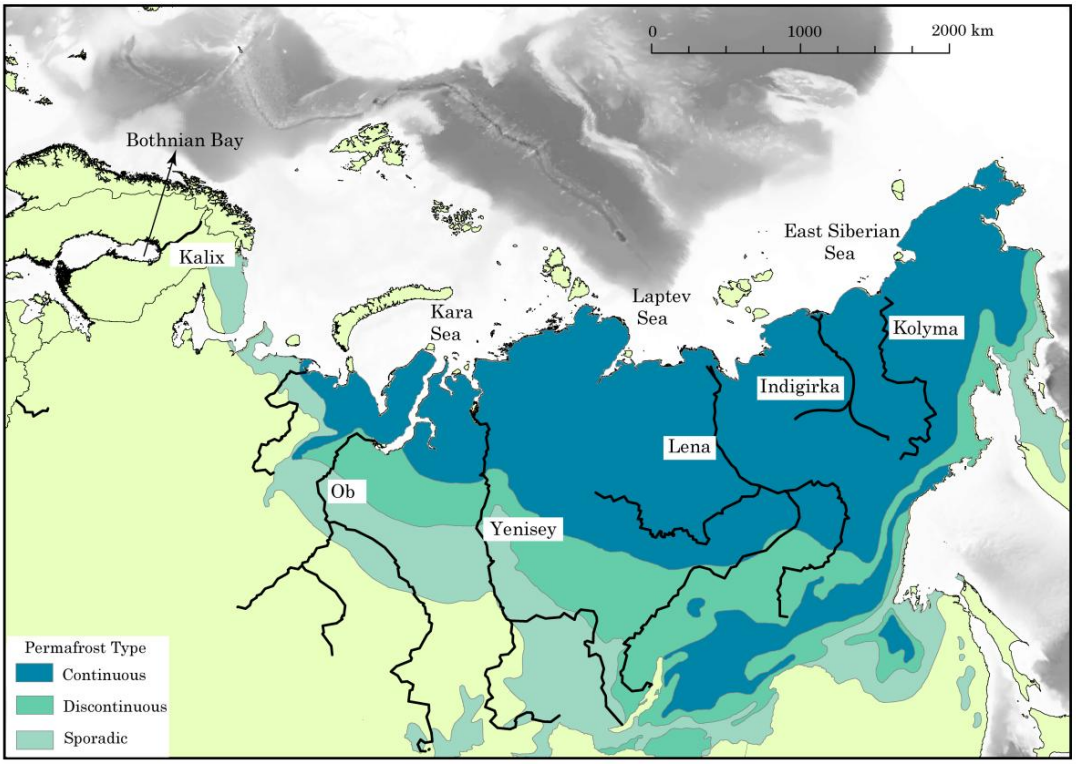

Figure 1. 1: Map showing permafrost types in the Arctic Region (data available at http://nsidc.org/data/docs/fgdc/ggd600_russia_pf_maps/). Black lines indicate major rivers.

Recent observations indicated that since the 1980s, the permafrost temperature increased globally and was between 0.5°C to 1°C in some parts of Alaska and up to 2°C in parts of the Eurasian Arctic (AMAP, 2012). This warming has increased the riverine flux from the Eurasian Arctic Rivers by 7% between 1936 and 1999 (Peterson et al., 2002). Furthermore, it may also lead to thaw-release of currently freeze-locked, 'old', soil/terrestrial OC (terrOC; Schuur et al., 2008), which can either breakdown to GHGs in the water column and surface sediments or be transported further and be reburied in the Arctic Ocean sediments. The amount and the composition of the terrOC transported to the Arctic Ocean may therefore be subject to increase/change now and in the future. Measurement of the magnitude and composition of current and prediction of future

fluxes of terrOC is therefore critical to understanding and predicting climate change in the Arctic and globally.

TerrOC transport has been the focus of previous research. Different mechanisms have been suggested for the regions under different types of permafrost. In western Siberia (Figure 1.1; Gustafsson et al., 2011) water can penetrate to deeper horizons due to discontinuous permafrost and carries material both from surface and deeper horizons while in the eastern region terrOC transport is mainly from the active layer (Figure 1.1; Gustafsson et al., 2011). Bulk radiocarbon age of OC increases from west to east Siberia, which has been mainly attributed to delay in the transport time due to increased permafrost coverage (Guo et al., 2004; van Dongen et al., 2008a). However, Guo et al. (2004) and van Dongen et al. (2008) suggested that, despite their older bulk radiocarbon ages, OC exported by the eastern GRARs is less degraded compared to that carried by the western GRARs. This older yet less degraded OC trend towards eastern Siberia is consistent with different permafrost coverage (Guo 2004; Gustafsson 2011).

Global warming will affect terrOC fluxes to the Arctic Ocean not only by increasing the river influx but also by increasing coastal erosion. Arctic sea ice cover is reduced so increasing the wave fetches and storm frequency. This is most likely along the Yedoma (ice complex) dominated coastlines of the East Siberian Sea (ESS; Figure 1.2). Recent research indicated that 4 times more terrOC (approximately 44 Mt of OC/yr; van Dongen et al., 2008a; Vonk et al., 2012) is released annually into ESS from coastal erosion than from rivers (10 Mt OC/yr; Rachold et al., 2004). Vonk et al. (2012) also showed, using a combination of bulk radiocarbon age and $\delta^{13}C$ analyses, that a major proportion (~57%) of terrOC in surface sediments from across the ESS originates from coastal erosion (Vonk et al., 2012) Therefore, quantification of both riverine terrOC fluxes and those derived from coastal erosion are required.

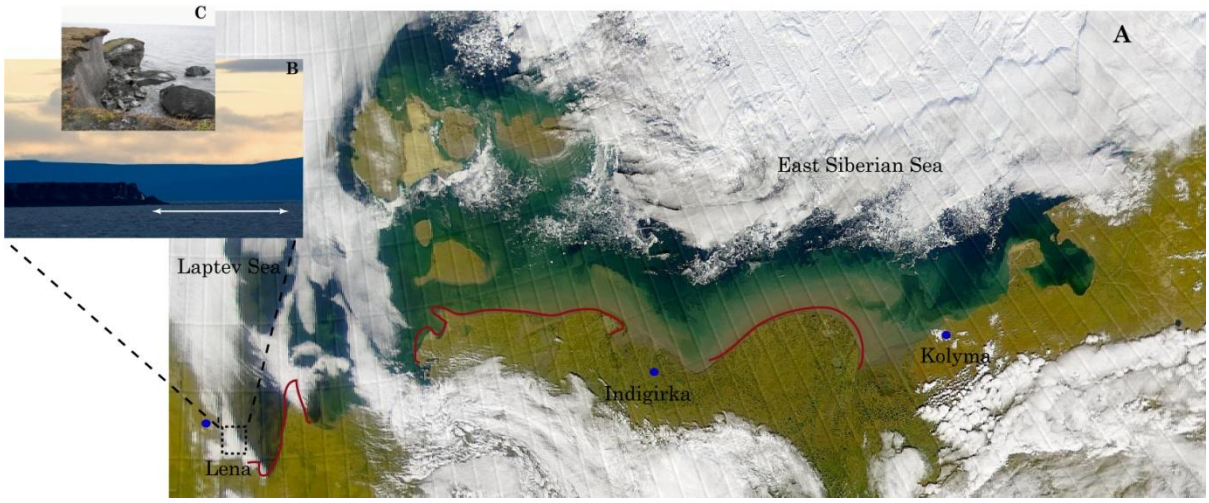

Figure 1. 2: Pictures showing (A) coastal erosion areas in the ESS (indicated as red lines; satellite image available at http://visibleearth.nasa.gov) (B) Moustakh Island (white line indicates eroded part of the island) (C) Eroding Yedoma (image available at http://isss08.wordpress.com)

1.2. Fate of terrestrial organic carbon on the Arctic Shelves

The fate of terrOC after it is released from the permafrost is one of the key factors controlling the future trajectory of warming in the Arctic region. Will the remobilized terrOC be degraded/ converted to GHGs, causing a positive feedback to global climate warming or will it behave conservatively and be transported down through the water column and be deposited in marine sediments with minimal net effect on the global warming?

It has been widely considered that in marine environments, terrOC is relatively refractory to degradation (Hedges et al., 1997; van Dongen et al., 2000). Based on the limited amount of data available at the time, Stein and MacDonald (2004) suggested that terrestrial particulate OC (POC) degradation in the Arctic Ocean was comparable to the average global degradation rate of fluvial POC in coastal environments. However, recent studies suggest that much of the terrOC may have already been degraded during its transport to marine environment (Keil et al., 1997) mainly close to

the point of origin (Karlsson et al., 2011; van Dongen et al., 2008b; Vonk et al., 2012). van Dongen et al. (2008b) suggested that 65% of terrestrial POC degrades close to the mouth of the sub-Arctic Kalix River suggesting that terrOC degradation is much larger than previously suggested by Stein and Macdonald (2004). Other studies suggested degradation of terrOC in the Arctic Ocean was also more active as demonstrated by loss of functional group - containing compounds (Vonk et al., 2010a; Vonk et al., 2008), high CO_2 and CH_4 flux above the East Siberian Shelf waters (Anderson et al., 2009; Semiletov et al., 2007; Shakhova and Semiletov, 2007) and CO_2 - saturated shelf waters (Semiletov et al., 2012). Vonk et al. (2012) showed that not only terrOC transported by rivers but also terrOC derived from coastal erosion behaves non-conservatively and degrades rapidly. Using a combination of bulk and molecular indices, it was estimated that about 66% of the carbon transported by coastal erosion escapes to the atmosphere with the remainder being buried in marine sediments (Vonk et al., 2012).

This less conservative behaviour of terrOC transported to the Arctic Ocean affects not only the GHGs flux but also the ocean pH. Atmospheric CO_2 is partly absorbed by the oceans balancing the CO_2 levels in the atmosphere; however increased emission of CO_2 causes a decrease in ocean pH levels, altering marine ecosystems (Sabine et al., 2004; The Royal Society, 2005). It has now been shown that Arctic waters are experiencing widespread ocean acidification (AMAP, 2013) and due to high freshwater and terrOC input, CO_2 neutralization capacity of the Arctic Ocean is low suggesting it is more sensitive to acidification (AMAP, 2013).

However, whilst the non-conservative nature of terrOC has been observed, its exact fate still remains unclear. In order to better understand the fate of terrOC transported to the Arctic Ocean, it is essential to determine the relative importance of marine and terrOC in the Arctic marine environment. Previously this has mainly been done using a range of bulk and molecular proxies (e.g. *n*-alkane, lignin proxies, C/N and

$^{13}C_{SOC}$; Feng et al., 2013; Gustafsson et al., 2011; Karlsson et al., 2011; Tesi et al., 2014; van Dongen et al., 2008a; Vonk et al., 2008; Vonk et al., 2010b). Bulk proxies provide very valuable information but can be biased by inorganic interferences and are not able to distinguish between inputs from different carbon pools such as plant or soil input. In addition, most of the molecular based proxies do not provide a complete understanding of terrOC behaviour since they only represent specific terrOC fractions. *n*-alkanes and lignin for instance are very useful markers to determine higher plant/ sphagnum derived terrOC (Feng et al., 2013; Tesi et al., 2014; Vonk and Gustafsson, 2009) but they do not allow inferences about the relative contribution of soil versus marine.

1.3. Microbial membrane lipids and related proxies

Recent discovery of Archaea and bacteria biomarkers and related proxies (i.e. glycerol dialkyl glycerol tetraethers (GDGTs) based BIT and bacteriohopanepolyols (BHPs) based R_{soil}) allow us to trace the soil OC in the marine realm.

1.3.1. GDGTs

GDGTs are membrane lipids synthesized by Archaea and some bacteria (Hopmans et al., 2000; Sinninghe Damsté et al., 2000). When the microorganism is viable, GDGTs are in their intact form with polar head groups present (Schouten et al., 2013). Polar head groups mainly consist of monohexose, dihexose and phosphohexose moieties (Liu et al., 2010; Peterse et al., 2011; Schouten et al., 2012; Sturt et al., 2004). Upon cell lysis, intact GDGTs lose their head groups and more resistant core GDGTs remain. Therefore, in the sedimentary record, they are preserved as core GDGTs and used as biomarkers for Archaea and bacteria. Of the core GDGTs, bacterially derived branched

GDGTs (br-GDGTs) consist of two C_{28} carbon skeletons with 4-6 methyl moieties (branches) and 0-2 cyclopentane moieties (Figure 1.3). The exact source of br-GDGTs still remains unknown but based on their branched alkyl chains and stereochemical configuration of the glycerol groups they were suggested to originate from bacteria (Weijers et al., 2006b). In fact, br-GDGTs have been identified in acidobacteria cultures but not been found in any other cultures to date (Sinninghe Damsté et al., 2012).

Isoprenoidal GDGTs (iso-GDGTs) consist of two isoprenoidal chains and have 0-8 cyclopentane moieties and in the case of crenarchaeol, 4 cyclopentane and 1 cyclohexane moieties (Figure 1.3). Unlike br-GDGTs, iso-GDGTs have been found in a number of different cultivated Archaea (Macalady et al., 2004; Schleper et al., 2010; Sinninghe Damsté et al., 2002; Uda et al., 2004). Crenarchaeol, for instance, is known to be produced primarily by Thaumarchaeota (DeLong 1998;Schouten 2000) while iso-GDGT-0, 1 and 4 were found in anaerobic methane oxidisers (Jahn et al., 2004; Knappy et al., 2011).

br-GDGTs are considered as 'soil markers' since they have been dominantly present in soils (Kim et al., 2006; Kim et al., 2010), peatlands (Weijers et al., 2006a; Weijers et al., 2004). However minor amounts can be found in the marine environments as well (Herfort et al., 2006; Hopmans et al., 2004; Kim et al., 2006). Recent studies showed that a proportion of br-GDGTs in the Arctic region may be produced within lakes and rivers rather than being transported solely from soil erosion (De Jonge et al., 2014; Peterse et al., 2014). This may indicate that br-GDGTs have a fluvial rather than soil origin. However, considering that GDGT compositions of Yedoma and permafrost are still unclear, further investigations are needed to deduce the contribution from rivers, Yedoma and permafrost. Iso-GDGTs, especially crenarchaeol, are abundantly found in marine settings, but are also observed in soils and peats in lower amounts

indicating minor in-situ production in these realms (Weijers et al., 2006b; Weijers et al., 2004).

Considering different origins of br- and iso-GDGTs, the "branched and isoprenoid tetraether" (BIT) index were suggested to track soil/terrOC in the marine environment (Hopmans et al., 2004). The BIT index is the ratio of br-GDGTs (sum of br-GDGT I, II and III; see figure 1.3 for structures), representing terrOC, to crenarchaeol, representing marine OC (equation [1]);

$$BIT = \frac{[\sum \text{br-GDGTs}]}{[\sum \text{br-GDGTs}] + [\text{crenarchaeol}]} \qquad [1]$$

The BIT index ranges between 0, representing no br-GDGTs therefore no soil contribution and 1, representing no crenarchaeol/ marine addition. BIT index has been successfully used to track soil/terrOC in a range of environments (Blaga et al., 2009; Doğrul Selver et al., 2012; Kim et al., 2012; Zhu et al., 2011).

However, while there are works on GDGTs distributions in soils (Rethemeyer et al., 2010), lakes (Shanahan et al., 2013; Peterse et al., 2014) and the marine environment (De Jonge et al., 2014; Rethemeyer et al., 2010) in the (sub-) Arctic region, there is a very limited number of work on the application of the BIT index in the Arctic Region (Belicka and Harvey, 2009; van Dongen et al., 2008a). GDGTs were analysed in the eastern GRAR estuary surface sediments and showed BIT values above 0.88 suggesting a dominant terrOC input to these sediments in line with other studies (Feng et al., 2013; Guo et al., 2004; Gustafsson et al., 2011). Due to the scarcity of the application of BIT index, it remains unclear if GDGT based proxies can be used to track terrOC in the Arctic environment.

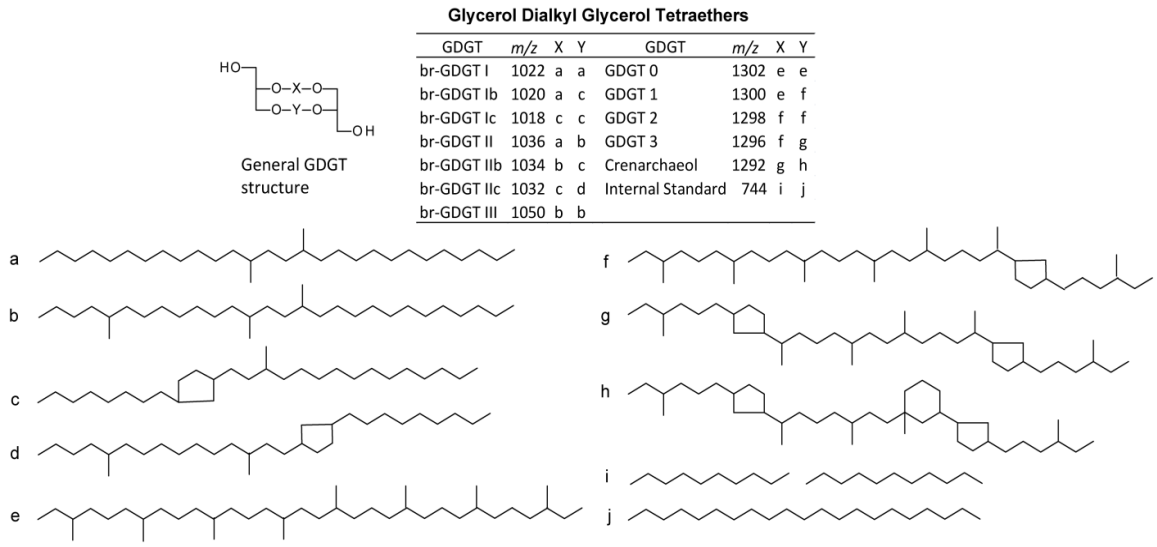

Figure 1. 3: Glycerol dialkyl glycerol tetraether (GDGT) structures

1.3.2. BHPs

Bacteriohopanepolyols (BHPs) are pentacyclic triterpenoids synthesized by prokaryotes (Ourisson and Rohmer, 1982) and can have 4-6 functional groups on their side chains at different positions (Rohmer et al., 1984). The nature of functional groups varies but they are mainly composed of hydroxyl groups (BHT) that can, in some compounds, be substituted with an amine group (aminobacteriohopanetriol, -tetrol, -pentol) or composite group (sugar moiety; BHT pentose) at the C-35 position (Figure 1.4). Some compounds (i.e. adenosylhopane and adenosylhopane related structures) contain a cyclised side chain. These side-chains are labile and it is the degradation products (core triterpenoid lipids) are usually preserved in sediments and soils (Brocks et al., 2005; Eigenbrode et al., 2008; Rohmer et al., 1980). However, functionalized BHPs can also be found in recent (Cooke et al., 2009) and older sediments (Cooke et al., 2008; Handley et al., 2010; van Dongen et al., 2006).

Based on the observations that adenosylhopane and adenosylhopane type BHP structures (Figure 1.4) have been observed abundantly in soils but are only present in

trace amounts in marine sediments they have been considered to be 'soil marker' BHPs (Cooke et al., 2008). However, while it can be present in minor amounts in terrestrial environments (Cooke, 2010; Talbot et al., 2007; van Winden et al., 2012), bacteriohopanetetrol (BHT) is suggested as a 'pseudo' marine compound since it is the most abundantly present BHP in marine sediments (Blumenberg et al., 2010; Farrimond et al., 2000; Sáenz et al., 2011; Zhu et al., 2011). For instance, BHT is the only BHP observed in marine sediments taken from coastal Svalbard (Rethemeyer et al., 2010). Similarly, along the Yangtze River-East China Sea transect, BHT abundance was approximately 40% in the river, while around 85% in the open shelf where it is one of the only 4 BHPs present (Zhu et al., 2011). Based on these observations, Zhu et al. (2011) developed a BHP proxy (R_{soil}) to trace the soil OC in the marine realm (equation [2]);

$$R_{soil}=\frac{[G1+2MeG1+\ G2+2MeG2+G3]}{[G1+2MeG1+\ G2+2MeG2+G3]+[BHT]} \qquad [2]$$

R_{soil} index is the ratio of soil marker BHPs (G1, 2MeG1, G2, 2MeG2, G3) to marine marker BHT (see Figure 1.4 for structures) and ranges between 0 – 1, with 0 representing solely marine contribution while 1 represents pure soil input.

BHPs have been analysed in the GRAR estuarine surface sediments and it was found that total BHP abundance and soil-marker BHPs contribution increased eastwards (Cooke et al., 2009). Since that study is the only one dealing with BHP distributions in the Arctic Ocean, more work is needed to better understand the fate/behaviour of BHPs in the Arctic region.

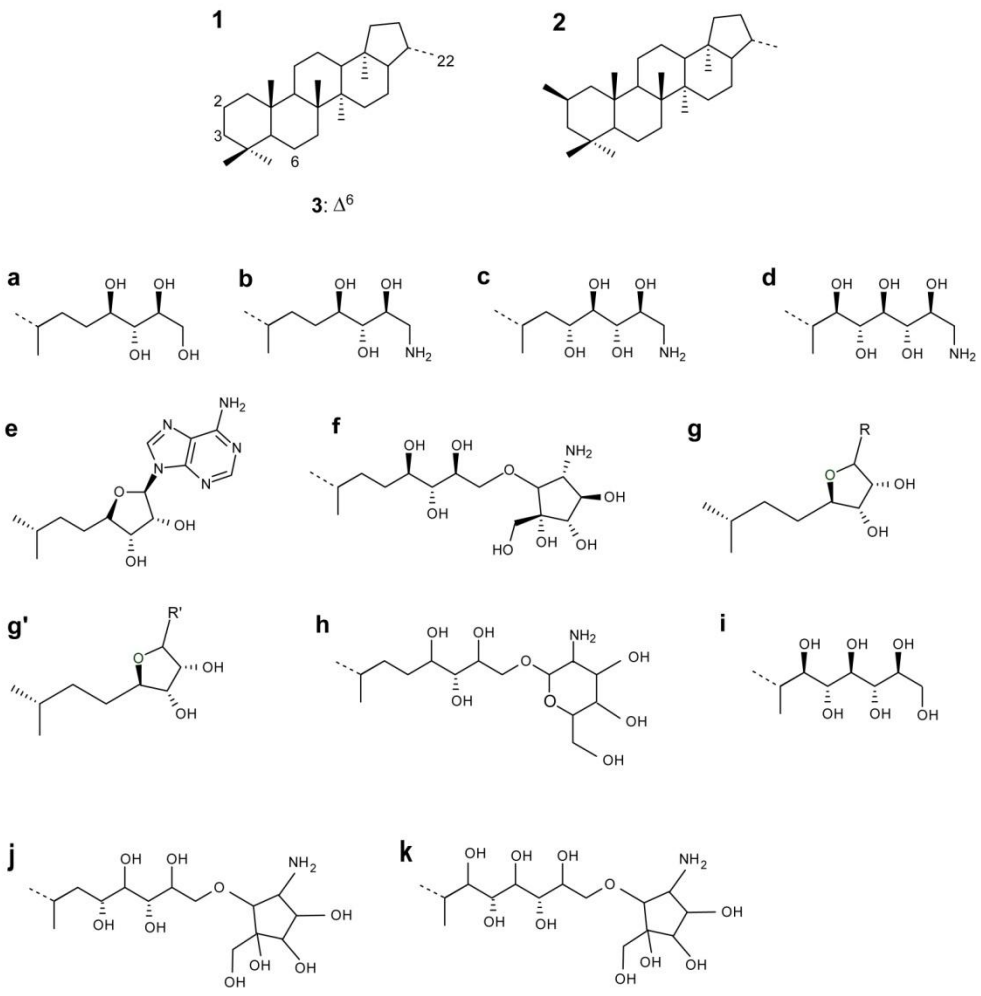

	Abbreviation	Structure[a]	m/z
Bacteriohopanetetrol	Δ^6BHT	3a	653
Bacteriohopanetetrol	BHT	1a	655
Bacteriohopanetetrol isomer	BHT isomer	1a'	655-II
Methyl bacteriohopanetetrol	2-Methyl BHT	2a	669
Bacteriohopanehexol	BHHexol	1i	771
Aminobacteriohopanetriol	Aminotriol	1b	714
Aminobacteriohopanetetrol	Aminotetrol	1c	772
Aminobacteriohopanepentol	Aminopentol	1d	830
Adenosylhopane	G1	1e	788
2Methyl-adenosylhopane	2Me-G1	2e	802
Adenosylhopane Type 2	G2	1g	761
2Me-adenosylhopane Type 2	2Me-G2	2g	775
Adenosylhopane Type 3	G3	1g'	802
2Me-adenosylhopane Type 3	2Me-G3	2g'	816
Bacteriohopanetetrol cyclitol ether	BHT cyclitol ether	1f	1002
Bacteriohopanetetrol glucosamine	BHT glucosamine	1h	1002
Bacteriohopanehexol cyclitol ether	BHhexol cyclitol ether	1k	1118
2Methyl-bacteriohopanehexol cyclitol ether	2Me-BHhexol ether	2k	1132
Bacteriohopanepentol cyclitol ether	BHpentol cyclitol ether	1j	1060

Figure 1. 4: Unacetylated bacteriohopanepolyol structures.

1.4. Macromolecular compounds

The lipids, which are the extractable part of the OC, only represent a relatively small fraction (5-10%) of total OC (Durand, 1980). The remaining 90-95% is part of the non-extractable fraction of OC containing macromolecular structures such as lignin, cellulose and other carbohydrate based structures, proteins and complex aliphatic macromolecular structures. Past research in the (Eurasian) Arctic region has mainly focused on the extractable fraction and far less is known about the biogeochemical cycling of the macromolecular OC in this region.

To date, only a few studies have analysed the macromolecular OC (Feng et al., 2013; Guo et al., 2004; Peulvé et al., 1996; Tesi et al., 2014) predominantly focusing of the cycling of lignin (Feng et al., 2013; Tesi et al., 2014). Feng et al. (2013) for instance showed that, using a combination of CuO oxidation analyses and compound specific radiocarbon analysis, vascular plant-derived lignin (phenols) in the Eurasian Arctic region are actively transported to the Arctic shelf seas by the GRARs and other rivers. However, (i) these lignin phenols mainly originate from young surface soils while, for instance, plant wax lipids predominantly originate from deeper, older, permafrost horizons and (ii) the mobilization mechanisms for this macromolecular part of the terrOC are different if compared to the rest of the terrOC. Climate warming, the presence/absence of permafrost and/or increased river run-off may impact the release of this type of OC differently if compared to other parts of the terrOC

In addition, it remains unclear how macromolecular terrOC behaves after it is released to the Arctic shelf seas. Will the remobilized macromolecular terrOC be degraded/ converted to GHGs in a similar way as the bulk of the terrOC, again causing a positive feedback to global climate warming or will it behave more conservatively? Recent analyses, again using CuO oxidation, suggested that lignin actually is more

reactive and therefore degrades faster than wax lipids, potentially causing a larger feedback than previously expected (Tesi et al., 2014). However lignin represents only a (small) part of the macromolecular OC fraction, indicating that it remains unclear to what extent these results are representative for the total macromolecular fraction.

This highlights that it is essential to analyse other parts of the (terrestrial) macromolecular OC. This can be done using Pyrolysis Gas Chromatography-Mass spectrometry (py–GC/MS) technique which, in contrast to CuO oxidation technique, gives a more general overview of the macromolecular composition. py–GC/MS is a common technique used for macromolecular analyses which thermally breaks down the macromolecular compounds into smaller compounds while retaining the information about the original macromolecule and provides insight into the biological bio-cursors such as protein, carbohydrate and lignin (McClymont et al., 2011).

Until now only a limited number of studies used py–GC/MS to analyse the macromolecular composition of the OC in samples from the (Eurasian) Arctic region (Guo et al., 2004; Peulvé et al., 1996). Peulvé et al. (1996), for instance, used py–GC/MS to study the macromolecular compositions of suspended particles and surface sediments from the Lena Delta and the Laptev Sea. Analyses of the marine suspended particles indicated a mixed input from marine and terrestrial origins whilst analyses of the surface sediments compositions suggested preservation of terrOC along with the influx of some marine (algal) derived OC. Similarly, Guo et al. (2004) analysed macromolecular compositions of GRAR estuary sediments along a west-east climosequence of the Siberian Arctic and based on an increase in the relative abundance of carbohydrate derived moieties (e.g. furfurals) towards eastern Siberia, it was suggested that the terrOC transported to the Eurasian Arctic shelf seas becomes less degraded toward the east. Combined these studies highlight that py–GC/MS can be used to analyse the composition of the macromolecular OC and could be helpful to

better understand the carbon cycling in this area. This means that more work is needed to better understand the fate/behaviour of macromolecular terrOC in the (Eurasian) Arctic region.

1.5. Aims and objectives

The aims of this thesis are to;

- determine the potential for GDGTs and BHPs for tracing the terrestrial/soil contribution in the (sub-) Arctic marine environment.
- investigate the relationships between different terrestrial (soil) vs. marine indices, the GDGT based BIT index , the BHP based R_{soil} index and $\delta^{13}C_{SOC}$, along river-shelf transects and across the ESS.
- determine to what extent GDGT and BHP based proxies can be used to distinguish between influxes of different carbon sources across the ESS.
- investigate the composition and biogeochemical fate of macromolecular terrOC transported to the Eurasian Arctic shelf.

To achieve these aims a number of objectives have been identified and these are:

- To characterise/quantify GDGTs and BHPs compositions in surface sediments along well studied (sub)-Arctic river-shelf transects (i.e. Kalix River- Bothnian Bay and Kolyma River- East Siberian Sea transects).

- To characterise/quantify the GDGTs compositions in surface sediments from across the ESS.

- To combine/correlate these molecular based BIT and R_{soil} proxies with bulk proxies ($\delta^{13}C_{SOC}$) along the (sub)-Arctic transects as well as across the ESS.

- To analyse the macromolecular composition of surface sediment samples along the Arctic climosequence (GRAR estuaries) and along the two (sub)-Arctic transects using pyrolysis–GC/MS.
- To compare the macromolecular compositions of terrOC transported from the areas with and without permanent permafrost.

1.6. Approach and thesis structure

This thesis contains a general introduction (**Chapter 1**) presenting the background of the research followed by four chapters written as scientific papers, a concluding chapter summarising the results of the thesis, outlines the recommendations for future work and appendices summarizing the methods utilized in this study. This allows each chapter to stand alone as piece of research, regardless of the repetition between chapters. Each of these chapters has either been published (**Chapter 2**) or will be submitted soon (**Chapters 3, 4 and 5**).

This thesis is separated into two main parts. The first part (**Chapters 2 to 4**) deals with tracing soil organic matter along two (sub-) Arctic river-ocean transects and across the ESS by using GDGTs, BHPs and related indices in combination with previously published bulk, molecular indices. **Chapter 2** utilizes BIT and R_{soil} proxies to better understand the behaviour of soil OC along Kalix River-Bothnian Bay transects which is considered as the westernmost representative of GRARs. The results of this study indicated that both BIT and R_{soil} are useful in the Arctic Region and both showed decreasing trends in an off-shore direction suggesting decreasing SOM contribution. A

slight modification in the R_{soil} index is proposed (R'_{soil}) for the use in the Arctic Region. **Chapter 3** deals with analyses of GDGTs and BHPs along the Kolyma River-East Siberian Sea transect and validates the use of BIT and R'_{soil} indices to trace soil OC in the eastern Siberia. Results are comparable to Chapter 2 indicating highest br-GDGT and soil marker BHPs concentrations and therefore highest soil OC contribution close to the river mouth. BIT and R'_{soil} indices showed declining trends in an off-shore direction suggesting an increasing marine OC input. Results revealed that the behaviour of BIT index is mainly controlled by substantial marine GDGTs contribution while R'_{soil} is suggested to be mainly governed by the degradation of soil marker BHPs.

Chapter 4 is a study of the distribution/ behaviour of GDGTs in the whole ESS. Results showed that br-GDGTs concentrations are higher in sediments taken close to river outflows. The BIT index followed a declining trend offshore indicating increased marine organic matter influence. The relationship between the BIT index and δ^{13}Csoc measurements is non-linear where in near shore sediments BIT index drops significantly before a considerable shift is observed in δ^{13}Csoc. In contrast, in offshore sediments they both show decreasing trends at. Results may indicate that on the ESS, BIT and δ^{13}Csoc are representative of different fractions of the terrestrial sediment exported to ESS, possibly BIT measuring fluvial input while δ^{13}Csoc reflecting both fluvial and coastal erosion input.

The second part of the thesis (**Chapter 5**) deals with the macromolecular fraction of sedimentary organic matter and discusses the changes in the macromolecular compositions of surface sediments along the Arctic climosequence (GRAR estuaries) to deduce the affect of different permafrost types. In addition, macromolecular compositions of surface sediments from two river (land)–ocean transects were analysed to gain more complete understanding of the fate of terrOC. Results suggested that, along the Arctic climosequence, the macromolecular

composition of GRAR estuary sediments is not controlled by the permafrost coverage but mainly by the river runoff and wetland coverage. In addition, although relative contributions varied, the macromolecular compound classes showed consistent trends along both river-ocean transects. Based on trends observed in phenols and pyridines and their strong correlations with other proxies along the Kolyma River-East Siberian Sea transect, phenols/ phenols+pyridines ratio was proposed as a macromolecular proxy to estimate relative input from terrestrial and marine inputs to the marine realm. **Chapter 6** brings various conclusions from the previous chapters together and outlines the future work that could be carried out.

Only scientific papers for which the author is the lead author have been included in this thesis. The author was responsible for writing the manuscripts and undertook the majority of the data reported unless otherwise stated. In addition, the author has contributed to a scientific paper published in G3 (Schouten et al., 2013). Details of this and conference presentations are given in appendix.

1.7. Author's and co-author's contributions to each chapter

- **Paper 1 (Chapter 2) -** *Author*-the lead investigator, extracting the samples for GDGTs-BHPs analyses, performing GDGT analysis and data interpretation, writing up the manuscript. *Helen M. Talbot*-analysing BHPs. *Örjan Gustafsson*-Sample collection. *Stephen Boult and Bart van Dongen*- sample collection, complete conceptual guidance and manuscript review.
- **Paper 2 (Chapter 3)** - *Author*-the lead investigator, extracting the samples for GDGTs-BHPs analyses, performing GDGT analysis and data interpretation, writing up the manuscript. *Robert Sparkes*-performing GDGT analysis and data interpretation. *Helen M. Talbot* and *Juliane Bischoff*- analysing BHPs. *Örjan*

Gustaffson, Igor Semiletov and *Oleg Dudarev*- sample collection. *Stephen Boult* and *Bart van Dongen*- sample collection, complete conceptual guidance and manuscript review.

- **Paper 3 (Chapter 4)-** *Author*-the lead investigator, extracting the samples for GDGTs analyses, performing GDGT analyses and data interpretation, writing up the manuscript. *Robert Sparkes*-modelling, performing GDGT analysis and data interpretation. *Örjan Gustaffson, Igor Semiletov* and *Oleg Dudarev*- sample collection. *Bart van Dongen*- sample collection, complete conceptual guidance and manuscript review.
- **Paper 4 (Chapter 5)-** *Author*-the lead investigator, performing py-GC/MS analysis and data interpretation, writing up the manuscript. *Robert Sparkes*-. py-GC/MS analysis. *Örjan Gustaffson, Igor Semiletov* and *Oleg Dudarev*- sample collection. *Stephan Boult* and *Bart van Dongen*- sample collection, complete conceptual guidance and manuscript review.

References

ACIA, 2004. Impacts of a Warming Arctic: Arctic Climate Impact and Assessment (ed. Hassol SJ) pp. 1-1020.

AMAP, 2012. Arctic Climate Issues 2011: Changes in Arctic Snow, Water, Ice and Permafrost. SWIPA 2011 Overview Report. Arctic Monitoring and Assessment Programme (AMAP), pp. xi + 97pp, Oslo.

AMAP, 2013. AMAP Assessment 2013: Arctic Ocean Acidification. Arctic Monitoring and Assessment Programme (AMAP). viii pp. + 99 pp., Oslo, Norway.

Anderson, L.G., Jutterström, S., Hjalmarsson, S., Wåhlström, I., Semiletov, I.P., 2009. Out-gassing of CO_2 from Siberian Shelf seas by terrestrial organic matter decomposition. Geophysical Research Letters 36, L20601.

Belicka, L.L., Harvey, H.R., 2009. The sequestration of terrestrial organic carbon in Arctic Ocean sediments: A comparison of methods and implications for regional carbon budgets. Geochimica et Cosmochimica Acta 73, 6231-6248.

Blaga, C., Reichart, G.-J., Heiri, O., Sinninghe Damsté, J.S., 2009. Tetraether membrane lipid distributions in water-column particulate matter and sediments: a study of 47 European lakes along a north–south transect. Journal of Paleolimnology 41, 523-540.

Blumenberg, M., Mollenhauer, G., Zabel, M., Reimer, A., Thiel, V., 2010. Decoupling of bio- and geohopanoids in sediments of the Benguela Upwelling System (BUS). Organic Geochemistry 41, 1119-1129.

Brocks, J.J., Love, G.D., Summons, R.E., Knoll, A.H., Logan, G.A., Bowden, S.A., 2005. Biomarker evidence for green and purple sulphur bacteria in a stratified Palaeoproterozoic sea. Nature 437, 866-870.

Brown, J., Ferrians, J., Heginbottom, O.J., Melnikov. , E.S., 1998. Circum-arctic map of permafrost and ground ice conditions. revised February 2001. National Snow and Ice Data Center. Digital media, Boulder, CO.

Cooke, M.P., 2010. The role of bacteriohopanepolyols as biomarkers for soil bacterial communities and soil derived organic matter. *PhD thesis*. Newcastle University, Newcastle.

Cooke, M.P., Talbot, H.M., Wagner, T., 2008. Tracking soil organic carbon transport to continental margin sediments using soil-specific hopanoid biomarkers: A case study from the Congo fan (ODP site 1075). Organic Geochemistry 39, 965-971.

Cooke, M.P., van Dongen, B.E., Talbot, H.M., Semiletov, I., Shakhova, N., Guo, L., Gustafsson, Ö., 2009. Bacteriohopanepolyol biomarker composition of organic matter exported to the Arctic Ocean by seven of the major Arctic rivers. Organic Geochemistry 40, 1151-1159.

De Jonge, C., Stadnitskaia, A., Hopmans, E.C., Cherkashov, G., Fedotov, A., Sinninghe Damsté, J.S., 2014. In situ produced branched glycerol dialkyl glycerol tetraethers in suspended particulate matter from the Yenisei River, Eastern Siberia. Geochimica et Cosmochimica Acta 125, 476-491.

Doğrul Selver, A., Talbot, H.M., Gustafsson, Ö., Boult, S., van Dongen, B.E., 2012. Soil organic matter transport along an sub-Arctic river- sea transect. Organic Geochemistry 51, 63-72.

Durand, B., 1980. Kerogen: Insoluble Organic Matter from Sedimentary Rocks. Editions technip.

Eigenbrode, J.L., Freeman, K.H., Summons, R.E., 2008. Methylhopane biomarker hydrocarbons in Hamersley Province sediments provide evidence for Neoarchean aerobiosis. Earth and Planetary Science Letters 273, 323-331.

Farrimond, P., Head, I.M., Innes, H.E., 2000. Environmental influence on the biohopanoid composition of recent sediments. Geochimica et Cosmochimica Acta 64, 2985-2992.

Feng, X., Vonk, J.E., van Dongen, B.E., Gustafsson, Ö., Semiletov, I.P., Dudarev, O.V., Wang, Z., Montluçon, D.B., Wacker, L., Eglinton, T.I., 2013. Differential mobilization of terrestrial carbon pools in Eurasian Arctic river basins. Proceedings of the National Academy of Sciences.

Friedlingstein, P., Cox, P., Betts, R., Bopp, L., von Bloh, W., Brovkin, V., Cadule, P., Doney, S., Eby, M., Fung, I., Bala, G., John, J., Jones, C., Joos, F., Kato, T., Kawamiya, M., Knorr, W., Lindsay, K., Matthews, H.D., Raddatz, T., Rayner, P., Reick, C., Roeckner, E., Schnitzler, K.G., Schnur, R., Strassmann, K., Weaver, A.J., Yoshikawa, C., Zeng, N., 2006. Climate- Carbon Cycle Feedback Analysis: Results from the C4MIP Model Intercomparison. Journal of Climate 19, 3337-3353.

Guo, L., Semiletov, I., Gustafsson, Ö., Ingri, J., Andersson, P., Dudarev, O., White, D., 2004. Characterization of Siberian Arctic coastal sediments: Implications for terrestrial organic carbon export. Global Biogeochemical Cycles 18, GB1036.

Gustafsson, Ö., van Dongen, B.E., Vonk, J.E., Dudarev, O.V., Semiletov, I.P., 2011. Widespread release of old carbon across the Siberian Arctic echoed by its large rivers. Biogeosciences 8, 1737-1743.

Handley, L., Talbot, H.M., Cooke, M.P., Anderson, K.E., Wagner, T., 2010. Bacteriohopanepolyols as tracers for continental and marine organic matter supply and phases of enhanced nitrogen cycling on the late Quaternary Congo deep sea fan. Organic Geochemistry 41, 910-914.

Hedges, J.I., Keil, R.G., Benner, R., 1997. What happens to terrestrial organic matter in the ocean? Organic Geochemistry 27, 195-212.

Herfort, L., Schouten, S., Boon, J. P., Woltering, M., Baas, M., Weijers, J. W. H., Sinninghe Damsté,J. S., 2006. Characterization of transport and deposition of terrestrial organic matter in the southern North Sea using the BIT index. Limnology Oceanography 51, 2196–2205.

Hopmans, E.C., Schouten, S., Pancost, R.D., van der Meer, M.T.J., Sinninghe Damsté, J.S., 2000. Analysis of intact tetraether lipids in archaeal cell material and sediments by high performance liquid chromatography/atmospheric pressure chemical ionization mass spectrometry. Rapid Communications in Mass Spectrometry 14, 585-589.

Hopmans, E.C., Weijers, J.W.H., Schefuß, E., Herfort, L., Sinninghe Damsté, J.S., Schouten, S., 2004. A novel proxy for terrestrial organic matter in sediments based on branched and isoprenoid tetraether lipids. Earth and Planetary Science Letters 224, 107-116.

IPCC, 2013. Climate Change 2013: The Physical Science Basis. Contribution of Working Group I to the Fifth Assessment Report of the Intergovernmental Panel on Climate Change (Ed. by T.F. Stocker, D. Qin, G.-K. Plattner, M. Tignor, S.K. Allen, J. Boschung, A. Nauels, Y. Xia, V. Bex and P.M. Midgley), pp. 1535 pp.

Jahn, U., Summons, R., Sturt, H., Grosjean, E., Huber, H., 2004. Composition of the lipids of Nanoarchaeum equitans and their origin from its host Ignicoccus sp. strain KIN4/I. Archives of Microbiology 182, 404-413.

Karlsson, E.S., Charkin, A., Dudarev, O.V., Semiletov, I.P., Vonk, J.E., Sánchez-García, L., Andersson, A., Gustafsson, Ö., 2011. Carbon isotopes and lipid biomarker investigation of sources, transport and degradation of terrestrial organic matter in the Buor-Khaya Bay, SE Laptev Sea. Biogeosciences 8, 1865-1879.

Keil, R.G., Mayer, L.M., Quay, P.D., Richey, J.E., Hedges, J.I., 1997. Loss of organic matter from riverine particles in deltas. Geochimica et Cosmochimica Acta 61, 1507-1511.

Kim, J.-H., Schouten, S., Buscail, R., Ludwig, W., Bonnin, J., Sinninghe Damsté, J.S., Bourrin, F., 2006. Origin and distribution of terrestrial organic matter in the NW Mediterranean (Gulf of Lions): Exploring the newly developed BIT index. Geochemistry Geophysics Geosystems 7, Q11017.

Kim, J.-H., van der Meer, J., Schouten, S., Helmke, P., Willmott, V., Sangiorgi, F., Koç, N., Hopmans, E.C., Sinninghe Damsté, J.S., 2010. New indices and calibrations derived from the distribution of crenarchaeal isoprenoid tetraether lipids: Implications for past sea surface temperature reconstructions. Geochimica et Cosmochimica Acta 74, 4639-4654.

Kim, J.-H., Zell, C., Moreira-Turcq, P., P., P.M.A., Abril, G., Mortillaro, J.-M., Weijers, J.W.H., Meziane, T., Sinninghe Damsté, J.S., 2012. Tracing soil organic carbon in the lower Amazon River and its tributaries using GDGT distributions and bulk organic matter properties. Geochimica et Cosmochimica Acta 90, 163-180.

Knappy, C., Nunn, C.M., Morgan, H., Keely, B., 2011. The major lipid cores of the archaeon Ignisphaera aggregans: implications for the phylogeny and biosynthesis of glycerol monoalkyl glycerol tetraether isoprenoid lipids. Extremophiles 15, 517-528.

Kuhry, P., Ping, C.-L., Schuur, E.A.G., Tarnocai, C., Zimov, S., 2009. Report from the International Permafrost Association: carbon pools in permafrost regions. Permafrost and Periglacial Processes 20, 229-234.

Liu, X.-L., Leider, A., Gillespie, A., Gröger, J., Versteegh, G.J.M., Hinrichs, K.-U., 2010. Identification of polar lipid precursors of the ubiquitous branched GDGT orphan lipids in a peat bog in Northern Germany. Organic Geochemistry 41, 653–660.

Macalady, J., Vestling, M., Baumler, D., Boekelheide, N., Kaspar, C., Banfield, J., 2004. Tetraether-linked membrane monolayers in Ferroplasma spp: a key to survival in acid. Extremophiles 8, 411-419.

McClymont, E.L., Bingham, E.M., Nott, C.J., Chambers, F.M., Pancost, R.D., Evershed, R.P., 2011. Pyrolysis GC–MS as a rapid screening tool for determination of peat-forming plant composition in cores from ombrotrophic peat. Organic Geochemistry 42, 1420-1435.

Ourisson, G., Rohmer, M., 1982. Prokaryotic polyterpenes: Phylogenetic precursors of sterols. Current topics in membranes and transport 17, 153-182.

Peterse, F., Hopmans, E.C., Schouten, S., Mets, A., Rijpstra, W.I.C., Sinninghe Damsté, J.S., 2011. Identification and distribution of intact branched tetraether lipids in peat and soils. Organic Geochemistry 42, 1007–1015

Peterse, F., Vonk, J. E., Holmes, R. M., Giosan, L., Zimov, N., and Eglinton, T. I., 2014. Branched glycerol dialkyl glycerol tetraethers in Arctic lake sediments: Sources

and implications for paleothermometry at high latitudes. Journal of Geophysical Research:Biogeosciences 119, 1738-1754

Peterson, B.J., Holmes, R.M., McClelland, J.W., Vörösmarty, C.J., Lammers, R.B., Shiklomanov, A.I., Shiklomanov, I.A., Rahmstorf, S., 2002. Increasing River Discharge to the Arctic Ocean. Science 298, 2171-2173.

Peulvé, S., Sicre, M., Saliot, A., De Leeuw, J., Baas, M., 1996. Molecular characterization of suspended and sedimentary organic matter in an Arctic delta. Limnol. Oceanogr 41, 488-497.

Rachold, V., Eicken, H., Gordeev, V.V., Grigoriev, M.N., Hubberten, H.W., Lisitzin, A.P., Shevchenko, V.P., Schirrmeister, L., 2004. Modern Terrigenous Organic Carbon Input to the Arctic Ocean. In: R. Stein, R. MacDonald (Eds.), The Organic Carbon Cycle in the Arctic Ocean (Ed. by R. Stein, R. MacDonald), pp. 33-55. Springer Berlin Heidelberg.

Rethemeyer, J., Schubotz, F., Talbot, H.M., Cooke, M.P., Hinrichs, K.-U., Mollenhauer, G., 2010. Distribution of polar membrane lipids in permafrost soils and sediments of a small high Arctic catchment. Organic Geochemistry 41, 1130-1145.

Rohmer, M., Bouvier-Nave, P., Ourisson, G., 1984. Distribution of Hopanoid Triterpenes in Prokaryotes. Journal of General Microbiology 130, 1137-1150.

Rohmer, M., Dastillung, M., Ourisson, G., 1980. Hopanoids from C30 to C35 in recent muds. Naturwissenschaften 67, 456-458.

Sabine, C.L., Feely, R.A., Gruber, N., Key, R.M., Lee, K., Bullister, J.L., Wanninkhof, R., Wong, C.S., Wallace, D.W.R., Tilbrook, B., Millero, F.J., Peng, T.-H., Kozyr, A., Ono, T., Rios, A.F., 2004. The Oceanic Sink for Anthropogenic CO_2. Science 305, 367-371.

Sáenz, J.P., Eglinton, T.I., Summons, R.E., 2011. Abundance and structural diversity of bacteriohopanepolyols in suspended particulate matter along a river to ocean transect. Organic Geochemistry 42, 774-780.

Schleper, C., Nicol, G.W., Robert, K.P., 2010. Ammonia-Oxidising Archaea- Physiology, Ecology and Evolution, Advances in Microbial Physiology, Volume 57, pp. 1-41. Academic Press.

Schouten, S., Pitcher, A., Hopmans, E.C., Villanueva, L., van Bleijswijk, J., Sinninghe Damsté, J.S., 2012. Distribution of core and intact polar glycerol dibiphytanyl glycerol tetraether lipids in the Arabian Sea Oxygen Minimum Zone: I: Selective preservation and degradation in the water column and consequences for the TEX_{86}. Geochimica et Cosmochimica Acta 98, 228-243.

Schouten, S., Hopmans, E.C., Rosell-Melé, A., Pearson, A., Adam, P., Bauersachs, T., Bard, E., Bernasconi, S.M., Bianchi, T.S., Brocks, J.J., Carlson, L.T., Castañeda, I.S., Derenne, S., Doğrul Selver, A., Dutta, K., Eglinton, T., Fosse, C., Galy, V., Grice, K., Hinrichs, K.-U., Huang, Y., Huguet, A., Huguet, C., Hurley, S., Ingalls, A., Jia, G., Keely, B., Knappy, C., Kondo, M., Krishnan, S., Lincoln, S., Lipp, J., Mangelsdorf, K., Martínez-García, A., Ménot, G., Mets, A., Mollenhauer, G., Ohkouchi, N., Ossebaar, J., Pagani, M., Pancost, R.D., Pearson, E.J., Peterse, F., Reichart, G.-J., Schaeffer, P., Schmitt, G., Schwark, L., Shah, S.R., Smith, R.W., Smittenberg, R.H., Summons, R.E., Takano, Y., Talbot, H.M., Taylor, K.W.R., Tarozo, R., Uchida, M., van Dongen, B.E., Van Mooy, B.A.S., Wang, J., Warren, C., Weijers, J.W.H., Werne, J.P., Woltering, M., Xie, S., Yamamoto, M., Yang, H., Zhang, C.L., Zhang, Y., Zhao, M., Sinninghe Damsté, J.S., 2013. An interlaboratory

study of TEX_{86} and BIT analysis of sediments, extracts, and standard mixtures. Geochemistry, Geophysics, Geosystems 14, 5263-5285.

Schuur, E.A.G., Bockheim, J., Canadell, J.G., Euskirchen, E., Field, C.B., Goryachkin, S.V., Hagemann, S., Kuhry, P., Lafleur, P.M., Lee, H., Mazhitova, G., Nelson, F.E., Rinke, A., Romanovsky, V.E., Shiklomanov, N., Tarnocai, C., Venevsky, S., Vogel, J.G., Zimov, S.A., 2008. Vulnerability of Permafrost Carbon to Climate Change: Implications for the Global Carbon Cycle. BioScience 58, 701-714.

Semiletov, I.P., Pipko, I.I., Repina, I., Shakhova, N.E., 2007. Carbonate chemistry dynamics and carbon dioxide fluxes across the atmosphere-ice-water interfaces in the Arctic Ocean: Pacific sector of the Arctic. Journal of Marine Systems 66, 204-226.

Semiletov, I.P., Shakhova, N.E., Sergienko, V.I., Pipko, I.I., Dudarev, O.V., 2012. On carbon transport and fate in the East Siberian Arctic land- shelf- atmosphere system. Environmental Research Letters 7, 015201.

Shakhova, N., Semiletov, I., 2007. Methane release and coastal environment in the East Siberian Arctic shelf. Journal of Marine Systems 66, 227-243.

Shanahan, T.M., Hughen, K.A., Van Mooy, B.A.S., 2013. Temperature sensitivity of branched and isoprenoid GDGTs in Arctic lakes. 64, pp. 119-128.

Sinninghe Damsté, J.S., Hopmans, E.C., Pancost, R.D., Schouten, S., Geenevasen, J.A.J., 2000. Newly discovered non-isoprenoid glycerol dialkyl glycerol tetraether lipids in sediments. Chemical Communications, 1683-1684.

Sinninghe Damsté, J.S., Rijpstra, W.I.C., Hopmans, E.C., Jung, M.-Y., Kim, J.-G., Rhee, S.-K., Stieglmeier, M., Schleper, C., 2012. Intact Polar and Core Glycerol Dibiphytanyl Glycerol Tetraether Lipids of Group I.1a and I.1b Thaumarchaeota in Soil. Applied and Environmental Microbiology.

Sinninghe Damsté, J.S., Rijpstra, W.I.C., Hopmans, E.C., Prahl, F.G., Wakeham, S.G., Schouten, S., 2002. Distribution of Membrane Lipids of Planktonic Crenarchaeota in the Arabian Sea. Applied and Environmental Microbiology 68, 2997-3002.

Stein, R., MacDonald, R.W., 2004. The Organic Carbon Cycle in the Arctic Ocean. Springer, Berlin.

Sturt, H.F., Summons, R.E., Smith, K., Elvert, M., Hinrichs, K.U., 2004. Intact polar membrane lipids in prokaryotes and sediments deciphered by highperformance liquid chromatography/electrospray ionization multistage mass spectrometry –new biomarkers for biogeochemistry and microbial ecology. Rapid Communications in Mass Spectrometry 18, 617–628.

Talbot, H.M., Rohmer, M., Farrimond, P., 2007. Rapid structural elucidation of composite bacterial hopanoids by atmospheric pressure chemical ionisation liquid chromatography/ion trap mass spectrometry. Rapid Communications in Mass Spectrometry 21, 880-892.

Tesi, T., Semiletov, I., Hugelius, G., Dudarev, O., Kuhry, P., Gustafsson, Ö., 2014. Composition and fate of terrigenous organic matter along the Arctic land- ocean continuum in East Siberia: Insights from biomarkers and carbon isotopes. 133, pp. 235-256.

The Royal Society, 2005. Ocean acidification due to increasing atmospheric carbon dioxide. Policy document 12/05. The Royal Society, London.

Uda, I., Sugai, A., Itoh, Y.H., Itoh, T., 2004. Variation in Molecular Species of Core Lipids from the Order Thermoplasmales Strains Depends on the Growth Temperature. Journal of Oleo Science 53, 399-404.

van Dongen, B.E., Irene C. Rijpstra, W., Philippart, C.J.M., de Leeuw, J.W., Sinninghe Damsté , J.S., 2000. Biomarkers in upper Holocene Eastern North Sea and Wadden Sea sediments. Organic Geochemistry 31, 1533-1543.

van Dongen, B.E., Semiletov, I., Weijers, J.W.H., Gustafsson, Ö., 2008a. Contrasting lipid biomarker composition of terrestrial organic matter exported from across the Eurasian Arctic by the five great Russian Arctic rivers. Global Biogeochemical Cycles 22, GB1011.

van Dongen, B.E., Talbot, H.M., Schouten, S., Pearson, P.N., Pancost, R.D., 2006. Well preserved Palaeogene and Cretaceous biomarkers from the Kilwa area, Tanzania. Organic Geochemistry 37, 539-557.

van Dongen, B.E., Zencak, Z., Gustafsson, Ö., 2008b. Differential transport and degradation of bulk organic carbon and specific terrestrial biomarkers in the surface waters of a sub-arctic brackish bay mixing zone. Marine Chemistry 112, 203-214.

van Winden, J.F., Talbot, H.M., Kip, N., Reichart, G.-J., Pol, A., McNamara, N.P., Jetten, M.S.M., Op den Camp, H.J.M., Sinninghe Damsté, J.S., 2012. Bacteriohopanepolyol signatures as markers for methanotrophic bacteria in peat moss. Geochimica et Cosmochimica Acta 77, 52-61.

Vonk, J.E., Gustafsson, Ö., 2009. Calibrating n-alkane Sphagnum proxies in sub-Arctic Scandinavia. Organic Geochemistry 40, 1085-1090.

Vonk, J.E., Sánchez-García, L., Semiletov, I.P., Dudarev, O.V., Eglinton, T.I., Andersson, A., Gustafsson, Ö., 2010a. Molecular and radiocarbon constraints on sources and degradation of terrestrial organic carbon along the Kolyma paleoriver transect, East Siberian Sea. Biogeosciences 7, 3153-3166.

Vonk, J.E., Sanchez-Garcia, L., van Dongen, B.E., Alling, V., Kosmach, D., Charkin, A., Semiletov, I.P., Dudarev, O.V., Shakhova, N., Roos, P., Eglinton, T.I., Andersson, A., Gustafsson, Ö., 2012. Activation of old carbon by erosion of coastal and subsea permafrost in Arctic Siberia. Nature 489, 137-140.

Vonk, J.E., van Dongen, B.E., Gustafsson, Ö., 2008. Lipid biomarker investigation of the origin and diagenetic state of sub-arctic terrestrial organic matter presently exported into the northern Bothnian Bay. Marine Chemistry 112, 1-10.

Vonk, J.E., van Dongen, B.E., Gustafsson, Ö., 2010b. Selective preservation of old organic carbon fluvially released from sub-Arctic soils. Geophysical Research Letters 37, L11605, DOI:10.1029/2010gl042909.

Weijers, J.W.H., Schouten, S., Hopmans, E.C., Geenevasen, J.A.J., David, O.R.P., Coleman, J.M., Pancost, R.D., Sinninghe Damsté, J.S., 2006a. Membrane lipids of mesophilic anaerobic bacteria thriving in peats have typical archaeal traits. Environmental Microbiology 8, 648-657.

Weijers, J.W.H., Schouten, S., Spaargaren, O.C., Sinninghe Damsté, J.S., 2006b. Occurrence and distribution of tetraether membrane lipids in soils: Implications for the use of the TEX_{86} proxy and the BIT index. Organic Geochemistry 37, 1680-1693.

Weijers, J.W.H., Schouten, S., van der Linden, M., van Geel, B., Sinninghe Damsté, J.S., 2004. Water table related variations in the abundance of intact archaeal membrane lipids in a Swedish peat bog. FEMS Microbiology Letters 239, 51-56.

Zhang, T., Barry, R.G., Knowles, K., Heginbottom, J.A., Brown, J., 2008. Statistics and characteristics of permafrost and ground-ice distribution in the Northern Hemisphere. Polar Geography 31, 47-68.

Zhu, C., Talbot, H.M., Wagner, T., Pan, J.-M., Pancost, R.D., 2011. Distribution of hopanoids along a land to sea transect: Implications for microbial ecology and the use of hopanoids in environmental studies Journal Limnology and Oceanography. Limnology and Oceanography 56, 1850-1865.

CHAPTER 2

Paper 1: Soil organic matter transport along an sub-Arctic river–sea transect

This chapter contains the following published paper:

Ayça Doğrul Selver, Helen M. Talbot, Örjan Gustafsson, Stephen Boult, Bart E. van Dongen.2012. Organic Geochemistry 51, 63–72.

Organic Geochemistry 51 (2012) 63–72

Contents lists available at SciVerse ScienceDirect

Organic Geochemistry

journal homepage: www.elsevier.com/locate/orggeochem

Soil organic matter transport along an sub-Arctic river–sea transect

Ayça Doğrul Selver [a], Helen M. Talbot [b], Örjan Gustafsson [c], Stephen Boult [a], Bart E. van Dongen [a,*]

[a] School of Earth, Atmospheric and Environmental Sciences and Williamson Research Centre for Molecular Environmental Science, University of Manchester, Manchester M13 9PL, UK
[b] School of Civil Engineering and Geosciences, Newcastle University, Newcastle upon Tyne NE1 7RU, UK
[c] Department of Applied Environmental Science (ITM) and the Bert Bolin Centre for Climate Research, Stockholm University, Sweden

ARTICLE INFO

Article history:
Received 20 April 2012
Received in revised form 1 August 2012
Accepted 2 August 2012
Available online 10 August 2012

ABSTRACT

Bacteriohopanepolyols (BHPs) and glycerol dialkyl glycerol tetraethers (GDGTs) have potential as soil-tracing biomarkers for the extensive shelves of the Arctic Ocean. In this work these biomarkers were analysed in surface sediments along a well characterised sub-Arctic transect in the northernmost Baltic Sea from the Kalix River to the central Bothnian Bay to assess their environmental behaviour and potential for tracing the contribution of soil in this type of system. There was a high BHP diversity and enhanced total BHP concentration in the estuarine sediments, whereas a much less diverse pattern could be observed in the open bay with lower total BHP concentration. In addition, both soil marker BHPs (adenosylhopanes) and branched GDGTs were substantially more abundant in the estuarine than the open bay sediments.

The R'_{soil} index, based on the R_{soil} index minus the contribution from the methylated soil marker BHPs, is suggested as a new approach for tracing soil derived organic matter (OM) in the (sub)-Arctic region. The index decreased along the transect in an off-river direction, correlating strongly with both the branched and isoprenoid tetraether (BIT) index and the stable carbon isotopic composition of the sedimentary organic carbon. These field results indicate that both the R'_{soil} and the BIT indices have potential for tracing soil derived OM in sub-Arctic to Arctic waters.

1. Introduction

Approximately half of the global soil organic carbon (OC) can be found in the Arctic region (Tarnocai et al., 2009), primarily locked in the pan-arctic permafrost. This is one of the so-called global climate vulnerable carbon pools (Gruber et al., 2004) and climate warming could cause a net redistribution of the terrestrial OC (terrOC) from these pan-arctic tundra/taiga areas, via the Arctic rivers to the Eurasian Arctic shelves. There is already evidence for increasing river discharge and change in the hydrological regime in these regions (Peterson et al., 2002; Dittmar and Kattner, 2003; Benner et al., 2004) and recent studies suggest that this might also have an effect on the release and decomposition of the terrOC, ultimately causing an increased release of greenhouse gases such as CO_2 and CH_4 (Guo et al., 2004, 2007; van Dongen et al., 2008a,b; Gustafsson et al., 2011).

This highlights the idea that determining the fate of the fluvially transported terrOC is also of major importance. Generally, research indicated that terrOC in the marine environment is more recalcitrant than marine OC (Hedges and Oades, 1997; Hedges et al., 1997). Most riverine particulate OC (POC) is preserved in estuarine sediments or degraded (Macdonald et al., 1998; Fernandes and Sicre, 2000; Amon et al., 2001; Dittmar and Kattner, 2003; Drenzek et al., 2007), with less than half transported off the shelf. However, actual data on the rate and extent of degradation of terrOC in the Arctic are limited, which forced Stein and Macdonald (2004) to assume that terrestrial POC degradation in the Arctic is identical to a 35% worldwide average for riverine POC in coastal environments in their first terrOC budget for the pan-Arctic shelves. More recent analysis indicates that a much larger proportion of the fluvially transported terrOC might be degraded near the river mouth than used in these budget estimates (van Dongen et al., 2008b; Vonk et al., 2010a; Karlsson et al., 2011). Van Dongen et al. (2008b), for instance, determined that ca. 65% of the terrestrial POC transported off the Kalix River is degraded in the coastal surface water. This non-conservative behaviour of terrOC on the Arctic shelves is supported by studies during the International Siberian Shelf Studies 2008 (ISSS08) expedition, indicating that ca. 30–50% of the terrestrial dissolved OC (DOC) and up to 66% of the terrestrial POC is lost annually during mixing in the Laptev and East Siberian seas (Alling et al., 2010; Sánchez-García et al., 2011). This suggests that the values used by Stein and Macdonald (2004) could be large underestimates and more terrOC might be degraded on Arctic Ocean shelves than previously thought, highlighting the potential for further mineralisation of this remobilized terrOC to greenhouse gases, causing a positive feedback to climate warming.

Given the difference in lability between terrOC and marine OC and the poorly constrained rate of loss of the former, it is critical to determine the relative concentration of each in Arctic

* Corresponding author. Tel.: +44 161 3067460; fax: +44 161 3069361.
E-mail address: Bart.vanDongen@manchester.ac.uk (B.E. van Dongen).

0146-6380/$ - see front matter © 2012 Elsevier Ltd. All rights reserved.
http://dx.doi.org/10.1016/j.orggeochem.2012.08.002

sediments. The differentiation of terrOC and marine OC is challenging, however, and has mostly been done at a bulk level using proxies such as C/N ratio and $\delta^{13}C$ composition (Fernandes and Sicre, 2000; Schubert and Calvert, 2001; Fahl et al., 2003; Guo et al., 2004; Drenzek et al., 2007; Vonk et al., 2008; van Dongen et al., 2008a). C/N values are likely depressed by nitrogen associated with mineral phases and therefore over-represent the marine contribution, as seen for other Arctic sediments (Schubert and Calvert, 2001; Fahl et al., 2003). In addition, none of these bulk methods can distinguish between terrestrial organic matter (OM) derived from plant material and soil. Recently, the discovery of specific microbial soil biomarkers has allowed the soil derived OC to be traced in other, non-Arctic, riverine system such as in a Yangtze River–East China Sea transect (Zhu et al., 2011).

Bacteriohopanepolyols (BHPs), synthesised by many prokaryotes (Ourisson and Albrecht, 1992), have polyfunctionalised side chains with a high degree of structural variability, including tetra-, penta- and hexafunctionalised structures (see Appendix A for structures; Rohmer, 1993). They have been observed in recent (Cooke et al., 2009 and references therein) and older sediments (up to ca. 70 Ma; van Dongen et al., 2006; Cooke et al., 2008a; Handley et al., 2010). Certain BHPs have been observed exclusively in soil and in sediments with a substantial terrestrial input (Talbot and Farrimond, 2007) and are therefore considered to be 'soil-markers' which can potentially be used to trace soil transport to marine sediments (Cooke et al., 2008a,b; Cooke et al., 2009; Zhu et al., 2011). Recently Zhu et al. (2011) successfully applied the BHP proxy, R_{soil}, based on the relative abundance of soil marker BHPs vs. bacteriohopanetetrol (BHT; Table 2), to trace the soil input to surface sediments along a river–estuary-shelf transect. BHT is used as a 'pseudo' marine representative since it is often the most abundant BHP in marine sediments (Farrimond et al., 2000; Blumenberg et al., 2010; Sáenz et al., 2011b; Zhu et al., 2011) and water columns (Wakeham et al., 2007; Sáenz et al., 2011a); however, it is not a pure marine end member as it is also present in a range of other environments including soil, peat and lacustrine environments (Talbot et al., 2003; Talbot and Farrimond, 2007; Cooke, 2010; van Winden et al., 2012). It is, however, currently the best option, as demonstrated by Zhu et al. (2011).

GDGTs are membrane lipids synthesised mainly by Archaea and are divided into two major groups, branched (br) and isoprenoid (iso) GDGTs (see Appendix A for structures). Studies indicate that br-GDGTs (br-GDGT I, II, III; m/z 1050, 1036, 1022 respectively; see Appendix A for structures) are synthesised mainly by anaerobic soil bacteria (Weijers et al., 2007), with acidobacteria as a potential source (Weijers et al., 2009; Sinninghe Damsté et al., 2011; Tierney et al., 2012), so are found predominantly in terrestrial environments (Hopmans et al., 2004; Weijers et al., 2006b). In contrast, marine Thaumarchaeota produce mainly iso-GDGTs, predominantly crenarchaeol (GDGT IV; Sinninghe Damsté et al., 2002; Schleper and Nicol, 2010). Iso-GDGTs have also been observed in soil and peat, although in considerably lower concentration (Weijers et al., 2004, 2006a). Based on these observations, an index was developed, the branched and isoprenoid tetraether (BIT) index, which can be used to trace fluvially transported soil OM to marine sediments (Hopmans et al., 2004). It is now widely used and has been successfully applied to trace soil derived carbon in the Congo River and Amazon River outflows (Hopmans et al., 2004; Kim et al., 2012) on the river dominated continental margins of the Mediterranean (Kim et al., 2006) and in OM rich turbidites from the Madeira abyssal plain (Huguet et al., 2008). Comparison with established molecular proxies, such as lignin–phenol based proxies, indicates that a clear correlation is not always observed (Walsh et al., 2008; Smith et al., 2010). Smith et al. (2010), for instance, observed no correlation between the relative presence of lignin phenols and the BIT index in surface sediments from Doubtful Sound (New Zealand). This could be caused by an increase in primary production but, considering that lignin is exclusively found in vascular plants, it is more likely due to a discrepancy between the relative amounts of soil OM and plant derived terrOM transported to the sediments (Smith et al., 2012). This further highlights the idea that soil specific proxies such as R_{soil} and BIT can be used alongside other established proxies to determine the relative input of soil, plant and marine OM to estuary sediments (Weijers et al., 2009).

Despite the extreme conditions, e.g. low temperature, recent studies of BHPs and GDGTs in surface sediments of Arctic river estuaries and the Chukchi and Beaufort seas indicate that terrOM is actively recycled in the soil of the drainage basin, resulting in a substantial contribution of terrestrially derived microbial lipids to the Arctic sediments (van Dongen et al., 2008a; Cooke et al., 2009; Taylor and Harvey, 2011). However, the extent to which these lipids can be used to trace a soil contribution to the Arctic shelves is unclear. The objectives of the present study were therefore to determine the potential for BHPs and GDGTs for tracing the soil contribution in the (sub-) Arctic marine environment using the GDGT based BIT index (Hopmans et al., 2004) and the recently developed BHP based R_{soil} index (Zhu et al., 2011). To this end, surface sediments along a well-studied (Gustafsson et al., 2000; Vonk et al., 2008, 2010b; van Dongen et al., 2008b) transect in the sub-Arctic northernmost Baltic Sea from the mouth of the unregulated Kalix River to central Bothnian Bay were analysed and the full BHP distributions and total BHP concentration measured to determine whether or not BHPs can be used as soil OM tracers in the Arctic environment.

2. Methods

2.1. Study area and sample collection

The Kalix River in northern Sweden, emptying into the Bothnian Bay (Fig. 1) and with a total catchment area of 23846 km^2, is one of the last unregulated major river systems in Europe and has a mean annual water discharge of ca. 300 $m^3 s^{-1}$ (Ingri et al., 2000, 2005), with peak flow during mid-May to late June and with a maximum discharge around 1600 $m^3 s^{-1}$. It can be considered to be an easily accessible model system for the western Russian Arctic Rivers, Ob and Yenisey, since it has a geochemistry similar to these rivers (Gustafsson et al., 2000; Guo et al., 2004; Ingri et al., 2005; Vonk et al., 2008). The Kalix River catchment area is sparsely populated and consists mainly of coniferous to boreal forest (55–65%) and peatland (17–20%) with <1% farmland (Ingri et al., 2005). The Kalix River estuary is characterised by weak tidal currents (<1 cm s^{-1}), is not influenced by major ice erosion and has an elongated low salinity ($\leqslant$3‰) zone, which stretches over 60 km into the estuary during spring (Gustafsson et al., 2000). This makes it an ideal location for studying processes in estuarine environments. Other major rivers draining into the Bothnian Bay are the Pite, Lule, Torne, Kemi, Li and Oulu (Fig. 1), in combination transporting ca. 790 kT/year of OC to the bay (Pettersson et al., 1997), of which ca. 7% originates from the Kalix River, meaning that land derived OM would be expected to have a significant impact on the basin. This also implies that stations further out into the open bay would have a substantial terrestrial input from other river systems.

Surface sediment samples were collected in the Kalix River–Bothnian Bay transect in early June 2005 using the research vessel KBV005 from the Umeå Marine Research Center (UMF, Norrbyn, Sweden), as described by Vonk et al. (2008). In short, an Ekman grab sampler was deployed to collect samples in an off Kalix River mouth transect (Fig. 1 and Table 1). Three of the sampling stations were situated in the Kalix River estuary (Stations A–C; Fig. 1) with a water depth up to 42 m, while the remaining three stations were

situated in the open Bothnian Bay (Stations D–F) with water depth between 80 and 83 m (Table 1). Sub-samples from the top 0–3 cm were obtained with stainless steel spatulas, transferred to pre-washed amber glass bottles, frozen immediately after collection and stored at −18 °C until analysis.

2.2. Extraction and fractionation

Methodology was adapted from Summons et al. (1994) and is based on Kates (1975) modification of the Bligh–Dyer method (Bligh and Dyer, 1959). Briefly, from each station 5 g (dry wt.) freeze-dried and homogenised sediment was ultrasonically extracted (3×; 40 °C, 1 h, followed by shaking 2–4 h and centrifugation, 15 min) with water:MeOH:dichloromethane (DCM) (4 ml, 10 ml, 5 ml) and the supernatants combined in another centrifuge tube. The sample was extracted again (2×) using the same solvent and the supernatants combined. The DCM fraction was recovered by addition of 5 ml water and 5 ml DCM, rotary evaporated to near dryness, transferred to a weighed vial using a solution of warm DCM:MeOH (2:1 v/v) and the solvent removed under a stream of N_2 to obtain the total lipid extract, which was split into aliquots.

One aliquot was used for GDGT analysis and was separated into polar and apolar fractions using Al_2O_3 column chromatography with hexane:DCM (1:1, v/v) and DCM:MeOH (1:1) as eluent, respectively. Analysis of GDGTs was carried out on the polar fraction using the method reported by Hopmans et al. (2004) via high performance liquid chromatography–atmospheric pressure chemical ionisation–mass spectrometry (HPLC–APCI–MS). A second aliquot was used for BHP analysis following the method described by Cooke et al. (2009) and analysed using LC–APCI–MS^n. In short, after addition of the internal standard (5α-pregnane-3β,20β-diol), the aliquot was acetylated, blown down to dryness and redissolved in a mixture of MeOH:propan-2-ol for analysis.

2.3. Instrumental analysis

Assignment of GDGTs was performed using an Agilent 1200 HPLC instrument coupled to an Agilent 6130 quadrupole MS instrument equipped with a multimode source operated in APCI positive ion mode using a similar instrumental setup as that described by McClymont et al. (2012). The GDGTs were analysed using normal phase LC–MS using a Grace Prevail Cyano HPLC column (3 μm, >150 mm × 2.1 mm i.d.) and a guard column of the same material. Separation was achieved at 30 °C with a flow rate of 0.2 ml min^{-1} and the following gradient profile: 1% isopropanol (IPA) in hexane (0–5 min), 1.8% IPA in hexane (at 25 min) and 10% IPA in hexane at 30 min (held 10 min). LC–MS settings were as follows: nebulizer pressure 20 psig, vaporiser temperature 250 °C, drying gas (N_2) flow 6 l/min and temperature 200 °C, capillary voltage 2 kV and corona 5 μA. In order to increase sensitivity/reproducibility, ion scanning was performed in single ion monitoring (SIM) mode using GDGT $[M+H]^+$ ions. The BIT index values were calculated according to the relative peak areas of the br-GDGTs with 4 (br-GDGT I), 5 (br-GDGT II) and 6 (br-GDGT III) methyl moieties, respectively, and crenarchaeol (cren), following the method of Hopmans et al. (2004):

$$\mathrm{BIT} = (\text{br-GDGTs I} + \mathrm{II} + \mathrm{III})/(\text{br-GDGTs I} + \mathrm{II} + \mathrm{III} + \text{cren}) \quad (1)$$

Identification and quantification of BHPs was accomplished using a Surveyor HPLC system (ThermoFinnigan, Hemel Hempstead, UK), fitted with a Phenomenex (Macclesfield, UK) Gemini C_{18} 5 μm HPLC column (150 mm × 3.0 mm i.d.) and a security guard column cartridge of the same material. Separation was achieved at 30 °C with a flow rate of 0.5 ml min^{-1} and using the following gradient profile: 90% A and 10% B (0 min), 59% A, 1% B and 40% C (at 25 min), then isocratic to 40 min (where A = MeOH, B = water and C = propan-2-ol; all HPLC grade, from Fisher Scientific [Loughborough, UK]) returning to the starting conditions in 5 min and stabilising for 15 min.

$LC–MS^n$ analysis was performed using a ThermoFinnigan LCQ ion trap mass spectrometer equipped with an APCI source operated in positive ion mode. LC–MS settings were as follows: capillary temperature 155 °C, APCI vaporiser temperature 400 °C, corona discharge current 8 μA, sheath gas flow 40 and auxiliary gas 10 (arbitrary units).

A semi-quantitative estimate of abundance (±20%) was calculated from the characteristic base peak ion peak areas of individual BHPs in mass chromatograms relative to the *m/z* 345 ($[M+H–CH_3COOH]^+$) base peak area response of the acetylated internal standard. Averaged relative response factors from a suite of five acetylated authentic BHP external standards were used to adjust the peak areas relative to that of the internal standard, where BHPs

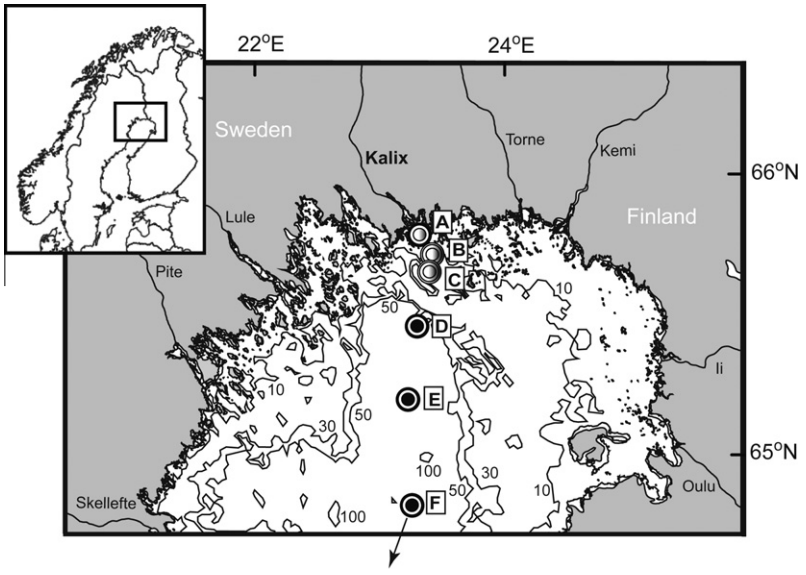

Fig. 1. Map of the Kalix River–Bothnian Bay transect showing sampling stations (exact locations are in Table 1). Open and closed circles indicate estuary and open bay stations, respectively.

Table 1
Sampling locations, BIT, $\delta^{13}C_{soc}$ and R_{soil} values of surface sediment samples from Kalix River–Bothnian Bay transect.

Sampling station	A	B	C	D	E	F
Location (N)	65°44.2′	65°40.2′	65°36.7′	65°25.5′	65°10.5′	63°00′
Location (E)	23°20.0′	23°26.0′	23°25.0′	23°19.0′	23°14.6′	22°51′
Distance from river mouth (km)[a]	13	22	29	50	78	304
Bottom depth (m)	13	30	42	82	83	80
Salinity	–	–	1.67[e]	–	3.00	4.87
BIT[b]	0.91	0.85	0.73	0.57	0.50	0.26
$\delta^{13}C_{SOC}$ (‰)[c]	−27.1	−27.4	−27.3	−26.1	−25.8	−24.5
R_{soil}[d]	0.25	0.38	0.40	0.26	0.08	0.08
R'_{soil}[d]	0.24	0.30	0.29	0.19	0.08	0.08

[a] Distance from 65°50N–23°10E.
[b] BIT = Branched and isoprenoid tetraether.
[c] SOC = Sedimentary organic carbon; data from Vonk et al. (2008).
[d] R_{soil} = (G1 + 2MeG1 + G2 + 2MeG2 + G3)/(BHT + G1 + 2MeG1 + G2 + 2MeG2 + G3) and R'_{soil} = (G1 + G2 + G3)/(BHT + G1 + G2 + G3); compound abbreviations as in Table 2.
[e] Since the practical salinity scale is only defined down to salinity 2, this value is regarded as "unofficial", but included here to define extend of mixing.

Table 2
BHP total abundance (μg/g TOC) and contribution to total BHPs (%), and GDGTs as a fraction of 1, in surface sediments from Kalix River–Bothnian Bay transect (BDL, below detection limit).

Compound	Abbreviation	Structure[a]	*m/z*	A	B	C	D	E	F
Bacteriohopanepolyols									
Bacteriohopanetetrol	BHT	1a	655	102(51)	181(44)	182(37)	99(72)	62(87)	83(84)
2Me-bacteriohopanetetrol	2Me-BHT	2a	669	8.4(4)	13(3)	9.6(2)	BDL	BDL	3.8(4)
Aminobacteriohopanetriol	Aminotriol	1b	714	11(5)	17(4)	37(8)	4.6(3)	3.6(5)	4.4(4)
Adenosylhopane Type 2	G2	1i	761	8.1(4)	12(3)	11(2)	3.1(2)	BDL	BDL
Aminobacteriohopanetetrol	Aminotetrol	1c	772	1.6(1)	BDL	BDL	BDL	BDL	BDL
2Me-adenosylhopane Type 2	2-Me G2	2i	775	1.1(1)	4.1(1)	5.3(1)	3.4(2)	BDL	BDL
Adenosylhopane	G1	1e	788	21(11)	59(14)	54(11)	14(10)	5.6(8)	7.4(7)
2Me-adenosyl hopane	2-MeG1	2e	802	BDL	29(7)	43.4(9)	6.7(5)	BDL	BDL
Adenosylhopane Type 3	G3	1i	802	3.4(2)	7.2(2)	9.6(2)	6.9(5)	BDL	BDL
Aminobacteriohopanepentol	Aminopentol	1d	830	1.8(1)	BDL	BDL	BDL	BDL	BDL
Bacteriohopanetetrol cyclitol ether	BHTcyclitol ether	1f	1002	27(13)	56(13)	111(23)	BDL	BDL	BDL
Bacteriohopanepentol cyclitol ether	BHpentol cyclitol ether	1g	1060	2.6(1)	4.2(1)	5.7(1)	BDL	BDL	BDL
Bacteriohopanehexol cyclitol ether	BHhexol cyclitol ether	1h	1118	1.6(1)	4.4(1)	4.6(1)	BDL	BDL	BDL
2Me-bacteriohopanehexol cyclitol ether	2Me-BHhexol cyclitol ether	2h	1132	1.7(1)	3.5(1)	3.1(1)	BDL	BDL	BDL
Other minor BHPs				10.7(5)	23.8(6)	12.5(3)	BDL	BDL	BDL
Total BHP concentration (μg/g TOC)				202	416	489	138	72	99
Glycerol dialkyl glycerol tetraethers									
br-GDGT I			1050	0.38	0.24	0.21	0.24	0.15	0.07
br-GDGT II			1036	0.31	0.29	0.23	0.29	0.16	0.10
br-GDGT III			1022	0.22	0.32	0.29	0.32	0.19	0.09
Crenarchaeol			1292	0.09	0.15	0.27	0.15	0.50	0.74

[a] See Appendix A.

containing one or more N atoms gave an averaged response ca. 12× that of the standard and those with no N atoms gave a response ca. 8× that of the standard (van Winden et al., 2012). The BHP based R_{soil} index values were calculated according to the relative concentration of the soil BHPs adenosylhopane (G1; structure 1e), 2Me-adenosylhopane (2MeG1; 2e), adenosylhopane type 2 (G2; 1i), 2Me-adenosylhopane type 2 (2MeG2; 2i) and andenosylhopane type 3 (G3; 1i′; Cooke et al., 2008a), respectively relative to the pseudo marine end member BHT (1a), following the method of Zhu et al. (2011):

$$R_{soil} = (G1 + 2MeG1 + G2 + 2MeG2 + G3)/(G1 + 2MeG1 + G2 + 2MeG2 + G3 + BHT) \quad (2)$$

3. Results

LC–MS revealed up to 20 different BHPs in the sediments. A general decrease in total BHP concentration between estuary (Stations A–B–C; Fig. 1) and open bay (D–E–F) sediments was observed, with a concentration ranging from 202 to 489 μg/g total OC (TOC) and from 72 to 138 μg/g TOC, respectively (Table 2 and Fig. 2).

Although some differences could be observed, all estuary sediments generally showed a comparable assemblage, with up to 16 different BHPs present. In all the estuary sediments, BHT (1a) was the most abundant, contributing between 37% and 51% to the total (Table 2). Other abundant BHPs were bacteriohopanetetrol cyclitol ether (1f) and adenosylhopane (1e). Concentration varied but these three BHPs comprised between 71% and 75% of the total (Table 2). The relative amount of soil-specific BHP markers (adenosylhopane (1e), 2Me-adenosylhopane (2e), adenosylhopane type structures including methylated homologues, 1i, 2i, 1i′ (Cooke et al., 2008a; Rethemeyer et al., 2010) in the estuary sediments varied from 18% to 37% of the total and the R_{soil} index varied between 0.25 and 0.40 (Table 1).

In contrast to the estuary sediments, the assemblage in the open bay sediments was less diverse, with only 3–7 BHPs above detection limit (Table 2). Again BHT was the most abundant BHP but with a substantially higher relative contribution (72–87%) than in the estuary sediments (Table 2 and Fig. 2). Other BHPs present in substantial amount in all three open bay sediments were adenosylhopane and aminobacteriohopanetriol (1b). Combined, these

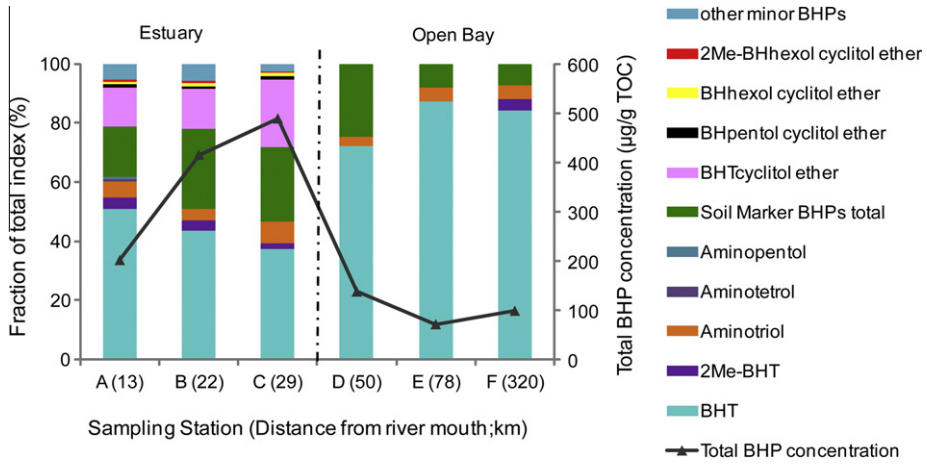

Fig. 2. Histogram of relative abundance of BHPs in Kalix River–Bothnian Bay transect surface sediments.

three structures comprised 85–100% of the total (Table 2 and Fig. 2). In contrast, bacteriohopanetetrol cyclitol ether, abundant in the estuary sediments, could not be detected in the open bay sediments. The relative amount of soil-specific BHPs in the open bay sediments was on average lower than in the estuary sediments, with values ranging from 7–24% (Table 2). Consequently, the R_{soil} index values between 0.08 and 0.26 (Table 1), were generally lower than for the estuary sediments.

LC–MS revealed a substantial amount of GDGTs in the transect sediments, with abundances expressed as a fraction of 1 in Table 2. The estuary sediments contained a much higher relative abundance of br-GDGTs than iso-GDGTs (Table 2), clearly reflected in relatively high BIT values from 0.73–0.91 (Table 1). In contrast, the open bay sediments were characterised by either comparable abundances of br- and iso-GDGTs (Station D) or a much higher relative abundance of iso-GDGTs (Station E and F), resulting in BIT index between 0.57 and 0.26 (Table 1).

4. Discussion

4.1. Soil OM input to Bothnian Bay

Detailed analysis of the suspended particulates of the Kalix River estuary indicated that a substantial part of the terr OC is degraded in the surface layer of the water column in the vicinity of the river mouth and is not preserved in the estuary sediments (van Dongen et al., 2008b). However, both elemental analysis and lipid biomarker analysis had shown that the OM in these estuary sediments is predominantly of terrestrial origin (Vonk et al., 2008). The detailed BHP analysis in the present study indicates that all Kalix River estuarine surface sediments were dominated by the same type of BHPs (e.g. BHPs 1a, 1f,1e,1b,2a,1i; Table 2), which also dominate the BHP signal in other major river systems and soils (i.e. major Russian Arctic Rivers and Yangtze River estuary sediments; Cooke et al., 2008b, 2009; Zhu et al., 2011) suggesting, in line with previous observations (Vonk et al., 2008), a high soil/terrestrially derived OC contribution. This is supported by the presence of substantial amounts of the soil-specific BHP markers in these estuary sediments, between 18% and 37% of the total, comparable with the contributions in other Arctic estuary sediments (Cooke et al., 2009; Taylor and Harvey, 2011) and in line with the average level of these soil-specific BHP markers in most European soils (Cooke et al., 2008a; Cooke, 2010).

Studies have indicated that the Kalix River has a geochemistry similar to that of the neighbouring western Russian Arctic rivers (Guo et al., 2004; Ingri et al., 2005; Vonk et al., 2008; Gustafsson et al., 2011). Lipid analysis of the same Kalix River–Bothnian Bay transect sediments showed, for instance, comparable terrestrial biomarker signatures, bulk $\delta^{13}C$ values and differences in ^{14}C signal between bulk OC and high molecular weight *n*-alkanes in the material released from the river, if compared with that of the western Russian Arctic rivers (Guo et al., 2004; Vonk et al., 2008; Gustafsson et al., 2011). The BHP analysis supports these observations, indicating that both the number (14–16) and type of BHPs and the total concentration (202–489 µg/g TOC) are comparable to those of the major Arctic river estuary sediments analysed by Cooke et al. (2009). In that study, between 11 (Ob estuary) and 15 (Indigirka and Mackenzie estuaries) BHPs were present at a total concentration ranging from 236 to 613 µg/g TOC. However, the number of structures is lower than that in the Yangtze River catchment sediments (21; Zhu et al., 2011) and the number usually observed in soil (at least 22 different BHPs; Cooke et al., 2009). Taken together, this shows that the Kalix River can, to a certain extent, be used as an easily accessible model for the river systems of the western Russian Arctic.

4.2. Marine vs. soil OM input along the transect

Substantial differences were observed along the transect between the estuary and the open bay. The estuary sediments were generally characterised by a substantial total amount of BHPs, up to 489 µg/g TOC, and high diversity (up to 16 BHPs; Table 2 and Fig. 2). In contrast, the open bay sediments showed substantially lower total BHP concentration, up to 138 µg/g TOC, and up to seven different structures. Earlier studies of surface sediment and suspended particulate OM samples along different river transects showed similar trends, with decreasing total BHP concentration and diversity (Cooke et al., 2008b, 2009; Taylor and Harvey, 2011; Zhu et al., 2011; Sáenz et al., 2011a). For instance, in a Yangtze River–East China Sea surface sediment transect, BHP diversity showed a seaward decrease, with the highest total abundance and an average of 14 BHPs nearshore vs. just 4 BHPs offshore. Similarly, a general decrease in total abundance from shallow to deep water was shown along a transect in the western Arctic (Taylor and Harvey, 2011). Interestingly, the same decreasing BHP diversity and concentration trend towards the marine environment was observed in a low latitude land-sea transect across the Island of San Salvador, the Bahamas (Pearson et al., 2009). However, the BHPs signatures here in the shallow open bay samples and the estuary, where seawater fully intrudes, were similar, suggesting that

similar depositional environment is a greater determinant of BHP composition than geographic location.

The apparent differences in the concentration and diversity of BHPs between open bay and estuarine stations may be primarily due to high soil OM influence in estuarine environments in combination with rapid BHP degradation along the transect, and/or in situ production (biosynthesis and diagenetic transformation) of marine derived BHPs (Zhu et al., 2010, 2011). Studies of the BHP composition of the Congo deep-sea fan sediments have suggested that adenosylhopane is less stable than other BHPs. In this setting it was the only BHP to show a typical diagenetic decay (overprinting strong cyclical variation in concentration) and it was not detected at all in samples over 950 ka, whilst other highly functionalised BHPs were still present at ca. 1.2 Ma (Cooke et al., 2008b; Handley et al., 2010). In addition, considering that BHT is not of pure marine origin but could have a substantial contribution from other environments, selective preservation of a recalcitrant pool of terrestrial BHPs could not be completely excluded, suggesting that the BHT in the open bay might be primarily of terrestrial origin (Sáenz et al., 2011a). Indeed, the BHT concentration was much lower in the open bay sediments than the estuary sediments (Table 2). However, this pattern is the opposite of the trend observed for other recalcitrant terrestrial biomarkers such as long chain *n*-alkanes showing increased relative contribution along the same transect (Vonk et al., 2008). This makes it unlikely that selective preservation could be a dominant factor in these sediments.

As mentioned above, adenosylhopane and adenosylhopane type structures are considered to be soil-specific biomarkers, transported fluvially to the marine environment (Cooke et al., 2008a; Sáenz et al., 2011b). Here, it was observed that there was a decreasing soil specific BHP contribution but relatively increasing BHT contribution in an off-river direction, as indicated by the R_{soil} index values (Table 1 and Fig. 3). This suggests a decreasing soil OM input throughout the Kalix River–Bothnian Bay transect, supporting the shift in $\delta^{13}C$ of the sedimentary OC, $\delta^{13}C_{soc}$, as observed by Vonk et al. (2008) for the same transect (Table 1 and Fig. 3). Smith et al. (2012) showed that proxies used to track soil OM in the marine environment, such as the BIT index, might be strongly dependent on the influx of marine derived material, indicating that the variation observed might reflect changes in the delivery of marine-derived OM to the sediments. The R_{soil} in the Kalix River–Bothnian Bay transect correlated strongly with both the total soil specific BHP concentrations ($r^2 = 0.89$; $p < 0.05$; $n = 6$) and BHT concentrations ($r^2 = 0.88$; $p < 0.05$; $n = 6$). This indicates that the variation in R_{soil} does not primary reflect changes in the delivery of marine-derived OM but suggests that it is a combination of both the preservation of soil and marine OM in the estuary sediments.

Besides the BHPs, the GDGT contribution indicates a shift from a soil to a more marine dominated input along the same transect, as illustrated by the GDGT based BIT index values (Table 1 and Fig. 3).

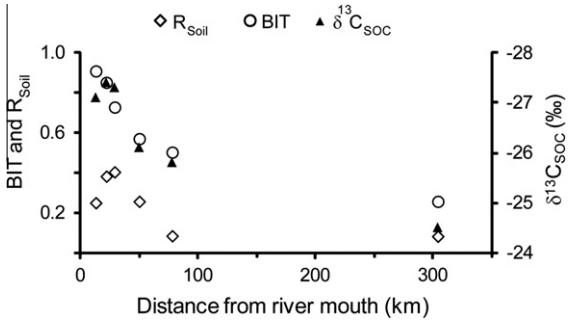

Fig. 3. Plot of BIT, R_{soil} and $\delta^{13}C_{soc}$ vs. distance from Kalix River mouth.

The estuary sediments were dominated by soil derived br-GDGTs, resulting in BIT values >0.73, comparable with, for instance, the GDGT composition in Russian Arctic River estuary sediments (van Dongen et al., 2008a). Also comparable with the BHPs and $\delta^{13}C_{soc}$, the BIT index dropped to 0.26, in line with a more marine contribution. This is likely due to degradation of br-GDGTs closer to the river mouth in combination with an increased in situ production of crenarchaeol.

As mentioned above, the majority of the terrOM is degraded near the Kalix River mouth (van Dongen et al., 2008a), resulting in a preferential preservation of the ballasted, older soil material in sediments (Vonk et al., 2010b). In addition, increased loss of functionality in a variety of lipid biomarkers, for instance, in the Kalix River Bothanian Bay transect sediments, suggested ongoing degradation of terrOM throughout this coastal system (Vonk et al., 2008). To summarise, both BIT and R_{soil} indicated decreasing trends in an off-river direction, supporting the earlier observations and suggesting that R_{soil} and BIT indices could indeed be used to track the soil derived OM in the Arctic region.

4.3. Comparison of different soil vs. marine indices

To compare the trends for the different terrestrial (soil) vs. marine indices along the transect, correlation plots were drawn between the different indices (R_{soil}, BIT and $\delta^{13}C_{soc}$; Fig 4). A strong correlation ($r^2 = 0.91$; $p < 0.05$; $n = 6$) is apparent between the BIT index and $\delta^{13}C_{soc}$ index, indicating that similar processes indeed affect these indices. Recent research indicates that a strong correlation between BIT and $\delta^{13}C_{soc}$ means that a substantial fraction of

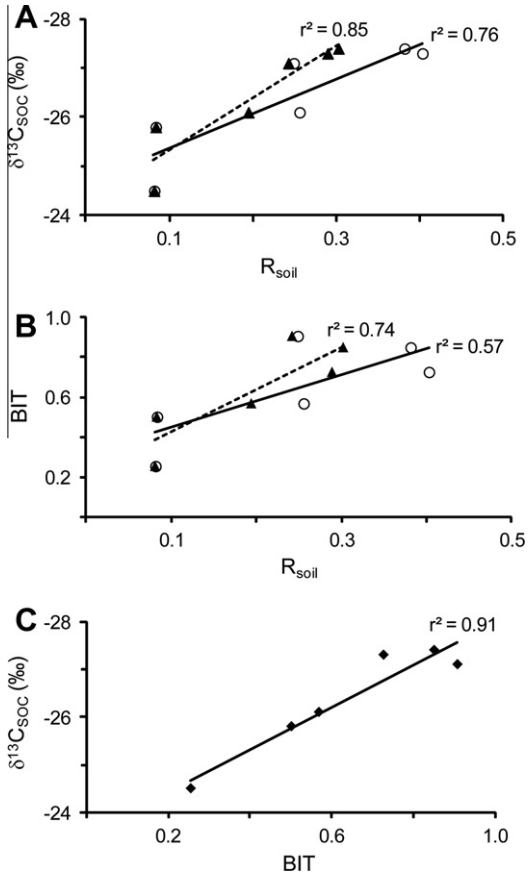

Fig. 4. Plots of R_{soil} index vs. (A) $\delta^{13}C_{soc}$ (B) BIT (open circles R_{soil}, triangles R'_{soil}) and (C) BIT index vs. $\delta^{13}C_{soc}$ in surface sediments of the Kalix River–Bothnian Bay transect.

the terrOM transported to the marine environment has a soil/peat origin (Smith et al., 2010), while a low correlation indicates lack of developed soil and peat in the local watershed (Walsh et al., 2008). Results from present study are in line with these observations and suggest that a substantial fraction of the terrOM transported to the marine environment in this sub-Arctic environment originates from the soil in the drainage basin. Crenarchaeol has also been observed in soil and peat (Weijers et al., 2004, 2006a) but these results indicate that a contribution from soil only plays a minor role here.

The correlation between R_{soil} and the other two indices is much lower than the correlation between the BIT and $\delta^{13}C_{soc}$ indices (Fig. 4). The R_{soil} index still strongly correlates with the $\delta^{13}C_{soc}$ index ($r^2 = 0.76$; $p < 0.05$; $n = 6$; Fig. 4C), although only a moderate correlation with the BIT index can be observed ($r^2 = 0.57$; $p = 0.15$; $n = 6$; Fig. 4B). This suggests that BHPs and GDGTs might behave differently in the marine environment. However, Zhu et al. (2011) observed a much better correlation between the two indices for the Yangtze River–East China Sea (ECS) shelf system, suggesting that this might be caused by local (Arctic) environmental conditions.

Alternative indices were explored to test if the correlations between R_{soil} and the other indices could be increased. Although individual BHP concentration naturally varies from station to station, closer examination of the soil marker BHPs indicates a substantial difference between the relative contributions of the non-methylated (G1, G2 and G3) and methylated (2-MeG1 and 2-MeG2) soil specific BHPs to the three estuary sediments (Table 2). In particular, the relative contribution of 2-MeG2 BHP varied substantially. While it could not be detected in the sediments from the station closest to the river mouth, it was abundantly present in the other two estuary sediments at 7–9% of the total BHPs (Table 2). At both of these two stations, 2-MeG2 was the second most abundant soil marker BHP. By comparison, G2, the most abundant soil marker BHP varied only slightly between the three stations, with a contribution between 11% and 14% of the total BHPs. The cause of the discontinuous presence of the methylated soil marker BHPs remains unclear.

Based on this discontinuous presence, we decided to exclude the methylated soil marker BHPs from the R_{soil} index, resulting in a new index labelled R'_{soil}:

$$R'_{soil} = (G1 + G2 + G3)/(G1 + G2 + G3 + BHT) \quad (3)$$

Compared with the R_{soil} index, the R'_{soil} index decreased along the transect in an off-river direction (Table 1). Furthermore, the slight change in the calculation of the BHP based proxy resulted in a significant increase in the correlation with the other two indices. The determination coefficients for the correlation between the R'_{soil} index and the BIT and the $\delta^{13}C_{soc}$ indices shifted from 0.57 to 0.74 and from 0.76 to 0.85, respectively ($p < 0.05$; $n = 6$; Fig. 4). This resulted in a strong correlation for all three indices along the transect ($r^2 = 0.74$–0.91), indicating that both R'_{soil} and the BIT have great potential for tracing soil derived OM in the (sub-)Arctic region.

To test if a (discontinuous) presence of the methylated soil marker BHPs also had an impact in other river transects, the R'_{soil} index was applied to the only other River-open bay transect for which BHP data and BIT and $\delta^{13}C_{soc}$ indices were available: the Yangtze River–ECS shelf system (Zhu et al., 2011). In contrast to the Kalix River–Bothnian Bay transect, exclusion of the methylated soil marker BHPs from the R_{soil} index in the Yangtze River – ECS transect did not cause a significant change in the correlation between the R_{soil} index and the other two indices (Fig. 5). At present, the cause of these differences remains unclear, but it highlights the possibility that environmental conditions could potentially have an impact on the soil marker BHP distribution pattern observed and subsequently on the R_{soil} index. Furthermore, it indicates that the range of the application of the R_{soil} proxy remains unclear and further work is necessary.

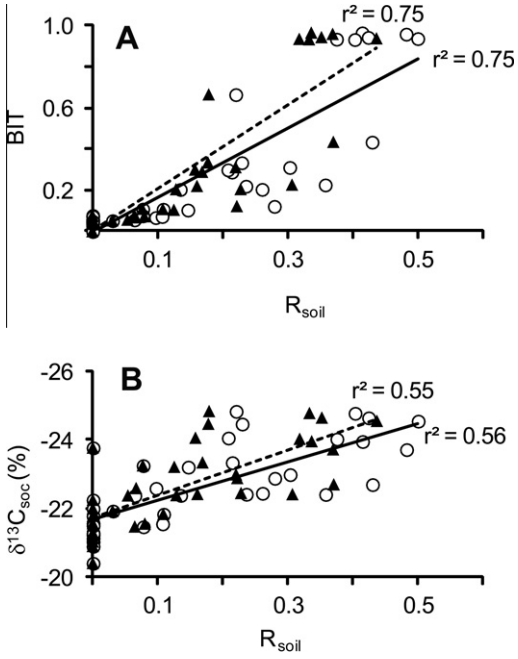

Fig. 5. Plots of R_{soil} and R'_{soil} (recalculated by us) indices vs. (A) BIT and (B) $\delta^{13}C_{soc}$ in surface sediments of the Yangtze River–East China Sea shelf system (data from Zhu et al., 2011; open circles R_{soil}, triangles R'_{soil}; $p < 0.05$; $n = 39$).

5. Conclusions

Surface sediments along a Kalix River–Bothnian Bay transect show high BHP diversity and enhanced total BHP concentration in the estuarine sediments. In contrast, much less diverse BHP patterns and lower total BHP concentration occur in the open bay sediments. Soil-marker BHPs and br-GDGTs were substantially more abundant in the estuary sediments than the open bay sediments, showing a decreasing trend along the transect in an off-river direction.

The BHP and GDGT based proxies, the BIT and R_{soil} indices, indicated decreasing trends, suggesting decreasing soil OM input, in an off-river direction.

Comparison of the different proxies indicates that BHP and GDGT based proxies can be used to track the relative contribution of terrestrial (soil) derived OM in the (sub-)Arctic marine environment. However, based on our findings it is proposed that the R'_{soil} index (i.e. the R_{soil} index minus the contribution from the methylated soil-marker BHPs) should be used instead to track the behaviour of the soil OM in the (sub-)Arctic region. Furthermore, the study again highlights the point that it is preferable not to use molecular based proxies, such as the BIT and R_{soil} indices, in isolation, but rather a multi-proxy approach, so that the behaviour of the individual proxies can be compared with that of others.

Acknowledgements

We gratefully acknowledge receipt of a PhD studentship for A.D.S., funded by the Ministry of National Education of Turkey. The study was also supported by the Swedish Research Council and the Nordic Council of Ministers. We thank Dr Zhu for providing the comparison data from the Yangtze River ECS system and

P. Lythgoe (University of Manchester) for invaluable assistance with LC–MS and The Science Research Infrastructure Fund (SRIF) from HEFCE for the ThermoFinnigan LCQ ion trap mass spectrometer (Newcastle University). We also thank two anonymous reviewers for constructive comments that helped improve the clarity of the paper.

Appendix A

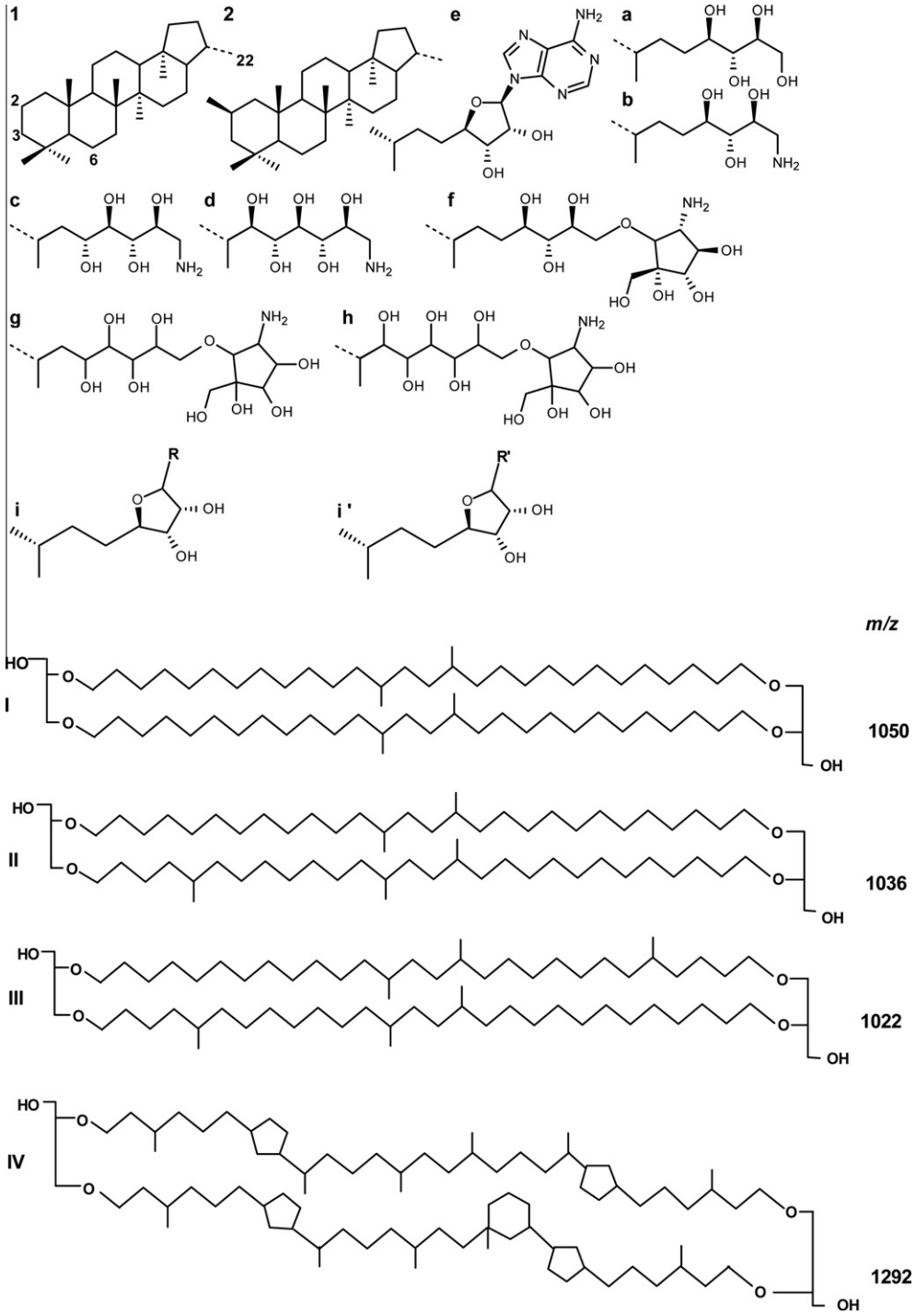

Associate Editor—**M.B. Yunker**

References

Alling, V., Sanchez-Garcia, L., Porcelli, D., Pugach, S., Vonk, J.E., van Dongen, B., Mörth, C.-M., Anderson, L.G., Sokolov, A., Andersson, P., Humborg, C., Semiletov, I., Gustafsson, Ö., 2010. Nonconservative behavior of dissolved organic carbon across the Laptev and East Siberian seas. Global Biogeochemical Cycles 24, GB4033. http://dx.doi.org/10.1029/2010gb003834.

Amon, R.M.W., Fitznar, H.-P., Benner, R., 2001. Linkages among the bioreactivity, chemical composition, and diagenetic state of marine dissolved organic matter. Limnology and Oceanography 46, 287–297.

Benner, R., Benitez-Nelson, B., Kaiser, K., Amon, R.M.W., 2004. Export of young terrigenous dissolved organic carbon from rivers to the Arctic Ocean. Geophysical Research Letters 31, L05305. http://dx.doi.org/10.1029/2003gl019251.

Bligh, E.G., Dyer, W.J., 1959. A rapid method of total lipid extraction and purification. Canadian Journal of Biochemistry and Physiology 37, 911–917.

Blumenberg, M., Mollenhauer, G., Zabel, M., Reimer, A., Thiel, V., 2010. Decoupling of bio- and geohopanoids in sediments of the Benguela Upwelling System (BUS). Organic Geochemistry 41, 1119–1129.

Cooke, M.P., 2010. The Role of Bacteriohopanepolyols as Biomarkers for Soil Bacterial Communities and Soil Derived Organic Matter. Ph.D. Thesis, University of Newcastle.

Cooke, M.P., Talbot, H.M., Farrimond, P., 2008a. Bacterial populations recorded in bacteriohopanepolyol distributions in soils from Northern England. Organic Geochemistry 39, 1347–1358.

Cooke, M.P., Talbot, H.M., Wagner, T., 2008b. Tracking soil organic carbon transport to continental margin sediments using soil-specific hopanoid biomarkers: a case study from the Congo fan (ODP site 1075). Organic Geochemistry 39, 965–971.

Cooke, M.P., van Dongen, B.E., Talbot, H.M., Semiletov, I., Shakhova, N., Guo, L., Gustafsson, Ö., 2009. Bacteriohopanepolyol biomarker composition of organic matter exported to the Arctic Ocean by seven of the major Arctic rivers. Organic Geochemistry 40, 1151–1159.

Dittmar, T., Kattner, G., 2003. The biogeochemistry of the river and shelf ecosystem of the Arctic Ocean: a review. Marine Chemistry 83, 103–120.

Drenzek, N.J., Montluçon, D.B., Yunker, M.B., Macdonald, R.W., Eglinton, T.I., 2007. Constraints on the origin of sedimentary organic carbon in the Beaufort Sea from coupled molecular ^{13}C and ^{14}C measurements. Marine Chemistry 103, 146–162.

Fahl, K., Stein, R., Gaye-Haake, B., Gebhardt, A.C., Kodina, L.A., Unger, D., Ittekkot, V., 2003. Biomarkers in surface sediments from the Ob and Yenisei estuaries and the southern Kara Sea: evidence for particulate organic carbon sources, pathways, and degradation. In: Stein, R., Fahl, K., Fütterer, D.K., Galimov, E.M., Stepanets, O.V. (Eds.), Proceedings in Marine Science: Siberian River Run-off in the Kara Sea, vol. 6. Elsevier, Amsterdam, pp. 329–348.

Farrimond, P., Head, I.M., Innes, H.E., 2000. Environmental influence on the biohopanoid composition of recent sediments. Geochimica et Cosmochimica Acta 64, 2985–2992.

Fernandes, M.B., Sicre, M.A., 2000. The importance of terrestrial organic carbon inputs on Kara Sea shelves as revealed by *n*-alkanes, OC and $\delta^{13}C$ values. Organic Geochemistry 31, 363–374.

Gruber, N., Friedlingstein, P., Field, C.B., Valentini, R., Heimann, M., Richey, J.E., Romero-Lankao, P., Schulze, C.C.-T., 2004. The vulnerability of the carbon cycle in the 21st century: an assessment of carbon–climate human interactions. In: Field, C.B., Raupach, M.R. (Eds.), The Global Carbon Cycle: Integrating Humans, Climate, and the Natural World. Island Press, Washington, DC, pp. 45–76.

Guo, L., Semiletov, I., Gustafsson, Ö., Ingri, J., Andersson, P., Dudarev, O., White, D., 2004. Characterization of Siberian Arctic coastal sediments: implications for terrestrial organic carbon export. Global Biogeochemical Cycles 18, GB1036. http://dx.doi.org/10.1029/2003gb002087.

Guo, L., Ping, C.-L., Macdonald, R.W., 2007. Mobilization pathways of organic carbon from permafrost to arctic rivers in a changing climate. Geophysical Research Letters 34, L13603. http://dx.doi.org/10.1029/2007gl030689.

Gustafsson, Ö., Widerlund, A., Andersson, P.S., Ingri, J., Roos, P., Ledin, A., 2000. Colloid dynamics and transport of major elements through a boreal river – brackish bay mixing zone. Marine Chemistry 71, 1–21.

Gustafsson, Ö., van Dongen, B.E., Vonk, J.E., Dudarev, O.V., Semiletov, I.P., 2011. Widespread release of old carbon across the Siberian Arctic echoed by its large rivers. Biogeosciences 8, 1737–1743.

Handley, L., Talbot, H.M., Cooke, M.P., Anderson, K.E., Wagner, T., 2010. Bacteriohopanepolyols as tracers for continental and marine organic matter supply and phases of enhanced nitrogen cycling on the late Quaternary Congo deep sea fan. Organic Geochemistry 41, 910–914.

Hedges, J.I., Oades, J.I., 1997. Comparative organic geochemistries of soils and marine sediments. Organic Geochemistry 27, 319–361.

Hedges, J.I., Keil, R.G., Benner, R., 1997. What happens to terrestrial organic matter in the ocean? Organic Geochemistry 27, 195–212.

Hopmans, E.C., Weijers, J.W.H., Schefuß, E., Herfort, L., Sinninghe Damsté, J.S., Schouten, S., 2004. A novel proxy for terrestrial organic matter in sediments based on branched and isoprenoid tetraether lipids. Earth and Planetary Science Letters 224, 107–116.

Huguet, C., de Lange, G.J., Gustafsson, Ö., Middelburg, J.J., Sinninghe Damsté, J.S., Schouten, S., 2008. Selective preservation of soil organic matter in oxidized marine sediments (Madeira Abyssal Plain). Geochimica et Cosmochimica Acta 72, 6061–6068.

Ingri, J., Widerlund, A., Land, M., Gustafsson, Ö., Andersson, P., Öhlander, B., 2000. Temporal variations in the fractionation of the rare earth elements in a boreal river; the role of colloidal particles. Chemical Geology 166, 23–45.

Ingri, J., Widerlund, A., Land, M., 2005. Geochemistry of major elements in a pristine boreal river system; hydrological compartments and flow paths. Aquatic Geochemistry 11, 57–88.

Karlsson, E.S., Charkin, A., Dudarev, O.V., Semiletov, I.P., Vonk, J.E., Sánchez-García, L., Andersson, A., Gustafsson, Ö., 2011. Carbon isotopes and lipid biomarker investigation of sources, transport and degradation of terrestrial organic matter in the Buor-Khaya Bay, SE Laptev Sea. Biogeosciences 8, 1865–1879.

Kates, M., 1975. Techniques of Lipidology: Isolation, Analysis and Identification of Lipids. North-Holland Publishing Company, Amsterdam.

Kim, J.-H., Schouten, S., Buscail, R., Ludwig, W., Bonnin, J., Sinninghe Damsté, J.S., Bourrin, F., 2006. Origin and distribution of terrestrial organic matter in the NW Mediterranean (Gulf of Lions): exploring the newly developed BIT index. Geochemistry Geophysics Geosystems 7, Q11017.

Kim, J.-H., Zell, C., Moreira-Turcq, Pérez, M.A.P., Abril, G., Mortillaro, J.-M., Weijers, J.W.H., Meziane, T., Sinninghe Damsté, J.S., 2012. Tracing soil organic carbon in the lower Amazon River and its tributaries using GDGT distributions and bulk organic matter properties. Geochimica et Cosmochimica Acta 90, 163–180.

Macdonald, R.W., Solomon, S.M., Cranston, R.E., Welch, H.E., Yunker, M.B., Gobeil, C., 1998. A sediment and organic carbon budget for the Canadian Beaufort Shelf. Marine Geology 144, 255–273.

McClymont, E.L., Ganeshram, R.S.S., Pichevin, L.E., Talbot, H., van Dongen, B., Thunell, R.C., Haywood, A.M., Singarayer, J.S., Valdes, P.J., 2012. Sea-surface temperature records of Termination 1 in the Gulf of California: challenges for seasonal and inter-annual analogues of tropical Pacific climate change. Paleoceanography 27. http://dx.doi.org/10.1029/2011PA02226.

Ourisson, G., Albrecht, P., 1992. Hopanoids. 1. Geohopanoids: the most abundant natural products on Earth? Accounts of Chemical Research 25, 398–402.

Pearson, A., Leavitt, W.D., Sáenz, J.P., Summons, R.E., Tam, M.C.M., Close, H.G., 2009. Diversity of hopanoids and squalene–hopene cyclases across a tropical land-sea gradient. Environmental Microbiology 11, 1208–1223.

Peterson, B.J., Holmes, R.M., McClelland, J.W., Vörösmarty, C.J., Lammers, R.B., Shiklomanov, A.I., Shiklomanov, I.A., Rahmstorf, S., 2002. Increasing river discharge to the Arctic Ocean. Science 298, 2171–2173.

Pettersson, C., Allard, B., Borén, H., 1997. River discharge of humic substances and humic-bound metals to the Gulf of Bothnia. Estuarine, Coastal and Shelf Science 44, 533–541.

Rethemeyer, J., Schubotz, F., Talbot, H.M., Cooke, M.P., Hinrichs, K.-U., Mollenhauer, G., 2010. Distribution of polar membrane lipids in permafrost soils and sediments of a small high Arctic catchment. Organic Geochemistry 41, 1130–1145.

Rohmer, M., 1993. The biosynthesis of triterpenoids of the hopane series in the Eubacteria: a mine of new enzyme reactions. Pure & Applied Chemistry 65, 1293–1298.

Sáenz, J.P., Eglinton, T.I., Summons, R.E., 2011a. Abundance and structural diversity of bacteriohopanepolyols in suspended particulate matter along a river to ocean transect. Organic Geochemistry 42, 774–780.

Sáenz, J.P., Wakeham, S.G., Eglinton, T.I., Summons, R.E., 2011b. New constraints on the provenance of hopanoids in the marine geologic record: bacteriohopanepolyols in marine suboxic and anoxic environments. Organic Geochemistry 42, 1351–1362.

Sánchez-García, L., Alling, V., Pugach, S., Vonk, J., van Dongen, B., Humborg, C., Dudarev, O., Semiletov, I., Gustafsson, Ö., 2011. Inventories and behavior of particulate organic carbon in the Laptev and East Siberian seas. Global Biogeochemical Cycles 25, GB2007. http://dx.doi.org/10.1029/2010gb003862.

Schleper, C., Nicol, G.W., 2010. Ammonia-oxidising archaea – physiology, ecology and volution. Advances in Microbial Physiology 57, 1–41.

Schubert, C.J., Calvert, S.E., 2001. Nitrogen and carbon isotopic composition of marine and terrestrial organic matter in Arctic Ocean sediments: implications for nutrient utilization and organic matter composition. Deep Sea Research Part I: Oceanographic Research Papers 48, 789–810.

Sinninghe Damsté, J.S., Schouten, S., Hopmans, E.C., van Duin, C.T., Geenevasen, J.A.J., 2002. Crenarchaeol: the characteristic core glycerol dibiphytanyl glycerol tetraether membrane lipid of cosmopolitan pelagic crenarchaeota. Journal of Lipid Research 43, 1641–1651.

Sinninghe Damsté, J.S., Rijpstra, W.I.C., Hopmans, E.C., Weijers, J.W.H., Foesel, B.U., Overmann, J., Dedysh, S.N., 2011. 13,16-Dimethyl octacosanedioic acid (iso-diabolic acid), a common membrane-spanning lipid of Acidobacteria subdivisions 1 and 3. Applied and Environmental Microbiology 77, 4147–4154.

Smith, R.W., Bianchi, T.S., Savage, C., 2010. Comparison of lignin phenols and branched/isoprenoid tetraethers (BIT index) as indices of terrestrial organic matter in Doubtful Sound, Fiordland, New Zealand. Organic Geochemistry 41, 281–290.

Smith, R.W., Bianchi, T.S., Li, X., 2012. A re-evaluation of the use of branched GDGTs as terrestrial biomarkers: implications for the BIT Index. Geochimica et Cosmochimica Acta 80, 14–29.

Stein, R., Macdonald, R.W., 2004. The Organic Carbon Cycle in the Arctic Ocean. Springer, Berlin, 363 pp.

Summons, R.E., Jahnke, L.L., Roksandic, Z., 1994. Carbon isotopic fractionation in lipids from methanotrophic bacteria: relevance for interpretation of the geochemical record of biomarkers. Geochimica et Cosmochimica Acta 58, 2853–2863.

Talbot, H.M., Farrimond, P., 2007. Bacterial populations recorded in diverse sedimentary biohopanoid distributions. Organic Geochemistry 38, 1212–1225.
Talbot, H.M., Summons, R., Jahnke, L., Farrimond, P., 2003. Characteristic fragmentation of bacteriohopanepolyols during atmospheric pressure chemical ionisation liquid chromatography/ion trap mass spectrometry. Rapid Communications in Mass Spectrometry 17, 2788–2796.
Tarnocai, C., Canadell, J.G., Schuur, E.A.G., Kuhry, P., Mazhitova, G., Zimov, S., 2009. Soil organic carbon pools in the northern circumpolar permafrost region. Global Biogeochemical Cycles 23, GB2023.
Taylor, K.A., Harvey, R.H., 2011. Bacterial hopanoids as tracers of organic carbon sources and processing across the western Arctic continental shelf. Organic Geochemistry 42, 487–497.
Tierney, J.E., Schouten, S., Pitcher, A., Hopmans, E.C., Sinninghe Damsté, J.S., 2012. Core and intact polar glycerol dialkyl glycerol tetraethers (GDGTs) in Sand Pond, Warwick, Rhode Island (USA): insights into the origin of lacustrine GDGTs. Geochimica et Cosmochimica Acta 77, 561–581.
van Dongen, B.E., Talbot, H.M., Schouten, S., Pearson, P.N., Pancost, R.D., 2006. Well preserved Palaeogene and Cretaceous biomarkers from the Kilwa area, Tanzania. Organic Geochemistry 37, 539–557.
van Dongen, B.E., Zencak, Z., Gustafsson, Ö., 2008b. Differential transport and degradation of bulk organic carbon and specific terrestrial biomarkers in the surface waters of a sub-Arctic brackish bay mixing zone. Marine Chemistry 112, 203–214.
van Dongen, B.E., Semiletov, I., Weijers, J.W.H., Gustafsson, Ö., 2008a. Contrasting lipid biomarker composition of terrestrial organic matter exported from across the Eurasian Arctic by the five great Russian Arctic rivers. Global Biogeochemical Cycles 22, GB1011. http://dx.doi.org/10.1029/2007gb002974.
van Winden, J.F., Talbot, H.M., Kip, N., Reichart, G.-J., Pol, A., McNamara, N.P., Jetten, M.S.M., Op den Camp, H.J.M., Sinninghe Damsté, J.S., 2012. Bacteriohopanepolyol signatures as markers for methanotrophic bacteria in peat moss. Geochimica et Cosmochimica Acta 77, 52–61.
Vonk, J.E., van Dongen, B.E., Gustafsson, Ö., 2008. Lipid biomarker investigation of the origin and diagenetic state of sub-Arctic terrestrial organic matter presently exported into the northern Bothnian Bay. Marine Chemistry 112, 1–10.
Vonk, J.E., Sánchez-García, L., Semiletov, I.P., Dudarev, O.V., Eglinton, T.I., Andersson, A., Gustafsson, Ö., 2010a. Molecular and radiocarbon constraints on sources and degradation of terrestrial organic carbon along the Kolyma paleoriver transect, East Siberian Sea. Biogeosciences 7, 3153–3166.
Vonk, J.E., van Dongen, B.E., Gustafsson, Ö., 2010b. Selective preservation of old organic carbon fluvially released from sub-Arctic soils. Geophysical Research Letters 37, L11605. http://dx.doi.org/10.1029/2010gl042909.
Wakeham, S.G., Amann, R., Freeman, K.H., Hopmans, E.C., Jørgensen, B.B., Putnam, I.F., Schouten, S., Sinninghe Damsté, J.S., Talbot, H.M., Woebken, D., 2007. Microbial ecology of the stratified water column of the Black Sea as revealed by a comprehensive biomarker study. Organic Geochemistry 38, 2070–2097.
Walsh, M.E., Ingalls, A.E., Keil, R.G., 2008. Sources and transport of terrestrial organic matter in Vancouver Island fjords and the Vancouver–Washington Margin: a multiproxy approach using $\delta^{13}C_{org}$, lignin phenols, and the ether lipid BIT index. Limnology and Oceanography 53, 1054–1063.
Weijers, J.W.H., Schouten, S., van der Linden, M., van Geel, B., Sinninghe Damsté, J.S., 2004. Water table related variations in the abundance of intact archaeal membrane lipids in a Swedish peat bog. FEMS Microbiology Letters 239, 51–56.
Weijers, J.W.H., Schouten, S., Hopmans, E.C., Geenevasen, J.A.J., David, O.R.P., Coleman, J.M., Pancost, R.D., Sinninghe Damsté, J.S., 2006a. Membrane lipids of mesophilic anaerobic bacteria thriving in peats have typical archaeal traits. Environmental Microbiology 8, 648–657.
Weijers, J.W.H., Schouten, S., Spaargaren, O.C., Sinninghe Damsté, J.S., 2006b. Occurrence and distribution of tetraether membrane lipids in soils: implications for the use of the TEX_{86} proxy and the BIT index. Organic Geochemistry 37, 1680–1693.
Weijers, J.W.H., Schouten, S., van den Donker, J.C., Hopmans, E.C., Sinninghe Damsté, J.S., 2007. Environmental controls on bacterial tetraether membrane lipid distribution in soils. Geochimica et Cosmochimica Acta 71, 703–713.
Weijers, J.W.H., Schouten, S., Schefuß, E., Schneider, R.R., Sinninghe Damsté, J.S., 2009. Disentangling marine, soil and plant organic carbon contributions to continental margin sediments: a multi-proxy approach in a 20,000 year sediment record from the Congo deep-sea fan. Geochimica et Cosmochimica Acta 73, 119–132.
Zhu, C., Talbot, H.M., Wagner, T., Pan, J.M., Pancost, R.D., 2010. Intense aerobic methane oxidation in the Yangtze Estuary: a record from 35-aminobacteriohopanepolyols in surface sediments. Organic Geochemistry 41, 1056–1059.
Zhu, C., Talbot, H.M., Wagner, T., Pan, J.M., Pancost, R.D., 2011. Distribution of hopanoids along a land to sea transect: implications for microbial ecology and the use of hopanoids in environmental studies. Limnology and Oceanography 56, 1850–1865.

CHAPTER 3

Paper 2: Distributions of bacterial and archaeal membrane lipids in surface sediments along a cross-shelf transect in central East Siberian Sea

This chapter contains the following paper which is in preparation to be submitted to the journal of Organic Geochemistry

Ayça Doğrul Selver[a], Robert B. Sparkes[a], Juliane Bischoff[b], Helen M. Talbot[b], Örjan Gustafsson[c], Igor P. Semiletov[d,e,f], Oleg V. Dudarev[e,f], Stephen Boult[a] and Bart E. van Dongen[a,*]

[a] School of Earth, Atmospheric and Environmental Sciences and Williamson Research Center, University of Manchester, Oxford Road, Manchester, M13 9PL, UK
[b] School of Civil Engineering and Geosciences, Newcastle University, Newcastle upon Tyne, NE1 7RU, UK
[c] Department of Applied Environmental Science (ITM) and the Bert Bolin Centre for Climate Research Stockholm University, Sweden
[d] Tomsk Polytechnic University,634050, Russia, Tomsk, Lenin Avenue, 30
[e] International Arctic Research Center, University of Alaska, Fairbanks, AK 99775-7340
[f] Pacific Oceanological Institute Far Eastern Branch of the Russian Academy of Sciences, Vladivostok 690041, Russia

* Corresponding Author: E-mail address: Bart.vandongen@manchester.ac.uk

Abstract

Enhanced climate warming affecting the Arctic region could have a dramatic impact on the soil organic carbon (OC) stored in the Eurasian permafrost and could increase the amounts of OC remobilized to the Arctic shelves. An improved understanding of the fate of this remobilized soil OC is essential to better understand the consequences for the Arctic and global carbon cycle. Glycerol Dialkyl Glycerol Tetraethers (GDGTs) and Bacteriohopanepolyols (BHPs) can be used to trace this remobilized soil OC. In this study, these biomarkers were analyzed in surface sediments along a 500 km cross-shelf transect from the mouth of the Kolyma River to the middle of the vast East Siberian Sea to assess their potential and that of the associated branched and isoprenoid tetraether (BIT) and R'_{soil} indices for tracing terrestrial derived OC in Arctic systems.

Both BHP and GDGT contributions indicate the highest contribution of soil OC to the total sediment OC collected close to the river mouths with the associated indices showed declining trends in an off-shore direction supporting an increasing marine OC input and/or a decrease in terrestrial OC. However, while the BHPs indicate a dominance of terrestrial derived OC at the start of the transect, the GDGTs suggest a much larger, almost 50%, marine OC input at this point. In addition, the BIT index showed an exponential decline along the transect, mainly controlled by substantial contributions of marine GDGTs, while the R'_{soil} revealed a linear trend primarily governed by the removal of soil marker BHPs.

These field results suggest that both biomarker approaches could be used to trace soil derived OC in the Arctic environment. However, using a single proxy approach is not recommended and may lead to an under or over estimation of the relative importance of terrOC. Using a multi-proxy approach is valuable to fully understand the fate of terrestrially derived OC along Arctic land-ocean transects.

3.1. Introduction

The Arctic terrestrial regions contain approximately half of all global soil organic carbon (Tarnocai et al., 2009), primarily locked in the first few meters of pan-Arctic permafrost. The widespread extent of this permafrost currently limits the exchange between this large organic carbon (OC) reservoir with other more active carbon pools, including the atmosphere. However, since this region is subjected to a warming at two to three times the global average rate (ACIA, 2004; Trenberth et al., 2007; Zwiers, 2002), dramatic changes in the release of soil carbon are expected to occur, including an increase in the amount of terrestrial/soil organic carbon transported to the Arctic shelf seas. There is, therefore, a requirement to better understand the fate of the terrestrial OC (terrOC) that is exported to the Arctic shelf seas (AMAP, 2012; Vonk and Gustafsson, 2013).

Although it has been widely accepted that in the marine realm, terrOC is more resistant to degradation than marine OC (Canuel and Martens, 1996; Hedges and Oades, 1997; van Dongen et al., 2000), recent studies indicated that a substantial proportion of the fluvially transported terrOC behaves non-conservatively and is degraded close to the point of origin (Karlsson et al., 2011; Tesi et al., 2014; van Dongen et al., 2008b; Vonk et al., 2012; Zhu et al., 2013). van Dongen et al. (2008b), for instance, showed that approximately 65% of the terrestrial particulate OC (POC) transported by the Kalix River is degraded within 30 km of the river mouth. A comparable proportion of the terrestrial POC is lost annually during mixing in the Laptev and East Siberian Seas (ESS; Alling et al., 2010; Sánchez-García et al., 2011). In addition, Vonk et al. (2012) determined that approximately 66% of the 44 x 10^{12} g/year of OC released by coastal erosion in the East Siberian region is degraded and transported to the atmosphere. High CO_2 and CH_4 fluxes to the atmosphere above the

ESS (Anderson et al., 2009; Semiletov et al., 2007; Semiletov et al., 2013; Shakhova and Semiletov, 2007; Shakhova et al., 2010) as well as CO_2 saturated shelf waters (Semiletov et al., 2013; Semiletov et al., 2012) further support the idea of more extensive OC degradation in the region than previously thought. Recent analyses indicate that Arctic waters are experiencing widespread ocean acidification (AMAP, 2013). Due to high freshwater and terrOC input, CO_2 neutralization capacity of the Arctic Ocean is low making these waters more sensitive to ocean acidification (AMAP, 2013). Climate enhanced remobilization and associated decomposition of terrOC may therefore not only cause an increase in the release of greenhouse gases into the atmosphere (Guo et al., 2007; Guo et al., 2004; Gustafsson et al., 2011) resulting into a positive feedback to climate warming but could also cause a further acidification of the Arctic Ocean (Sabine et al., 2004; The Royal Society, 2005) which ultimately alters marine ecosystems.

In order to better understand the rate of loss of the terrOC transported to the Arctic shelf seas, it is essential to determine the relative importance of marine and terrOC in the Arctic marine environment. This has been mainly done at a bulk level using proxies such as C/N ratio and $\delta^{13}C$ of the sedimentary organic carbon (SOC; Drenzek et al., 2007; Fernandes and Sicre, 2000; Guo et al., 2004; Vonk et al., 2008). However, considering that these proxies cannot be used to distinguish between different terrestrial carbon sources, for instance the relative input of soil and plant derived OC; other biomarker based proxies are needed. Recently, the discovery of specific microbial soil biomarkers has resulted in the development of a number of proxies that can be used to trace the soil derived OC along riverine systems (Doğrul Selver et al., 2012; Sáenz et al., 2011a; Zhu et al., 2011a; Zhu et al., 2013). The first molecular based proxy is based on Glycerol Dialkyl Glycerol Tetraether (GDGT) membrane lipids and has been applied in a variety of settings (e.g. Doğrul Selver et al.,

2012; Huguet et al., 2012; Schouten et al., 2012b; Weijers et al., 2011; Weijers et al., 2009; Weijers et al., 2007). Branched GDGTs (br-GDGT; see Figure 3S.1 for structures), produced by anaerobic soil bacteria (Weijers et al., 2007), are mainly found in terrestrially dominated environments (Hopmans et al., 2004; Peterse et al., 2011; Sinninghe Damsté et al., 2009; Tierney and Russell, 2009; Weijers et al., 2006). In contrast, isoprenoidal GDGTs (iso-GDGTs), specifically crenarchaeol, are mainly synthesized by marine Thaumarchaeota (Schleper et al., 2010; Sinninghe Damsté et al., 2002). Iso-GDGTs are also present in terrestrial environments but in substantially lower abundance (Weijers et al., 2006; Weijers et al., 2004). The GDGT related branched and isoprenoid tetraether (BIT) index (Hopmans et al., 2004) is developed based on these assumptions and has successfully been applied to trace fluvially transported soil OC to marine sediments worldwide (Schouten et al., 2012a).

A second biomarker proxy is based on Bacteriohopanepolyols (BHPs), which are pentacyclic triterpenoids with polyfunctionalized side chains (see Figure 3S.1 for structures; Rohmer, 1993). BHPs are synthesized by various bacteria (Ourisson and Rohmer, 1982; Ourisson et al., 1987) and observed in recent as well as older sediments (Cooke et al., 2008b; Cooke et al., 2009; Handley et al., 2010; van Dongen et al., 2006). Some BHPs, such as adenosylhopane and related BHP compounds, have a terrestrial origin and are therefore considered to be 'soil marker' BHPs (Figure 3S.1; Talbot and Farrimond, 2007). On the other hand, bacteriohopanetetrol (BHT) although typically present in all environments (Cooke, 2010; Talbot and Farrimond, 2007; Talbot et al., 2003; van Winden et al., 2012), is usually the most abundant BHP in marine sediments (Blumenberg et al., 2010; Sáenz et al., 2011b) and therefore is used as a 'pseudo' marine representative end-member. Zhu et al. (2011a) used the relative abundance of soil marker BHPs versus BHT (R_{soil} proxy) to trace the soil input to surface sediments along the Yangtze River–East China Sea transects. Recent research indicated that the R'_{soil}

index (R_{soil} index minus the contribution from the methylated soil marker BHPs; see Figure 3S.1) can also be used to trace soil derived OC in the (sub)-Arctic region (Doğrul Selver et al., 2012).

Both BHPs and GDGTs have been observed in Arctic shelf sediments (Cooke et al., 2009; De Jonge et al., 2014; Doğrul Selver et al., 2012; Ho et al., 2014; Taylor and Harvey, 2011; van Dongen et al., 2008a) including the East Siberian Shelf (Cooke et al., 2009; van Dongen et al., 2008a) however the extent to which these lipids can be used to trace a terrestrial/soil contribution to the East Siberian Shelf remains unclear. The objectives of the present study were to determine to what extent GDGT and BHP based proxies can be used for tracing the terrestrial (soil) contributions on the East Siberian Shelf. To this end, surface sediments along a transect from the mouth of the Kolyma River to the middle of the ESS were analyzed. The outcomes of the BHP and GDGT analyses were compared with the results of other proxies used to trace terrestrial contributions ($\delta^{13}C_{SOC}$ and $\delta^{15}N$) to determine whether or not molecular based proxies can be used to trace the various OC sources in the Arctic environment.

3.2. Methods

3.2.1. Study area and sample collection

The Kolyma River in north-eastern Siberia, with a total catchment area of $647*10^3$ km^2 (Stein and MacDonald, 2004) is the largest Arctic river basin completely underlain by continuous permafrost (Holmes et al., 2011) with active layer depths ranging from 0.2m in the north to 1m in the south of the catchment (Uhlířová et al., 2007). Tundra vegetation is the dominant vegetation along the coast while taiga forests are more dominant in the rest of the basin (Huh et al., 1998). The Kolyma River has a mean

annual water discharge of 114 km^3/yr (Cooper et al., 2008) with a peak flow during late May-early June and estimated annual transport of 0.46 Tg dissolved organic carbon (DOC) and 0.31 Tg of particulate organic carbon (POC; Lobbes et al., 2000).

Eight surface sediment samples were collected along a transect tracing the Kolyma palaeoriver canyon in September 2008 during International Siberian Shelf Study expedition (ISSS-08; Figure 3.1; Semiletov and Gustafsson, 2009) with a dual gravity corer (GEMAX) or, in the case of stations YS-34B and YS-41, a van Veen grab sampler. The sampling station closest to the Kolyma river mouth, Station YS-34B (46 km of the rover mouth), was the only station situated in an area with a water depth <20 m (10m depth; Table 3.1). All other stations were situated further off the river mouth (100 to 513 km) with water depth between 31 and 49 m (Table 3.1). Sub-samples of the grab samples were obtained with stainless steel spatulas, transferred to pre-cleaned polyethylene containers and kept frozen until analysis. The sediment cores were sliced into 1cm sections and processed similarly. Total sedimentary organic carbon (SOC), $\delta^{13}C$ of the SOC ($\delta^{13}C_{soc}$) were determined previously (Vonk et al., 2010) and ranged from 8 to 13.6 %, -27.3 to -23.9 ‰ respectively (Table 3.1). $\delta^{15}N$ values were measured on triplicate samples using an isotope mass spectrometer (Euro Hydra 20/20, University of California, Davis Stable Isotope Facility, USA).

In addition to the marine sediments three Yedoma samples, taken from the Kolyma River catchment area (69.46 °N – 161.79 °E; Tesi et al., 2014), were analysed to determine the relative amounts of br-GDGTs in these type of sediments. These samples were collected from exposed river banks and represent the composition of terrestrial material that is transported to shelf.

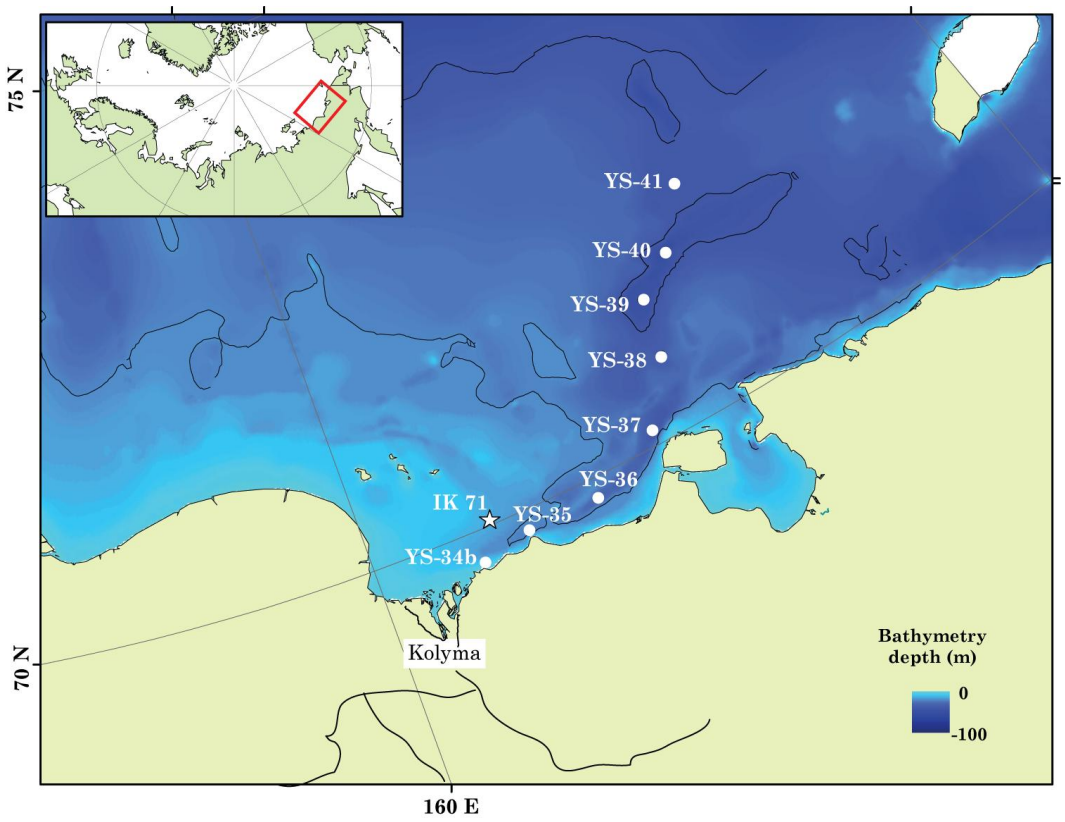

Figure 3. 1: Map of the Kolyma River-ESS transect showing sampling stations (YS-xx; exact locations are in Table 1). The star is a reference station IK-71 (van Dongen et al. 2008). Bathymetry data from Amante and Eakins (2009).

Table 3. 1: Sampling locations, BIT, δ^{13}Csoc and R'_{soil} values of surface sediment samples from Kolyma River-ESS transect.

	YS-34B	YS-35	YS-36	YS-37	YS-38	YS-39	YS-40	YS-41
Longitude (N)	69.71	69.82	69.82	70.14	70.70	71.22	71.48	71.97
Latitude (E)	162.69	164.06	166.00	168.01	169.13	169.37	170.55	171.79
Distance from river mouth (km)[a]	46	100	174	258	334	392	443	513
Bottom depth(m)	10	31	32	42	36	44	49	43
Salinity	29.9	30.6	30.8	31.1	31.6	32.4	32.9	33.2
TOC (%)[b,c]	11.2	12.2	8.0	9.4	10.0	12.3	13.6	13.2
$\delta^{13}C_{soc}$ (‰)[b,d]	-27.3	-26.8	-26.0	-25.7	-25.3	-24.3	-23.9	-23.9
$\delta^{15}N$ (‰)	4.24	5.90	6.69	7.91	8.17	8.80	9.34	9.34
BIT[e]	0.51	0.28	0.12	0.07	0.05	0.02	0.02	0.03
R'_{soil} [f]	0.57	0.46	0.38	0.30	0.17	0.13	0.08	0.07

[a] Distance from 69.65 °N-161.50 °E.
[b] Data taken from Vonk et al. (2010)
[c] Total Organic Carbon
[d] SOC = Sedimentary Organic Carbon
[e] BIT = Branched and isoprenoid tetraether index
[f] R'_{soil} = (G1 + G2 + G3)/(G1 + G2 + G3+BHT); compound abbreviations as in Table 2.

3.2.2. Extraction and fractionation

Freeze dried sediment samples were extracted using a modified Bligh-Dyer method as described by (Tierney et al., 2012). Briefly, 5 g (dry wt.) of sediment were ultrasonically extracted (at 40 ^{o}C for 10 minutes followed by centrifugation at 2500 rpm for 5 minutes) with a mixture of methanol: dichloromethane: aqueous phase (MeOH:DCM: aqueous phase, 2:1:0.8,v/v/v) with aqueous phase consisting of 0.05 M phosphate buffer at pH~7.4. This process was repeated two additional times using the same solvent mixture and the supernatants were combined. The DCM fractions were recovered by addition of phosphate buffer and DCM to the supernatants. The combined DCM fractions were rotary evaporated to near dryness, transferred to vials using a solution of DCM:MeOH (2:1 v/v) and evaporated to dryness under a stream of N_2 to obtain the total lipid extracts which were split into three aliquots (Tierney et al., 2012).

The first set of aliquots were used for GDGT analysis and separated into core lipid (CL) and intact polar lipid (IPL) fractions using silica column chromatography with 4 ml hexane:ethyl acetate (1:1, v/v) and 8 ml MeOH as eluents, respectively. After separation, 0.2 μg of C_{46} GDGT standard was added into the CL fractions and dried under N_2 flow. CL fractions were redissolved in hexane: isopropanol (99:1) and filtered through 0.45 μm PTFE filter. Analysis of GDGTs were carried on the CL fractions using the method reported by Hopmans et al. (2004) via high performance liquid chromatography-atmospheric pressure chemical ionization-mass spectrometry (HPLC–APCI–MS).

The second set of aliquots was used for BHP analysis following the same method described by (Cooke et al., 2009). Briefly, after addition of the internal standard (5α-pregnane-3β,20β-diol), each aliquot was acetylated, blown down to dryness using N_2 and redissolved in MeOH:propanol (60:40) for analysis on LC–APCI-MS^n.

3.2.3. Instrumental analysis

Identifications of the GDGTs were performed using an Agilent 1200 HPLC coupled to an Agilent 6130 quadrupole MS instrument equipped with a multimode source operated in APCI positive ion mode using a similar instrumental setup as described by McClymont et al. (2012). The GDGTs were analysed using normal phase LC–MS with a Grace Prevail Cyano HPLC column (3 μm, >150 mm x 2.1 mm i.d.) and a guard column of the same material. Separation was achieved at 30ºC with a flow rate of 0.2 ml min^{-1} and the following gradient profile: 1% isopropanol (IPA) in hexane (0–5 min), 1.8% IPA in hexane (at 25 min) and 10% IPA in hexane (at 30 min, held for 10 min). Conditions for APCI were: nebulizer pressure 20 psig, vaporiser temperature 250ºC, drying gas (N_2) flow 6 l/min and temperature 200ºC, capillary voltage 2 kV and corona 5 μA. In order to increase sensitivity/ reproducibility, ion scanning was performed in single ion monitoring (SIM) mode using GDGT $[M+H]^+$ ions.

Quantification of individual GDGTs were made by using a combination of the peak areas of the compounds, the C_{46} GDGT standard and correction factors for GDGTs. Correction factors were determined based on the peak areas of a synthetic mixture with known concentrations of GDGTs. These correction factors were applied to minimize the differences in mass spectrometric response between compounds allowing the determination of the individual GDGT concentrations present (Schouten et al., 2013). BIT index values were calculated according to the corrected peak areas of the branched GDGTs (br-GDGT) and crenarchaeol (equation [1]).

$$\mathrm{BIT}=\frac{\sum[\text{br-GDGTs}]}{\sum[\text{br-GDGTs}]+[\text{crenarchaeol}]} \qquad [1]$$

The triplicate analyses yielded standard errors of ±1 to 12 μg/g TOC for crenarchaeol and ± < 0.1 to 0.8 μg/g TOC for br-GDGTs resulting in a standard error of ± 0 to 0.04 for BIT index.

Identification and quantification of BHPs was accomplished using a Surveyor HPLC system (ThermoFinnigan, Hemel Hempstead, UK) equipped with a Gemini C_{18} column (5 μm, 150 mm x 3.0 mm I.D.) and a security guard column of the same material, both from Phenomenex (Macclesfield, UK). Separation was achieved at a flow rate of 0.5 ml min^{-1} at 30 ºC with the following gradient: 90% A and 10% B (0 min); 59% A, 1% B and 40% C (at 25 min), then isocratic to 70 min (where A = MeOH, B = water and C = propan-2-ol; all HPLC grade, purchased from Fisher Scientific [Loughborough, UK]) returning to the starting conditions in 5 min and stabilising for 15 min.

LC–MS^n analysis was conducted using a ThermoFinnigan LCQ ion trap mass spectrometer equipped with an APCI source interface operated in positive ion mode. Instrument settings were as follows: capillary temperature 155°C, APCI vaporiser temperature 400°C, corona discharge current 8 μA, sheath gas flow 40 and auxiliary gas 10 (arbitrary units).

A semi-quantitative estimate of was calculated from the characteristic base peak ion peak areas of individual BHPs in mass chromatograms relative to the base peak area response of the acetylated 5α-pregnane-3β,20β-diol internal standard. The reproducibility of a triplicate injection was 3-6% (standard error: ± 1 – 4 μg/g TOC) for BHT and 5-8 % (standard error: ±1 – 2 μg/g TOC) for adenosylhopane in the samples, resulting in an absolute standard error of on average ± 0.01 for R'_{soil}. Averaged relative response factors from a suite of five acetylated authentic BHP external standards are used to adjust the peak areas relative to that of the internal standard, where BHPs containing one or more N atoms give an averaged response ca. 12 times that of the

standard and those with no N atoms give a response approximately 8 times that of the standard (Cooke, 2010; van Winden et al., 2012).

The BHP based R'_{soil} indices were calculated according to the relative concentrations of the soil BHPs adenosylhopane (G1; structure 1e), adenosylhopane type 2 (G2; 1g), and adenosylhopane type 3 (G3; 1g'; Doğrul Selver et al., 2012), respectively and bacteriohopanetetrol (BHT; 1a; equations [2]).

$$R'_{soil} = \frac{[G1 + G2 + G3]}{[G1 + G2 + G3] + [BHT]} \qquad [2]$$

3.3. Results

3.3.1. GDGTs compositions

In all sediment samples, substantial amounts of br- and iso-GDGTs were detected (Table 3.2). Along the transect, summed GDGT concentration showed a general increase from 62 µg/g TOC in the sediments collected at the station YS-34B to 1413 µg/g TOC in those from YS-40 (Table 3.2 and figure 3.2a). With the exception of YS-35, all GDGT distribution patterns in the sediments were dominated by GDGT-0 with concentrations between 25 µg/g TOC in the sediment from YS-34B and 774 µg/g TOC for YS-40,making up between 38% and 57% of the summed GDGT concentrations (Table 3.2 and figure 3.2a). Beside GDGT-0, substantial amounts of crenarchaeol were also present in all sediment samples with summed concentrations varying between 18 and 597 µg/g TOC equivalent to 29% – 42% of the summed GDGT concentrations (Table 3.2). Crenarchaeol was the most abundant GDGT present in the sediment collected at station YS-35. Other iso-GDGTs were also present but in lower amounts (up 26 µg/g TOC). Besides these iso-GDGTs, br-GDGTs were also present, predominantly br-GDGT

II and III, with summed concentrations ranging from 6 (YS-39) to 41 μg/g TOC (YS-35 and 36) equivalent to 1% – 31% of the summed GDGTs present (Table 3.2). Minor amounts of br-GDGTs with cyclic units were also detected in all sediments with the exception of YS-34B. BIT index values declined from 0.51 at station YS-34B to 0.03 at station YS-41 showing a decreasing trend in an offshore direction (Table 3.1 and Figure 3.3a). The summed br-GDGTs concentrations in the Yedoma samples varied between 119 and 136 ng/g sediment (not shown).

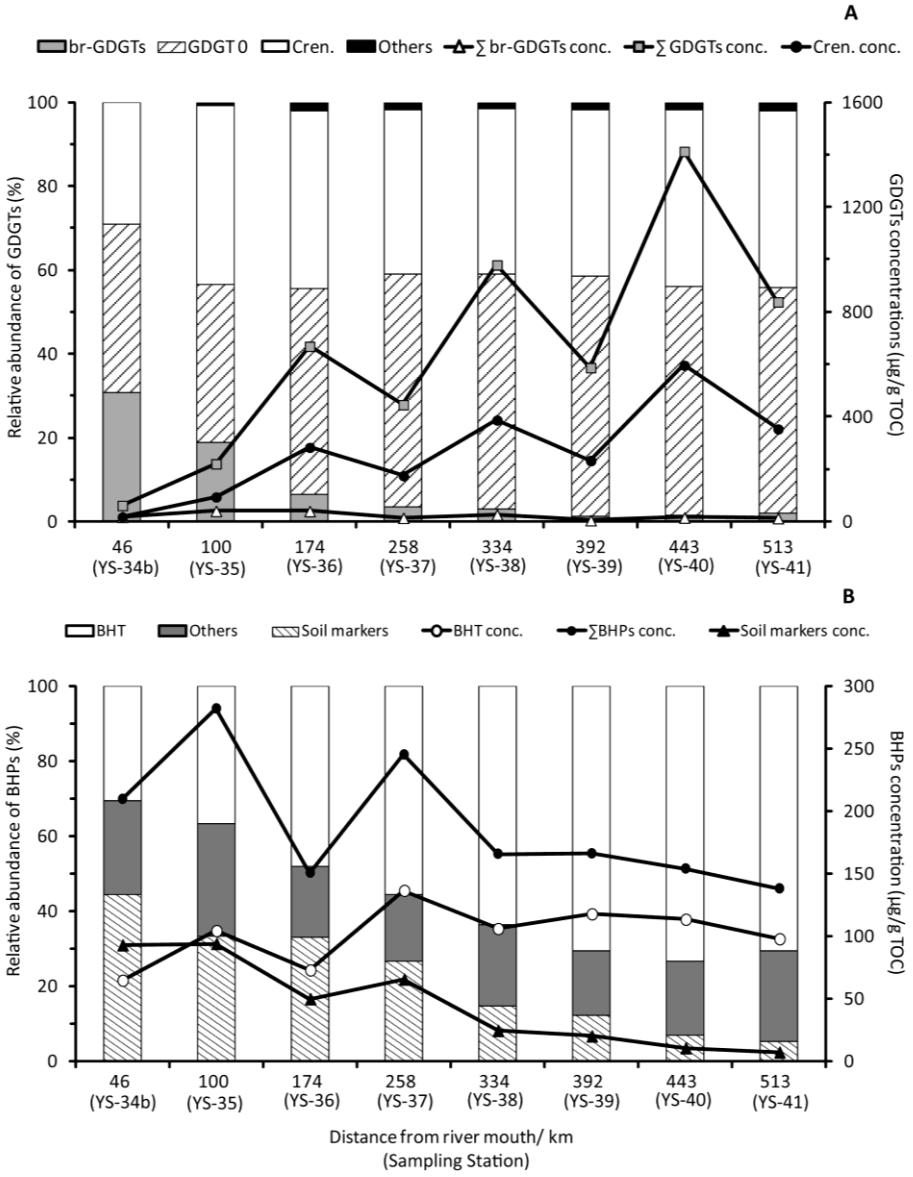

Figure 3. 2: Histograms of relative abundance and concentrations (μg/g TOC) of (A) GDGTs and (B) BHPs in the Kolyma River-ESS transect surface sediments.

3.3.2. BHPs compositions

LC–MS analyses showed that up to 16 different BHP structures, 6 of which are ascribed as soil marker BHPs, were present in the Kolyma River-ESS transect sediments (Table 3.2). The maximum amount of 16 different BHP structures were detected in the YS-34B, 36 and 37 sediments while only 11 BHP structures could be detected at YS-41. Total BHP concentration showed a general decrease along the Kolyma River-ESS transect from 209 μg/g TOC in the sediment collected at YS-34B to 138 μg/g TOC in the sediment obtained at YS-41 (Table 3.2 and Figure 3.2B). BHT was the most abundant BHP structure present in all sediments analysed, with concentrations ranging between 64 and 136 μg/g TOC constituting 31% to 74% of the summed BHP concentrations. Other abundant BHPs present were adenosylhopane (4.1 to 56 μg/g TOC), adenosylhopane type II (2.3 to 28 μg/g TOC) and aminotriol (5.6 to 29 μg/g TOC; Table 3.2). Although individual concentrations varied, these 3 BHPs constituted between 10% – 43% of the summed BHP concentrations (Table 3.2). Besides BHT and these other 3 dominant compounds, moderate to minor amounts of other BHPs were also detected in the sediments varying between 18% and 35% (Table 3.2). Summed soil marker BHPs (adenosylhopane and adenosylhopane type structures) concentrations decreased relatively from 93 μg/g TOC at YS-34B to 6.9 μg/g TOC at YS-41, equivalent to 44% – 5% of the summed BHPs concentration present (Table 3.2 and Figure 3.2b).

Throughout the transect, R'_{soil} values declined from 0.51 at station YS-34B to 0.13 at station YS-41 showing a decreasing trend in an offshore direction (Table 3.1 and Figure 3.3a).

Table 3. 2: Total abundances of GDGTs and BHPs (µg/g TOC) and contribution to total GDGTs and BHPs (%; in brackets) in surface sediments from the Kolyma River-ESS transect

	Abbreviation	Structure[a]	m/z	YS-34	YS-35	YS-36	YS-37	YS-38	YS-39	YS-40	YS-41
Glycerol Dialkyl Glycerol Tetraethers											
Crenarchaeol			1292	18(29)	95(43)	267(41)	176(39)	388(40)	234(40)	597(42)	354(42)
GDGT 0			1302	25(40)	83(38)	330(51)	248(55)	549(56)	337(57)	774(55)	454(54)
GDGT I			1300	BDL	1.8(1)	9.4(1)	5.8(1)	11(1)	8.4(1)	18(1)	11(1)
GDGT II			1298	BDL	BDL	3.3(0.5)	1.5(0.3)	2.2(0.2)	1.7(0.3)	4.4(0.3)	3.5(0.4)
GDGT III			1296	BDL	BDL	2.0(0.3)	1.1(0.2)	2.4(0.2)	1.4(0.2)	3.5(0.2)	2.1(0.3)
br-GDGT I			1022	4.1(7)	9(4)	10(1)	3.2(0.7)	5.2(0.5)	0.7(0.1)	0.8(0.1)	1.9(0.2)
br-GDGT II			1036	8.8(14)	17(7)	15(2)	4.2(0.9)	8.0(0.8)	1.1(0.2)	3.3(0.2)	3.0(0.4)
br-GDGT III			1050	6.1(10)	11(5)	12(2)	4.9(1)	8.1(0.8)	2.3(0.4)	6.1(0.4)	4.3(0.5)
∑Cyclic br-GDGTs[b]				BDL	4.2(2)	3.7(0.6)	2.5(0.5)	5.7(0.6)	1.9(0.3)	5.7(0.4)	4.6(0.6)
∑GDGT				62	221	653	447	980	588	1413	839
Bacteriohopanepolyols											
Bacteriohopanetetrol	Δ^6BHT	3a	653	3.2(2)	4.8(2)	2.4(2)	5.4(2)	4.3(3)	4.0(2)	3.2(2)	2.7(2)
Bacteriohopanetetrol	BHT	1a	655	64(31)	104(37)	73(49)	136(56)	106(64)	117(71)	113(74)	97(71)
Bacteriohopanetetrol isomer	BHT isomer	1a'	655-II	10(5)	11(4)	9(6)	12(5)	9(6)	10(6)	13(9)	11(8)
Methyl bacteriohopanetetrol	2-Methyl BHT	2a	669	4.3(2)	7.2(3)	3.8(3)	6.1(2)	4.1(2)	4.2(3)	4.8(3)	2.4(2)
Bacteriohopanehexol	BHHexol	1i	771	1.9(0.9)	2.4(0.9)	1.1(0.7)	2.2(0.9)	1.0(0.6)	BDL	BDL	BDL
Aminobacteriohopanetriol	Aminotriol	1b	714	11(5)	29(10)	6.3(4)	10(4)	10(6)	6.3(4)	5.6(4)	11(8)
Aminobacteriohopanetetrol	Aminotetrol	1c	772	1.9(0.9)	5.3(2)	0.7(0.4)	0.8(0.3)	0.9(0.5)	0.3(0.2)	BDL	0.9(0.7)
Aminobacteriohopanepentol	Aminopentol	1d	830	2.9(1)	5.7(2)	0.7(0.5)	0.4(0.2)	0.8(0.5)	BDL	BDL	BDL
Adenosylhopane	G1	1e	746+788+830[c]	56(27)	53(19)	23(15)	33(14)	13(8)	10(6)	6.1(4)	4.1(3)
2Me-adenosylhopane	2Me-G1	2e	760+802+844[c]	1.4(0.7)	BDL	1.3(0.8)	1.5(0.6)	0.83(0.5)	BDL	BDL	BDL
Adenosylhopane Type 2	G2	1g	761	23(11)	28(10)	18(12)	20(8)	8.4(5)	5.5(3)	3.4(2)	2.3(2)
2Me-adenosylhopane Type 2	2Me-G2	2g	775	4.0(2)	4.5(2)	3.4(2)	4.0(2)	1.5(0.9)	1.0(0.6)	BDL	BDL
Adenosylhopane Type 3	G3	1g'	802	5.8(3)	5.8(2)	3.2(2)	4.2(2)	0.9(0.5)	2.0(1)	0.8(0.5)	0.5(0.4)
2Me-adenosylhopane Type 3	2Me-G3	2g'	816	2.3(1)	2.4(0.8)	1.3(0.9)	1.9(0.8)	BDL	1.2(0.7)	BDL	BDL
Bacteriohopanetetrol cyclitol ether	BHT cyclitol ether	1f	1002+1044[d]	15(7)	17(6)	2.4(2)	3.9(2)	3.0(2)	2.4(1)	2.1(1)	4.9(4)
Bacteriohopanetetrol glucosamine	BHT glucosamine	1h	1002	1.3(0.6)	1.5(0.5)	0.7(0.5)	1.0(0.4)	1.1(0.7)	0.9(0.5)	1.1(0.7)	0.8(0.6)
∑BHPs				209	281	150	244	164	166	154	138

[a] See Figure 3S.1; [b] summed concentrations of br-GDGT Ib,Ic and IIb, IIc ; BDL =below detection limit; [c] Diacetate, triacetate and tetraacetate, respectively; [d] Heptaacetate and octaacetate

3.4. Discussion

3.4.1. Origin of the near shore organic carbon

GDGT distributions in all sediments along the Kolyma River-ESS transect were dominated by GDGT 0 and crenarchaeol (≥ 69 % of summed GDGT concentrations). Although the lowest relative abundance of these iso-GDGTs was found closest to the river mouth, at the station YS-34B (69% of the summed GDGT concentrations), it suggests a substantial marine OC input within 46 km of the river mouth. The presence of substantial amounts of iso-GDGTs in sediments and suspended particulate matter taken close to river mouths, indicating a substantial influx of marine derived OC, are not uncommon and have been observed previously (Doğrul Selver et al., 2012; Herfort et al., 2006; Kim et al., 2007; Strong et al., 2012). Recent analyses of surface sediments collected in the estuaries of the Kalix River (Sweden; Doğrul Selver et al., 2012) and Yangtze River (China; Zhu et al., 2011b), for instance, also indicated the presence of significant amount of crenarchaeol close to the river mouths.

The presence of substantial amounts of br-GDGTs (both with and without cyclic units) in the stations close to river mouth (YS-34B and 35) suggests a terrestrial influx. Br-GDGTs are produced in abundance in soils and peats (Weijers et al., 2006) and accepted to be predominantly transported to marine environment by rivers and erosion (Hopmans et al., 2004). Indeed Peterse et al. (2014) recently showed that the br-GDGTs present in Kolyma River suspended particulate matter and lake surface sediments in the Kolyma River catchment were mainly derived from (surface) soils, either indirectly delivered by the river, or directly through thawing. However, this study also showed that additional br-GDGT production may take place in lakes/rivers. These results are in line with other studies from (non-) Arctic regions (Herfort et al., 2006; Kim et al.,

2007; De Jonge et al., 2014) suggesting a mixed origin of the br-GDGTs observed along the transect.

Analyses of the Yedoma samples from the Kolyma River catchment area indicated low br-GDGTs concentrations, 2 to 4 times lower than those observed in the surface sediments taken close to river mouth. In addition, lake sediments from the same region showed high br-GDGT concentrations comparable to those observed in the estuary sediments (Peterse et al., 2014) indicating that the contribution of yedoma/coastal erosion is minimal. Combined these observation suggest that the majority of the br-GDGTs present in the Kolyma estuary sediments originated from in-situ production in the Kolyma river.

The presence of substantial amount of br-GDGTs and iso-GDGTs is reflected in the BIT index and resulted in a value of 0.51 in the sediment at YS-34B suggests that only about 50% of the OM present in the sediment is of terrestrial origin. In line with previous studies (Doğrul Selver et al., 2012; Smith et al., 2010), this is most likely due to a combination of both removal of the terrestrial derived OC by the time it reaches 46 km out of river mouth and a substantial influx of marine-derived OC. In contrast, previous GDGT analysis of a sediment taken close to YS-34B (station IK-71; Figure 3.1) showed much higher relative br-GDGTs abundances relative to crenarchaeol (van Dongen et al., 2008). This resulted in a much higher BIT index value (0.91) suggesting a higher dominance of terrestrial derived OC. However, in this previous study no internal standard was used and correction factors were not applied. Schouten et al. (2013) recently showed that this could cause a bias in calculations of concentrations and BIT index values.

The substantial influx of marine-derived OC as suggested by the GDGT analyses is not supported by other analyses on the same sediment sample (Vonk et al., 2010; Vonk et al., 2012; Tesi et al., 2014). The depleted $\delta^{13}C_{SOC}$ value of sediment from

YS-34B (-27.3‰; Vonk et al., 2010), the high concentration of HMW *n*-alkanes (1170 µg/g TOC; Vonk et al., 2010) and the substantial amounts of lignin markers (28 mg/g TOC; Tesi et al., 2014) combined suggest a dominance of terrOC. Indeed a dual carbon isotopic mixing model, based on both bulk ^{13}C and ^{14}C analyses, suggested considerably greater terrOC contribution (approximately 85%; Vonk et al., 2012) if compared to the GDGT based estimation. In addition, the BHP analyses also suggest a much lower influx of marine-derived OC. Soils usually have high BHP diversity (Cooke et al., 2008a; Xu et al., 2009; Zhu et al., 2011a), particularly if compared to sediments or suspended matter from marine dominated areas. Saenz et al. (2011), for instance, analysed suspended particulate matter from a river-ocean transect off the Pacific coast of Panama and found 8 BHPs in estuarine and only 1 BHP in open ocean samples. In line with other sediments from river catchments (Doğrul Selver et al., 2012; Zhu et al., 2011a) the BHP analyses of the sediment at station YS-34B show a large diversity (Table 3.2; Figure 3.2B). 16 different BHPs were present, 6 of which are soil marker BHPs, suggesting a predominant terrestrial influx. In addition, the BHP composition at station YS-34B is in line with the analyses at IK-71 (Cooke et al., 2009), which showed 13 different BHPs.

In addition to the relative composition, the relatively high abundance of soil marker BHPs (44% of the total BHPs) at station YS-34B supports the inference of a high terrestrial influx, when compared to the relative contribution of soil marker BHPs generally observed in soils worldwide (average 28%; Cooke, 2010; Cooke et al., 2009). Analyses of soil profiles in the Arctic region for instance, indicated that up to 50% of the total BHPs were soil marker BHPs in soil profiles taken in Svalbard (Rethemeyer et al., 2010) and up to 52% in Canadian soils (Xu et al., 2009). The dominance of soil (terrestrial) derived BHPs is well reflected in the R'_{soil} index resulting in a value of 0.57 in the YS-34B sediment, and is slightly higher that the R'_{soil} index (0.44) calculated

based on the BHP concentration observed at IK-71 (Cooke et al., 2009). Considering that R_{soil} indexes have been reported to range between 0.5 – 0.8 in terrestrial environments (Zhu et al., 2011a), the R'_{soil} index suggest that >71% of the OC present in the sediment at station YS-34B is of terrestrial origin. These are comparable to the outcome of the a dual carbon isotopic mixing model (Vonk et al., 2012) and lignin analyses (Tesi et al., 2014) on the same sediment supporting the hypothesis that most of the terrOC is not degraded/removed during the first 46 km of its transport of the river mouth.

To summarise, $\delta^{13}C_{SOC}$ (Vonk et al., 2010) BHP composition and R'_{soil} index (present study), lignin and other terrestrial lipid analyses (Vonk et al., 2010; Tesi et al., 2014) and the outcome of the dual carbon isotopic mixing model using ^{13}C and ^{14}C (Vonk et al., 2012) all indicate that the organic material transported to the sediment at station YS-34B, the start of the transect studied, is heavily dominated by terrOC. However, GDGT analyses contradicts this suggesting a much lower terrOC derived dominance most likely due to a combination of both a higher removal of the br-GDGTs if compared to the other terrOC and a substantial influx of iso-GDGTs (e.g. crenarchaeol).

3.4.2. Organic carbon input and removal along the transect

Besides the dominance of terrOC at station YS-34B, previous studies indicated, based on lipid and isotope analyses of suspended particulate matter and surface sediments, an increasing marine derived OC contribution along the Kolyma River-ESS transect off-shore (Vonk et al., 2010; Vonk et al., 2012). For instance, the declining HMW / LMW *n*-alkanes ratio (from 51.2 to 19), enrichment in $\delta^{13}C_{SOC}$ (from -27.3‰ to -23.9‰) and $\delta^{15}N$ values (from 4.2‰ to 9.3‰; Vonk et al., 2010) indicate an increasing addition

of marine-derived OC in an off-shore direction. In addition, using a 3-end member mixing model that included bulk radiocarbon age and $\delta^{13}C_{SOC}$ data, Vonk et al. (2010) observed an increasing marine, a decreasing riverine and a constant coastal erosion OC contribution with an increasing distance from the river mouth.

Along the transect, the BHPs diversity decreased from 16 compounds (at YS-34B) to 11 (at YS-41) mainly due to loss of methylated soil markers, BHHexol and Aminopentol (Table 3.2). Earlier studies showed similar declining tendency in BHP diversity across other land-sea transects such as along the Kalix River-Bothnian Bay transect (Doğrul Selver et al., 2012) and the Yangtze River-East China Sea transect (Zhu et al., 2011b) as well as a river–ocean transect off the Pacific coast of Panama (Sáenz et al., 2011a). The particular loss of methylated soil markers is typical and has been observed previously, such as along the Kalix River-Bothnian Bay transect (Doğrul Selver et al., 2012).

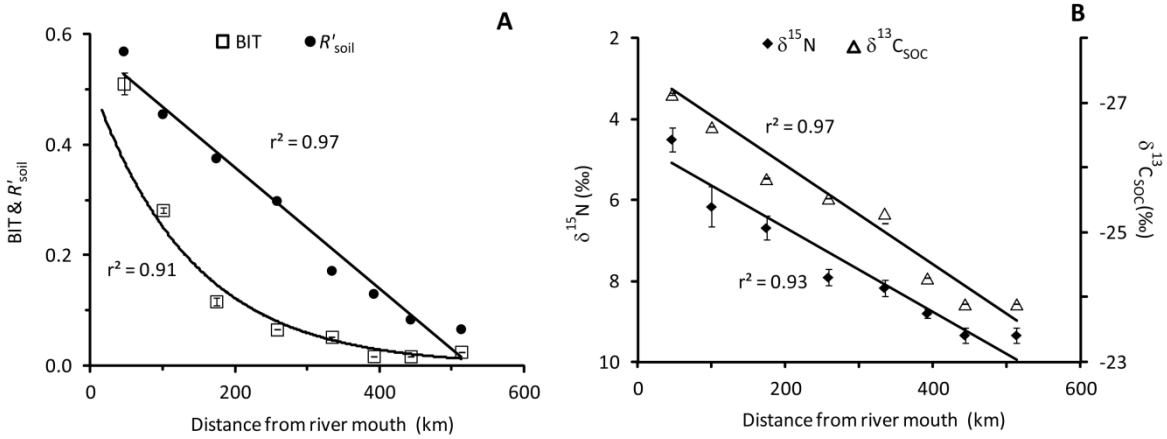

Figure 3. 3: Plots of (A) BIT and R'_{soil} and (B) $\delta^{13}C_{soc}$ and $\delta^{15}N$ vs. distance from Kolyma River mouth.

As well as the reduction in BHP diversity, the increasing contributions of crenarchaeol (from 18 to 354 µg/g TOC) and decreasing br-GDGTs (from 19 to 14 µg/g TOC) and soil marker BHPs contributions (from 93 to 6.9 µg/g TOC) were also be

observed along the same transect (Figure 3.2 and Table 3.2). These changes are reflected in the BIT and R'_{soil} indices and reveal declining trends (from 0.51 to 0.02 and from 0.57 to 0.07, respectively) along the transect. In line with previous studies for other river-ocean transects (Doğrul Selver et al., 2012; Smith et al., 2010; Zhu et al., 2011a) this further suggests a shift to a more marine-dominated environment in an off-shore direction.

Although all proxies indicate a general shift towards a more marine dominated environment, a remarkable difference can be observed in the behaviour of BIT index compared to the other indices. The bulk proxies (i.e. $\delta^{13}C_{SOC}$ and $\delta^{15}N$) and the R'_{soil} all revealed a clear linear decreasing trend with distance from the river mouth with r^2 values between 0.91 and 0.97 (p <0.05, n = 8; Figure 3.3). In contrast, the BIT index showed an exponentially decreasing trend (r^2 = 0.91, p <0.05, n = 8; Figure 3.3). In addition, when plotted against each other very high linear correlations were observed between R'_{soil}, $\delta^{13}C_{SOC}$ and $\delta^{15}N$ indices (r^2 between 0.93 and 0.97, p<0.05, n = 8; Figure 3.4B, C and F). Similarly, BIT also strongly correlates with R'_{soil}, $\delta^{13}C_{SOC}$ and $\delta^{15}N$ (r^2 between 0.95 and 0.97, p<0.05, n=8; Figure 3.4A, D and E) but only if an exponential correlation is applied. Previous studies showed that BIT index was linearly correlated with $\delta^{13}C_{SOC}$ as well as with R'_{soil} (Doğrul Selver et al., 2012; Smith et al., 2012; Zhu et al., 2011a). Smith et al. (2010) attributed this linear correlation between the BIT index and $\delta^{13}C_{SOC}$ to the geographical conditions (i.e. forested catchment area, steep fjord slopes and high annual rainfall) which resulted in enhanced input of soil derived OC. The difference in behaviour between the BIT index and the bulk indices could be caused by an influx of a substantial amount of resistant plant derived OC, such as lignin. Previous studies have showed that the BIT index only shows a weak correlation with lignin phenol proxies (Smith et al., 2010; Walsh et al., 2008). Consequently, in systems with a dominant soil OC input, such as Fiordland, New Zealand, the BIT index strongly

correlated with $\delta^{13}C_{SOC}$ (Smith et al., 2010), while in systems with a low soil input but high input of plant derived OC, such as the Vancouver Island Fjords, no significant correlation between the BIT index and the $\delta^{13}C_{SOC}$ could be observed (Walsh et al., 2008). However, such an influx would not only have an effect on the correlation between the BIT index and the $\delta^{13}C_{SOC}$ along the transect, but also should have a comparable effect on the correlation between the R'_{soil} index and the $\delta^{13}C_{SOC}$. The absence of such an effect indicates that a substantial influx of resistant plant derived OC is not likely the major cause of the difference in trends observed.

Another possible cause is the difference in the removal of br-GDGTs, soil marker BHPs and other terrestrial derived OC throughout the transect. This can be attributed to difference of susceptibility to degradation of the different compound classes. However, Tesi et al. (2014) recently showed that sediment sorting could also play an important factor. Lignin phenols, for instance, are removed faster if compared to wax lipids in the Arctic environment. Lignin tends to be adsorbed on larger particles, becoming part of the heavier fraction in the water column and subsequently transported to surface sediments much closer to the river mouths if compared to wax lipids that are mainly adsorbed on finer (lighter) particles. It remains unclear if sediment sorting also plays an important role in the case of GDGTs or BHPs. However, more importantly soil marker BHPs appear to be removed faster in comparison to br-GDGTs (6 fold versus 2 fold decrease in concentrations in an off-shore direction, respectively; Table 3S.1) which is in line with a study in Yangtze River-East China Sea transect (Zhu et al., 2013). Therefore this moderate decline in br-GDGTs, and thus degradation and/or sediment sorting, cannot completely explain the exponential behaviour of the BIT index.

Another possible explanation for the observed correlations is based on the most striking difference observed in the addition of the marine components crenarchaeol and

BHT. Although fluctuations are observed between the different stations, possibly due to influx from Long Strait, a general substantially high crenarchaeol input was observed relative to a considerably lower pseudo marine end member BHT input (24 times versus 2 times increase towards offshore, respectively). Combining these with the relative removal rates of the terrestrial component as discussed above suggest that the relatively higher soil marker BHPs removal was not compensated by addition of BHT. In contrast, lower br-GDGT removal was overwhelmed by high crenarchaeol addition, possibly causing the exponential decrease in the BIT index observed. Assuming that the influx of crenarchaeol is extremely high in this area, particularly in comparison with the transport of other marine derived OC to the sediments, this would also explain the trends observed between the BIT and the bulk indices.

Given the predominance of coastal erosion in this part of the Eastern Siberia Sea (Semiletov et al., 2012; Vonk et al., 2012), which may account for the majority of the bulk $\delta^{13}C_{SOC}$ signal, it is not unlikely that the trends observed are partly caused by contributions of the different terrestrial end-members, e.g. fluvial versus coastal erosion. In contrast to the br-GDGTs, which are likely predominantly produced in the river itself (De Jonge et al., 2014) the strong correlation between $R'_{soil,}$ $\delta^{13}C_{SOC}$ and $\delta^{15}N$, suggests that the major source of BHPs to the marine system may be coastal erosion rather than fluvial transport. However, to fully understand and quantify the origin/contribution of the specific compound classes on the Arctic Shelf, reliable end-member values from terrestrial, including river, Yedoma and coastal erosion, and distal marine settings are required.

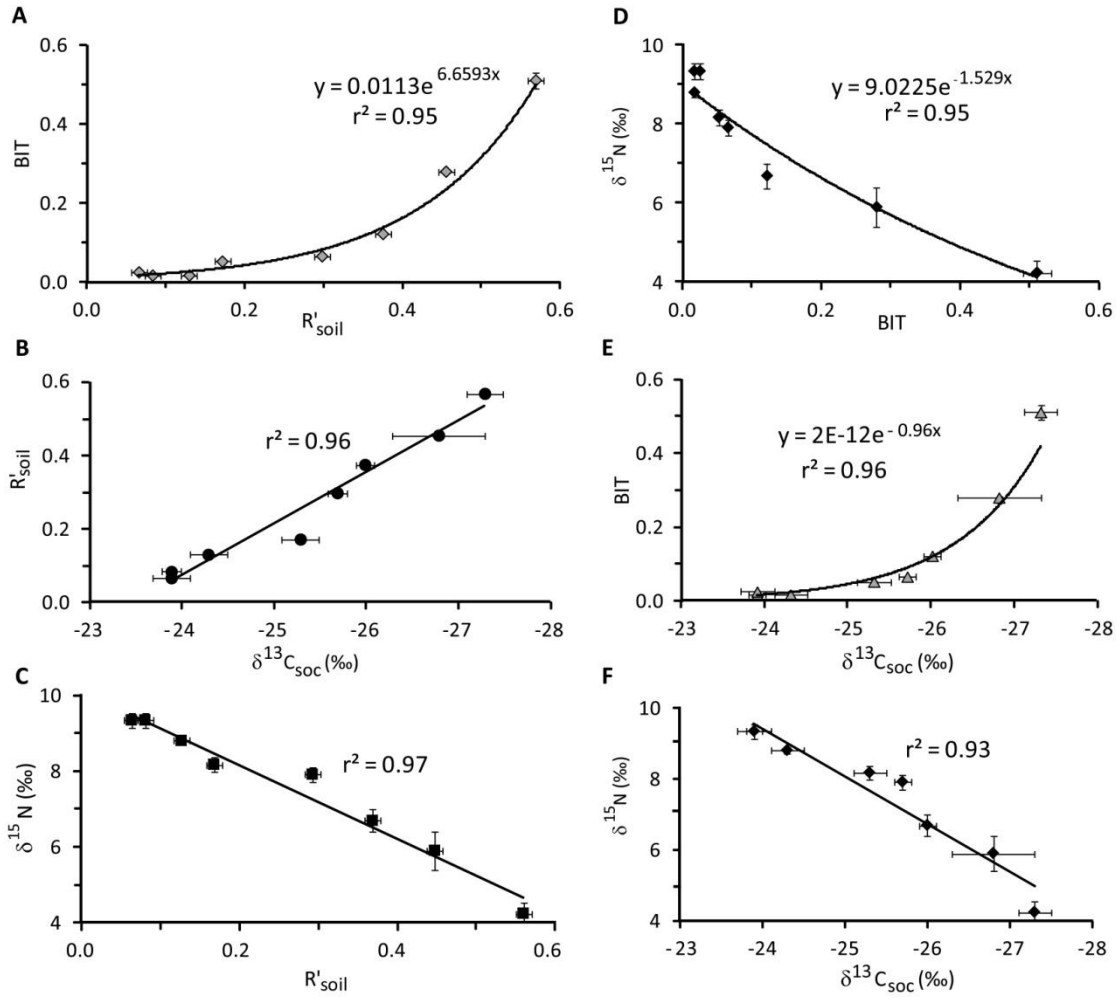

Figure 3. 4: Plots of R'_{soil} index vs. (A) BIT, (B) $\delta^{13}C_{soc}$ and (C) $\delta^{15}N$, (D) $\delta^{15}N$ vs. BIT, (E) BIT vs. $\delta^{13}C_{soc}$ and (F) $\delta^{15}N$ vs. $\delta^{13}C_{soc}$ in surface sediments of the Kolyma River-ESS transect.

3.4.3. Implications for carbon cycling

From the above, it is clear that all indices support previous studies (Tesi et al., 2014; Vonk et al., 2010; Vonk et al., 2012) showing a reduction of the influx of terrestrial derived OC in surface sediments along the Kolyma River-ESS transect. Likewise, soil marker BHPs and br-GDGTs show similar declining trends but the magnitude of reduction is different. Consequently, the BIT index decreases faster than the R'_{soil} index offshore, in contrast to measurements elsewhere (Zhu 2013). This apparent paradox

can be resolved by understanding the factors that control both indices. Since the relatively high loss in soil marker BHPs was not compensated by the increase in BHT (Table 3S.1), R'_{soil} is mainly controlled by the removal of soil marker BHPs. On the other hand, due to significantly high input of crenarchaeol compared to minor decrease in br-GDGTs, the BIT index appeared to be primarily controlled by the addition of crenarchaeol. Thus, these two proxies provide complementary insights into the offshore processes.

These field results suggest that both biomarker approaches could be used to trace soil derived OC in the Arctic environment. However, in line with previous studies using only a single proxy may give an incomplete characterization of the system and could lead to an under or over estimation of the relative importance of the different contributions. Using a multi-proxy approach is valuable to deduce the relative inputs of marine and terrestrial OC and combined with the outcomes of previous analyses of the same sediments (Tesi et al., 2014; Vonk et al., 2010) has generated a much stronger understanding of the processes acting along the Kolyma River-ESS transect. Therefore, this study highlights the importance of combining different proxies to better understand the fate of terrOC in the marine environment.

If such a multi-proxy approach is applied to other parts of the Arctic region, such as the whole East Siberian Arctic shelf, this could give us a better understanding of the fate of the terrOC exported to the Arctic shelf seas. This would include effects on ocean acidification and the exchange with other more active carbon pools, including the atmosphere.

3.5. Conclusions

This study showed that of all the sediments along the Kolyma River- East Siberian Sea transect, the highest total BHPs concentration as well as the highest BHP diversity was observed at the station closest to river mouth indicating high terrestrial input at the start of the transect. Along with a drop in the diversity and the total BHPs concentration, soil marker BHPs concentrations declined towards offshore suggesting an ongoing loss of soil marker BHPs and a shift to more marine dominated system.

Conversely, the lowest total GDGTs concentration was observed at the start of the transect with iso-GDGTs comprising almost 50% of the total GDGTs. This suggest that, unlike the BHPs results, there is an almost equal contribution of marine and terrOC at the start of the transect, relatively close to the river mouth. Total GDGTs concentration showed an increase in an offshore direction mainly due to the input of iso-GDGTs whereas br-GDGT contributions dropped along the transect. Taken together, these trends in GDGTs suggested a removal of br-GDGTs and a shift towards a more marine dominated system in an offshore direction.

Both bulk ($\delta^{13}C_{SOC}$ and $\delta^{15}N$) and molecular based indices (BIT and R'_{soil}) changed in an off-shore direction supporting an increasing marine OC input. However a prominent difference was observed in the behaviour of BIT index compared to the other indices. BIT index showed an exponential decline while all the other indices revealed linear trends throughout the transect. This exponential behaviour of BIT index is mainly controlled by the substantial addition of crenarchaeol while R'_{soil} is primarily governed by the removal of soil marker BHPs.

These field results suggest that both biomarker approaches can be used to trace terrOC in the Arctic environment. However, in line with the outcomes of previous studies, the results of this study highlighted that using a single proxy approach to trace

terrOC in the Arctic environment may lead to an under or over estimation of the relative importance of the different contributions. Using a multi-proxy approach is valuable to deduce the relative inputs of marine and terrestrial OC and leads to a better understanding of the processes acting along land-ocean transects in the Arctic region.

Acknowledgements

We gratefully acknowledge receipt of a NERC research grant (NE/I024798/I) to BEvD and HMT, a PhD studentship to ADS funded by the Ministry of National Education of Turkey and financial support as an Academy Research Fellow to ÖG from the Swedish Royal Academy of Sciences through a grant from the Knut and Alice Wallenberg Foundation. We thank the crew and personnel of the *R/V Yakob Smirnitskyi* and all colleagues in the International Siberian Shelf Study (ISSS) Program for support, including sampling. We thank P. Lythgoe (University of Manchester) for invaluable assistance with LC–MS, T. Tesi for providing the Yedoma samples for the Kolyma catchment area and the Science Research Infrastructure Fund (SRIF) From HEFCE for the TermoFinnigan LCQ ion trap mass spectrometer (Newcastle University). The ISSS program, is supported by the Knut and Alice Wallenberg Foundation, the Far Eastern Branch of the Russian Academy of Sciences, the Swedish Research Council, the US National Oceanic and Atmospheric Administration, the Russian Foundation of Basic Research, the Swedish Polar Research Secretariat, the Nordic Council of Ministers and the US National Science Foundation.

Supplementary Data

Figure 3S. 1: GDGT and BHP structures referred to in the text

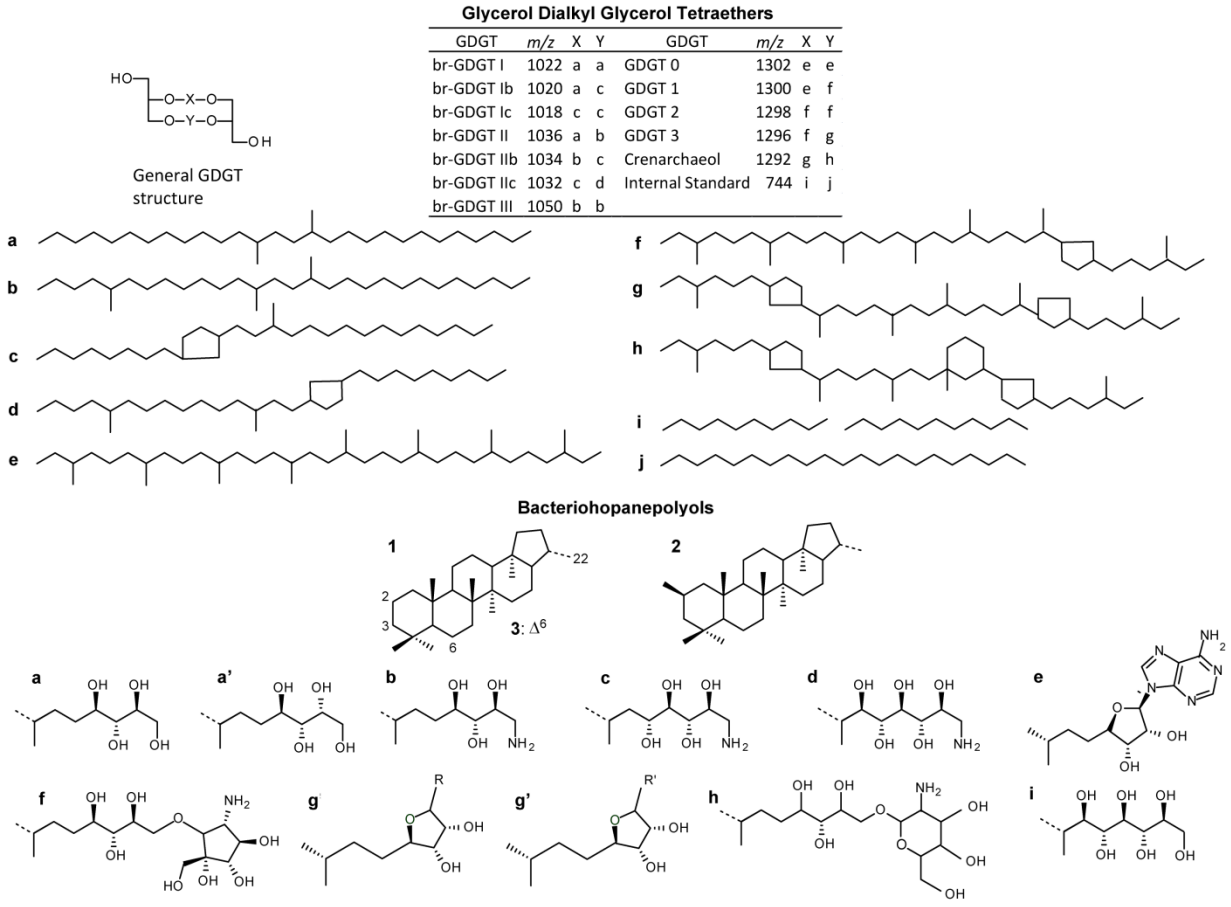

Table 3S. 1: Concentrations of GDGTs and BHPs in surface sediments along the Kolyma River-ESS transect (ng/g sed.)

Abbreviation	Structure	YS-34B	YS-35	YS-36	YS-37	YS-38	YS-39	YS-40	YS-41
Glycerol Dialkyl Glycerol Tetraethers									
Cren		204	1156	2138	1650	3882	2873	8117	4673
GDGT 0		280	1016	2640	2329	5492	4141	10528	5991
GDGT I		0	22	75	55	106	104	248	148
GDGT II		0	0	27	14	22	21	60	46
GDGT III		0	0	16	10	24	17	47	28
br-GDGTIII		68	133	95	46	81	28	84	56
br-GDGTII		99	202	123	40	80	14	45	39
br-GDGTI		45	115	78	30	52	9	11	25
∑Cyclic br-GDGTs		0	51	30	23	57	23	78	61
Bacteriohopanepolyols									
Δ^6BHT	3a	35	58	19	51	43	49	43	36
BHT	1a	720	1269	580	1280	1057	1445	1539	1287
BHT isomer	1a'	113	130	75	117	95	128	183	139
2-Methyl BHT	2a	48	87	31	57	41	52	65	32
BHHexol	1i	21	29	9	21	10	BDL	BDL	BDL
Aminotriol	1b	124	354	50	94	100	78	76	147
Aminotetrol	1c	21	64	5	8	9	4	BDL	12
Aminopentol	1d	32	70	6	4	8	BDL	BDL	BDL
BHT cyclitol ether	1e	169	204	19	37	30	30	29	65
BHT Glucosamine	2e	15	18	5	10	11	11	15	10
G1	1g	627	652	180	315	125	125	125	125
2Me-G1	2g	16	BDL	10	14	8	BDL	BDL	BDL
G2	1g'	258	337	143	190	85	68	46	30
2Me-G2	2g'	45	55	27	38	15	13	BDL	BDL
G3	1f	65	71	26	39	9	24	11	7
2Me-G3	1h	26	29	11	17	BDL	15	BDL	BDL

BDL: Below Detection Limit

References

ACIA, 2004. Impacts of a Warming Arctic: Arctic Climate Impact and Assessment (ed. Hassol SJ) pp. 1-1020.

Alling, V., Sanchez-Garcia, L., Porcelli, D., Pugach, S., Vonk, J.E., van Dongen, B., Mörth, C.-M., Anderson, L.G., Sokolov, A., Andersson, P., Humborg, C., Semiletov, I., Gustafsson, Ö., 2010. Nonconservative behavior of dissolved organic carbon across the Laptev and East Siberian seas. Global Biogeochemical Cycles 24, GB4033, DOI:10.1029/2010gb003834.

Amante, C. and Eakins, B.W., 2009. ETOPO1 1 Arc-Minute Global Relief Model: Procedures, Data Sources and Analysis. NOAA Technical Memorandum NESDIS NGDC-24. National Geophysical Data Center, NOAA.

AMAP, 2012. Arctic Climate Issues 2011: Changes in Arctic Snow, Water, Ice and Permafrost. SWIPA 2011 Overview Report. Arctic Monitoring and Assessment Programme (AMAP), pp. xi + 97pp, Oslo.

AMAP, 2013. AMAP Assessment 2013: Arctic Ocean Acidification. Arctic Monitoring and Assessment Programme (AMAP). viii pp. + 99 pp., Oslo, Norway.

Anderson, L.G., Jutterström, S., Hjalmarsson, S., Wåhlström, I., Semiletov, I.P., 2009. Out-gassing of CO_2 from Siberian Shelf seas by terrestrial organic matter decomposition. Geophysical Research Letters 36, L20601.

Blumenberg, M., Mollenhauer, G., Zabel, M., Reimer, A., Thiel, V., 2010. Decoupling of bio- and geohopanoids in sediments of the Benguela Upwelling System (BUS). Organic Geochemistry 41, 1119-1129.

Canuel, E.A., Martens, C.S., 1996. Reactivity of recently deposited organic matter: Degradation of lipid compounds near the sediment-water interface. Geochimica et Cosmochimica Acta 60, 1793-1806.

Cooke, M.P., 2010. The role of bacteriohopanepolyols as biomarkers for soil bacterial communities and soil derived organic matter. *PhD thesis*. Newcastle University, Newcastle.

Cooke, M.P., Talbot, H.M., Farrimond, P., 2008a. Bacterial populations recorded in bacteriohopanepolyol distributions in soils from Northern England. Organic Geochemistry 39, 1347-1358.

Cooke, M.P., Talbot, H.M., Wagner, T., 2008b. Tracking soil organic carbon transport to continental margin sediments using soil-specific hopanoid biomarkers: A case study from the Congo fan (ODP site 1075). Organic Geochemistry 39, 965-971.

Cooke, M.P., van Dongen, B.E., Talbot, H.M., Semiletov, I., Shakhova, N., Guo, L., Gustafsson, Ö., 2009. Bacteriohopanepolyol biomarker composition of organic matter exported to the Arctic Ocean by seven of the major Arctic rivers. Organic Geochemistry 40, 1151-1159.

Cooper, L.W., McClelland, J.W., Holmes, R.M., Raymond, P.A., Gibson, J.J., Guay, C.K., Peterson, B.J., 2008. Flow-weighted values of runoff tracers ($\delta^{18}O$, DOC, Ba, alkalinity) from the six largest Arctic rivers. Geophysical Research Letters 35.

De Jonge, C., Stadnitskaia, A., Hopmans, E.C., Cherkashov, G., Fedotov, A., Sinninghe Damsté, J.S., 2014. In situ produced branched glycerol dialkyl glycerol tetraethers in suspended particulate matter from the Yenisei River, Eastern Siberia. Geochimica et Cosmochimica Acta 125, 476-491.

Doğrul Selver, A., Talbot, H.M., Gustafsson, Ö., Boult, S., van Dongen, B.E., 2012. Soil organic matter transport along an sub-Arctic river- sea transect. Organic Geochemistry 51, 63-72.

Drenzek, N.J., Montluçon, D.B., Yunker, M.B., Macdonald, R.W., Eglinton, T.I., 2007. Constraints on the origin of sedimentary organic carbon in the Beaufort Sea from coupled molecular ^{13}C and ^{14}C measurements. Marine Chemistry 103, 146-162.

Fernandes, M.B., Sicre, M.A., 2000. The importance of terrestrial organic carbon inputs on Kara Sea shelves as revealed by *n*-alkanes, OC and $\delta^{13}C$ values. Organic Geochemistry 31, 363-374.

Guo, L., Ping, C.-L., Macdonald, R.W., 2007. Mobilization pathways of organic carbon from permafrost to arctic rivers in a changing climate. Geophysical Research Letters 34, L13603.

Guo, L., Semiletov, I., Gustafsson, Ö., Ingri, J., Andersson, P., Dudarev, O., White, D., 2004. Characterization of Siberian Arctic coastal sediments: Implications for terrestrial organic carbon export. Global Biogeochemical Cycles 18, GB1036.

Gustafsson, Ö., van Dongen, B.E., Vonk, J.E., Dudarev, O.V., Semiletov, I.P., 2011. Widespread release of old carbon across the Siberian Arctic echoed by its large rivers. Biogeosciences 8, 1737-1743.

Handley, L., Talbot, H.M., Cooke, M.P., Anderson, K.E., Wagner, T., 2010. Bacteriohopanepolyols as tracers for continental and marine organic matter supply and phases of enhanced nitrogen cycling on the late Quaternary Congo deep sea fan. Organic Geochemistry 41, 910-914.

Hedges, J.I., Oades, J.M., 1997. Comparative organic geochemistries of soils and marine sediments. Organic Geochemistry 27, 319-361.

Herfort, L., Schouten, S., Boon, J.P., Woltering, M., Baas, M., Weijers, J.W.H., Sinninghe Damsté, J.S., 2006. Characterization of Transport and Deposition of Terrestrial Organic Matter in the Southern North Sea Using the BIT Index. Limnology and Oceanography 51, 2196-2205.

Ho, S.L., Mollenhauer, G., Fietz, S., Martínez-Garcia , A., Lamy, F., Rueda, G., Schipper, K., Méheust , M., Rosell-Melé , A., Stein, R., Tiedemann, R., 2014. Appraisal of TEX_{86} and and $TEX^{L}86$ thermometries in subpolar and polar regions. Geochimica et Cosmochimica Acta 131, 213-226.

Holmes, R., McClelland, J., Peterson, B., Tank, S., Bulygina, E., Eglinton, T., Gordeev, V., Gurtovaya, T., Raymond, P., Repeta, D., Staples, R., Striegl, R., Zhulidov, A., Zimov, S., 2011. Seasonal and Annual Fluxes of Nutrients and Organic Matter from Large Rivers to the Arctic Ocean and Surrounding Seas. Estuaries and Coasts 35, 369-382.

Hopmans, E.C., Weijers, J.W.H., Schefuß, E., Herfort, L., Sinninghe Damsté, J.S., Schouten, S., 2004. A novel proxy for terrestrial organic matter in sediments based on branched and isoprenoid tetraether lipids. Earth and Planetary Science Letters 224, 107-116.

Huguet, A., Wiesenberg, G.L.B., Gocke, M., Fosse, C., Derenne, S., 2012. Branched tetraether membrane lipids associated with rhizoliths in loess: Rhizomicrobial overprinting of initial biomarker record. Organic Geochemistry 43, 12-19.

Huh, Y., Panteleyev, G., Babich, D., Zaitsev, A., Edmond, J., M., 1998. The fluvial geochemistry of the rivers of Eastern Siberia:II. Tributaries of the Lena, Omoloy, Yana, Indigirka, Kolyma, and Anadyr draining the collisional/accretionary zone of

the Verkhoyansk and Cherskiy ranges. Geochimica et Cosmochimica Acta 62, 2053-2075.

Karlsson, E.S., Charkin, A., Dudarev, O.V., Semiletov, I.P., Vonk, J.E., Sánchez-García, L., Andersson, A., Gustafsson, Ö., 2011. Carbon isotopes and lipid biomarker investigation of sources, transport and degradation of terrestrial organic matter in the Buor-Khaya Bay, SE Laptev Sea. Biogeosciences 8, 1865-1879.

Kim, J.-H., Ludwig, W., Schouten, S., Kerhervé, P., Herfort, L., Bonnin, J., Sinninghe Damsté, J.S., 2007. Impact of flood events on the transport of terrestrial organic matter to the ocean: A study of the Têt River (SW France) using the BIT index. Organic Geochemistry 38, 1593-1606.

Lobbes, J.M., Fitznar, H.P., Kattner, G., 2000. Biogeochemical characteristics of dissolved and particulate organic matter in Russian rivers entering the Arctic Ocean. Geochimica et Cosmochimica Acta 64, 2973-2983.

Ourisson, G., Rohmer, M., 1982. Prokaryotic polyterpenes: Phylogenetic precursors of sterols. Current topics in membranes and transport 17, 153-182.

Ourisson, G., Rohmer, M., Poralla, K., 1987. Prokaryotic Hopanoids and other Polyterpenoid Sterol Surrogates. Annual Review of Microbiology 41, 301-333.

Peterse, F., Hopmans, E.C., Schouten, S., Mets, A., Rijpstra, W.I.C., Sinninghe Damsté , J.S., 2011. Identification and distribution of intact polar branched tetraether lipids in peat and soil. Organic Geochemistry 42, 1007-1015.

Peterse, F., Vonk, J. E., Holmes, R. M., Giosan, L., Zimov, N., and Eglinton, T. I., 2014. Branched glycerol dialkyl glycerol tetraethers in Arctic lake sediments: Sources and implications for paleothermometry at high latitudes. Journal of Geophysical Research:Biogeosciences 119, 1738-1754

Rethemeyer, J., Schubotz, F., Talbot, H.M., Cooke, M.P., Hinrichs, K.-U., Mollenhauer, G., 2010. Distribution of polar membrane lipids in permafrost soils and sediments of a small high Arctic catchment. Organic Geochemistry 41, 1130-1145.

Rohmer, M., 1993. The Biosynthesis of Triterpenoids of the Hopane Series in the Eubacteria: A Mine of New Enzyme Reactions. Pure& Applied Chemistry 65, 1293-1298.

Sabine, C.L., Feely, R.A., Gruber, N., Key, R.M., Lee, K., Bullister, J.L., Wanninkhof, R., Wong, C.S., Wallace, D.W.R., Tilbrook, B., Millero, F.J., Peng, T.-H., Kozyr, A., Ono, T., Rios, A.F., 2004. The Oceanic Sink for Anthropogenic CO_2. Science 305, 367-371.

Sáenz, J.P., Eglinton, T.I., Summons, R.E., 2011a. Abundance and structural diversity of bacteriohopanepolyols in suspended particulate matter along a river to ocean transect. Organic Geochemistry 42, 774-780.

Sáenz, J.P., Wakeham, S.G., Eglinton, T.I., Summons, R.E., 2011b. New constraints on the provenance of hopanoids in the marine geologic record: Bacteriohopanepolyols in marine suboxic and anoxic environments. Organic Geochemistry 42, 1351-1362.

Sánchez-García, L., Alling, V., Pugach, S., Vonk, J., van Dongen, B.E., Humborg, C., Dudarev, O., Semiletov, I., Gustafsson, Ö., 2011. Inventories and behavior of particulate organic carbon in the Laptev and East Siberian seas. Global Biogeochemical Cycles 25, GB2007.

Schleper, C., Nicol, G.W., Robert, K.P., 2010. Ammonia-Oxidising Archaea- Physiology, Ecology and Evolution, Advances in Microbial Physiology, Volume 57, pp. 1-41. Academic Press.

Schouten, S., Hopmans, E.C., Rosell-Melé, A., Pearson, A., Adam, P., Bauersachs, T., Bard, E., Bernasconi, S.M., Bianchi, T.S., Brocks, J.J., Carlson, L.T., Castañeda, I.S., Derenne, S., Doğrul Selver, A., Dutta, K., Eglinton, T., Fosse, C., Galy, V., Grice, K., Hinrichs, K.-U., Huang, Y., Huguet, A., Huguet, C., Hurley, S., Ingalls, A., Jia, G., Keely, B., Knappy, C., Kondo, M., Krishnan, S., Lincoln, S., Lipp, J., Mangelsdorf, K., Martínez-García, A., Ménot, G., Mets, A., Mollenhauer, G., Ohkouchi, N., Ossebaar, J., Pagani, M., Pancost, R.D., Pearson, E.J., Peterse, F., Reichart, G.-J., Schaeffer, P., Schmitt, G., Schwark, L., Shah, S.R., Smith, R.W., Smittenberg, R.H., Summons, R.E., Takano, Y., Talbot, H.M., Taylor, K.W.R., Tarozo, R., Uchida, M., van Dongen, B.E., Van Mooy, B.A.S., Wang, J., Warren, C., Weijers, J.W.H., Werne, J.P., Woltering, M., Xie, S., Yamamoto, M., Yang, H., Zhang, C.L., Zhang, Y., Zhao, M., Sinninghe Damsté, J.S., 2013. An interlaboratory study of TEX_{86} and BIT analysis of sediments, extracts, and standard mixtures. Geochemistry, Geophysics, Geosystems 14, 5263-5285.

Schouten, S., Hopmans, E.C., Sinninghe Damsté, J.S., 2012a. The organic geochemistry of glycerol dialkyl glycerol tetraether lipids: A review. Organic Geochemistry 54, 19-61.

Schouten, S., Pitcher, A., Hopmans, E.C., Villanueva, L., van Bleijswijk, J., Sinninghe Damsté, J.S., 2012b. Intact polar and core glycerol dibiphytanyl glycerol tetraether lipids in the Arabian Sea oxygen minimum zone: I. Selective preservation and degradation in the water column and consequences for the TEX_{86}. Geochimica et Cosmochimica Acta 98, 228-243.

Semiletov, I., Gustafsson, Ö., 2009. East Siberian Shelf Study Alleviates Scarcity of Observations. Eos, Transactions American Geophysical Union 90, 145-146.

Semiletov, I.P., Pipko, I.I., Repina, I., Shakhova, N.E., 2007. Carbonate chemistry dynamics and carbon dioxide fluxes across the atmosphere-ice-water interfaces in the Arctic Ocean: Pacific sector of the Arctic. Journal of Marine Systems 66, 204-226.

Semiletov, I.P., Shakhova, N.E., Pipko, I.I., Pugach, S.P., Charkin, A.N., Dudarev, O.V., Kosmach, D.A., Nishino, S., 2013. Space–time dynamics of carbon and environmental parameters related to carbon dioxide emissions in the Buor-Khaya Bay and adjacent part of the Laptev Sea. Biogeosciences 10, 5977-5996.

Semiletov, I.P., Shakhova, N.E., Sergienko, V.I., Pipko, I.I., Dudarev, O.V., 2012. On carbon transport and fate in the East Siberian Arctic land- shelf- atmosphere system. Environmental Research Letters 7, 015201.

Shakhova, N., Semiletov, I., 2007. Methane release and coastal environment in the East Siberian Arctic shelf. Journal of Marine Systems 66, 227-243.

Shakhova, N., Semiletov, I., Salyuk, A., Yusupov, V., Kosmach, D., Gustafsson, Ö., 2010. Extensive Methane Venting to the Atmosphere from Sediments of the East Siberian Arctic Shelf. Science 327, 1246-1250.

Sinninghe Damsté, J.S., Ossebaar, J., Abbas, B., Schouten, S., Verschuren, D., 2009. Fluxes and distribution of tetraether lipids in an equatorial African lake: Constraints on the application of the TEX_{86} palaeothermometer and BIT index in lacustrine settings. Geochimica et Cosmochimica Acta 73, 4232-4249.

Sinninghe Damsté, J.S., Schouten, S., Hopmans, E.C., Van Duin, C.T., Geenevasen, J.A.J., 2002. Crenarchaeol: the characteristic core glycerol dibiphytanyl glycerol tetraether membrane lipid of cosmopolitan pelagic crenarchaeota. Journal of Lipid Research 43, 1641-1651.

Smith, R.W., Bianchi, T.S., Li, X., 2012. A re-evaluation of the use of branched GDGTs as terrestrial biomarkers: Implications for the BIT Index. Geochimica et Cosmochimica Acta 80, 14-29.

Smith, R.W., Bianchi, T.S., Savage, C., 2010. Comparison of lignin phenols and branched/isoprenoid tetraethers (BIT index) as indices of terrestrial organic matter in Doubtful Sound, Fiordland, New Zealand. Organic Geochemistry 41, 281-290.

Stein, R., MacDonald, R.W., 2004. The Organic Carbon Cycle in the Arctic Ocean. Springer, Berlin.

Strong, D.J., Flecker, R., Valdes, P.J., Wilkinson, I.P., Rees, J.G., Zong, Y.Q., Lloyd, J.M., Garrett, E., Pancost, R.D., 2012. Organic matter distribution in the modern sediments of the Pearl River Estuary. Organic Geochemistry 49, 68-82.

Talbot, H.M., Farrimond, P., 2007. Bacterial populations recorded in diverse sedimentary biohopanoid distributions. Organic Geochemistry 38, 1212-1225.

Talbot, H.M., Summons, R., Jahnke, L., Farrimond, P., 2003. Characteristic fragmentation of bacteriohopanepolyols during atmospheric pressure chemical ionisation liquid chromatography/ion trap mass spectrometry. Rapid Communications in Mass Spectrometry 17, 2788-2796.

Tarnocai, C., Canadell, J.G., Schuur, E.A.G., Kuhry, P., Mazhitova, G., Zimov, S., 2009. Soil organic carbon pools in the northern circumpolar permafrost region. Global Biogeochemical Cycles 23, GB2023.

Taylor, K.A., Harvey, R.H., 2011. Bacterial hopanoids as tracers of organic carbon sources and processing across the western Arctic continental shelf. Organic Geochemistry 42, 487-497.

Tesi, T., Semiletov, I., Hugelius, G., Dudarev, O., Kuhry, P., Gustafsson, Ö., 2014. Composition and fate of terrigenous organic matter along the Arctic land- ocean continuum in East Siberia: Insights from biomarkers and carbon isotopes. 133, pp. 235-256.

The Royal Society, 2005. Ocean acidification due to increasing atmospheric carbon dioxide. Policy document 12/05. The Royal Society, London.

Tierney, J.E., Russell, J.M., 2009. Distributions of branched GDGTs in a tropical lake system: Implications for lacustrine application of the MBT/CBT paleoproxy. Organic Geochemistry 40, 1032-1036.

Tierney, J.E., Schouten, S., Pitcher, A., Hopmans, E.C., Sinninghe Damsté, J.S., 2012. Core and intact polar glycerol dialkyl glycerol tetraethers (GDGTs) in Sand Pond, Warwick, Rhode Island (USA): Insights into the origin of lacustrine GDGTs. Geochimica et Cosmochimica Acta 77, 561-581.

Trenberth, K.E., P.D., J., Ambenje, P., et al., 2007. Observations: surface and atmospheric climate change. In: Climate Change 2007: The Physical Science Basis. Contribution of Working Group I to the Fourth Assessment Report of the Intergovernmental Panel on Climate Change (Ed. by S. Solomon, Qin, D., Manning, M., Chen, Z., Marquis,M., Averyt, K.B., Tignor, M., Miller, H.I.), Cambridge, UK and New York,NY, USA.

Uhlířová , E., Šantrůčková , H., Davidov, S.P., 2007. Quality and potential biodegradability of soil organic matter preserved in permafrost of Siberian tussock tundra. Soil Biology and Biochemistry 39, 1978-1989.

van Dongen, B.E., Irene C. Rijpstra, W., Philippart, C.J.M., de Leeuw, J.W., Sinninghe Damsté , J.S., 2000. Biomarkers in upper Holocene Eastern North Sea and Wadden Sea sediments. Organic Geochemistry 31, 1533-1543.

van Dongen, B.E., Semiletov, I., Weijers, J.W.H., Gustafsson, Ö., 2008a. Contrasting lipid biomarker composition of terrestrial organic matter exported from across the Eurasian Arctic by the five great Russian Arctic rivers. Global Biogeochemical Cycles 22, GB1011.

van Dongen, B.E., Talbot, H.M., Schouten, S., Pearson, P.N., Pancost, R.D., 2006. Well preserved Palaeogene and Cretaceous biomarkers from the Kilwa area, Tanzania. Organic Geochemistry 37, 539-557.

van Dongen, B.E., Zencak, Z., Gustafsson, Ö., 2008b. Differential transport and degradation of bulk organic carbon and specific terrestrial biomarkers in the surface waters of a sub-arctic brackish bay mixing zone. Marine Chemistry 112, 203-214.

van Winden, J.F., Talbot, H.M., Kip, N., Reichart, G.-J., Pol, A., McNamara, N.P., Jetten, M.S.M., Op den Camp, H.J.M., Sinninghe Damsté, J.S., 2012. Bacteriohopanepolyol signatures as markers for methanotrophic bacteria in peat moss. Geochimica et Cosmochimica Acta 77, 52-61.

Vonk, J.E., Gustafsson, Ö., 2013. Permafrost-carbon complexities. Nature Geoscience 6, 675-676.

Vonk, J.E., Sánchez-García, L., Semiletov, I.P., Dudarev, O.V., Eglinton, T.I., Andersson, A., Gustafsson, Ö., 2010. Molecular and radiocarbon constraints on sources and degradation of terrestrial organic carbon along the Kolyma paleoriver transect, East Siberian Sea. Biogeosciences 7, 3153-3166.

Vonk, J.E., Sanchez-Garcia, L., van Dongen, B.E., Alling, V., Kosmach, D., Charkin, A., Semiletov, I.P., Dudarev, O.V., Shakhova, N., Roos, P., Eglinton, T.I., Andersson, A., Gustafsson, Ö., 2012. Activation of old carbon by erosion of coastal and subsea permafrost in Arctic Siberia. Nature 489, 137-140.

Vonk, J.E., van Dongen, B.E., Gustafsson, Ö., 2008. Lipid biomarker investigation of the origin and diagenetic state of sub-arctic terrestrial organic matter presently exported into the northern Bothnian Bay. Marine Chemistry 112, 1-10.

Walsh, M.E., Ingalls, A.E., Keil, R.G., 2008. Sources and transport of terrestrial organic matter in Vancouver Island fjords and the Vancouver–Washington Margin: A multiproxy approach using $\delta^{13}C_{org}$, lignin phenols, and the ether lipid BIT index. Limnology and Oceanography 53, 1054-1063.

Weijers, J.W.H., Bernhardt, B., Peterse, F., Werne, J.P., Dungait, J.A.J., Schouten, S., Sinninghe Damsté, J.S., 2011. Absence of seasonal patterns in MBT-CBT indices in mid-latitude soils. Geochimica et Cosmochimica Acta 75, 3179-3190.

Weijers, J.W.H., Blaga, C.I., Werne, J.P., Sinninghe Damsté, J.S., 2009. Microbial membrane lipids in lake sediments as a paleothermometer. PAGES news 17.

Weijers, J.W.H., Schouten, S., Spaargaren, O.C., Sinninghe Damsté, J.S., 2006. Occurrence and distribution of tetraether membrane lipids in soils: Implications for the use of the TEX_{86} proxy and the BIT index. Organic Geochemistry 37, 1680-1693.

Weijers, J.W.H., Schouten, S., van den Donker, J.C., Hopmans, E.C., Sinninghe Damsté, J.S., 2007. Environmental controls on bacterial tetraether membrane lipid distribution in soils. Geochimica et Cosmochimica Acta 71, 703-713.

Weijers, J.W.H., Schouten, S., van der Linden, M., van Geel, B., Sinninghe Damsté, J.S., 2004. Water table related variations in the abundance of intact archaeal membrane lipids in a Swedish peat bog. FEMS Microbiology Letters 239, 51-56.

Xu, Y., Cooke, M.P., Talbot, H.M., Simpson, M.J., 2009. Bacteriohopanepolyol signatures of bacterial populations in Western Canadian soils. Organic Geochemistry 40, 79-86.

Zhu, C., Talbot, H.M., Wagner, T., Pan, J.-M., Pancost, R.D., 2011a. Distribution of hopanoids along a land to sea transect: Implications for microbial ecology and the use of hopanoids in environmental studies Journal Limnology and Oceanography. Limnology and Oceanography 56, 1850-1865.

Zhu, C., Wagner, T., Talbot, H.M., Weijers, J.W.H., Pan, J.-M., Pancost, R.D., 2013. Mechanistic controls on diverse fates of terrestrial organic components in the East China Sea. Geochimica et Cosmochimica Acta 117, 129-143.

Zhu, C., Weijers, J.W.H., Wagner, T., Pan, J.-M., Chen, J.-F., Pancost, R.D., 2011b. Sources and distributions of tetraether lipids in surface sediments across a large river-dominated continental margin. Organic Geochemistry 42, 376-386.

Zwiers, F.W., 2002. Climate change: The 20-year forecast. Nature 416, 690-691.

CHAPTER 4

Paper 3: GDGT distributions on the East Siberian Sea: implications for organic carbon export, burial and degradation

This chapter contains the following paper which is in preparation to be submitted to the journal Biogeosciences

Ayça Doğrul Selver[a], Robert B. Sparkes[a], Juliane Bischoff[b], Helen M. Talbot[b], Örjan Gustafsson[c], Igor P. Semiletov[d,e,f], Oleg V. Dudarev[e,f], Stephen Boult[a] and Bart E. van Dongen[a,*]

[a] School of Earth, Atmospheric and Environmental Sciences and Williamson Research Center, University of Manchester, Oxford Road, Manchester, M13 9PL, UK
[b] School of Civil Engineering and Geosciences, Newcastle University, Newcastle upon Tyne, NE1 7RU, UK
[c] Department of Applied Environmental Science (ITM) and the Bert Bolin Centre for Climate Research Stockholm University, Sweden
[d] Tomsk Polytechnic University,634050, Russia, Tomsk, Lenin Avenue, 30
[e] International Arctic Research Center, University of Alaska, Fairbanks, AK 99775-7340
[f] Pacific Oceanological Institute Far Eastern Branch of the Russian Academy of Sciences, Vladivostok 690041, Russia

* Corresponding Author: E-mail address: Bart.vandongen@manchester.ac.uk

Abstract

Siberian permafrost contains a globally-significant pool of organic carbon (OC) that is vulnerable to enhanced warming in this region. OC release by both fluvial and coastal erosion has been reported in the region, but the behaviour of this material in the Arctic Ocean is poorly understood. The balance between OC deposition and degradation on the East Siberian Arctic Shelf (ESAS) can determine the nature of the feedback between a changing climate and enhanced permafrost thawing and erosion in this area. In this study we couple measurements of glycerol dialkyl glycerol tetraethers (GDGTs) with bulk geochemical observations in order to determine the sources of OC to the ESAS, the behaviour of specific biomarkers on the shelf and the balance between delivery and removal of different carbon pools. Branched GDGT (br-GDGT) concentrations were highest close to river mouths, yet low in "Yedoma" permafrost deposits, suggesting that br-GDGTs are mostly delivered by fluvial erosion, and may be a tracer for this in complex sedimentary environments. Br-GDGT concentrations and the BIT index reduced quickly offshore, demonstrating a rapid reduction in river influence. δ^{13}Csoc values changed at a different rate to the BIT index, suggesting that OC on the shelf is not only sourced from fluvial erosion, but that erosion of coastal sediments delivers substantial quantities of OC to the Arctic Ocean. A model was created to investigate the OC export from fluvial, coastal and marine sources on the ESAS. The model of is able to recreate the biomarker and bulk observations and provide estimates for the influence of fluvial and coastal OC across the whole shelf. Whilst rivers deliver 72 % of br-GDGTs to the ESAS, coastal erosion delivers 43 % of the OC and 87 % of the mineral sediment.

4.1. Introduction

Understanding natural processes and feedbacks within the global carbon cycle is necessary for modelling and preparing for continuing climate change. High latitudes hold nearly half of the global soil carbon stores (Tarnocai et al., 2009), and are a poorly-understood region. Arctic permafrost carbon, in the form of tundra and taiga (~1000 PgC), terrestrial ice complexes (Yedoma; ~400 PgC) and submarine permafrost (~1400 PgC), is a significantly larger pool than that of atmospheric CO_2 (~760 PgC; Shakhova et al., 2010; Soloviev et al., 1987; Tarnocai et al., 2009; Zimov et al., 2006) and is liable to become an active part of the carbon cycle in the region during the next century (Gustafsson et al., 2011). Observations and predictions of global climate change have shown that the Polar Regions are disproportionately affected by climate warming (IPCC, 2013) leading to increased permafrost thawing, erosion of coastal permafrost and destabilisation of submarine permafrost (Vonk et al., 2012). Recent experiments showed that long-term warming of permafrost reorganises the soil carbon stock, increasing microbial activity in the mineral soil layer while also increasing the vegetation stock at the surface (Sistla et al., 2013). Changing pervasiveness of permafrost (i.e. from continuous to discontinuous coverage) introduces permeability, and allows groundwater flow to interact with deeply-buried carbon (Feng et al., 2013; Gustafsson et al., 2011). This activation of deep carbon will not only lead to direct oxidation and release of greenhouse gases (GHGs; e.g. CO_2, CH_4), but also to increased erosion and offshore transport from the permafrost layer to the Arctic Ocean, enhanced by (already observed) increased river discharge (Peterson et al., 2002). Ultimately these processes can lead to increased terrestrial organic carbon (terrOC) input to the Arctic Ocean where it can interact with the biosphere. However, the fate of terrOC in the Arctic Ocean remains poorly understood.

Carbon stored within permafrost and Yedoma is only released to the atmosphere if it becomes an active part of the carbon cycle. Conservative transport from terrestrial to marine environment (e.g. deposition as organic-rich sediment) has no net effect on global atmospheric carbon dioxide levels. However, any degradation during transport will release GHGs to the atmosphere (Arndt et al., 2013), causing a positive feedback effect on climate change. Previous studies of global offshore behaviour of terrOC have suggested that there is extensive degradation/removal once terrestrial material is delivered to the marine realm (Hedges et al., 1997), whilst others have documented significant offshore terrOC burial, even over long transport distances (Galy et al., 2007; Kao et al., 2014). Therefore, understanding the fate of terrOC after it is transported to the Arctic marine environment is critical to quantify the carbon cycle in this region.

Recently, a number of studies were published focusing on bulk and molecular level investigations of sediments exported from the Canadian and Siberian regions to better understand the behaviour of terrOC in lakes, rivers, estuaries and shelves (Belicka and Harvey, 2009; Cooke et al., 2009; Feng et al., 2013; Fernandes and Sicre, 2000; Guo et al., 2004; Gustafsson et al., 2011; Tesi et al., 2014; van Dongen et al., 2008; Vonk et al., 2012; Yunker et al., 1995). These studies have suggested the presence of terrOC in marine settings and a shift from terrestrial to marine-dominated environments with increasing distance offshore. However, Vonk et al. (2012) showed that terrOCOC inputs from coastal erosion are also a significant part of the Arctic carbon cycle and highlighted the potential for approximately 44 x 10^{12} g/year of terrOC to be mobilised from permafrost coastal erosion, of which 66 % could be released to the atmosphere.

Glycerol Dialkyl Glycerol Tetraethers (GDGTs) have been identified as biomarker molecules for terrestrial and marine organic matter (Schouten et al., 2013). Sourced from the cell membranes of bacteria and thaumarchaeota, they have been

found in a range of terrestrial and marine sediments dating back millions of years (Jenkyns et al., 2012; van Dongen et al., 2006). Branched GDGTs (br-GDGTs) contain 4-6 methyl branches along two C_{28} alkyl chains (Figure 4S.1) and are produced by terrestrial bacteria mainly in peats and soils (Weijers et al., 2006; Weijers et al., 2007). They have also been found to be abundant in other terrestrial settings, including lakes and rivers (Blaga et al., 2009; De Jonge et al., 2014). Isoprenoidal GDGTs contain two C_{40} isoprenoid chains with varying number of cyclopentane rings. One of these, crenarchaeol, which is dominantly produced by marine Thaumarchaeota, contains a cyclohexane unit in addition to 4 cyclopentane rings (Figure 4S.1). The ratio of br-GDGTs to crenarchaeol forms the basis of the Branched and Isoprenoid Tetraether (BIT) index (Hopmans et al., 2004) that is a proxy for tracing terrestrial material in marine environment. The BIT index has been used to infer terrestrial to marine transitions along river-ocean transects in (sub)-Arctic and non-Arctic Regions (Doğrul Selver et al., 2012; Kim et al., 2006; Zhu et al., 2011b). Recent studies have inferred that a proportion of br-GDGTs in the Arctic region may be produced within rivers rather than being transported entirely from soil erosion during freshet, and that br-GDGTs and BIT can be used to trace fluvial erosion offshore (De Jonge et al., 2014; Peterse et al., 2014). Therefore, the relationship between river outflows and the Arctic Shelf is worth investigating to understand the delivery of organic matter to the Arctic Ocean and its eventual fate. Differences in amount, distribution and fate between coastal and fluvial OC delivery can have severe implications for climate change and feedbacks.

Here we use a combination of GDGTs and stable carbon isotope proxies measured on a wide range of surface sediments from across the East Siberian Arctic Shelf (ESAS), including transects of the major Russian Arctic Rivers in this area (Lena, Indigirka and Kolyma) and areas of coastal erosion, to investigate the transport and fate of terrestrial organic carbon in a region which has experienced little scientific

investigation but is likely to experience extreme climate change in the next century. Combination of these proxies allows us to (i) differentiate between the different fractions of terrOC (coastal ice complex OC and river transported terrOC) which will likely have different degradation potentials and (ii) observe whether bulk OCand a specific fraction of the terrOC behave similarly.

4.2. Methods

4.2.1. Study area and sample collection

Samples used in the present study were collected from across the ESAS (130 to 175 °E; Figure 4.1). This area, including the Laptev and East Siberian Seas, spans the outflows of the Lena, Yana, Indigirka and Kolyma Rivers, with a combined drainage area of 3.7×10^6 km^2 and a discharge of 7.3×10^{11} m^3/y (Table 4.1; Gordeev, 2006). Annual organic carbon export into the Laptev and East Siberian seas is approximately $10x\ 10^{12}$ g/y (Rachold et al., 2004; Stein and MacDonald, 2004). The Lena River is the largest of the rivers in this region and forms a substantial delta reaching in to the Arctic Ocean, whilst the other three form smaller, more tide-dominated deltas. Due to a reduction in sea ice, potentially enhanced by climate warming, this region is also the site of severe coastal erosion of Yedoma, which has been estimated to deliver approximately 44×10^{12} g/y to the ESAS (Vonk et al., 2012). Focussing on the drainage basins, Eastern Siberia is a region with predominantly continuous permafrost, with the subsoil remaining permanently below 0°C and being impermeable to water flow (Permafrost Subcommittee, 1988). Eurasian permafrost soils contain 120 000 MtC, of which 74% is stored within continuous permafrost (Tarnocai et al., 2009); the majority of the continuous permafrost exists within the East Siberian region. At the surface there are

many small lakes and seasonal ice cover for up to nine months per year, with the majority of the sediment and water discharge during the early summer (Gordeev, 2006). Offshore there is a narrow channel between the coastline at ~140 °E and the New Siberian Islands, known as the Dmitry Laptev Strait splitting the ESAS up into two distinct areas, the Laptev Sea and East Siberian Sea (Figure 4.1). The New Siberian Islands themselves are remnants of the Great Arctic Plain, which once covered 1.6×10^6 km^2 between the modern coastline and the shelf edge, and was inundated during the Early-Middle Holocene, and now exists as substantial subsea permafrost (Kienast et al., 2005). Samples in this study were separated into groups representing the Buor-Khaya Bay, Dmitry Laptev Strait, Nearshore ESAS (<150 km from river outflows) and Offshore ESAS (>150 km from river outflows). In total, 92 sediment samples were collected in September 2008 during the International Siberian Shelf Study expedition (ISSS-08; Figure 4.1; Semiletov and Gustafsson, 2009), along with six samples from terrestrial Yedoma. Briefly, sediment cores and surface sediments were collected with a dual gravity corer (GEMAX) and a van Veen grab sampler. The sediment cores were sliced into 1 cm sections and, transferred to pre-cleaned polyethylene containers with stainless steel spatulas. Similarly, surface sections of the grab samples were obtained with stainless steel spatulas, transferred to pre-cleaned polyethylene containers. In addition, Yedoma samples were collected from river bank erosion profiles close to the mouths of the Indigirka and Kolyma rivers (Tesi et al., 2014). All sediments were kept frozen until analysis, in order to mitigate microbial degradation, and subsequently preserved by freeze- or oven-drying (50°C).

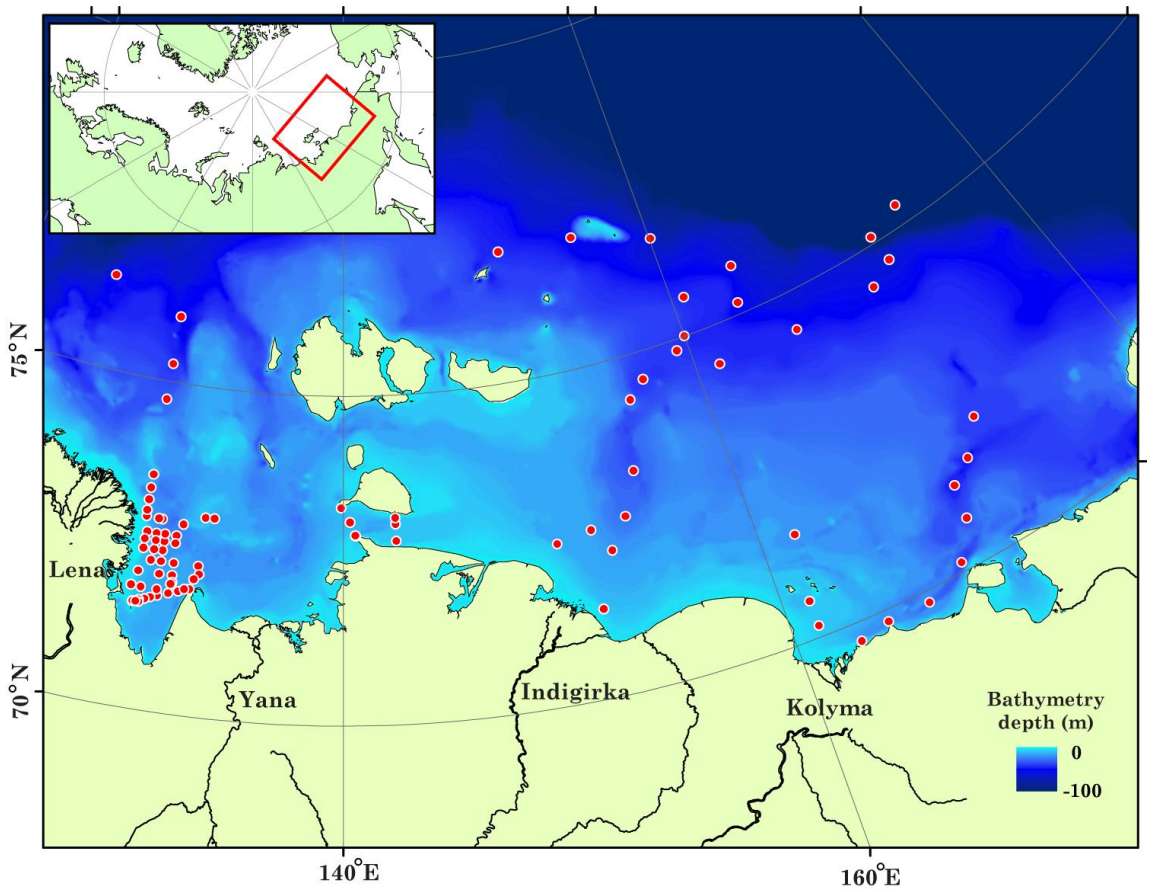

Figure 4. 1: Map of the East Siberian Arctic Shelf showing the location of the ISSS-08 sampling stations and outflows of four Great Russian Arctic Rivers. Bathymetry data from Amante and Eakins (2009).

4.2.2. Extraction and instrumental analysis

Freeze dried sediment samples were extracted using a modified Bligh-Dyer method as described by Doğrul Selver et al. (submitted). Approximately five grams (dry wt.) of sediment were ultrasonically extracted (at 40 °C for 10 min) using 19 ml of a mixture of methanol: dichloromethane: aqueous phase (MeOH:DCM: aqueous phase, 2:1:0.8 v/v/v) with the aqueous phase consisting of 0.05 M phosphate buffer at pH 7.4. Samples were centrifuged for five minutes at 2500 r.p.m., supernatants were collected and the extractions were repeated two additional times using the same solvent mixture. The DCM fractions were recovered by addition of 5ml each of phosphate buffer and DCM to

the supernatants. Combined DCM fractions were rotary evaporated to near dryness, transferred to vials using a solution of DCM:MeOH (2:1 v/v) and evaporated to dryness under a stream of N_2 to obtain the total lipid extracts (Tierney et al., 2012).

Aliquots (1/3 of the TLE) were separated into core lipid (CL) and intact polar lipid (IPL) fractions using silica column chromatography with 4 ml hexane:ethyl acetate (1:1, v/v) and 8 ml MeOH as eluents, respectively. After separation, 0.2 μg of a synthetic C_{46} GDGT standard was added to the CL fractions, which were dried under N_2, re-dissolved in Hexane:Isopropanol (99:1 v/v) and filtered through a 0.45 μm PTFE filter. GDGTs analysis was carried on the CL fractions via high performance liquid chromatography-atmospheric pressure chemical ionization-mass spectrometry (HPLC-APCI-MS) using the method reported by Hopmans et al. (2004). Analyses were performed using an Agilent 1200 HPLC coupled to an Agilent 6130 quadrupole MS instrument equipped with a multimode source operated in APCI positive ion mode using a similar instrumental setup as described by McClymont et al. (2012). The GDGTs were analysed using normal phase LC–MS with a Grace Prevail Cyano HPLC column (3 μm, 150 mm x 2.1 mm i.d.) and a guard column of the same material. Separation was achieved at 30 °C with a flow rate of 0.2 ml min^{-1} and the following gradient profile: 1 % isopropanol (IPA) in hexane (0–5 min), 1.8 % IPA in hexane (at 25 min) and 10 % IPA in hexane (at 30 min, held for 10 min). Conditions for APCI were: nebulizer pressure 20 psig, vaporiser temperature 250 °C, drying gas (N_2) flow 6 L/min and temperature 200 °C, capillary voltage 2 kV and corona 5 μA. In order to increase sensitivity/ reproducibility, ion scanning was performed in single ion monitoring (SIM) mode using GDGT $[M+H]^+$ ions. Peak areas were measured, and concentrations of individual GDGTs were calculated using a combination of the peak area of the C_{46} synthetic standard and a series of response factors for each GDGT calculated based on the peak areas of a sample with known concentrations. This corrects for the differences in

ionisation between compounds, as shown by Schouten et al. (2013). BIT index values were calculated according to the corrected peak areas of the branched GDGTs (br-GDGT) and crenarchaeol (Cren), following the method of Hopmans et al. (2004):

$$\mathrm{BIT} = \frac{[\sum \text{br-GDGTs}]}{[\sum \text{br-GDGTs}] + [\text{crenarchaeol}]} \qquad [1]$$

The BIT index ranges between a value of approximately one in a purely terrestrial setting and zero in a marine setting. Crenarchaeol can also be found in some terrestrial settings, including soils and rivers (De Jonge et al., 2014; Weijers et al., 2006; Zell et al., 2013), leading to BIT measurements of slightly less than one.

To complement these measurements, a model was created to simulate sediment export from fluvial and coastal erosion, and the associated influx of GDGTs and OC to the ESAS. Offshore locations were modelled as receiving organic matter from a combination of three sources. River erosion delivered sediment, OC and br-GDGTs as a series of point sources along the coastline. Coastal erosion delivered sediment and OC but no GDGTs as a linear source along the entire coastline, whilst marine productivity supplied OC and crenarchaeol in marine settings but no sediment. Full model details and parameters are included in the supplementary information.

The dual nature of inputs to the shelf, fluvial point sources and linear coastal erosion, means that distributions of terrestrial material across the shelf may be a function of both the distance from river mouths and coastlines. When investigating the across-shelf trends, the position of samples in relation to the nearest river outflow was used because the measured GDGT concentrations near to fluvial outflows are much higher than in coastal settings away from river mouths.

4.3. Results and Discussion

Sedimentary [Total] Organic Carbon (SOC) (data from Vonk et al., 2012) ranged from 0.68 to 2.25 wt% with the highest values in the Buor-Khaya Bay and being relatively uniform across the rest of the ESAS. 0 – 100 km from the river outflows, TOC averaged 1.81 ± 0.10 %, at 100 – 800 km it averaged 0.88 ± 0.06 % (Table 4.1).

4.3.1. GDGT concentrations

LC–MS analyses revealed a wide range of br-GDGTs and crenarchaeol concentrations in the sediments (Figures 4.2a & b). Br-GDGTs concentrations ranged from below detection limit (BDL) to 2046 ng/g sed. (BDL to 180 µg/g SOC) with the highest concentrations in sediments close to river mouths, especially the Lena River mouth, which is the largest of the rivers in the study area and exports the largest amount (20×10^6 t/ y) of sediment (Gordeev et al., 2006). Within the Buor-Khaya Bay, the highest br-GDGT concentrations were observed in the south-western corner of the bay, beside the major outflows of the Lena Delta, and decreased with distance across the bay. Nearshore ESAS samples showed an average br-GDGT concentration of 203 ng/g sed. (30 µg/g SOC) whilst ESAS offshore samples had an average concentration of 136 ng/g sed. (14 µg/g SOC; Figure 4S.2a).

When plotted against the distance from river outflows, br-GDGT concentrations decreased steeply offshore (Figure 4.3a). Samples within 100 km of the river mouths had an average br-GDGTs concentration of 668 ± 65 ng/g sed., by 300 – 400 km offshore the concentration was only 129±31 ng/g sed., and 700 – 800 km offshore the average was 13±11 ng/g sed. (Table 4.1 and Table 4S.1). The br-GDGTs concentration decrease showed a power-law distribution ($y = ax^b$) with an exponent of $b = -0.92$ and an r^2 value

of 0.52. In a similar analysis, Zhu et al. (2013) found power-law relationships between water depth (roughly equivalent to distance offshore) and concentrations of GDGTs and other biomarkers in the East China Sea. Our results indicate that the rapid offshore decrease in br-GDGTs concentrations is not an isolated observation. The sharp decrease in br-GDGTs concentration could be either due to a rapid sedimentation of br-GDGTs-rich material close to the shoreline, or the degradation of GDGT compounds during transport to the more distal locations.

Table 4. 1: Summed br-GDGTs and Crenarchaeol concentrations, BIT, $\delta^{13}C_{SOC}$ and TOC values on the ESAS , grouped by distance from river mouths

Distance from rivers (km)[a]	n	∑br-GDGTs (ng/g sed.)	Crenarchaeol (ng/g sed.)	BIT	δ^{13}Csoc (‰)[b]	TOC (%)
0-100	46	668	475	0.58	-26.0	1.81
100-200	13	227	781	0.32	-25.9	0.79
200-300	12	306	815	0.37	-26.6	0.96
300-400	5	129	3595	0.04	-24.6	0.94
400-500	5	136	2611	0.05	-24.6	0.91
500-600	3	84	2164	0.04	-23.7	0.78
600-700	6	62	1984	0.03	-22.8	0.83
700-800	2	13	971	0.01	-21.4	0.97

[a] Distance was measured radially from a series of outflows shown in the NOAA GSHGG river dataset.
[b] Data from Vonk et al., 2012.

Crenarchaeol concentrations ranged from 24 to 8116 ng/g sed. (2.05 to 656 µg/g SOC) with the lowest values in the coastal areas and the highest values at site YS-40, 391 km offshore from the Kolyma river outflow (Figures 4.3b & 4S.2b, location details in Table 4S.2). Other regions of high crenarchaeol concentration were the area east of longitude 165°E, and north of the Lena Delta. The most distal sediments showed a reduction in crenarchaeol concentration, with mean values of ~970 ng/g sed. (197 µg/g SOC) in the samples collected at the edge of the shelf. Crenarchaeol trends offshore were also non-linear, with the concentration peaking 300 – 400 km from the river

mouths (average concentration 3600 ± 1200 ng/g sed.). Nearshore and far offshore the average values were much lower (0 – 100 km: 480±50 ng/g sed., 700-800 km: 970±774 ng/g sed.; Table 4.1). A similar pattern in marine production has been observed in other transects of the Arctic coast, such as offshore northern Alaska (Belicka and Harvey, 2009) and may be due to a combination of (local) factors. Close to the shore, the influx of fresh water and sediment could reduce primary productivity, whilst far offshore ice cover throughout most of the year may have the same effect (Cremer, 1999; Sakshaug and Slagstad, 1992; Xiao et al., 2013). Measurements of dinosterol and brassicasterol, biomarkers for open-water phytoplankton, in the Laptev Sea (Xiao et al., 2013) showed a similar pattern; although the maximum concentrations of these biomarkers were 76 – 79 °N, further offshore than the crenarchaeol peak. It has been suggested that maximum primary productivity is in the open water and polynyas between the terrestrially-bound fast ice and the permanent open ocean ice sheet.

Onshore, in Yedoma samples, total br-GDGTs concentrations were 81 ± 52 ng/g sed., and crenarchaeol concentrations 114 ± 41 ng/g sed. These values are very low compared to the ESAS samples, especially the br-GDGTs concentrations compared to samples collected in the Buor-Khaya Bay or close to river outflows (Figure 4S.2). This suggests that erosion of Yedoma is unlikely to be the main source of br-GDGTs to the ESAS.

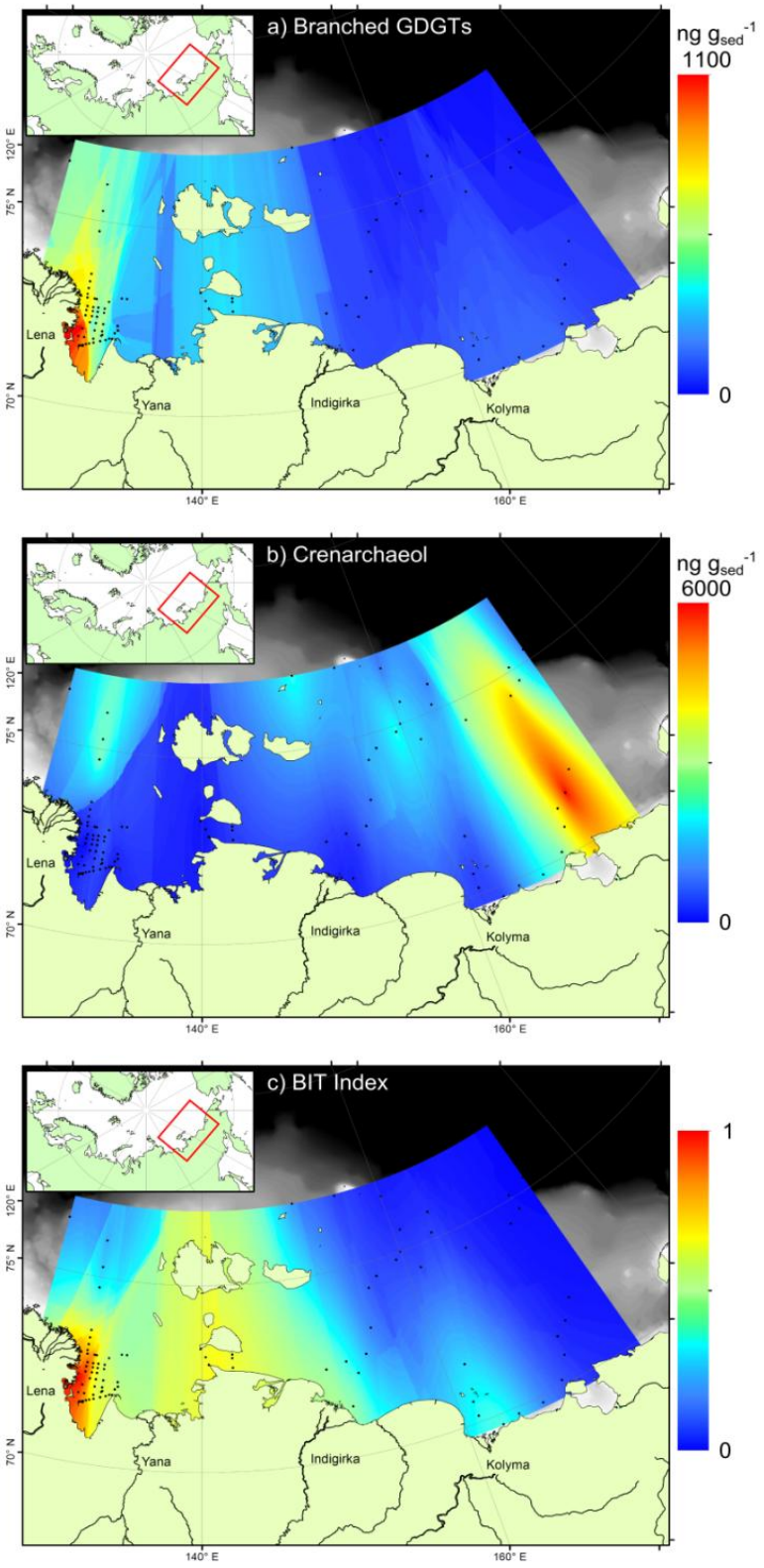

Figure 4. 2: Maps of a) Summed br-GDGTs and b) Crenarchaeol concentrations, and c) the BIT index on the ESAS. Maps were interpolated using a kriging algorithm. Black dots represent the locations of ISSS-08 stations.

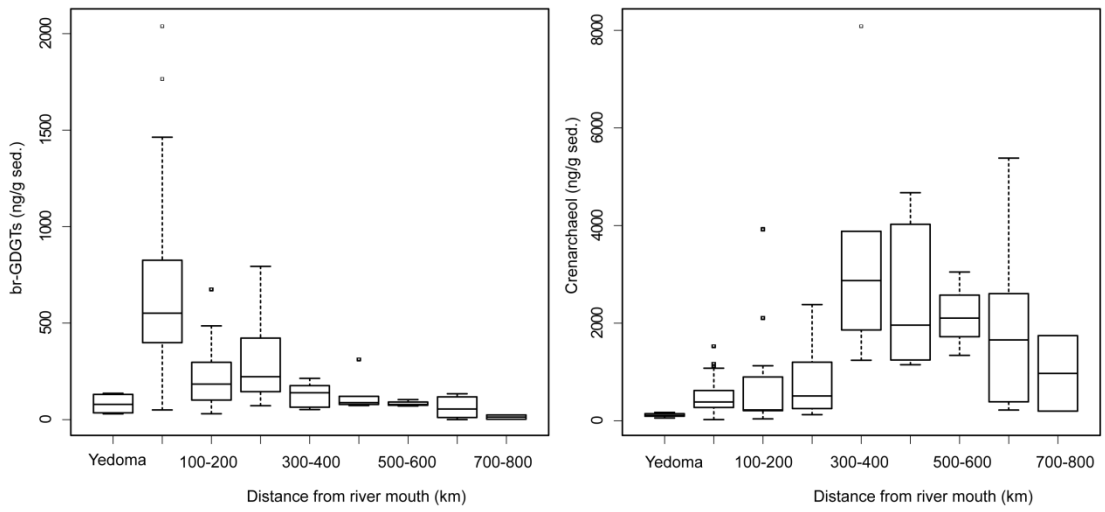

Figure 4. 3: Boxplots summarising the concentrations of a) br-GDGTs and b) Crenarchaeol on the ESAS, grouped by distance from river , and in Yedoma samples. Thick lines represent the median values, boxes the 25th and 75th percentiles, whiskers the maximum and minimum values within 1.5 times the inter-quartile range and square symbols outliers.

4.3.2. Spatial GDGT distributions and BIT

Br-GDGTs and crenarchaeol showed very different concentration relationships across the shelf (Figures 4.2a & b and 4.3). Plotting crenarchaeol concentration against br-GDGTs concentration showed that all nearshore samples are grouped together, having low crenarchaeol concentrations, whilst all offshore ESAS samples are in a distinct group with high crenarchaeol and low br-GDGT concentrations (Figure 4.4). The existence of these two groups was reflected in the BIT index (Figure 4.2c). BIT was highest in the Buor-Khaya Bay, especially close to the Lena River outflows (Figure 4.2c). The stations closest to the Lena (TB-30, 40, 46, 47 and 48) had an average BIT value of 0.91, compared to the bay as a whole which had an average BIT value 0.58 (Table 4S.2). Given a terrestrial BIT value of 1 (Hopmans et al., 2004), this strongly suggests a terrestrial source of the sediment deposited here, and a fluvial source to the br-GDGTs (De Jonge et al., 2014; Peterse et al 2014), and is similar to patters seen in other

locations (Doğrul Selver et al., 2012; Zhu et al., 2013). The BIT index values averaged 0.58 ±0.03 in the 100 km closest to all river outflows, dropping to 0.04 ±0.01 when 300 – 400 km offshore. A strong relationship was observed when the BIT index is plotted against the distance from the outflows of major rivers (Figure 4.5a). The BIT index decreased rapidly in the first 150 km offshore before reducing more slowly across the ESAS. This was seen for the Lena, Indigirka and Kolyma regions, as well as the open shelf, however, this pattern was not seen in the Dmitry Laptev Strait, which is a long distance from any river outflows but has a relatively high BIT value of 0.55 ±0.06. Excluding data from the Dimitry Laptev Strait, which will be discussed separately, there is a strong power-law correlation ($y=ax^{-b}$) between BIT and distance from rivers, with a value for exponent b of -1.209 (Figure 4.5a; $r^2=0.85$, $p<0.005$). To test this further, the BIT index of offshore transects from the Lena, Indigirka and Kolyma rivers were plotted against distance from river outflows in log-log space (Figure 4.5b). The gradients of the associated trendlines correspond to the exponential value (b) of each transect. The values for the Lena (b = 0.903) and Indigirka (b = 0.953) are comparable but the values for the Kolyma seems substantially higher (b = 1.302), denoting a more rapid shift to a marine-dominated system. However, the sediments from the most distal part of the Kolyma transect appear to have abnormally low BIT values compared to the nearshore sediments. These sediments are in a region that can potentially be influenced by inflow of Pacific Ocean water from the Bering Strait (Tesi et al., 2014), where incoming nutrients could stimulate primary productivity. The nearshore section of the Kolyma transect gives a b value (0.945) comparable to the other two rivers. The similarity of each major river transect studied, each showing a power-law reduction in BIT with distance despite a spatial separation of 100s of km, suggests that the processes affecting br-GDGT degradation and crenarchaeol production are similar across the whole ESAS. The absolute amounts of br-GDGTs and crenarchaeol differ for each river (Figures 4.2a

& b and Figure 4S.3a), and each river outflow has a different BIT value for a given distance offshore (Figures 4.2c and 4.5b), yet the rate of reduction offshore is comparable.

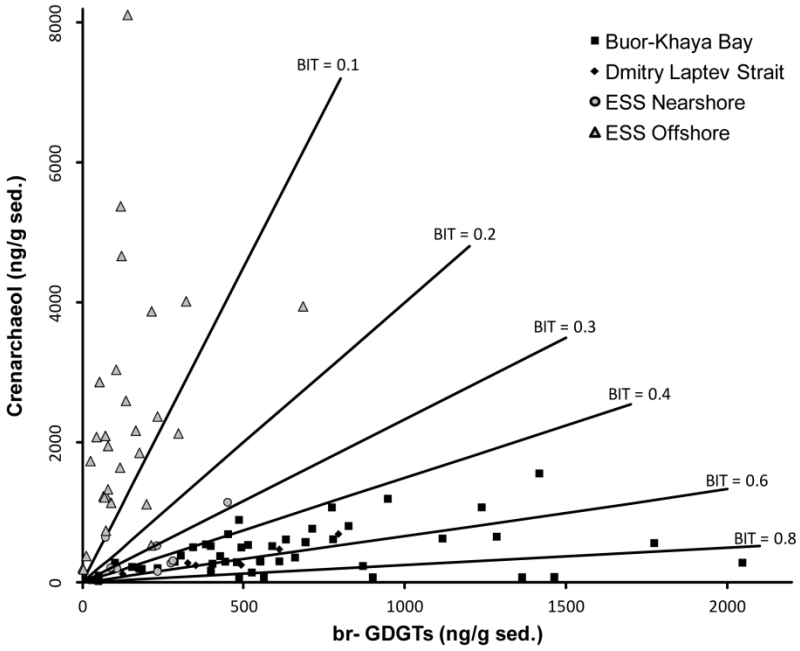

Figure 4. 4: Plot of crenarchaeol versus br-GDGTs concentration in sediment from the Buor-Khaya Bay, Dmitry Laptev Strait, nearshore and offshore ESAS. Labelled contours represent the BIT index values.

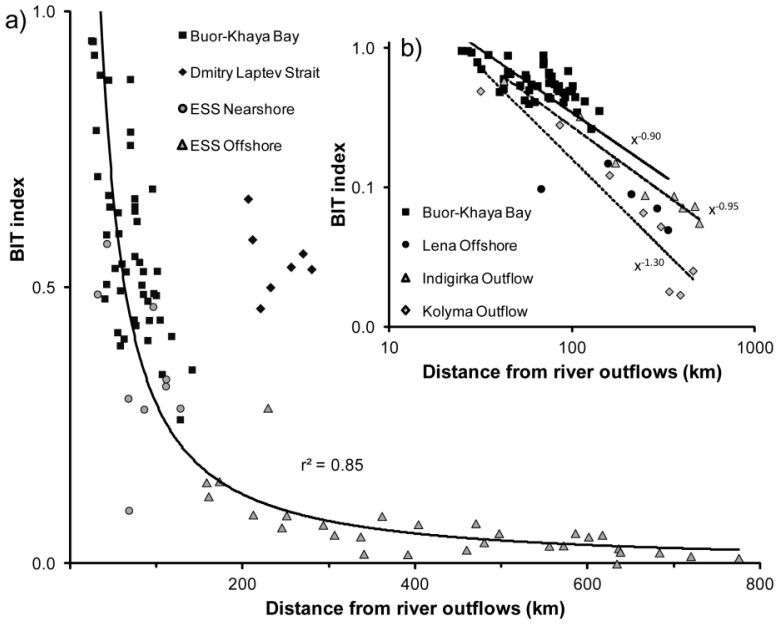

Figure 4. 5: Plot of BIT index versus linear distance from river mouths. a) plotted in linear space, showing the strong power-law relationship between the BIT and distance (with the exception of the Dmitry Laptev Strait samples) and b) plotted in log-log space.

The Dmitry Laptev Strait is unusual for its relatively high BIT index compared to its location, over 200 km from a major river outflow. This area is a region of high coastal erosion and the outflow of the Lena and Yana rivers is channelled through the Dmitry-Laptev Strait. Considering that the BIT index appears to decrease with the distance from fluvial outflows (Figure 4.5a), and therefore br-GDGTs are likely delivered by rivers, one possibility could be that minor rivers discharging into this area are providing the br-GDGTs to give enhanced BIT index values. However, br-GDGT concentrations in this area are not considerably high (Figures 4.2a and 4S.2a), and there is a decreasing trend eastward from the Lena Delta that these samples follow. In addition, the crenarchaeol concentrations in this region are very low (Figure 4.2b and 4S.2b) which leads to the high BIT index values in the area. The low crenarchaeol concentration in the Dmitry Laptev Strait sediments may be due to sea-ice cover reducing primary productivity. Indeed, Sakshaug and Slagstad (1992) found that later

melting times for sea-ice cover reduced seasonal primary productivity. Retreating ice causes a plankton bloom and initiates the growing season in that area. Xiao et al. (2013) report that the boundary between sea ice and continentally-anchored fast ice forms open-water polynyas roughly equivalent to the peak crenarchaeol regions, and the fast ice then retreats throughout the summer. Summer sea ice coverage is higher in the Dmitry Laptev Strait than other coastal areas which could lead to the extremely low crenarchaeol concentrations. Future changes in ice cover will likely lead to increased marine productivity in this region, and may therefore reduce BIT values (Arrigo et al., 2008).

4.3.3. Stable Carbon isotopes and BIT

Stable carbon isotope values ($\delta^{13}C_{SOC}$) can be used as a bulk proxy for marine versus terrestrial influence on sediment OC composition. Marine productivity produces material with more enriched $\delta^{13}C_{SOC}$ value compared to terrOC. $\delta\ ^{13}C_{SOC}$ values (data from Vonk et al., 2012) ranged from -21.2 to -27.5 ‰, with most depleted values in the Dmitry Laptev Strait, and most enriched values on the distal shelf, again showing a transition from terrestrial to marine dominance offshore. The Buor-Khaya Bay samples were also depleted, although less than the Dmitri Laptev Strait, and showed no significant variation across the Bay (Figure 4.6).

A linear relationship between $\delta^{13}C_{SOC}$ and distance offshore was observed. For samples from the Indigirka and Kolyma outflows and the offshore ESAS, the correlation was very strong (r^2= 0.90) which is in contrast to the BIT index, which showed a strong non-linear relationship with distance offshore. The relationship between $\delta^{13}C_{SOC}$ and BIT was therefore also non-linear with a strong correlation between the two (Figure 4.6). This was observed in the Kolyma River transect and attributed to the higher

removal rate of br-GDGTs compared to other fractions of terrOC and/or a significantly higher crenarchaeol addition compared to addition of other marine compounds (Doğrul Selver et al., submitted). In the present study, for the first time, decoupled offshore trends in BIT and $\delta^{13}C_{SOC}$ were observed.

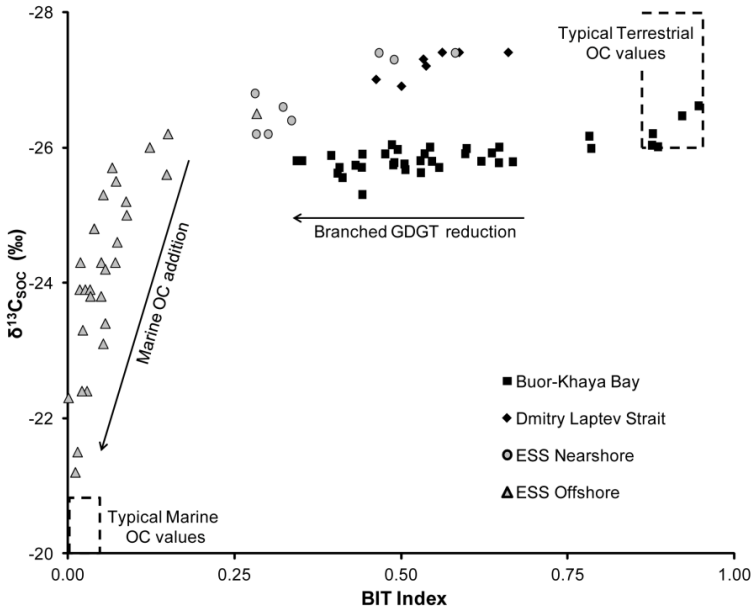

Figure 4. 6: Plot of $\delta^{13}C_{SOC}$ (data from Vonk et al., 2012) versus BIT index. Typical values for terrestrial and marine end-member samples are shown.

In the Buor-Khaya Bay, Dmitry Laptev Strait and within 150 km of the coastline, the $\delta^{13}C_{SOC}$ values were between -25 ‰ and -28 ‰ and showed no significant trend, whilst the BIT value dropped from 1 to 0.28 in an offshore direction. Greater than 150 km offshore, the BIT values decreased from 0.22 to 0, and the $\delta^{13}C_{SOC}$ values enriched from -26 ‰ to -21 ‰, creating an inflection at $\delta^{13}C_{SOC}$ = -26 ‰ and BIT =0.25. Considering that both $\delta^{13}C_{SOC}$ and BIT are used as proxies to quantify the proportion of terrestrial and marine material in offshore sediments (Belicka and Harvey, 2009; Doğrul Selver et al., submitted; Doğrul Selver et al., 2012; Karlsson et al., 2011; Smith et al., 2012; Zhu et al., 2011a), this apparent disagreement, which has not been observed

elsewhere, may suggests that on the ESAS, the proxies reflect different fractions of the terrestrial sediment export. Vonk et al. (2012) showed that the Yedoma, which dominate the East Siberian coastline, are at least as rich in organic carbon as topsoil, yet measurements of GDGTs in these complexes produced low concentrations (Table 4S.2). Therefore, erosion of coastal ice complexes would affect the $\delta^{13}C_{SOC}$ value of the sediments without significantly changing BIT values. Thus, BIT may be measuring inputs from GDGT-rich fluvial sources whilst $\delta^{13}C_{SOC}$ integrates both fluvial influx and coastal erosion. An alternative explanation is that the br-GDGTs responsible for the BIT index that were removing at a different rate compared to the bulk terrestrial organic carbon signal (Zhu et al., 2013). If br-GDGTs, which made up a small proportion of the OC load of the sampled sediments (less than 1/10 000), are removed more rapidly than bulk matter, which may contain large amounts of resistant molecules such as lignin phenols or plant wax lipids (Feng et al., 2013; Tesi et al., 2014), then the two proxies are likely to have a non-linear relationship. This finding raises suspicion about the usefulness of the BIT index as a proxy for the proportion of terrOC in a bulk sediment sample where coastal erosion plays a large role, but introduces the possibility of its use as a more specific proxy for fluvial input.

4.3.4. Modelling OC and GDGT delivery

To further investigate the sources and offshore behaviour of GDGTs and OC on the ESAS, a simple model was created to simulate the deposition and degradation of terrestrial and marine material (Figure 4S.3). A full description of the model is available in the supplementary information.

Our dataset, and other recent studies, have shown that fluvial systems in this region contain large amounts of br-GDGTs and OC (De Jonge et al., 2014; Peterse et al.,

2014). We modelled fluvial delivery of sediment, OC and GDGTs from GRARs as a series of point sources, from which material spread across the ESAS in a radial pattern. This leads to concentrations decreasing across the shelf in a 1/distance pattern. The Siberian Arctic coastline experiences rapid coastal erosion, delivering large amounts of sediment and OC to the Arctic Ocean each year (Vonk et al., 2012). This process was modelled as a linear source of material stretching along the entire longitudinal range of this study. The OC, GDGTs and sediment delivered by coastal erosion decreased proportional to the distance from the coastline. Marine primary productivity peaks in the mid-latitude samples (Figure 4.3b). This feature was reproduced simply in the model, with low marine OC and crenarchaeol deposition close to the coastline and far offshore.

A degradation factor was applied to the model, to simulate oxidation of organic matter in the water column. In the absence of more detailed studies a simple rule was applied in which OC and biomarkers were degraded proportional to the distance travelled from source. The initial conditions for sediment, OC and GDGT supply from fluvial and coastal erosion were taken from this and previous studies (Gordeev, 2006; Vonk et al., 2012).

Applying measured starting conditions and simple processes, the model reproduced measured offshore distributions of br-GDGTs, Crenarchaeol, TOC, $\delta^{13}C_{SOC}$ and BIT (Figure 4.7). Transects from the river outflows were successfully reproduced, and the low-crenarchaeol high-BIT behaviour of the Dmitry Laptev Strait was also qualitatively replicated. The model was then applied to the whole ESAS region included in this study, to avoid sampling bias. In the model, rivers delivered 13 % of the sediment to the ESAS, but 72 % of the br-GDGTs, which supports the use of the BIT index as a proxy for fluvial rather than coastal sediment and terrOC delivery. OC supply to the shelf was 40 % fluvial, 44 % coastal and 16 % marine primary productivity. These

findings are comparable to Vonk et al. (2012), although in their numerical model the role of coastal erosion was somewhat greater. Using the degradation functions provided above, the model predicts that 23 % of the exported terrOC was degraded between delivery and sampling (since this study only considers surface sediments, later diagenesis is ignored, but likely to be substantial (Arndt et al., 2013). Using published sediment delivery estimates (Rachold et al., 2002; Gordeev, 2006) this degradation equates to 0.7 Tg/y across the whole shelf, whilst 2.79 Tg/y is deposited. Of this deposition, 1.13 Tg/y comes from fluvial erosion, 1.23 Tg/y from coastal erosion of yedoma and 0.43 Tg/y from burial of marine primary productivity. Again, these numbers are somewhat lower than predicted by previous studies (Dudarev et al., 2006; Semiletov et al., 2011, 2012, 2013; Vonk et al., 2012), which suggested a greater rate of coastal erosion in this region. Further study of coastal erosion rates is clearly needed.

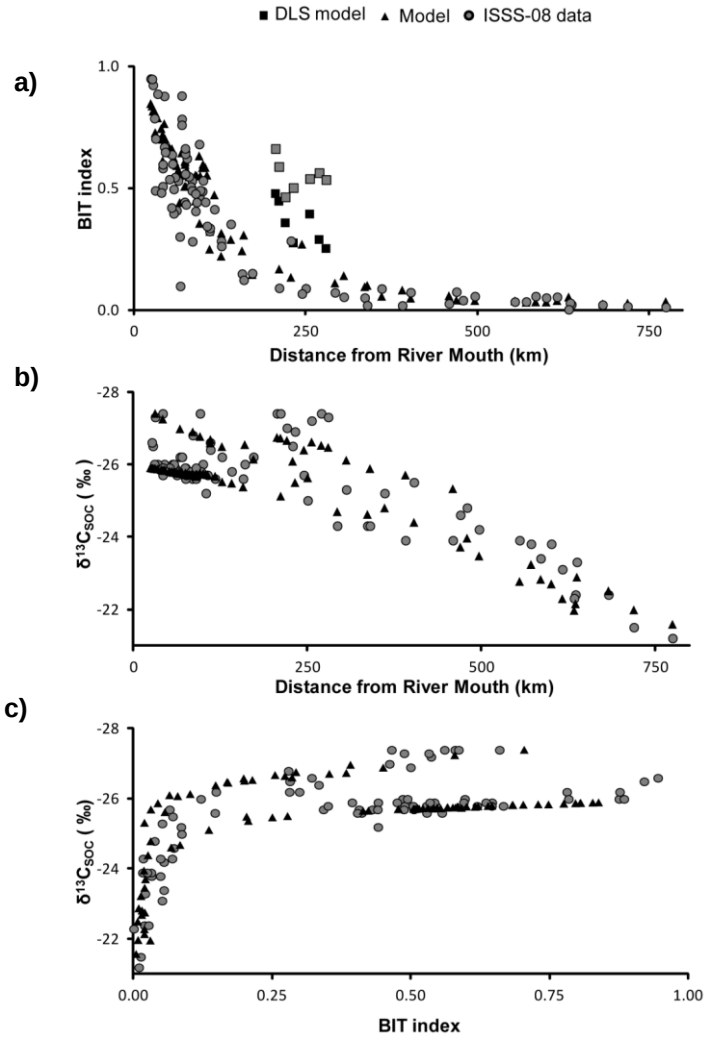

Figure 4. 7: Comparison plots of sample parameters with modelled values. Grey symbols represent observed data from this study and Vonk et al. (2012), black symbols are modelled values. a) BIT index versus distance from river outflows. Samples from the Dmitry Laptev Strait are shown separately, demonstrating how this region is offset from the general offshore-reduction trend in BIT, and showing the model recreating this trend. b) $\delta^{13}C_{SOC}$ versus distance from river outflow c) $\delta^{13}C_{SOC}$ versus BIT index.

4.3.5. Use of br-GDGTs as a proxy for river-derived sediment

The patterns observed in the BIT and $\delta^{13}C_{SOC}$ proxies suggest that the BIT index may be used not as a proxy for bulk soil export but for fluvial sediment delivery. Both the power-law reduction in BIT in an offshore direction and the non-linear relationship between BIT and $\delta^{13}C_{SOC}$ can be explained by the interaction of three carbon pools. The

model suggests that the majority of the br-GDGTs are due to input of OC from rivers discharging to the East Siberian Sea, whilst BIT is less representative of coastal erosion. As a bulk proxy, $\delta^{13}C_{SOC}$ is measuring the integrated effect of coastal erosion of terrestrial material, fluvial input and marine productivity, and therefore follows a different trend. Thus, samples close to outflows are river dominated, nearshore samples are coastal erosion dominated and offshore samples are marine-enriched. The west-east decrease in BIT values (Figure 4.2c) may also be explained by a fluvial signal, since the easternmost rivers are both smaller will deliver lower amounts of br-GDGTs during the spring freshet (Peterse et al., 2014).

4.4. Conclusions

Samples from the ESAS, including several offshore transects of Great Russian Arctic Rivers, show that sediments on the ESAS are terrestrially dominated near to river outflows and in the Buor-Khaya Bay in agreement with earlier studies. The BIT index shows that there is a trend towards marine organic matter domination offshore. This transition is quite rapid, occurring within 150 km of the shoreline following a power-law distribution along all river transects. There is a non-linear relationship between the BIT index and $\delta^{13}C_{SOC}$ measurements, suggesting that offshore transport of material in this region is a complex process. Modelling of fluvial and coastal erosion is able to reproduce the observed signals and suggests that br-GDGTs are primarily delivered by rivers. Fluvial delivery of br-GDGTs and topsoil, coupled with coastal erosion of permafrost ice complexes can explain the patterns seen on the shelf and raises the possibility of using br-GDGTs as a proxy for fluvially-delivered material in these sedimentary settings.

Acknowledgements

We gratefully acknowledge receipt of a NERC research grant (NE/I024798/1 and NE/I027967/1) to B.E.v.D and H.M.T., a PhD studentship to A.D.S. funded by the Ministry of National Education of Turkey and financial support as an Academy Research Fellow to O.G. from the Swedish Royal Academy of Sciences through a grant from the Knut and 410 Alice Wallenberg Foundation. We thank the crew and personnel of the R/V Yakob Smirnitskyi and all colleagues in the International Siberian Shelf Study (ISSS) Program for support, including sampling. We thank P. Lythgoe (University of Manchester) for invaluable assistance with LC–MS and T. Tesi for providing the Yedoma samples for the Kolyma catchment area. The ISSS program is supported by the Knut and Alice Wallenberg Foundation, the Far Eastern Branch of the Russian Academy of Sciences, the Swedish Research Council, the US National Oceanic and Atmospheric Administration, the Russian Foundation of Basic Research, the Swedish Polar Research Secretariat, the Nordic Council of Ministers and the US National Science Foundation.

Supplementary Data

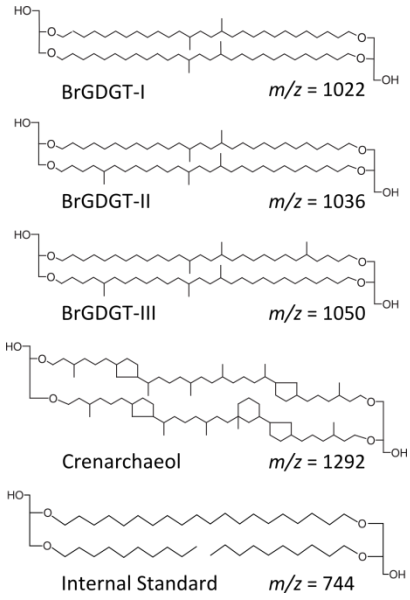

Figure 4S. 1: Structures of GDGTs and the synthetic C_{46} internal standard referred in the text.

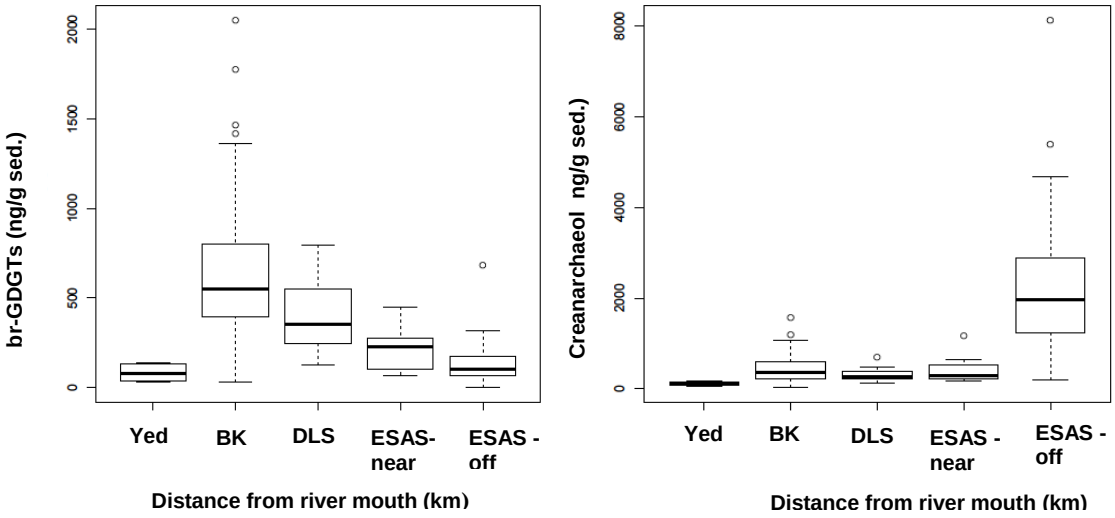

Figure 4S. 2: Boxplots summarising the concentrations of a) br-GDGTs and B) Crenarchaeol on the ESAS, grouped by sampling regions. Thick lines show the median values, boxes the 25th and 75th percentiles, whiskers the maximum and minimum values within 1.5 times the inter-quartile range and square symbols outliers beyond this threshold.Yed:Yedoma, BK:Buor-Khaya Bay, DLS:Dimitry Laptev Strait, ESAS-near: ESAS nearshore; ESAS-off: ESAS offshore

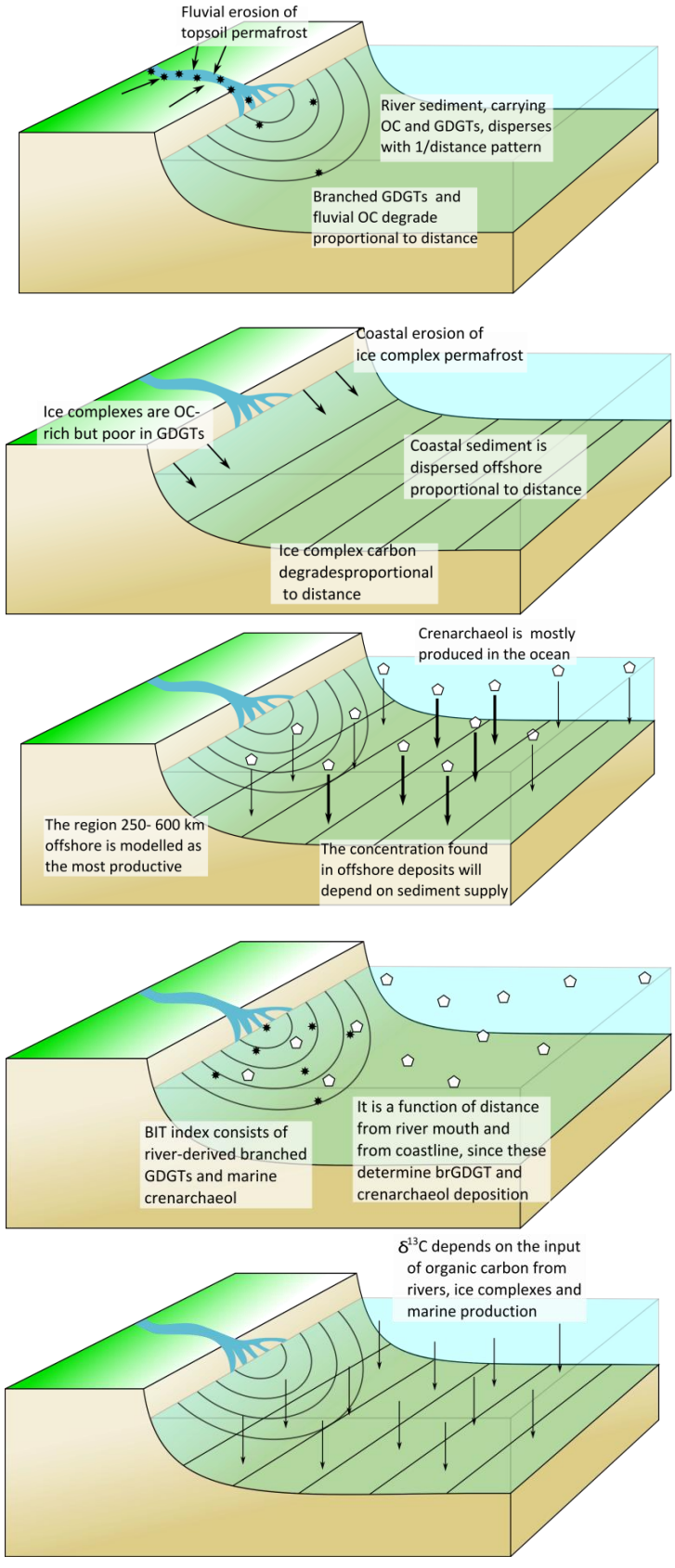

Figure 4S. 3: Cartoon demonstrating the principles behind the model used to understand carbon export and degradation on the ESAS.

Table 4S. 1: Basin area, water discharge, sediment discharge and continuous permafrost coverage values of East Siberian Rivers.

River	Basin Area[a] (10^3 km^2)	Water Discharge[a] (km^3/ y)	Sediment Discharge[a] (10^6 t/ y)	Continuous Permafrost[a,b] (%)
Lena	2448	523	20.7	71
Yana	225	32	4	100
Indigirka	360	54	11.1	100
Kolyma	647	122	10.1	99

[a] Data from Gordeev et al., 2006
[b] Kotlyakov and Khromova, 2002

Table 4S. 2: Sampling locations, TOC, $\delta^{13}C_{soc}$, BIT values and GDGTs concentrations of surface sediments from ESAS

Sample	Latitude	Longitude	Distance from river mouth (km)	Bottom depth (m)	TOC (%)[a]	$\delta^{13}C$ (‰)[b]	Crenarchaeol (µg/g TOC)	br-GDGT III (µg/g TOC)	br-GDGT II (µg/g TOC)	br-GDGT I (µg/g TOC)	Total GDGTs	BIT
ESS Off shore												
YS-4	75.99	129.98	293	50	1.34	-24.3	163	4	4	4	175	0.07
YS-5	75.27	130.02	212	43	1.48	NA	161	5	6	5	177	0.09
YS-6	74.72	130.02	158	32	1.86	-25.6	213	13	14	9	249	0.15
YS-28	72.65	154.19	173	28	0.87	-26.2	130	7	9	6	152	0.15
YS-31	71.59	161.69	229	20	0.56	-26.5	96	11	17	10	134	0.28
YS-36	69.82	166.00	160	32	0.80	-26.0	267	12	15	10	304	0.12
YS-37	70.14	168.01	245	42	0.94	-25.7	176	5	4	3	188	0.07
YS-38	70.70	169.13	306	36	1.00	-25.3	388	8	8	5	410	0.05
YS-39	71.22	169.37	340	44	1.23	-24.3	234	2	1	0.8	238	0.02
YS-40	71.48	170.55	391	49	1.36	-23.9	597	6	3	0.8	607	0.02
YS-41	71.97	171.79	459	43	1.32	-23.9	354	4	3	2	363	0.03
YS-86	75.30	174.40	775	200	0.89	NA	22	0.1	0.0	0.1	22	0.01
YS-88	75.10	172.19	720	142	1.04	-21.5	168	1	0.6	0.6	170	0.01
YS-90	74.67	172.39	683	63	0.85	-22.4	246	2	1	1	251	0.02
YS-91	74.43	170.85	638	56	0.82	-23.3	656	7	4	3	671	0.02
YS-93	74.42	166.00	572	51	0.80	-23.8	381	6	4	3	394	0.03
YS-95	74.42	161.34	480	45	0.97	-24.8	202	3	3	2	210	0.04
YS-98	75.55	160.75	555	48	0.77	-23.9	273	5	2	2	282	0.03
YS-99	75.17	163.59	586	50	0.77	-23.4	174	3	3	4	184	0.06
YS-100	75.72	164.08	636	58	0.76	-22.4	51	0.5	0.5	0.5	52	0.03
YS-102	76.56	160.07	634	69	0.77	-22.3	28	BDL	BDL	BDL	28	0.00
YS-104	76.93	155.17	617	57	0.91	-23.1	135	2	2	3	142	0.05
YS-106	76.97	150.29	601	43	0.87	-23.8	299	7	4	4	315	0.05
YS-111	75.00	160.01	497	46	0.80	-24.2	156	3	3	3	165	0.06
YS-112	74.83	159.33	470	42	0.88	-24.6	373	6	5	16	400	0.07
YS-116	74.58	157.00	404	36	0.60	-25.5	191	5	6	4	206	0.07
YS-118	74.33	156.01	361	28	0.71	-25.2	262	7	9	9	287	0.09
YS-120	73.29	155.17	251	33	0.99	-25.0	76	2	3	2	83	0.09
YS-131	76.40	125.47	337	50	0.40	-24.3	310	6	5	5	326	0.05
ESS Nearshore												
YS-8	73.57	130.01	68	14	0.18	NA	364	14	15	10	402	0.10
YS-26	72.46	150.60	96	1	0.87	-27.4	37	12	14	6	69	0.47
YS-27	72.57	152.37	128	18	0.41	-26.2	54	6	9	6	75	0.28
YS-29	72.20	153.17	111	18	0.63	-26.6	35	5	7	4	52	0.32
YS-30	71.36	152.15	42	9	1.35	-27.4	12	6	8	3	30	0.58
YS-32	70.57	161.22	111	9	0.42	-26.4	50	8	10	7	75	0.33
YS-33	70.17	161.22	67	8	0.40	-26.2	134	21	23	13	192	0.30
YS-34B	69.71	162.69	32	10	1.12	-27.3	18	6	9	4	37	0.51
YS-35	69.82	164.06	86	31	1.22	-26.8	95	11	17	9	132	0.28
Dimitry-Laptev Sea												
YS-20	73.31	139.89	233	8	0.39	-26.9	32	11	15	6	64	0.50
YS-21	73.09	140.35	221	15	0.81	-27.0	24	8	9	4	45	0.46
YS-22	72.88	140.63	207	20	1.18	-27.4	21	15	19	7	63	0.66
YS-22B	72.89	140.62	212	15	1.07	-27.4	23	12	14	6	56	0.59
YS-23	72.79	142.67	256	10	0.91	-27.2	31	13	16	7	67	0.54
YS-24	73.05	142.67	270	15	0.77	-27.4	62	30	36	14	141	0.56
YS-25	73.14	142.67	280	10	1.02	-27.3	68	32	34	12	146	0.53

BDL: below detection limit; NA: not analysed

Table 4S. 2: Continued

Sample	Latitude	Longitude	Distance from river mouth	Bottom depth (m)	TOC (%)[a]	$\delta^{13}C$ (‰)[b]	Crenarchaeol (µg/g TOC)	br-GDGT III (µg/g TOC)	br-GDGT II (µg/g TOC)	br-GDGT I (µg/g TOC)	Total GDGTs	BIT
						Buor-Khaya Bay						
TB-17	72.29	132.92	118	21	1.51	-25.6	36	7	11	8	62	0.41
TB-18	72.17	133.00	107	16	0.80	-25.8	13	2	3	2	19	0.34
TB-19	72.09	132.78	100	14	0.47	-26.0	34	9	14	9	66	0.49
TB-20	71.93	132.62	96	NA	0.08	NA	30	19	28	15	92	0.68
TB-22	71.88	132.11	105	15	0.40	-25.3	10	2	3	2	17	0.44
TB-23	71.83	131.67	97	20	1.59	-25.8	19	5	8	5	37	0.49
TB-24	71.76	131.17	85	16	1.87	-25.6	28	9	14	9	60	0.53
TB-25	71.72	130.83	81	13	1.88	-25.8	31	10	17	11	67	0.55
TB-26	71.69	130.58	78	13	2.09	-25.8	14	7	10	5	37	0.62
TB-27	71.66	130.33	75	11	1.90	-26.0	19	12	15	7	54	0.65
TB-28	71.62	130.04	70	5	2.15	-26.2	7	9	11	5	31	0.78
TB-30	71.87	129.83	45	5	2.04	-26.0	3	9	10	4	27	0.88
TB-31	71.86	130.32	56	12	2.25	-25.9	14	8	11	6	39	0.64
TB-32	71.86	131.09	75	12	1.90	-25.7	33	10	18	13	74	0.56
TB-33	72.09	131.09	65	15	2.20	-25.8	17	5	9	5	37	0.53
TB-34	72.29	131.09	63	16	1.90	-25.7	12	3	4	2	20	0.41
TB-35	72.46	131.09	60	17	2.30	-26.0	25	8	14	8	55	0.54
TB-36	72.59	131.10	58	17	2.12	-25.9	33	7	10	5	54	0.39
TB-37	72.71	131.09	57	19	2.39	-26.0	8	4	6	3	21	0.60
TB-38	72.93	130.84	59	20	2.35	-26.0	22	5	9	6	43	0.49
TB-39	72.93	130.66	52	20	2.30	-25.9	47	16	24	13	101	0.53
TB-40	72.93	130.03	35	6	1.50	-26.0	5	14	16	7	42	0.88
TB-43	72.89	131.93	90	22	1.56	-25.6	33	5	10	7	55	0.40
TB-44	72.71	131.66	74	19	2.09	-25.9	57	11	20	13	103	0.44
TB-45	72.70	130.66	42	15	2.24	-25.9	13	6	9	5	33	0.60
TB-46	72.70	130.18	28	6	2.58	-26.5	3	13	15	6	38	0.92
TB-47	72.45	130.12	25	NA	2.78	NA	3	20	23	9	56	0.95
TB-48	72.59	130.12	27	7	3.81	-26.6	2	13	16	7	38	0.95
TB-49	72.59	130.68	45	14	2.02	-25.8	10	6	10	5	31	0.67
TB-50	72.59	131.66	76	18	1.82	-25.7	29	6	10	6	51	0.43
TB-52	72.45	130.67	46	18	1.34	-25.8	23	13	19	10	64	0.65
TB-54	72.28	130.59	42	10	0.88	-25.7	52	14	24	15	105	0.51
TB-55	72.29	131.72	83	17	1.97	-25.8	41	10	19	13	83	0.50
TB-56	72.10	131.72	85	15	1.80	-25.7	30	7	13	9	58	0.49
TB-57	72.00	131.77	92	10	1.83	-25.7	21	5	7	5	38	0.44
TB-59	72.09	130.06	30	11	1.87	-26.0	13	17	20	9	59	0.78
YS-9	73.37	130.00	55	23	1.35	NA	80	16	26	15	137	0.42
YS-10	73.18	130.00	40	20	1.48	NA	52	15	22	11	100	0.48
YS-11	73.02	129.99	32	11	1.97	NA	5	4	6	3	18	0.70
YS-12B	71.92	132.39	101	10	0.13	NA	161	53	82	46	342	0.53
YS-13	71.97	131.70	90	19	1.89	-25.9	83	20	33	23	158	0.48
YS-14	71.63	130.05	70	7	1.91	-26.2	15	40	48	19	122	0.88
YS-15	71.63	130.05	70	11	2.60	NA	22	26	30	13	90	0.76
YS-16	71.63	130.32	75	11	2.08	NA	30	18	24	12	84	0.64
YS-17	71.63	130.19	75	10	1.35	NA	49	34	42	19	144	0.66
YS-18	73.03	133.00	128	15	0.17	NA	169	18	25	16	228	0.26
YS-19	73.04	133.46	142	27	1.82	-25.8	49	7	11	9	76	0.35

A model of offshore OC and GDGT delivery

The model considers the export of GDGT biomarker molecules and organic carbon (OC) across the entire area of the ESAS included in this study. It is a simplified model in which a small number of processes and parameters are able to replicate the observed patterns across the ESAS. The model considers the delivery of sediment from both rivers and coastal erosion, and the organic carbon and GDGTs associated with this material. Combining this with marine primary productivity we can model the delivery of sediment, terrestrial organic carbon and marine carbon to each position on the ESAS, and calculate the BIT index and $\delta^{13}C_{SOC}$ values that would be generated by that delivery. Rivers are point sources of sediment, OC and biomarkers, distributed along the ESAS coastline.

Measurements in this study showed that br-GDGT concentrations were highest at the mouths of GRARs. From the river mouth, material was modelled as spreading out in a 1/distance radial pattern, such that sediment, OC and GDGTs from fluvial sources were primarily deposited close to the river mouth, and concentrations dropped rapidly offshore. For simplicity, surface and deep current effects were ignored. Since GRAR outflow points are distributed 100s of km apart along the shoreline, the effects of interactions between river inputs was ignored - each position on the ESAS was modelled as only being affected by the closest river. Measurements of rivers (De Jonge et al., 2014), lakes (Peterse et al., 2014) and nearshore marine sediments from the region showed that br-GDGTs were abundant in fluvial sediment, along with some crenarchaeol. OC and GDGT concentrations in fluvial material were parameterized using samples from this study collected closest to the river mouths.

Coastal erosion is a major source of sediment and to the ESAS, and is prevalent along a majority of the East Siberian Arctic coastline (Rachold et al., 2002; Vonk et al.,

2012). The delivery of sediment, OC and GDGTs from coastal erosion was modelled as a linear source, assuming that all sections of the coastline were acting as a source of material. This leads to sediment, OC and GDGT deposition rates decreasing proportional to the distance from source, in a linear fashion. OC and GDGT input from coastal erosion was parameterized from measurements in this study and published data. Measurements from two vertical Yedoma permafrost transects showed that GDGT concentrations were low throughout, so the coastal erosion sediment was a minor source of GDGTs to the ESAS. OC concentration in the Yedoma samples was similar to fluvial sediments. Coastal-sourced sediment was given a carbon isotopic signature matching the source area -23‰ in the Laptev Sea and -27‰ in the ESAS.

Degradation during transport is an important consideration for terrOC and GDGTs; however it is currently very poorly understood and could only be parameterized as a simplified process. Since transport exposes OC and GDGTs to oxygenated water, degradation of both terrestrial OC and GDGTs was modelled as a function of the distance travelled from source. The model used a linear relationship between distance travelled and proportion degraded, such that by a given distance offshore (defined as 800 km) all of the material was modelled as having been degraded. Obviously this is a simplification, since there are some recalcitrant fractions of OC that would certainly survive transport across the whole shelf - graphite particles have been observed far across the ESAS using the Raman Spectroscopy technique of Sparkes et al. (2013) - but in the absence of a comprehensive degradation study in this region it is not possible to include a more thorough model.

In the model, marine primary productivity produces both marine OC and crenarchaeol. Observations of crenarchaeol distribution in the ESAS sediments, and of marine biomarkers in this region (Xiao et al., 2013), showed that productivity was maximum at intermediate distances across the shelf, and reduced close to the shore and

far offshore. These areas exhibit winter sea-ice cover for longer amounts of the year, which will reduce primary productivity, whilst the region between the polar ice cap and the terrestrially-bound fast ice contains open-water polynyas (Xiao et al., 2013). A simple parabolic distribution was used to model the production of both marine OC and crenarchaeol.

Each point on the ESAS was evaluated using GIS software that measured the distance to the closest river mouth and the closest coastline. These were given the values D_{riv} and D_{coast} respectively. This allowed the delivery of sediment, OC and GDGTs to be modelled for each location. Fluvial OC and GDGTs are a function of $1/D_{riv}$. Yedoma OC and GDGTs are a function of D_{coast}, as are marine OC and crenarchaeol. Having modelled the delivery of sediment, OC and GDGTs for each position on the shelf, TOC, $\delta^{13}C_{SOC}$ and BIT values were calculated for comparison with measured data and application to the whole shelf carbon cycle.

References

Amante, C. and Eakins, B.W., 2009. ETOPO1 1 Arc-Minute Global Relief Model: Procedures, Data Sources and Analysis. NOAA Technical Memorandum NESDIS NGDC-24. National Geophysical Data Center, NOAA.

Arndt, S., Jørgensen, B.B., LaRowe, D.E., Middelburg, J.J., Pancost, R.D., Regnier, P., 2013. Quantifying the degradation of organic matter in marine sediments: A review and synthesis. Earth-Science Reviews 123, 53-86.

Arrigo, K.R., van Dijken, G., Pabi, S., 2008. Impact of a shrinking Arctic ice cover on marine primary production. Geophysical Research Letters 35.

Belicka, L.L., Harvey, H.R., 2009. The sequestration of terrestrial organic carbon in Arctic Ocean sediments: A comparison of methods and implications for regional carbon budgets. Geochimica et Cosmochimica Acta 73, 6231-6248.

Blaga, C., Reichart, G.-J., Heiri, O., Sinninghe Damsté, J.S., 2009. Tetraether membrane lipid distributions in water-column particulate matter and sediments: a study of 47 European lakes along a north–south transect. Journal of Paleolimnology 41, 523-540.

Cooke, M.P., van Dongen, B.E., Talbot, H.M., Semiletov, I., Shakhova, N., Guo, L., Gustafsson, Ö., 2009. Bacteriohopanepolyol biomarker composition of organic matter exported to the Arctic Ocean by seven of the major Arctic rivers. Organic Geochemistry 40, 1151-1159.

Cremer, H., 1999. Distribution patterns of diatom surface sediment assemblages in the Laptev Sea (Arctic Ocean). Marine Micropaleontology 38, 39-67.

De Jonge, C., Stadnitskaia, A., Hopmans, E.C., Cherkashov, G., Fedotov, A., Sinninghe Damsté, J.S., 2014. In situ produced branched glycerol dialkyl glycerol tetraethers in suspended particulate matter from the Yenisei River, Eastern Siberia. Geochimica et Cosmochimica Acta 125, 476-491.

Doğrul Selver, A., Sparkes, R.B., Bischoff, J., Talbot, H.M., Gustafsson, Ö., Semiletov, I.P., Dudarev, O.V., Boult, S., van Dongen, B.E., submitted. Distributions of bacterial and archaeal membrane lipids in surface sediments along the Kolyma Palaeoriver transect, East Siberian Sea.

Doğrul Selver, A., Talbot, H.M., Gustafsson, Ö., Boult, S., van Dongen, B.E., 2012. Soil organic matter transport along an sub-Arctic river- sea transect. Organic Geochemistry 51, 63-72.

Feng, X., Vonk, J.E., van Dongen, B.E., Gustafsson, Ö., Semiletov, I.P., Dudarev, O.V., Wang, Z., Montluçon, D.B., Wacker, L., Eglinton, T.I., 2013. Differential mobilization of terrestrial carbon pools in Eurasian Arctic river basins. Proceedings of the National Academy of Sciences.

Fernandes, M.B., Sicre, M.A., 2000. The importance of terrestrial organic carbon inputs on Kara Sea shelves as revealed by *n*-alkanes, OC and $\delta^{13}C$ values. Organic Geochemistry 31, 363-374.

Galy, V., France-Lanord, C., Beyssac, O., Faure, P., Kudrass, H., Palhol, F., 2007. Efficient organic carbon burial in the Bengal fan sustained by the Himalayan erosional system. Nature 450, 407-410.

Gordeev, V.V., 2006. Fluvial sediment flux to the Arctic Ocean. Geomorphology 80, 94-104.

Guo, L., Semiletov, I., Gustafsson, Ö., Ingri, J., Andersson, P., Dudarev, O., White, D., 2004. Characterization of Siberian Arctic coastal sediments: Implications for terrestrial organic carbon export. Global Biogeochemical Cycles 18, GB1036.

Gustafsson, Ö., van Dongen, B.E., Vonk, J.E., Dudarev, O.V., Semiletov, I.P., 2011. Widespread release of old carbon across the Siberian Arctic echoed by its large rivers. Biogeosciences 8, 1737-1743.

Hedges, J.I., Keil, R.G., Benner, R., 1997. What happens to terrestrial organic matter in the ocean? Organic Geochemistry 27, 195-212.

Hopmans, E.C., Weijers, J.W.H., Schefuß, E., Herfort, L., Sinninghe Damsté, J.S., Schouten, S., 2004. A novel proxy for terrestrial organic matter in sediments based on branched and isoprenoid tetraether lipids. Earth and Planetary Science Letters 224, 107-116.

IPCC, 2013. Climate Change 2013: The Physical Science Basis. Contribution of Working Group I to the Fifth Assessment Report of the Intergovernmental Panel on Climate Change (Ed. by T.F. Stocker, D. Qin, G.-K. Plattner, M. Tignor, S.K. Allen, J. Boschung, A. Nauels, Y. Xia, V. Bex and P.M. Midgley), pp. 1535 pp.

Jenkyns, H.C., Schouten-Huibers, L., Schouten, S., Sinninghe Damsté, J.S., 2012. Warm Middle Jurassic- Early Cretaceous high-latitude sea-surface temperatures from the Southern Ocean. Clim. Past 8, 215-226.

Kao, S.J., Hilton, R.G., Selvaraj, K., Dai, M., Zehetner, F., Huang, J.C., Hsu, S.C., Sparkes, R., Liu, J.T., Lee, T.Y., Yang, J.Y.T., Galy, A., Xu, X., Hovius, N., 2014. Preservation of terrestrial organic carbon in marine sediments offshore Taiwan: mountain building and atmospheric carbon dioxide sequestration. Earth Surface Dynamics 2, 127-139.

Karlsson, E.S., Charkin, A., Dudarev, O.V., Semiletov, I.P., Vonk, J.E., Sánchez-García, L., Andersson, A., Gustafsson, Ö., 2011. Carbon isotopes and lipid biomarker investigation of sources, transport and degradation of terrestrial organic matter in the Buor-Khaya Bay, SE Laptev Sea. Biogeosciences 8, 1865-1879.

Kienast, F., Schirrmeister, L., Siegert, C., Tarasov, P., 2005. Palaeobotanical evidence for warm summers in the East Siberian Arctic during the last cold stage. Quaternary Research 63, 283-300.

Kim, J.-H., Schouten, S., Buscail, R., Ludwig, W., Bonnin, J., Sinninghe Damsté, J.S., Bourrin, F., 2006. Origin and distribution of terrestrial organic matter in the NW Mediterranean (Gulf of Lions): Exploring the newly developed BIT index. Geochemistry Geophysics Geosystems 7, Q11017.

Kim, J.-H., Zell, C., Moreira-Turcq, P., P., P.M.A., Abril, G., Mortillaro, J.-M., Weijers, J.W.H., Meziane, T., Sinninghe Damsté, J.S., 2012. Tracing soil organic carbon in the lower Amazon River and its tributaries using GDGT distributions and bulk organic matter properties. Geochimica et Cosmochimica Acta 90, 163-180.

McClymont, E.L., Ganeshram, R.S.S., Pichevin, L.E., Talbot, H., van Dongen, B., Thunell, R.C., Haywood, A.M., Singarayer, J.S., Valdes, P.J., 2012. Sea-surface temperature records of Termination 1 in the Gulf of California: Challenges for seasonal and inter-annual analogues of tropical Pacific climate change. Paleoceanography 27, DOI:10.1029/2011PA02226.

Permafrost Subcommittee, 1988. Glossary of Permafrost and Related Ground-ice Terms. National Research Council of Canada, Ottawa.

Peterse, F., Vonk, J. E., Holmes, R. M., Giosan, L., Zimov, N., and Eglinton, T. I., 2014. Branched glycerol dialkyl glycerol tetraethers in Arctic lake sediments: Sources and

implications for paleothermometry at high latitudes. Journal of Geophysical Research:Biogeosciences 119, 1738-1754.

Peterson, B.J., Holmes, R.M., McClelland, J.W., Vörösmarty, C.J., Lammers, R.B., Shiklomanov, A.I., Shiklomanov, I.A., Rahmstorf, S., 2002. Increasing River Discharge to the Arctic Ocean. Science 298, 2171-2173.

Rachold, V., Eicken, H., Gordeev, V.V., Grigoriev, M.N., Hubberten, H.W., Lisitzin, A.P., Shevchenko, V.P., Schirrmeister, L., 2004. Modern Terrigenous Organic Carbon Input to the Arctic Ocean. In: R. Stein, R. MacDonald (Eds.), The Organic Carbon Cycle in the Arctic Ocean (Ed. by R. Stein, R. MacDonald), pp. 33-55. Springer Berlin Heidelberg.

Sakshaug, E., Slagstad, D., 1992. Sea ice and wind: Effects on primary productivity in the Barents Sea. Atmosphere-Ocean 30, 579-591.

Schouten, S., Hopmans, E.C., Rosell-Melé, A., Pearson, A., Adam, P., Bauersachs, T., Bard, E., Bernasconi, S.M., Bianchi, T.S., Brocks, J.J., Carlson, L.T., Castañeda, I.S., Derenne, S., Doğrul Selver, A., Dutta, K., Eglinton, T., Fosse, C., Galy, V., Grice, K., Hinrichs, K.-U., Huang, Y., Huguet, A., Huguet, C., Hurley, S., Ingalls, A., Jia, G., Keely, B., Knappy, C., Kondo, M., Krishnan, S., Lincoln, S., Lipp, J., Mangelsdorf, K., Martínez-García, A., Ménot, G., Mets, A., Mollenhauer, G., Ohkouchi, N., Ossebaar, J., Pagani, M., Pancost, R.D., Pearson, E.J., Peterse, F., Reichart, G.-J., Schaeffer, P., Schmitt, G., Schwark, L., Shah, S.R., Smith, R.W., Smittenberg, R.H., Summons, R.E., Takano, Y., Talbot, H.M., Taylor, K.W.R., Tarozo, R., Uchida, M., van Dongen, B.E., Van Mooy, B.A.S., Wang, J., Warren, C., Weijers, J.W.H., Werne, J.P., Woltering, M., Xie, S., Yamamoto, M., Yang, H., Zhang, C.L., Zhang, Y., Zhao, M., Sinninghe Damsté, J.S., 2013. An interlaboratory study of TEX_{86} and BIT analysis of sediments, extracts, and standard mixtures. Geochemistry, Geophysics, Geosystems 14, 5263-5285.

Semiletov, I., Gustafsson, Ö., 2009. East Siberian Shelf Study Alleviates Scarcity of Observations. Eos, Transactions American Geophysical Union 90, 145-146.

Semiletov, I. P., Pipko, I. I., Shakhova, N. E., Dudarev, O. V., Pugach, S. P., Charkin, A. N., McRoy, C. P., Kosmach, D., and Gustafsson, O., 2011. Carbon transport by the Lena River from its headwaters to the Arctic Ocean, with emphasis on fluvial input of terrestrial particulate organic carbon vs. carbon transport by coastal erosion. Biogeosciences, 8, 2407–2426.

Semiletov, I. P., Shakhova, N. E., Sergienko, V. I., Pipko, I. I., and Dudarev, O. V., 2012. On carbon transport and fate in the East Siberian Arctic land- shelf- atmosphere system. Environmental Research Letters, 7, 015 201.

Semiletov, I. P., Shakhova, N. E., Pipko, I. I., Pugach, S. P., Charkin, A. N., Dudarev, O. V., Kosmach, D. A., and Nishino, S., 2013. Space-time dynamics of carbon and environmental parameters related to carbon dioxide emissions in the Buor-Khaya Bay and adjacent part of the Laptev Sea. Biogeosciences, 10, 5977–5996.

Shakhova, N., Semiletov, I., Salyuk, A., Yusupov, V., Kosmach, D., Gustafsson, Ö., 2010. Extensive Methane Venting to the Atmosphere from Sediments of the East Siberian Arctic Shelf. Science 327, 1246-1250.

Sistla, S.A., Moore, J.C., Simpson, R.T., Gough, L., Shaver, G.R., Schimel, J.P., 2013. Long-term warming restructures Arctic tundra without changing net soil carbon storage. Nature, 615–618

Smith, R.W., Bianchi, T.S., Li, X., 2012. A re-evaluation of the use of branched GDGTs as terrestrial biomarkers: Implications for the BIT Index. Geochimica et Cosmochimica Acta 80, 14-29.

Soloviev, V.A., Ginzburg, G.D., Telepnev, E.V., Mikhaluk, Y.N., 1987. Cryothermia and Gas Hydrates in the Arctic Ocean (VNIIOkeangeolia)

Stein, R., MacDonald, R.W., 2004. The Organic Carbon Cycle in the Arctic Ocean. Springer, Berlin.

Tarnocai, C., Canadell, J.G., Schuur, E.A.G., Kuhry, P., Mazhitova, G., Zimov, S., 2009. Soil organic carbon pools in the northern circumpolar permafrost region. Global Biogeochemical Cycles 23, GB2023.

Tesi, T., Semiletov, I., Hugelius, G., Dudarev, O., Kuhry, P., Gustafsson, Ö., 2014. Composition and fate of terrigenous organic matter along the Arctic land- ocean continuum in East Siberia: Insights from biomarkers and carbon isotopes. 133, pp. 235-256.

Tierney, J.E., Russell, J.M., 2009. Distributions of branched GDGTs in a tropical lake system: Implications for lacustrine application of the MBT/CBT paleoproxy. Organic Geochemistry 40, 1032-1036.

Tierney, J.E., Schouten, S., Pitcher, A., Hopmans, E.C., Sinninghe Damsté, J.S., 2012. Core and intact polar glycerol dialkyl glycerol tetraethers (GDGTs) in Sand Pond, Warwick, Rhode Island (USA): Insights into the origin of lacustrine GDGTs. Geochimica et Cosmochimica Acta 77, 561-581.

van Dongen, B.E., Semiletov, I., Weijers, J.W.H., Gustafsson, Ö., 2008. Contrasting lipid biomarker composition of terrestrial organic matter exported from across the Eurasian Arctic by the five great Russian Arctic rivers. Global Biogeochemical Cycles 22, GB1011.

van Dongen, B.E., Talbot, H.M., Schouten, S., Pearson, P.N., Pancost, R.D., 2006. Well preserved Palaeogene and Cretaceous biomarkers from the Kilwa area, Tanzania. Organic Geochemistry 37, 539-557.

Vonk, J.E., Sanchez-Garcia, L., van Dongen, B.E., Alling, V., Kosmach, D., Charkin, A., Semiletov, I.P., Dudarev, O.V., Shakhova, N., Roos, P., Eglinton, T.I., Andersson, A., Gustafsson, Ö., 2012. Activation of old carbon by erosion of coastal and subsea permafrost in Arctic Siberia. Nature 489, 137-140.

Weijers, J.W.H., Schouten, S., Spaargaren, O.C., Sinninghe Damsté, J.S., 2006. Occurrence and distribution of tetraether membrane lipids in soils: Implications for the use of the TEX_{86} proxy and the BIT index. Organic Geochemistry 37, 1680-1693.

Weijers, J.W.H., Schouten, S., van den Donker, J.C., Hopmans, E.C., Sinninghe Damsté, J.S., 2007. Environmental controls on bacterial tetraether membrane lipid distribution in soils. Geochimica et Cosmochimica Acta 71, 703-713.

Xiao, X., Fahl, K., Stein, R., 2013. Biomarker distributions in surface sediments from the Kara and Laptev seas (Arctic Ocean): indicators for organic-carbon sources and sea-ice coverage. Quaternary Science Reviews 79, 40-52.

Yunker, M.B., Macdonald, R.W., Veltkamp, D.J., Cretney, W.J., 1995. Terrestrial and marine biomarkers in a seasonally ice-covered Arctic estuary -- integration of multivariate and biomarker approaches. Marine Chemistry 49, 1-50.

Zell, C., Kim, J.-H., Moreira-Turcq, P., Gwenaël Abril, Hopmans, E.C., Bonnet, M.-P., Sobrinho, R.L., Sinninghe Damsté, J.S., 2013. Disentangling the origins of branched tetraether lipids and crenarchaeol in the lower Amazon River: Implications for GDGT-based proxies. Limnologhy Oceanography 58, 343-353.

Zhu, C., Talbot, H.M., Wagner, T., Pan, J.-M., Pancost, R.D., 2011a. Distribution of hopanoids along a land to sea transect: Implications for microbial ecology and the

use of hopanoids in environmental studies Journal Limnology and Oceanography. Limnology and Oceanography 56, 1850-1865.

Zhu, C., Wagner, T., Talbot, H.M., Weijers, J.W.H., Pan, J.-M., Pancost, R.D., 2013. Mechanistic controls on diverse fates of terrestrial organic components in the East China Sea. Geochimica et Cosmochimica Acta 117, 129-143.

Zhu, C., Weijers, J.W.H., Wagner, T., Pan, J.-M., Chen, J.-F., Pancost, R.D., 2011b. Sources and distributions of tetraether lipids in surface sediments across a large river-dominated continental margin. Organic Geochemistry 42, 376-386.

Zimov, S.A., Schuur, E.A.G., Chapin, F.S., 2006. Permafrost and the Global Carbon Budget. Science 312, 1612-1613.

CHAPTER 5

Paper 4: Characterization of macromolecular organic matter in the Arctic Region by py-GC/MS

This chapter contains the following paper which is in preparation to be submitted to the journal of Organic Geochemistry

Ayça Doğrul Selver[a], Robert B. Sparkes[a], Örjan Gustafsson[b], Igor P. Semiletov[c,d,e], Oleg V. Dudarev[d,e], Stephen Boult[a] and Bart E. van Dongen[a,*]

[a] School of Earth, Atmospheric and Environmental Sciences and Williamson Research Center, University of Manchester, Oxford Road, Manchester, M13 9PL, UK
[b] Department of Applied Environmental Science (ITM) and the Bert Bolin Centre for Climate Research Stockholm University, Sweden
[c] Tomsk Polytechnic University,634050, Russia, Tomsk, Lenin Avenue, 30
[d] International Arctic Research Center, University Alaska Fairbanks, PO Box 757340, Fairbanks, AK, USA
[e] Pacific Oceanological Institute Far Eastern Branch of the Russian Academy of Sciences, Vladivostok 690041, Russia

* Corresponding Author: E-mail address: Bart.vandongen@manchester.ac.uk

Abstract

Understanding the fate of terrestrial organic carbon (terrOC) in the Arctic Region is of major importance since it may influence the future trajectory of the global carbon cycle and ultimately of global warming. However, the fate of macromolecular fraction of terrOC in the Arctic Region still remains unclear. In this study, surface sediment samples from Great Russian Arctic River (GRAR) estuaries along an Eurasian Arctic climosequence as well as from two river ocean transects (Kalix River-Bothnian Bay and Kolyma River-East Siberian Sea transects) were analysed for their macromolecular compositions. Results indicated that the wetland coverage (sphagnum vs higher plants) and river runoff are likely to be the main controlling factors influencing the terrestrial macromolecular composition in the GRAR estuaries while the presence/absence of continuous permafrost does not have any effect on it.

Along both of transects, compound classes followed the same trends with furfurals and pyridines showing increasing and phenols decreasing trends in an off-river direction. The phenols to pyridines ratio is suggested as a new macromolecular proxy for tracing terrOC in the Eurasian Arctic Region and showed a strong correlation with other terrestrial versus marine proxies ($\delta^{13}N$,$\delta^{15}N$, BIT and R'_{soil}). The analyses indicate that a substantial part of the macromolecular terrOC is removed during transport along the shelf. In line with previous observations this suggests a non-conservative behaviour for this part of the terrOC.

5.1. Introduction

When considering the global carbon cycle, rivers are the main mechanism by which terrestrial material is transported to the oceans (Milliman et al., 1999) providing an

integrated signal of their watersheds. River dominated coastal shelves are important for carbon burial and transformation before the material is transported further into the ocean (Hedges and Keil, 1995). The Arctic Ocean, which can be considered to be a 'grand estuary' (AMAP, 2013; McClelland et al., 2004), is a unique example because it receives 10% of the global river flux and corresponding terrestrial organic carbon(terrOC) from Siberian and Canadian Rivers (Raymond et al., 2007; Schlünz and Schneider, 2000) yet only accounts for the 1% of the world's ocean volume (Aagaard and Carmack, 1989; Gordeev et al., 1996; Rachold et al., 2004). Considering that the Northern latitude soils, including all major Arctic river watersheds, hold approximately half of the global soil organic carbon (OC; 1672 Pg of OC; Schuur et al., 2008), the Arctic Region is a key location for studying the behaviour/fate of terrOC in the marine environment.

Recent reports show that this region is warming twice as fast as other parts of the world (IPCC, 2013) and it is expected that the Arctic Region is one of the areas where changes on biogeochemical cycles will first be observed (Serreze et al., 2000). The vast amounts of soil OC, currently freeze-locked in the permafrost, is vulnerable to global warming and can be relocated through various processes including permafrost thawing, increased river runoff and coastal erosion (Stendel and Cristen 2002; Vonk 2010). Indeed, in parts of the Eurasian Arctic region, global warming has already caused an increase in permafrost temperatures of up to 2°C between 1971 – 2010 (Schuur et al., 2008) and an increase in discharge rates of the main Eurasian rivers up to 7% (Peterson et al., 2002). More recently, Vonk et al. (2012) showed that coastal erosion could be an important process through which vast amount of terrOC are transported to the Arctic shelf. Particularly, the Yedoma (organic rich, old deposits) which dominate the East Siberian Sea coast (ESS; Vonk et al., 2010; Vonk et al., 2012) is currently affected by coastal erosion resulting in 44 ± 10 MT of terrOC transported to the ESS annually. This amount will likely increase in the next decades due to diminishing sea ice cover

resulting in increased storm frequency and wave fetch (Stein and MacDonald, 2004; Vonk et al., 2010).

The fate of terrOC in the Arctic Region is still a matter of debate. Stein and MacDonald (2004) previously suggested that degradation rates of terrestrial particulate organic carbon (POC) in coastal Arctic environments were comparable to global average degradation rate of riverine POC. However recent studies suggest that a much bigger proportion of the river transported terrOC is degraded in the water column, mainly close to the point of origin (Karlsson et al., 2011; Sánchez-García et al., 2011; Tesi et al., 2014; van Dongen et al., 2008b; Vonk et al., 2012). Van Dongen et al. (2008b), for instance, showed that 65% of terrestrial particulate organic carbon transported by the Kalix River is degraded in the inner low salinity zone close to the river mouth (within 60 km out of the river). Yedoma has been shown to be highly labile upon its remobilisation (Vonk et al., 2013a; Vonk et al., 2013b; Zimov et al., 2006) and therefore terrOC released by coastal erosion also behaves non-conservatively. Combined, these studies suggest that the estimates of Stein and Macdonald (2004) may be too low and a much larger proportion of the remobilized terrOC may be degraded and released into the atmosphere as greenhouse gases (GHGs) than previously thought, causing a positive feedback to global climate warming (IPCC, 2007; Mitchell, 1989; Raval and Ramanathan, 1989).

However, previous studies investigating the composition and fate of the terrOC transported to the Arctic shelf primarily focused on the extractable fraction, (Belicka and Harvey, 2009; Benner et al., 2005; Doğrul Selver et al., 2012; Drenzek et al., 2007; Fernandes and Sicre, 2000; Gustafsson et al., 2011; Karlsson et al., 2011; van Dongen et al., 2008a; Vonk et al., 2010; Vonk et al., 2012; Yunker et al., 1995); much less is known about the non-extractable part of the terrOC. This non-extractable OC constitutes the biggest proportion of bulk OC transported to the Arctic Ocean and contains macromolecular compounds such as lignin and cellulose. Until now, only a few studies

have analysed (parts) of the macromolecular terrOC transported to the Siberian Arctic shelves (Feng et al., 2013; Guo et al., 2004; Peulvé et al., 1996b; Tesi et al., 2014). Guo et al. (2004), for instance, analysed the macromolecular OC compositions of Great Russian Arctic Rivers (GRAR) estuary surface sediments using pyrolysis-gas chromatography/ mass spectrometry (py-GC/MS). Based on the increasing relative abundance of carbohydrate moieties towards eastern Siberia, they suggested that the terrOC transported to the Arctic Ocean via the eastern GRARs was less degraded thanOC transported by the western GRARs. In addition, Feng et al. (2013) showed, by analysing the radiocarbon age of specific lignin moieties in the same set of GRAR sediments, that the vascular plant derived lignin phenols may originate from young surface soils while wax lipids mainly derive from deeper permafrost horizons, implying that climate induced remobilisation may cause old permafrost carbon release.

In addition, it remains poorly understood how macromolecular terrOC behaves after it is transported to the Arctic Ocean. Recent lignin analyses on the ESS indicate that lignin may degrade faster than wax lipids (Tesi et al., 2014) suggesting that macromolecular terrOC may also behave non-conservatively. However, lignin represents only one part of the macromolecular fraction of the remobilized terrOC therefore it remains unclear to what extent these results are representative for the bulk macromolecular fraction. Thus, the aim of this paper is to improve our understanding of the composition and fate of terrestrial macromolecular OC transported to the Eurasian Arctic shelf systems and to better understand the effects of different hydrogeographic characteristics on the OC remobilized. For this, sediments from two river- ocean transects (Kolyma River- East Siberian Sea (ESS) and Kalix-River-Bothnian Bay transects) as well as sediments from major river estuaries along the Russian Arctic coastline were analysed to better understand the fate of the remobilized terrestrial macromolecular OC.

5.2. Materials and Methods

5.2.1. Study area and sample collection

The five GRARs and the Kalix River span over 5000 km (140 °E longitude; Figure 5.1) and represent different climatology, permafrost coverage and vegetation types. The eastern GRARs (Lena, Indigirka, and Kolyma Rivers) flow into the Laptev Sea and the East Siberian Sea (Figure 5.1A) and their watersheds are located in the continuous permafrost region covered with vast amounts of deciduous forest. The climate in the eastern GRAR drainage basins is semi- arid to arid, with average summer temperatures of between +7 °C and +9 °C and winter temperatures below −40 °C. Of these GRARs, the Kolyma River is the easternmost river and has the largest Arctic river basin completely underlain by continuous permafrost (Holmes et al., 2011).

The two western GRARs (Ob and Yenisey) drain into the Kara Sea and their watersheds are mainly located on the discontinuous permafrost region covered mainly by mosses and shrubs. The average summer temperatures are comparable to those of eastern Siberia but winter temperatures are higher (around −20 °C). Due to the wetter and warmer climate, there are more extensive peats and wetlands in the western GRAR drainage areas compared to those of the eastern GRARs (Kremenetski et al., 2003; Tarnocai et al., 2009).

The GRARs combined have a freshwater discharge of around 1900 km^3/ yr (Table 5.1) by far the greatest proportion of the total freshwater discharge to the Arctic Ocean (Opsahl et al., 1999). The highest discharge is from the Yenisey River carrying approximately 36 % of the total GRAR flow (~673 km^3/yr), while the lowest discharge is from the Indigirka River carrying only 3% of the total GRAR discharge (~54 km^3/yr).

The sub-Arctic Kalix River is considered to be the western extension of the western GRARs, since its geochemistry is similar to those of these rivers (Guo et al., 2004; Gustafsson et al., 2000; Ingri et al., 2005; Vonk et al., 2008). The Kalix River is in the Kalix–Torne river system having a watershed mainly consisting of coniferous to boreal forest (55–65%) and peatland (17–20%; Ingri et al., 2005) and together with other Finnish and Swedish rivers (e.g. Lule, Kemi and Oulu Rivers), runs into Bothnian Bay. The mean annual water discharge of the Kalix River is approximately 10 km^3/yr (Ingri et al., 2005; Ingri et al., 2000), accounting for 7% of the total annual discharge to Bothnian Bay, peaking in mid-May-late June (Ingri et al., 2005).

Surface sediment samples from the GRAR estuaries, the Kolyma River-ESS and the Kalix River-Bothnian Bay transect were collected during different scientific cruises. Surface sediment samples from the Ob and Yenisey estuaries were obtained using a van Veen grab sampler during the third Russia-United States cruise 2005 (R/V Ivan Kireev September 2005 cruise) in the Kara Sea (Figure 5.1 and Table 5.1). The Indigirka and Kolyma estuary surface sediments were collected during the Russia-United States cruise in 2004 (R/V Ivan Kireev September 2004 cruise) in the East Siberian and Laptev Seas using a van Veen grab sampler. Sub-samples were taken from 0– 2 cm of the grab samples and transferred into pre-combusted glass jars.

Kalix River– Bothnian Bay transect surface sediments (Figure 5.1B) were obtained in early June 2005 using the research vessel KBV005 from the Umea Marine Research Center (UMF, Norrbyn, Sweden), as described by Vonk et al. (2008). An Ekman grab sampler was used to collect samples and sub-samples were taken with stainless steel spatula, transferred to glass bottles. All samples were kept frozen (20°C) until analysis.

The Kolyma River- ESS transect (Figure 5.1C) and the off-shore (YS-88) surface sediments were taken in September 2008 during the International Siberian Shelf Study

expedition (ISSS-08; Figure 5.1 and Table 5.1). Lena estuary (TB-30) surface sediment was collected during a sub-expedition carried out during ISSS-08 expedition in the Buor-Khaya Bay. The sediments were collected along a river mouth-shelf transect following the old palaeoriver transect (Vonk et al., 2010) spanning approximately 467 km from station YS-34B (46 km out of the river mouth) to station YS-41 (513 km out of the river mouth). The additional surface sediment (YS-88), not part of the transect, from the ESS was collected near the edge of the shelf (approximately 700 km from the Kolyma river mouth). Samples were collected with a dual gravity corer or a van Veen grab (YS-34B and YS-41) sampler. The sub-samples of the grab samples and the top section of the core samples were obtained with stainless steel spatulas and transferred to pre-cleaned polyethelene containers.

In addition to the marine sediments, three Yedoma samples were collected from an exposed river bank profile in the Kolyma River catchment area in 2013 (69.46 °N – 161.79 °E; Figure 5.1C; Tesi et al., 2014). These samples are used as representative of the composition of terrestrial material transported to the shelf.

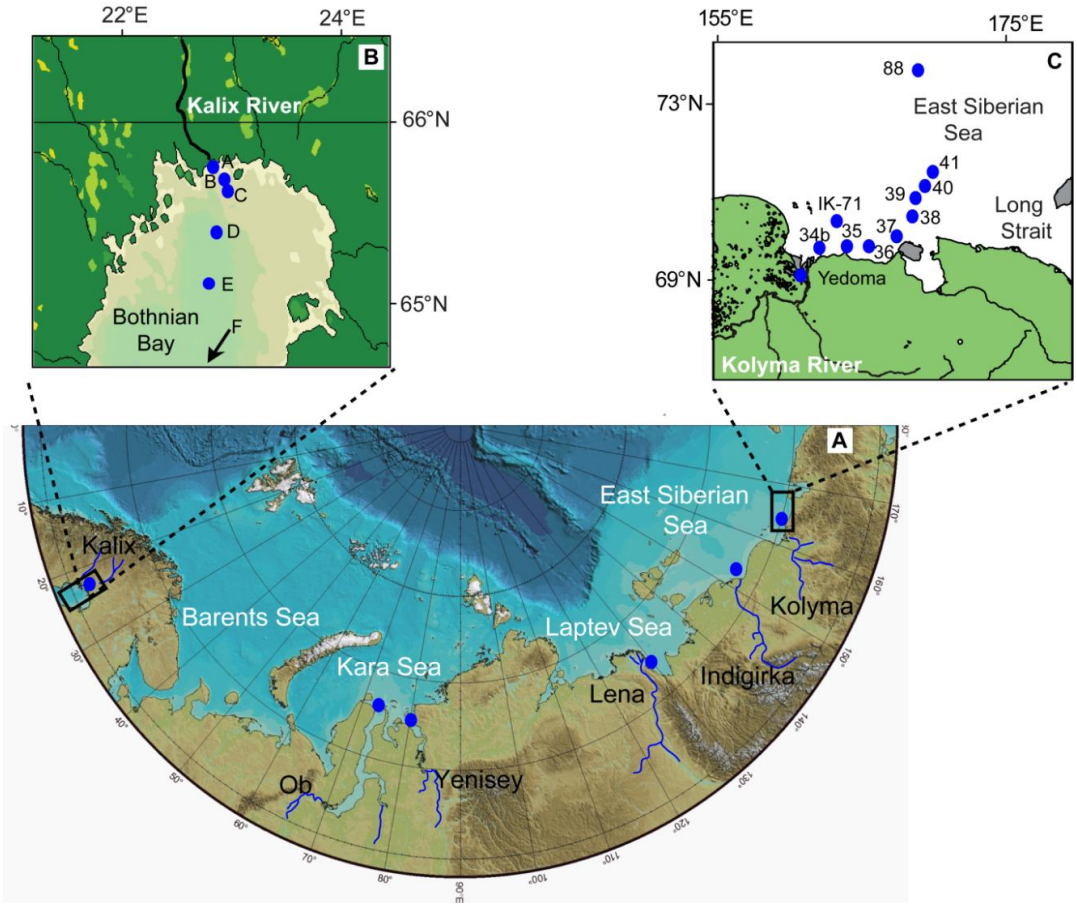

Figure 5. 1: Maps of (A) the Eurasian Arctic Region, (B) the Kalix River-Bothnian Bay region and (C) the Kolyma river- ESS transect showing approximate sampling locations (exact locations are given in Table 5.1).

Table 5. 1: Sample details of surface sediment samples from Kalix River–Bothnian Bay transect, GRARs and Kolyma River- ESS transect

Kalix River-Bothnian Bay transect [a]						
Sample ID	A	B	C	D	E	F
Longitude (N)	65°44	65°40	65°36	65°25	65°10	63°00'
Latitude (E)	23°20	23°26	23°25	23°19	23°14	22°51
Distance from river mouth (km)	13	22	29	50	78	304
TOC (mg/g dw)[e,f]	45.8	24.2	16.0	15.4	16.3	15.0
δ^{13}Csoc (‰)[e,g]	-27.1	-27.4	-27.3	-26.1	-25.8	-24.5
TN (mg/g dw) [e,h]	4.2	2.4	1.6	1.5	1.5	1.2
HMW *n* -alkanes (µg/g TOC)[e,i]	380	440	490	820	840	ND
HMW /LMW *n* -alkanes[e,j]	7.1	8.4	29.0	11.4	33.8	ND
TOC/TN[e,f,h]	10.9	10.1	10.0	10.3	10.9	12.5

GRARs						
	Kalix[a]	Ob[b]	Yenisey[b]	Lena[c]	Indigirka[d]	Koyma[d]
Sample ID	A	1	2	TB-30	IK-43	IK-71
Longitude (N)	65.44	72.65	72.61	71. 52	72.06	70.00
Latitude (E)	23.20	73.44	79.86	129.5	150.46	163.70
Basin Area (10^6 km^2)[k]	0.024	2.54-2.99	2.44-2.59	2.40-2.49	0.34-0.36	0.65-0.66
Water runoff (mm/yr)[l]	417.0	145.0	263.0	245.0	159.0	209.0
Discharge (km^3/yr)[l]	10.0	427.0	673.0	588.0	54.0	136.0
Wetland coverage (%)[m]	20.0	11.0	3.0	1.0	3.0	1.0
Continuous permafrost coverage(%)[n]	5.0	2.0	33.0	79	100.0	100.0
TOC (mg/g dw)[p,f]	45.8	9.2	19.4	20.4	14.6	17.3
δ^{13}Csoc (‰)[p,g]	-27.1	-27.4	-26.5	-26	-26.6	-26.7
TN (mg/g dw)[p,h]	4.2	0.9	1.9	1.36	0.99	1.1
HMW n-alkanes (µg/g OC)[p,i]	380	1800	910	604	1700	1200
TOC/TN[p,f,h]	10.9	10.0	10.5	15.0	14.7	15.9
C25/ C25+C29[p,r]	0.65	0.52	0.44	0.35	0.38	0.41
Lignin phenols concentration (mg/g OC)[s]	14.4	13.4	11.2	ND	21.4	22.8

Kolyma River-ESS transect [c]										
Sample ID	Yedoma	YS-34b	YS-35	YS-36	YS-37	YS-38	YS-39	YS-40	YS-41	YS-88
Longitude (N)	69.46	69.71	69.82	69.82	70.14	70.70	71.22	71.48	71.97	75.10
Latitude (E)	161.79	162.69	164.06	166.00	168.01	169.13	169.37	170.55	171.79	172.19
Distance from river mouth (km)	ND	46	100	174	258	334	392	443	513	720
TOC (mg/g dw)[t,f]	ND	11.2	12.2	8.02	9.4	10	12.3	13.6	13.2	10.4
δ^{13}Csoc[t,g]	ND	-27.3	-26.8	-26	-25.7	-25.3	-24.3	-23.9	-23.9	-21.5
TN (mg/g dw)[t,h]	ND	1.1	1.4	1.2	1.4	1.5	2.0	2.2	2.2	1.89
HMW *n* -alkanes(µg/g TOC)[t,i]	ND	1170	639	2820	1370	948	747	675	628	ND
HMW /LMW *n* -alkane[t,j]	ND	51.2	53.1	26.3	43.9	33.7	8.21	22.7	19	ND
TOC/TN[t,f,h]	ND	10.0	8.9	6.8	6.7	6.5	6.1	6.2	6.1	5.5
δ^{15}N (‰)[u]	ND	4.24	5.9	6.69	7.91	8.17	8.8	9.34	6.1	10.2
Lignin concentration (mg/g OC)[v]	240	28.4	16	10.8	5.9	6.4	3.2	1.7	2.1	ND

[a] Collected during ODEN cruise in 2005, [b] Collected during 3rd Russia-United States cruise in 2005, [c] Collected during the International Siberian Shelf Study expedition in 2008 and yedoma samples were collected in 2013, [d] Collected during the 2nd Russia-United States cruise in 2004, [e] Data from Vonk et al. (2008), [f] TOC = total organic carbon, [g] SOC = sedimentary organic carbon, [h] TN = total nitrogen, [i] HMW = High molecular weight (>C20), [j] LMW = low molecular weight(C17-19), [k] Data from Holmes et al (2002), Goordev et al. (1996) and Rachold (2004), [l] Data from Ingri et al. (2005), Holmes et al. (2013) and Stein and Macdonald (2004), [m] Data from Ingri et al. (2005) and 'watersheds of the world (http://archive.wri.org), [n] Data from Gustafsson et al. (2011), [p] Data from van Dongen et al. (2008), [r]Ratio of C25 to the sum of C25 and C29 *n*-alkanes, [s] Data from Feng et al. (2013), [t] Data from Vonk et al. (2010), [u] Data from Doğrul Selver (submitted), [v] Data from Tesi et al. (2014)

5.2.2. Pyrolysis-gas chromatography/ mass spectrometry

Dried, solvent extracted sediments were used for py–GC/MS analyses. All samples were analysed using an Agilent GC/ MSD system fitted with a CDS-5200 series pyrolysis unit setup in trap mode. Briefly, between 15 and 20 mg of sediment was weighted into 3 separate quartz sample tubes with a known amount of internal standard (5α-androstane) added to one of the tubes. All three samples were pyrolysed at 700°C for 20 seconds and loaded on the same trap. After pyrolysis of the third sample, the trap was unloaded at 320°C for 4 minutes and pyrolysis moieties were transferred to the gas chromatograph (GC) via a heated transfer line. Moieties were analysed using an Agilent 7890A GC fitted with a HP-5 fused capillary column (J+W Scientific; 5% diphenyl-dimethylpolysiloxane; 30 m length, 250 µm ID, 0.25 µm film thickness) coupled to an Agilent 5975 MSD single quadrupole mass spectrometer operating in electron ionization mode (scanning a range of m/z 50 to 650 at 2.7 scans second^{-1}; ionisation energy 70 eV). The pyrolysis transfer line and injector temperatures were set at 350°C, the heated interface at 280°C, the EI source at 230°C and the MS quadrupole at 150°C. Helium was used as the carrier gas and the samples were introduced in split mode (split ratio 5:1, constant flow of 5 ml/min). The oven was programmed from 40˚C (held for 5 min) to 250˚C at 4˚C min^{-1}, held at this temperature for 0 min before being heated to 300˚C at 20˚C min^{-1} and held at this temperature for 1 min.

Approximately 70 of the most abundant pyrolysis moieties were identified in each pyrogram (Figure 5S.1; Table 5S.1). Compounds were identified by comparison of retention times, NIST library and spectra to those reported in the literature (Schellekens et al., 2009; Vancampenhout et al., 2009). The major compounds were comparable in each pyrogram, although the relative proportions were different. Of all pyrolysis moieties analysed, following the method by Guo et al. (2009), an index set of 9

moieties was selected, divided into five different categories (Table 5.2) based on the nature and/or origin of the moiety, to show key difference between sediments. Comparable to Guo et al. (2004) the ion chromatogram of the most abundant ion in each of the 9 moieties was extracted from the total ion chromatogram. The area assigned to each selected moiety was equal to the area under the trace of the most abundant ion only. The percentage of total for each moiety/category was calculated by dividing the area of the individual moiety or summed area of the moieties in the same category by the sum of the areas of all 9 selected moieties for each sediment analysed (Guo et al., 2004; Guo et al., 2009; White and Beyer, 1999).

The selected categories were furfurals, alkylbenzenes, phenols, cyclopentanones, aromatics and pyridines. The approach used was not intended to represent all compounds present and the percentage of total determined is not directly related to the actual abundance of each category present but can be used to show difference between the sediments analysed.

Table 5. 2: List of most representative py- GC/MC moieties.

Compounds	Category	Class
Furfural, Methyl furfural	Furfurals	Carbohydrates
Dimethyl benzene	Alkylbenzenes	Aromatics
Phenol	Phenols	Phenols
Methylcyclopentanone	Cyclopentanones	Carbohydrates
Indene, naphtalene	Aromatics	Aromatics
Pyridine, Me-pyridine	Pyridines	N-containing compounds

5.3. Results

The Kalix river estuary sediment was the only sediment of all those collected along Eurasian Arctic climosequence that was dominated by furfurals (35% of total; Figure 5.2C and Table 5S.2). The relative abundance of furfurals in the other estuarine sediments was substantially lower, ranging from 7% in the Kolyma estuarine sediment to 14% in the Yenisey estuarine sediment. All other estuarine sediments were dominated by phenols, comprising from 47% in the Yenisey to 58% in the Indigirka and Kolyma estuarine sediments (Figure 5.3B and Table 5S.2). The relative abundance of phenols in the Kalix river sediment was 27%, substantially lower than in the other estuarine sediments. The relative abundances of the pyridines and alkylbenzenes were substantially lower and they varied between 10% and 24% and 6% and 9%, respectively (Figure 5.2B and Table 5S.2). Cyclopentanones were below detection limit in the Kalix and Ob estuarine sediments and comprised up to 3% in the other sediments.

In all sediments taken from the Kalix River-Bothnian Bay transect, furfurals were always the most abundant class of compounds present, followed by phenols and pyridines (Table 5S.2). Furfurals (35%) and phenols (27%) were the two most abundant classes in the sediment taken at station A, closest to the Kalix river mouth, followed by pyridines (18%), aromatics (12%) and minor contributions of alkylbenzenes and cyclopentanones (combined 8%; Figure 5.2A and Table 5S.2). Moving from station A to station F, in an off-river direction, the relative abundances of furfurals and pyridines increased to 43% and 22%, respectively, while the relative abundances of abundances of the phenols and aromatics dropped to 18% and 6%, respectively. The relative abundances of alkylbenzenes (between 7 and 9%) and cyclopentanone (between 0.5 and 1.3%) stayed relatively stable along the same transect (Figure 5.2A and Table 5S.2).

In the sediment closest to Kolyma River mouth (YS-34b), phenols comprised 50% of the total abundance followed by pyridines (15%), aromatics (13%) and furfurals (12%). Alkylbenzene and cyclopentanones together made up 10% of the total index of YS-34b sediment. This relative distribution pattern is comparable to the Yedoma samples taken from the Kolyma River watershed, which on average were also dominated by phenols (40%) , pyridines (24%) and furfurals (18%) with minor contributions of aromatics, alkylbenzene and cyclopentanones (combined 19%; Figure 5.2C and Table 5S.2). Along the Kolyma River-ESS transect, from station YS-34b to YS-41, although some variations were observed, the relative abundance of furfurals and pyridines generally increased from 12% to 29% and from 15% to 38%, respectively, whilst the abundance of the phenols decreased from 50% to 30% (Figure 5.3C and Table 5S.2). A slight decrease in the aromatics (13 – 7%) and alkylbenzenes (9 – 5%) abundances was also observed while cyclopentanone abundances did not show any significant change throughout the transect (Figure 5.2C and Table 5S.2). The surface sediment collected further offshore in the ESS (YS-88), was dominated by pyridines (53%) with lesser amount of aromatics (25%) and furfurals (21%; Figure 5.2C and Table 5S.2). Alkylbenzenes comprised only 1.5 % of the total fraction while phenols and cyclopentanones were below detection limit (Figure 5.2C and Table 5S.2).

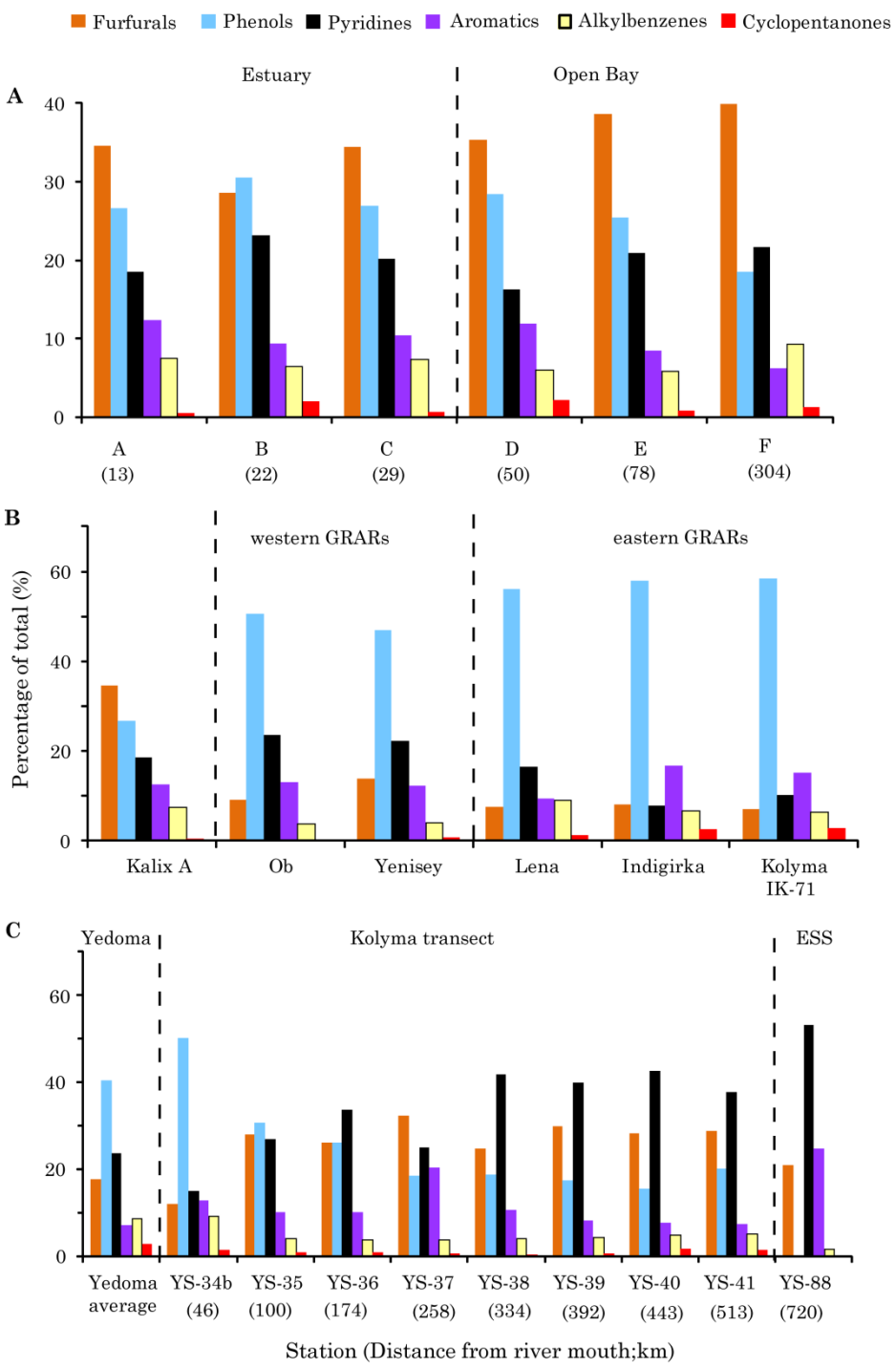

Figure 5. 2: Relative abundances (given as percentage of total) of categories present in surface sediments of (A) the Kalix River-Bothnian Bay transect, (B) river estuaries along the Eurasian Arctic climosequence from west to east and (C) the Kolyma River-ESS transect. Results of analyses of Yedoma and ESS sediment are given as end member composition.

5.4. Discussion

5.4.1. Terrestrial macromolecular organic carbon transported via the major Arctic rivers

Previous analyses have shown that the OC in the estuary sediments collected along the Eurasian Arctic climosequence are primarily of terrestrial origin (Cooke et al., 2009; Feng et al., 2013; Guo et al., 2004; van Dongen et al., 2008a). Bulk geochemical analyses of the same GRAR estuary sediments such as $\delta^{13}C_{SOC}$ (ranging between -25 and -27‰) and TOC/TN ratios (varying between 10 and 16) suggested a predominantly terrestrial origin of the OC present (van Dongen et al., 2008a). In addition, lipid analyses indicated a dominance of terrestrially derived biomarkers such as high molecular weight (HMW) *n*-alkanes, *n*-alcohols and *n*-alkanoic acids as well as branched glycerol dialkyl glycerol tetraethers and β-sitosterol in the same sediment set. Similarly, Cooke et al. (2009) analysed the bacteriohopanepolyol (BHP) compositions of the same estuarine sediments, which indicated a dominance of soil marker BHPs composing between 18% (Ob) and 37 % (Indigirka) of total BHPs, comparable to concentration observed in sediments close to Kalix River mouth (18%; Doğrul Selver et al., 2012) and Kolyma River mouth (30%; Doğrul Selver et al.,submitted), Feng et al. (2013) observed a high abundance of lignin phenols in these sediments again supporting a dominance of terrOC in these estuarine sediments. In addition, recent analyses revealed that the average lignin concentration in the Yedoma samples taken from the Kolyma River catchment (24 mg/g OC; Tesi et al., 2014) were comparable to the amount observed in the Kolyma estuarine sediment (IK-71, 28.4 mg/g OC; Feng et al., 2013). The similar relative macromolecular composition of the Yedoma samples and the Kolyma estuarine sediment (Figure 5.2C) observed in the present study supports the previous works.

Together these results indicate that the macromolecular compositions observed in all sediments close to the river mouths are predominantly terrestrial derived.

The most abundant compound classes in all sediments analysed were furfurals, phenols and pyridines (Figure 5.2B, Table 5S.2). Furfurals are derived from polysaccharides that can be associated with both terrestrial (Bracewell et al., 1980; Saiz-Jimenez and De Leeuw, 1986) and marine origins (Peulvé et al., 1996a; Van Heemst et al., 1996). The presence of substantial amounts of furfurals in estuarine sediments or particulate organic matter (POM) has been observed previously (Fabbri et al., 2005; Guo et al., 2004; Guo et al., 2009; Peulvé et al., 1996a; Peulvé et al., 1996b). Analyses of Arctic estuarine sediments, for example, indicated a high abundance of furfurals (>35%; Guo et al., 2004), while analyses of non-Arctic environment indicated a much lower relative abundance (7%; Fabbri et al., 2005).

Along the climosequence, the relative amount of furfurals was substantially higher in the western GRAR (9 – 14%) and Kalix Station A (35%) sediments if compared to the eastern GRAR sediments (7 – 8%). Relatively high amounts of carbohydrate pyrolysis moieties have been observed in sphagnum and sphagnum dominated peat (McClymont et al., 2011; Saiz-Jimenez and De Leeuw, 1986). Considering that sphagnum is the dominant vegetation cover in the western Eurasian Arctic region (Ingri et al., 2005; Parviainen and Luoto, 2007) it is not unlikely that this resulted in a relative high influx of carbohydrate derived macromolecular OC in this region.

The relative amounts of pyridines (22 – 24%) were also relatively higher in the western GRAR sediments compared to those of the eastern GRARs (8 – 17%). Pyridines are nitrogen containing compounds and are mainly derived from the pyrolysis of polypeptides (Bracewell and Robertson, 1984). They are mainly attributed to aquatic microorganisms however they can also be formed by microbial degradation of lignin (Buurman et al., 2007). The slight decrease in furfurals and pyridines from west to east,

contradicts the previous study by Guo (2004) where similar estuarine surface sediments were analysed across the Arctic climosequence. Briefly, they observed increasing furfural and decreasing nitrogen-containing compounds abundances from west to east. Based on the increasing furfural trend, it was suggested that surface sediments in the east were 'fresher' possibly due to the presence of continuous permafrost coverage (van Dongen et al., 2008a). The reason for conflicting results with Guo et al. (2004) remains unclear but may be due to different sampling times and locations.

Aromatics and alkylbenzenes did not show any significant change throughout the climosequence (Figure 5.2B). Aromatic compounds can be released from different parent macromolecules and have little diagnostic value for identifying biological precursors however have been observed abundantly in some estuary sediments (Fabbri et al., 2005). Cyclopentanones are, like furfurals, derived from polysaccharides (Saiz-Jimenez and De Leeuw, 1986) and suggested as being common in the pyrolysates of aquatic organic matter (Guo et al., 2009). However based on dissolved organic matter fraction analyses in the Mississippi River plume, Guo et al. (2009) suggested that cyclopentanones may also have other, non-aquatic, sources (Guo et al., 2009).

In contrast to furfurals and pyridines, relatively higher phenols abundances were observed the eastern GRAR estuarine sediments (56 – 58%) compared to those from the western river estuaries (27 – 50%). Phenols can have multiple terrestrial origins such as lignin and proteins (van Bergen et al., 1998) but can also be derived from algal polyphenols (van Heemst et al., 1999). Substantial amounts of phenolic compounds have been observed in surface sediments from the Lena Delta Peulve et al. (1996b). Similarly, Fabbri et al. (2005) found phenolic compounds that are up to 20% of the total in surface sediment taken close to Po River mouth, Italy. Considering the substantial amounts of lignin phenols in sediments from the ESS (Feng et al., 2013; Tesi et al., 2014), it is very

likely that the phenols observed in the estuary sediments are predominantly derived from lignin.

The relative abundance of lignin is generally high in higher plants (Sarkanen and Ludwig, 1972), particularly compared to for instance sphagnum, suggesting that phenols can be used as a marker for other (non - sphagnum) plants, such as shrubs, in this region. Previous research has indicated that the C25/C25+C29 *n*-alkane ratio can be used as a proxy for relative amounts of sphagnum present (Vonk and Gustafsson, 2009). This is based on the observations that the C25 *n*-alkane is abundant in sphagnum while higher plants are dominated by C29-C31 *n*-alkanes (Nott et al., 2000; Pancost et al., 2002; Vonk and Gustafsson, 2009). The relative amount of furfurals to the summed amounts of furfurals and phenol, furfurals/furfurals+phenol ratio, present in these estuarine sediments correlated well with the C25/C25+C29 ratio (r^2=0.77, p<0.05, n=6; Figure 5.3A), suggesting that the ratio of relative amounts of furfurals to phenols can indeed be used to determine the relative amounts of sphagnum present in the watersheds. In addition, it suggests that the macromolecular input in the western areas is dominated by sphagnum derived OC, while the OC in the eastern areas is predominantly from non sphagnum/ vascular plant dominated vegetation that is in line with the dominant vegetation cover in the Eurasian Arctic regions (Vonk and Gustafsson, 2009). In addition, increasing amount of lignin phenols (Feng et al., 2013) and plant wax lipids from west to east (van Dongen et al., 2008a) supports the decreasing sphagnum abundance in the eastern GRAR basins.

Correlating the furfurals/furfurals+phenols ratio with some hydrogeographical data (obtained from Feng et al., 2013) allow to infer about terrOC transport mechanisms and to deduce the affects of different environmental/geographical conditions on the macromolecular compositions in the different regions along the Eurasian Arctic climosequence.

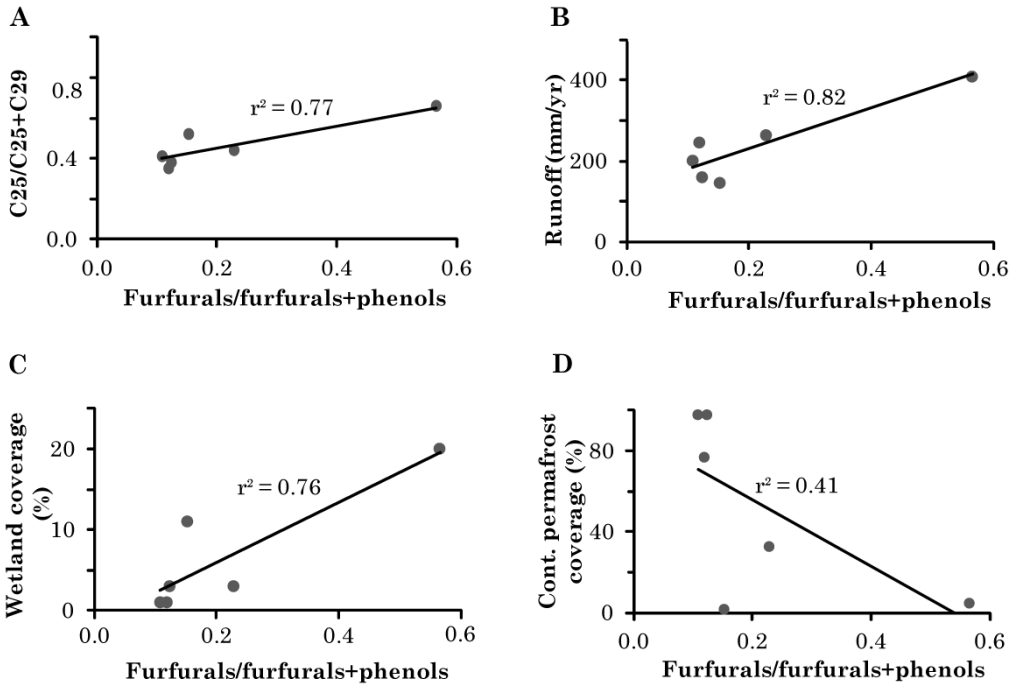

Figure 5. 3: Plots of the ratio of furfurals to phenols+furfurals vs.(A) the ratio of C25 vs. C25+C29 *n*-alkane (data from Gustafsson et al., 2011), (B) runoff, (C) wetland coverage and (D) continuous permafrost coverage (data from Gustafsson et al. (2011) of sediments taken in surface sediments from Kalix River and GRARs estuaries. Runoff and wetland coverage data from Ingri et al. (2005), Holmes et al. (2013) and Stein and Macdonald (2004).

The furfurals/furfurals+phenols ratio strongly correlates with runoff (r^2=0.82; p<0.05, n=6; Figure 5.3B) and wetland coverage (r^2=0.76, p<0.05, n=6; Figure 5.3C) likely indicating that these macromolecular fraction of terrOC may predominantly originate from the upper sections of contemporary wetlands drained by these rivers. In contrast, continuous permafrost coverage (r^2=0.41, p>0.05, n=6; Figure 5.3D) did not correlate with furfurals/furfurals+phenols ratio implying that, in contrast to earlier observations (Guo et al., 2004), permafrost does not have a major control on the transport of these macromolecular terrOC fractions.

5.4.2. Behaviour of macromolecules along river-ocean transects

5.4.2.1. Kolyma River-ESS transect

All Kolyma River-ESS transect sediment samples were dominated by furfurals, phenol and pyridines combined composing 75% (YS-37) to 87% (YS-39) of the total abundance. In an offshore direction, the relative phenol abundances decreased from 50% (at YS-34b) to 20% (at YS-41, Figure 5.4A). As mentioned previously, phenols could be derived from multiple terrestrial and marine sources. However a strong correlation with lignin concentrations, recently determined in the same sediments using the CuO oxidation method, (r^2=0.96, p<0.05, n=8; Figure 5.4B; Tesi et al., 2014) suggests that the phenols in these sediments are primarily lignin derived. In addition, phenols abundance moderately correlates with $\delta^{13}C_{SOC}$ values (r^2=0.66, p<0.05, n=8; Figure 5.4D) supporting the predominantly terrestrial origin. Considering that the phenols abundance was below detection limit in the sediment collected at YS-88, indicates that phenols were removed before the transported OC reaches this part of the open shelf.

Pyridines abundances increased from 15% to 38 % in an offshore direction along the same transect (Figure 5.4A) and dominated the sediment collected at station YS-88 (53%). The increasing pyridines abundance coincides with a shift towards more marine $\delta^{15}N$ values (r^2=0.74, p<0.05, n=8; Figure 5.4C) and $\delta^{13}C_{SOC}$ (r^2=0.71, p<0.05, n=8; Figure 5.4D). This suggests that, although pyridines were present in Yedoma samples, pyridines in these sediments were mainly of marine origin, indicating that, pyridines can be used as a 'pseudo marine' marker.

Along the Kolyma River-ESS transect, the relative abundance of furfurals increased from 12% to 29 % most likely caused by an increased marine contribution of carbohydrate material in an offshore direction. However, this increase was not uniform

and the relative abundance of furfurals in the sediment collected furthest offshore (YS-88) was considerably lower if compared to the end of the transect (YS-41). It is likely that local conditions/processes such increased annual sea ice cover could have reduce marine (polysaccharide) production further off shore.

Combined the trends observed for both the phenols and pyridines raises the possibility of using the phenols/(phenols+pyridines) ratio as a proxy to determine the relative proportion of marine versus terrestrial macromolecular OC input in these sediments. The phenols/(phenols+pyridines) ratio strongly correlate with other terrestrial vs. marine proxies such as the $\delta^{15}N$ (r^2=0.89, p<0.05, n=8; Figure 5.4E), TOC/TN ratio (r^2=0.89, p<0.05, n=8; Figure 5.4E), BIT (r^2=0.95, p<0.05, n=8; Figure 5.4F) and R'_{soil} indices (r^2=0.85, p<0.05, n=8; Figure 5.4F), and $\delta^{13}C_{SOC}$ (r^2=0.77, p<0.05, n=8; Figure 5.4G) suggesting that indeed this proxy could be used as a macromolecular proxy to trace terrOC in the marine environment. Assuming a terrestrial end-member phenols/(phenols+pyridines) ratio of 0.63, based on the average value of the Yedoma samples analysed, and a marine end-member value of 0, based on the value of YS-88, the relative percentage of terrestrial derived macromolecular OC can be determined (Figure 5.4H). Results indicate a reduction in the %terrOC in an offshore direction, resulting in around 50% terrOC about 400km out of the river. Except for the sediment taken from YS-34b, these percentages are comparable to the %terrOC values previously reported by using $\delta^{13}C$ and $\Delta^{14}C$ values (Figure 5.4H; Vonk et al., 2012). This suggests that, comparable to the bulk of the OC, a substantial part of the macromolecular terrOC is removed during transport along the shelf. In line with previous observations (Karlsson et al., 2011; Sánchez-García et al., 2011; van Dongen et al., 2008a; Vonk et al., 2012), this suggests a non-conservative behaviour for this part of the terrOC. However, the substantial differences observed in the YS-34b sediment raises the suspicion on using Yedoma as a sole terrestrial end-member.

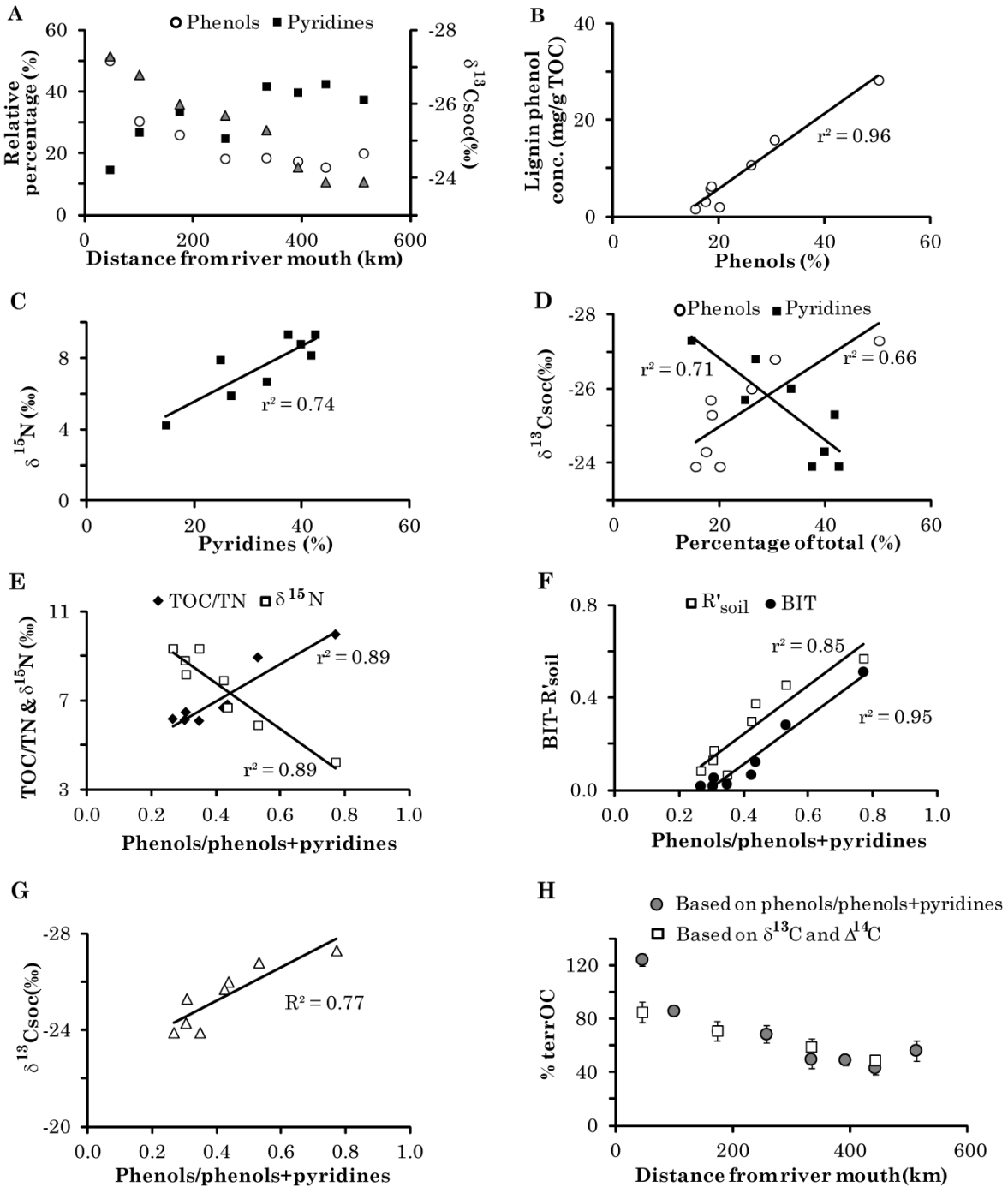

Figure 5. 4: Plots of (A) relative percentage of pyridines and phenols and δ^{13}Csoc versus distance from river mouth, (B) relative abundance of phenols vs. Lignin phenol (data from Tesi et al., 2014) concentration, (C) abundance of pyridines vs. δ^{15}N (data from Doğrul Selver et al.,submitted), (D) relative abundance of phenols and pyridines vs. δ^{13}Csoc (data from Vonk et al., 2010), and the ratio of phenols to phenols+pyridines vs. (E) TOC to TN and δ^{15}N , (F) R'_{soil} and BIT indices and (G) δ^{13}Csoc and (H) Phenol to pyridines and δ^{13}C - Δ^{14}C based (data from Vonk et al., 2012) % of terrOC plotted against distance from river mouth of sediments obtained from taken along the Kolyma River-ESS transect.

5.4.2.2. Kalix River-Bothnian Bay transect

Comparable to the Kolyma River-ESS transect, furfurals, phenols and pyridines were the most abundant compounds in all sediments along the Kalix River-Bothnian Bay transect, composing > 80% of the total. However, in contrast to Kolyma River-ESS transect, furfurals were the most abundant compounds in almost all of these sediments. This relatively high furfural abundance at the start of the transect is, as explained previously, most likely due to a high runoff in combination with a high percentage of sphangnum cover in the watershed. Considering that the abundance of furfurals increased towards open bay (35 to 43%, Figure 5.5A) in an off-river direction. This increased furfurals abundance coincided with a more marine $\delta^{13}C_{SOC}$ signature (r^2=0.82, p<0.05, n=6; Figure 5.5B) which may suggest an addition of marine derived polysaccharide material. However, considering fluvial input from other rivers into the Bothnian Bay, addition of other terrestrial derived polysaccharide material cannot be completely neglected.

In contrast to the furfurals and the trend observed in the Kolyma River-ESS transect, the relative pyridine abundances varied and overall increased only slightly (from 18% to 22% in an offshore direction). This slight increase might indicate a (increased) marine contribution, but given the potential terrestrial influx of other rivers, a predominant terrestrial origin throughout the transect cannot be completely excluded.

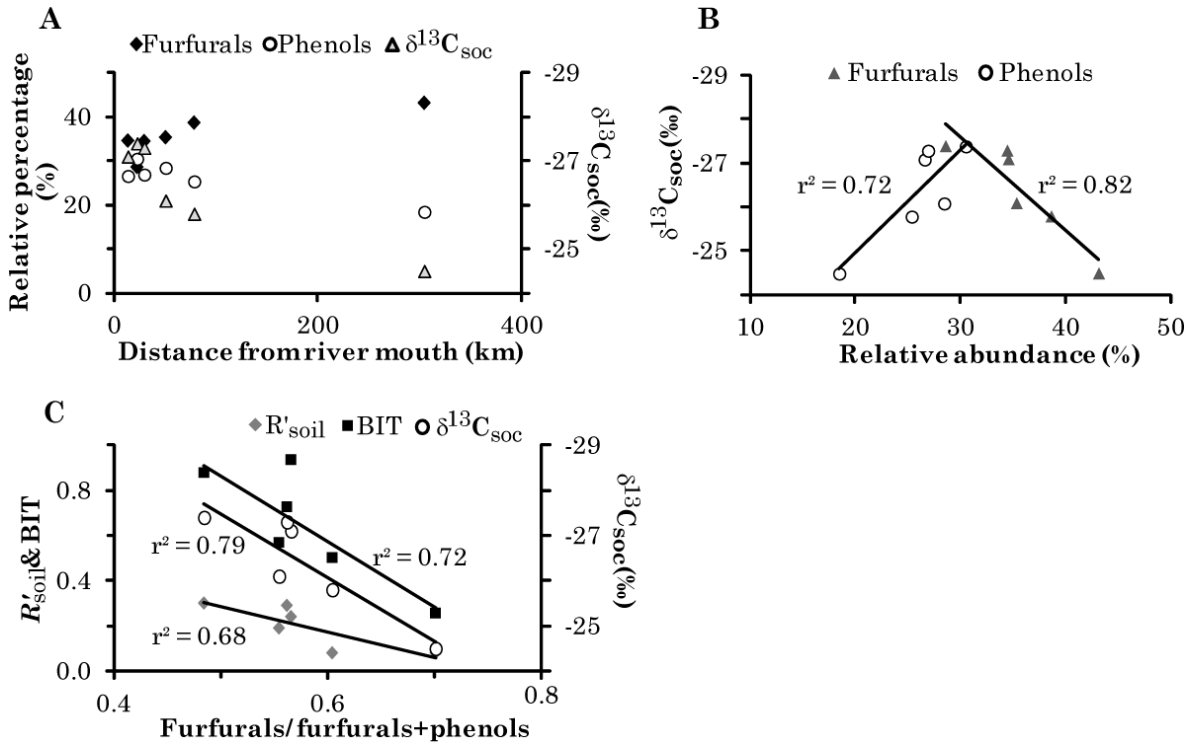

Figure 5. 5: Plots of the (A) relative percentage of furfurals, phenols and δ^{13}Csoc (data from Vonk et al. 2008) versus distance from river mouth, (B) relative abundance of furfurals and phenols vs. δ^{13}Csoc and (C) the ratio of furfurals to furfurals +phenols vs. R'_{soil} and BIT indices (data from Doğrul Selver et al., 2012) of sediments taken along the Kalix River Bothnian Bay transect.

Phenols revealed a decreasing abundance along the transect from 27% at station A to 18% at station F. The strong correlation with more marine $\delta^{13}C_{SOC}$ values (r^2=0.72, p<0.05, n=6; Figure 5.5B) suggest its terrestrial/plant origin most likely from lignin, comparable to the Kolyma River-ESS transect. Based on these indications, the furfurals/(furfurals+phenols) ratio was investigated for its applicability in defining marine versus terrOC input in the Kalix transect. Furfurals/ (furfurals+phenols) ratio correlated moderately/strongly with BIT, R'_{soil} (obtained from Doğrul Selver et al., 2012; r^2= 0.72 and 0.68, p<0.05, n=6; Figure 5.5C) and $\delta^{13}C_{SOC}$ (obtained from Vonk et al., 2010; r^2= 0.79; p<0.05, n=6; Figure 5.5C) indicating that it may be used as a proxy for marine versus terrOC contribution in this area. However, due to lack of endmember

values it remains to be seen exactly how much of the furfurals and phenols is marine and /or terrestrial derived.

5.5. Conclusions

The macromolecular composition analyses of estuary sediments from all GRARs indicate that the relative abundance of furfurals and pyridines decreased from west to east along Eurasian Arctic climosequence, while the phenol abundance increased. Analyses indicated that the wetland coverage (sphagnum vs higher plants) and river runoff are likely to be the main controlling factors influencing the terrestrial macromolecular composition in the GRAR estuaries while the presence/absence of continuous permafrost type does not have any effect.

Along both the Kalix River-Bothnian Bay and Kolyma River-ESS transects compound classes followed the same trends with furfurals and pyridines showing increasing while phenols showing decreasing trends in an off-river direction. Based on the phenols and pyridines trends observed, a phenols to pyridines ratio was investigated for its potential to be used as a new proxy to trace macromolecular terrOC in the Eurasian Arctic Region. This proxy showed a strong correlation with other terrestrial versus marine proxies ($\delta^{13}C_{SOC}$,$\delta^{15}N$, BIT and R'_{soil}) along the same transect suggesting that it can indeed can be used as a proxy to trace macromolecular terrOC in the Arctic region. The analyses indicate that a substantial part of the macromolecular terrOC is removed during transport along the shelf. In line with previous observations this suggests a non-conservative behaviour for this part of the terrOC.

Acknowledgements

We gratefully acknowledge receipt of a PhD studentship to ADS funded by the Ministry of National Education of Turkey and financial support as an Academy Research Fellow to ÖG from the Swedish Royal Academy of Sciences through a grant from the Knut and Alice Wallenberg Foundation. We thank all colleagues in the International Siberian Shelf Study (ISSS); third and fourth Russia-United States and ODEN cruises for sampling. We thank H. Jones (University of Manchester) for assistance with py/GC-MS, T. Tesi for providing the Yedoma samples for the Kolyma catchment area.

Supplementary data

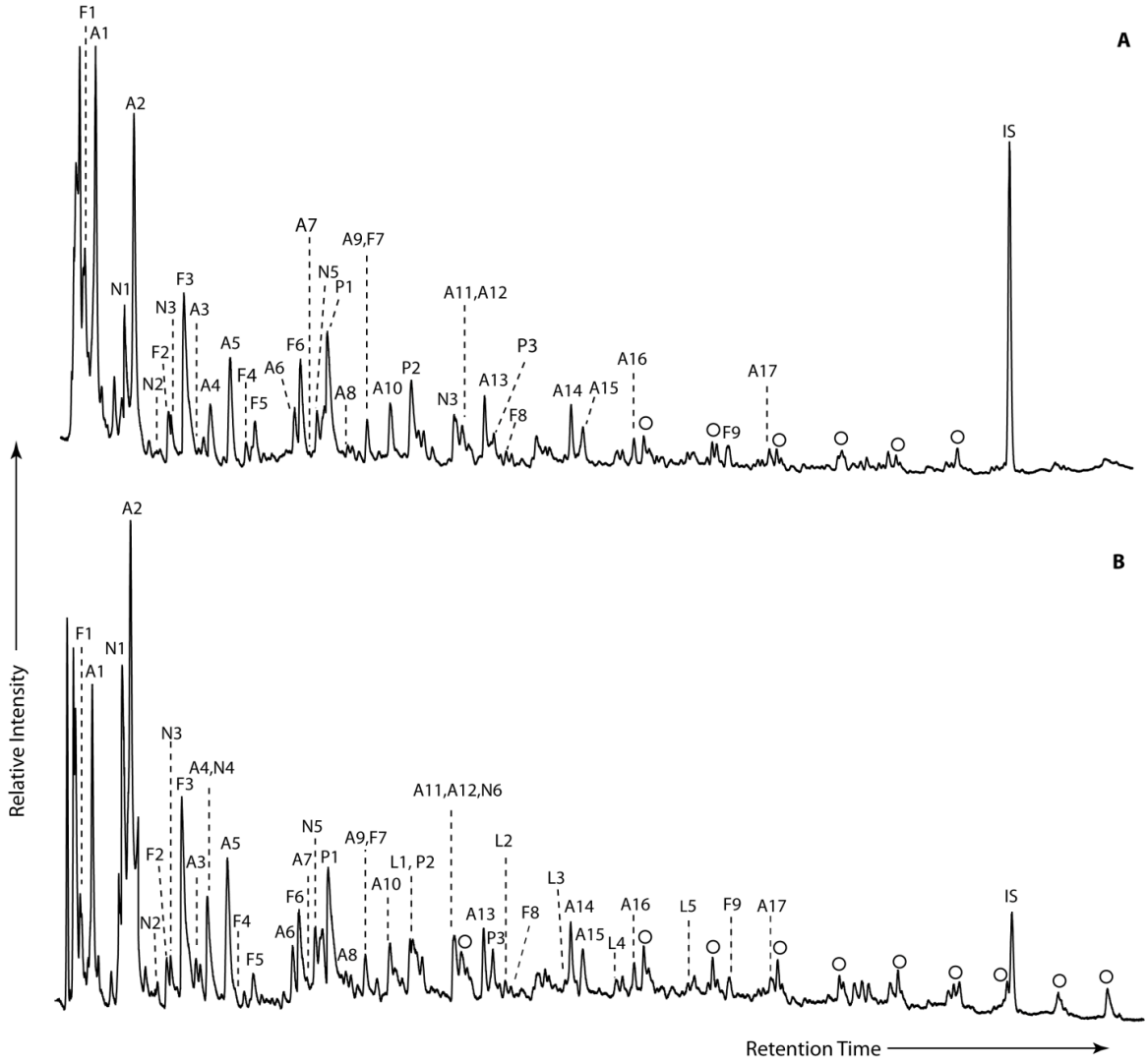

Figure 5S. 1 Partial py-GC/MS total ion pyrogram of surface sediments from (A) Kalix River-Bothnian Bay transect (Station A) and (B) Kolyma River-ESS transect (station YS-36). Peak assignments are given in Table 5S.1. IS: Internal standard, ○: *n*-alkane/alkene doublets.

Table 5S. 1: List of py-GC/MS moieties found in the sediment samples including compound code, compound name, masses and average retention times (RT).

Code	Name	Masses	RT	Code	Name	Masses	RT
	Polysaccharide Compounds				*Lipids*		
F1	3-methyl furan	82,53	2.39		C11 alkane	57,71	17.54
F2	3-furaldehyde	95,96	6.22		C12 alkane	57,71	21.29
F3	2-furaldehyde (furfural)	96,95	6.89		C13 alkane	57,71	24.79
F4	2-Methyl-2-cyclopentanone	67,96	9.72		C14 alkane	57,71	28.06
F5	Acetylfuran	110,109	10.15		C15 alkane	57,71	31.15
F6	5-methyl furfural	110,109	12.2		C16 alkane	57,71	34.07
F7	2,3-Dimethyl-2-cyclopentanone	67,110	15.32		C17 alkane	57,71	36.85
F8	4,7-dimethyl-benzofuran,	146,145	21.81		C18 alkane	57,71	39.49
F9	Dibenzofuran	168,139	31.65		C19 alkane	57,71	42.02
	Aromatics-PAHs				C20 alkane	57,71	44.38
A1	Benzene	78,77	2.85		C21 alkane	57,71	46.67
A2	Toluene	91,92	4.59		C22 alkane	57,71	48.85
A3	Ethyl benzene	91,106	7.75		C23 alkane	57,71	51.01
A4	1,2 dimethyl benzene	91,106	8.06		C24 alkane	57,71	53.02
A5	Styrene	104,103	9.03		C11 alkene	55,69	17.21
A6	Benzaldehyde	77,106	11.92		C12 alkene	55,69	20.99
A7	Ethyl-methyl benzene	105,120	12.58		C13 alkene	55,69	24.5
A8	Trimethyl benzene	105, 120	14.31		C14 alkene	55,69	27.8
A9	Indene	116, 115	15.16		C15 alkene	55,69	30.9
A10	Acetophenone	105,77	16.28		C16 alkene	55,69	33.87
A11	Tetramethyl benzene	119,134	19.46		C17 alkene	55,69	36.65
A12	3-methyl-indene	130, 115	19.53		C18 alkene	55,69	39.3
A13	Napthalene	128	20.59		C19 alkene	55,69	41.83
A14	2-me napthalene	142,141	24.50		C20 alkene	55,69	44.26
A15	1-me napthalene	142,141	25.07		C21 alkene	55,69	46.53
A16	Biphenyl	154	27.32		C22 alkene	55,69	48.77
A17	Fluorene	166,165	33.54		C23 alkene	55,69	50.95
	Protein/Lignin markers				C24 alkene	55,69	52.86
P1	Phenol	94,66	13.44		*Lignin compounds*		
P2	3-methyl phenol	108,107	17.42	L1	Guaiacol	109, 124	17.23
P3	Dimethyl phenol	122,107	21.03	L2	4-methyl guaiacol	123, 138	21.23
	N-containing compounds			L3	4-ethyl 2-methoxy phenol	137, 152	24.25
N1	Pyridine	79,52	4.25	L4	4-vinyl 2-methoxy phenol	135, 150	25.58
N2	2-Furan carbonitrile	93,64	5.83	L5	Isoeugenol	164,77	29.9
N3	Me-pyridine	93,66	6.43	L6	Dimethoxy propenyl phenol	194, 91	37.19
N4	Me-pyridine	94,66	8.03				
N5	Benzonitrile	103,76	12.94				
N6	Benzyl nitrile	117,90	19.22				

Table 5S. 2: Relative abundance of compound classes (%) in surface sediments along the Kalix River-Bothnian Bay transect, across the Arctic climosequence and Yedoma-Kolyma River-ESS transect.

	Furfurals	Phenols	Pyridines	Aromatics	Alkylbenzenes	Cyclopentanones
Kalix River-Bothnian Bay transect						
A	35	27	18	12	7	0.5
B	29	31	23	9	6	2.0
C	34	27	20	10	7	0.6
D	35	28	16	12	6	2.2
E	39	25	21	8	6	0.8
F	43	18	22	6	9	1.3
Arctic Climosequence						
Kalix	35	27	18	12	7	0.5
Ob	9	50	24	13	4	BDL
Yenisey	14	47	22	12	4	1
Lena	8	56	17	9	9	1
Indigirka	8	58	8	17	7	3
Kolyma	7	58	10	15	6	3
Yedoma-Kolyma River-ESS transect						
Yedoma deep	19	47	20	6	5	3
Yedoma middle	19	38	28	8	4	2
Yedoma shalllow	15	36	23	7	16	2
Yedoma average	18	40	24	7	9	3
YS-34b	12	50	15	13	9	1.2
YS-35	28	30	27	10	4	0.7
YS-36	26	26	34	10	4	0.8
YS-37	32	18	25	20	4	0.7
YS-38	25	19	42	11	4	0.2
YS-39	30	17	40	8	4	0.7
YS-40	28	16	43	8	5	1.7
YS-41	29	20	38	7	5	1.3
YS-88	21	BDL	53	25	2	BDL

BDL: below detection limit

References

Amante, C. and Eakins, B.W., 2009. ETOPO1 1 Arc-Minute Global Relief Model: Procedures, Data Sources and Analysis. NOAA Technical Memorandum NESDIS NGDC-24. National Geophysical Data Center, NOAA.

Aagaard, K., Carmack, E.C., 1989. The Role of Sea Ice and Other Fresh Water in the Arctic Circulation. J. Geophys. Res. 94, 14485-14498.

AMAP, 2013. AMAP Assessment 2013: Arctic Ocean Acidification. Arctic Monitoring and Assessment Programme (AMAP). viii pp. + 99 pp., Oslo, Norway.

Belicka, L.L., Harvey, H.R., 2009. The sequestration of terrestrial organic carbon in Arctic Ocean sediments: A comparison of methods and implications for regional carbon budgets. Geochimica et Cosmochimica Acta 73, 6231-6248.

Benner, R., Louchouarn, P., Amon, R.M.W., 2005. Terrigenous dissolved organic matter in the Arctic Ocean and its transport to surface and deep waters of the North Atlantic. Global Biogeochemical Cycles 19, GB2025.

Bracewell, J.M., Robertson, G.W., 1984. Quantitative comparison of the nitrogen-containing pyrolysis products and amino acid composition of soil humic acids. Journal of Analytical and Applied Pyrolysis 6, 19-29.

Bracewell, J.M., Robertson, G.W., Welch, D.I., 1980. Polycarboxylic acids as the origin of some pyrolysis products characteristics of soil organic matter. Journal of Analytical and Applied Pyrolysis 2, 239-248.

Buurman, P., Peterse, F., Almendros Martin, G., 2007. Soil organic matter chemistry in allophanic soils: a pyrolysis-GC/MS study of a Costa Rican Andosol catena. European Journal of Soil Science 58, 1330-1347.

Cooke, M.P., van Dongen, B.E., Talbot, H.M., Semiletov, I., Shakhova, N., Guo, L., Gustafsson, Ö., 2009. Bacteriohopanepolyol biomarker composition of organic matter exported to the Arctic Ocean by seven of the major Arctic rivers. Organic Geochemistry 40, 1151-1159.

Doğrul Selver, A., Sparkes, R.B., Bischoff, J., Talbot, H.M., Gustafsson, Ö., Semiletov, I.P., Dudarev, O.V., Boult, S., van Dongen, B.E., submitted. Distributions of bacterial and archaeal membrane lipids in surface sediments along the Kolyma Palaeoriver transect, East Siberian Sea.

Doğrul Selver, A., Talbot, H.M., Gustafsson, Ö., Boult, S., van Dongen, B.E., 2012. Soil organic matter transport along an sub-Arctic river- sea transect. Organic Geochemistry 51, 63-72.

Drenzek, N.J., Montluçon, D.B., Yunker, M.B., Macdonald, R.W., Eglinton, T.I., 2007. Constraints on the origin of sedimentary organic carbon in the Beaufort Sea from coupled molecular ^{13}C and ^{14}C measurements. Marine Chemistry 103, 146-162.

Fabbri, D., Sangiorgi, F., Vassura, I., 2005. Pyrolysis-GC-MS to trace terrigenous organic matter in marine sediments: a comparison between pyrolytic and lipid markers in the Adriatic Sea. Analytica Chimica Acta 530, 253-261.

Feng, X., Vonk, J.E., van Dongen, B.E., Gustafsson, Ö., Semiletov, I.P., Dudarev, O.V., Wang, Z., Montluçon, D.B., Wacker, L., Eglinton, T.I., 2013. Differential mobilization of terrestrial carbon pools in Eurasian Arctic river basins. Proceedings of the National Academy of Sciences.

Fernandes, M.B., Sicre, M.A., 2000. The importance of terrestrial organic carbon inputs on Kara Sea shelves as revealed by *n*-alkanes, OC and $\delta^{13}C$ values. Organic Geochemistry 31, 363-374.

Gordeev, V.V., Martin, J.M., Sidorov, I.S., Sidorova, M.V., 1996. A reassessment of the Eurasian river input of water, sediment, major elements, and nutrients to the Arctic Ocean. American Journal of Science 296, 664-691.

Guo, L., Semiletov, I., Gustafsson, Ö., Ingri, J., Andersson, P., Dudarev, O., White, D., 2004. Characterization of Siberian Arctic coastal sediments: Implications for terrestrial organic carbon export. Global Biogeochemical Cycles 18, GB1036.

Guo, L., White, D.M., Xu, C., Santschi, P.H., 2009. Chemical and isotopic composition of high-molecular-weight dissolved organic matter from the Mississippi River plume. Marine Chemistry 114, 63-71.

Gustafsson, Ö., van Dongen, B.E., Vonk, J.E., Dudarev, O.V., Semiletov, I.P., 2011. Widespread release of old carbon across the Siberian Arctic echoed by its large rivers. Biogeosciences 8, 1737-1743.

Gustafsson, Ö., Widerlund, A., Andersson, P.S., Ingri, J., Roos, P., Ledin, A., 2000. Colloid dynamics and transport of major elements through a boreal river - brackish bay mixing zone. Marine Chemistry 71, 1-21.

Hedges, J.I., Keil, R.G., 1995. Sedimentary organic matter preservation: an assessment and speculative synthesis. Marine Chemistry 49, 81-115.

Holmes, R., McClelland, J., Peterson, B., Tank, S., Bulygina, E., Eglinton, T., Gordeev, V., Gurtovaya, T., Raymond, P., Repeta, D., Staples, R., Striegl, R., Zhulidov, A., Zimov, S., 2011. Seasonal and Annual Fluxes of Nutrients and Organic Matter from Large Rivers to the Arctic Ocean and Surrounding Seas. Estuaries and Coasts 35, 369-382.

Ingri, J., Widerlund, A., Land, M., 2005. Geochemistry of Major Elements in a Pristine Boreal River System; Hydrological Compartments and Flow Paths. Aquatic Geochemistry 11, 57-88.

Ingri, J., Widerlund, A., Land, M., Gustafsson, Ö., Andersson, P., Ã–hlander, B.r., 2000. Temporal variations in the fractionation of the rare earth elements in a boreal river; the role of colloidal particles. Chemical Geology 166, 23-45.

IPCC, 2007. Climate Change 2007: the physical science basis (Ed. by S. Solomon, D. Qin, M. Manning, Z. Chen, M. Marquis, K.B. Averyt, M. Tignor and H.L. Miller (eds.)), pp. 996, Cambridge, United Kingdom.

IPCC, 2013. Climate Change 2013: The Physical Science Basis. Contribution of Working Group I to the Fifth Assessment Report of the Intergovernmental Panel on Climate Change (Ed. by T.F. Stocker, D. Qin, G.-K. Plattner, M. Tignor, S.K. Allen, J. Boschung, A. Nauels, Y. Xia, V. Bex and P.M. Midgley), pp. 1535 pp.

Karlsson, E.S., Charkin, A., Dudarev, O.V., Semiletov, I.P., Vonk, J.E., Sánchez-García, L., Andersson, A., Gustafsson, Ö., 2011. Carbon isotopes and lipid biomarker investigation of sources, transport and degradation of terrestrial organic matter in the Buor-Khaya Bay, SE Laptev Sea. Biogeosciences 8, 1865-1879.

Kremenetski, K.V., Velichko, A.A., Borisova, O.K., MacDonald, G.M., Smith, L.C., Frey, K.E., Orlova, L.A., 2003. Peatlands of the Western Siberian lowlands: current knowledge on zonation, carbon content and Late Quaternary history. Quaternary Science Reviews 22, 703-723.

McClelland, J.W., Holmes, R.M., Peterson, B.J., Stieglitz, M., 2004. Increasing river discharge in the Eurasian Arctic: Consideration of dams, permafrost thaw, and fires as potential agents of change. Journal of Geophysical Research 109, D18102.

McClymont, E.L., Bingham, E.M., Nott, C.J., Chambers, F.M., Pancost, R.D., Evershed, R.P., 2011. Pyrolysis GC–MS as a rapid screening tool for determination of peat-forming plant composition in cores from ombrotrophic peat. Organic Geochemistry 42, 1420-1435.

Milliman, J.D., Farnsworth, K.L., Albertin, C.S., 1999. Flux and fate of fluvial sediments leaving large islands in the East Indies. Journal of Sea Research 41, 97-107.

Mitchell, J.F.B., 1989. The "Greenhouse" effect and climate change. Reviews of Geophysics 27, 115-139.

Nott, C.J., Xie, S., Avsejs, L.A., Maddy, D., Chambers, F.M., Evershed, R.P., 2000. n-Alkane distributions in ombrotrophic mires as indicators of vegetation change related to climatic variation. Organic Geochemistry 31, 231-235.

Opsahl, S., Benner, R., Amon, R.M.W., 1999. Major Flux of Terrigenous Dissolved Organic Matter Through the Arctic Ocean. Limnology and Oceanography 44, 2017-2023.

Pancost, R.D., Baas, M., van Geel, B., Sinninghe Damsté, J.S., 2002. Biomarkers as proxies for plant inputs to peats: an example from a sub-boreal ombrotrophic bog. Organic Geochemistry 33, 675-690.

Parviainen, M., Luoto, M., 2007. Climate envelopes of mire complex types in Fennoscandia Geografiska Annaler: Series A, Physical Geography 89, 137-151.

Peterson, B.J., Holmes, R.M., McClelland, J.W., Vörösmarty, C.J., Lammers, R.B., Shiklomanov, A.I., Shiklomanov, I.A., Rahmstorf, S., 2002. Increasing River Discharge to the Arctic Ocean. Science 298, 2171-2173.

Peulvé, S., Leeuw, J.W.d., Sicre, M.A., Baas, M., Saliot, A., 1996a. Characterization of macromolecular organic matter in sediment traps from the northwestern Mediterranean Sea. Geochimica et Cosmochimica Acta 60, 1239-1259.

Peulvé, S., Sicre, M., Saliot, A., De Leeuw, J., Baas, M., 1996b. Molecular characterization of suspended and sedimentary organic matter in an Arctic delta. Limnol. Oceanogr 41, 488-497.

Rachold, V., Eicken, H., Gordeev, V.V., Grigoriev, M.N., Hubberten, H.W., Lisitzin, A.P., Shevchenko, V.P., Schirrmeister, L., 2004. Modern Terrigenous Organic Carbon Input to the Arctic Ocean. In: R. Stein, R. MacDonald (Eds.), The Organic Carbon Cycle in the Arctic Ocean (Ed. by R. Stein, R. MacDonald), pp. 33-55. Springer Berlin Heidelberg.

Raval, A., Ramanathan, V., 1989. Observational determination of the greenhouse effect. Nature 342, 758-761.

Raymond, P.A., McClelland, J.W., Holmes, R.M., Zhulidov, A.V., Mull, K., Peterson, B.J., Striegl, R.G., Aiken, G.R., Gurtovaya, T.Y., 2007. Flux and age of dissolved organic carbon exported to the Arctic Ocean: A carbon isotopic study of the five largest arctic rivers. Global Biogeochemical Cycles 21, GB4011.

Saiz-Jimenez, C., De Leeuw, J.W., 1986. Chemical characterization of soil organic matter fractions by analytical pyrolysis-gas chromatography-mass spectrometry. Journal of Analytical and Applied Pyrolysis 9, 99-119.

Sánchez-García, L., Alling, V., Pugach, S., Vonk, J., van Dongen, B.E., Humborg, C., Dudarev, O., Semiletov, I., Gustafsson, Ö., 2011. Inventories and behavior of particulate organic carbon in the Laptev and East Siberian seas. Global Biogeochemical Cycles 25, GB2007.

Sarkanen, K.V., Ludwig, C.H., 1972. Lignins: Occurrence, formation, structure and reactions, Eds., John Wiley & Sons, Inc., New York, 1971. 916 pp. John Wiley & Sons, Inc.

Schellekens, J., Buurman, P., Pontevedra-Pombal, X., 2009. Selecting parameters for the environmental interpretation of peat molecular chemistry - A pyrolysis-GC/MS study. Organic Geochemistry 40, 678-691.

Schlünz, B., Schneider, R.R., 2000. Transport of terrestrial organic carbon to the oceans by rivers: re-estimating flux- and burial rates. International Journal of Earth Sciences 88, 599-606.

Schuur, E.A.G., Bockheim, J., Canadell, J.G., Euskirchen, E., Field, C.B., Goryachkin, S.V., Hagemann, S., Kuhry, P., Lafleur, P.M., Lee, H., Mazhitova, G., Nelson, F.E., Rinke, A., Romanovsky, V.E., Shiklomanov, N., Tarnocai, C., Venevsky, S., Vogel, J.G., Zimov, S.A., 2008. Vulnerability of Permafrost Carbon to Climate Change: Implications for the Global Carbon Cycle. BioScience 58, 701-714.

Serreze, M.C., Walsh, J.E., Chapin, F.S., Osterkamp, T., Dyurgerov, M., Romanovsky, V., Oechel, W.C., Morison, J., Zhang, T., Barry, R.G., 2000. Observational Evidence of Recent Change in the Northern High-Latitude Environment. Climatic Change 46, 159-207.

Stein, R., MacDonald, R.W., 2004. The Organic Carbon Cycle in the Arctic Ocean. Springer, Berlin.

Tarnocai, C., Canadell, J.G., Schuur, E.A.G., Kuhry, P., Mazhitova, G., Zimov, S., 2009. Soil organic carbon pools in the northern circumpolar permafrost region. Global Biogeochemical Cycles 23, GB2023.

Tesi, T., Semiletov, I., Hugelius, G., Dudarev, O., Kuhry, P., Gustafsson, Ö., 2014. Composition and fate of terrigenous organic matter along the Arctic land- ocean continuum in East Siberia: Insights from biomarkers and carbon isotopes. 133, pp. 235-256.

van Bergen, P.F., Nott, C.J., Bull, I.D., Poulton, P.R., Evershed, R.P., 1998. Organic geochemical studies of soils from the Rothamsted Classical Experiments- IV. Preliminary results from a study of the effect of soil pH on organic matter decay. Organic Geochemistry 29, 1779-1795.

van Dongen, B.E., Semiletov, I., Weijers, J.W.H., Gustafsson, Ö., 2008a. Contrasting lipid biomarker composition of terrestrial organic matter exported from across the Eurasian Arctic by the five great Russian Arctic rivers. Global Biogeochemical Cycles 22, GB1011.

van Dongen, B.E., Zencak, Z., Gustafsson, Ö., 2008b. Differential transport and degradation of bulk organic carbon and specific terrestrial biomarkers in the surface waters of a sub-arctic brackish bay mixing zone. Marine Chemistry 112, 203-214.

Van Heemst, J.D.H., Peulve, S., De Leeuw, J.W., 1996. Novel algal polyphenolic biomacromolecules as significant contributors to resistant fractions of marine dissolved and particulate organic matter. Organic Geochemistry 24, 629-640.

van Heemst, J.D.H., van Bergen, P.F., Stankiewicz, B.A., de Leeuw, J.W., 1999. Multiple sources of alkylphenols produced upon pyrolysis of DOM, POM and recent sediments. Journal of Analytical and Applied Pyrolysis 52, 239-256.

Vancampenhout, K., Wouters, K., De Vos, B., Buurman, P., Swennen, R., Deckers, J., 2009. Differences in chemical composition of soil organic matter in natural ecosystems from different climatic regions: A pyrolysis- GC/MS study. Soil Biology and Biochemistry 41, 568-579.

Vonk, J.E., Gustafsson, Ö., 2009. Calibrating n-alkane Sphagnum proxies in sub-Arctic Scandinavia. Organic Geochemistry 40, 1085-1090.

Vonk, J.E., Mann, P.J., Davydov, S., Davydova, A., Spencer, R.G.M., Schade, J., Sobczak, W.V., Zimov, N., Zimov, S., Bulygina, E., Eglinton, T.I., Holmes, R.M., 2013a. High biolability of ancient permafrost carbon upon thaw. Geophysical Research Letters 40, 2689-2693.

Vonk, J.E., Mann, P.J., Dowdy, K.L., Davydova, A., Davydov, S.P., Zimov, N., Spencer, R.G.M., Bulygina, E.B., Eglinton, T.I., Holmes, R.M., 2013b. Dissolved organic carbon loss from Yedoma permafrost amplified by ice wedge thaw. Environmental Research Letters 8, 035023.

Vonk, J.E., Sánchez-García, L., Semiletov, I.P., Dudarev, O.V., Eglinton, T.I., Andersson, A., Gustafsson, Ö., 2010. Molecular and radiocarbon constraints on sources and degradation of terrestrial organic carbon along the Kolyma paleoriver transect, East Siberian Sea. Biogeosciences 7, 3153-3166.

Vonk, J.E., Sanchez-Garcia, L., van Dongen, B.E., Alling, V., Kosmach, D., Charkin, A., Semiletov, I.P., Dudarev, O.V., Shakhova, N., Roos, P., Eglinton, T.I., Andersson, A., Gustafsson, Ö., 2012. Activation of old carbon by erosion of coastal and subsea permafrost in Arctic Siberia. Nature 489, 137-140.

Vonk, J.E., van Dongen, B.E., Gustafsson, Ö., 2008. Lipid biomarker investigation of the origin and diagenetic state of sub-arctic terrestrial organic matter presently exported into the northern Bothnian Bay. Marine Chemistry 112, 1-10.

White, D., Beyer, L., 1999. Pyrolysis-gas chromatography/mass spectrometry and pyrolysis-gas chromatography/flame ionization detection analysis of three Antarctic soils. Journal of Analytical and Applied Pyrolysis 50, 63-76.

Yunker, M.B., Macdonald, R.W., Veltkamp, D.J., Cretney, W.J., 1995. Terrestrial and marine biomarkers in a seasonally ice-covered Arctic estuary -- integration of multivariate and biomarker approaches. Marine Chemistry 49, 1-50.

Zimov, S.A., Schuur, E.A.G., Chapin, F.S., 2006. Permafrost and the Global Carbon Budget. Science 312, 1612-1613.

CHAPTER 6

Conclusions and future work

6.1. Conclusions

The main objectives of this work were to (i) characterise GDGTs and BHPs compositions in surface sediments along the Eurasian (sub)-Arctic river-shelf transects as well as in surface sediments from across the ESS and compare the related BIT and R_{soil} indices with other previously published terrestrial vs marine proxies and (ii) analyse the macromolecular composition of surface sediments from the estuaries along an Eurasian Arctic climosequence as well as along two (sub)-Arctic River-ocean transects and to compare the macromolecular compositions of terrOC transported from the areas with and without permanent permafrost.

In summary this work showed that:

- Analyses of GDGTs and BHPs in sediments from the Eurasian (sub)-Arctic regions revealed that these microbial lipids are present in all sediment samples analysed. A general relative decrease in soil/terrestrial marker compounds and

associated increase in marine marker compounds can be observed along transects of the shoreline/ river mouths.

- GDGT and BHP related indices (BIT and R_{soil}) can be used in the (sub)-Arctic Region to trace terrOC in the marine realm, however a slight modification in the R_{soil} index was suggested (R'_{soil}) for use in the Arctic Region. Similar to other proxies, such as $\delta^{13}C_{SOC}$ and $\delta^{15}N$, BIT and R'_{soil} indices show decreasing trends along river/shoreline-ocean transects in line with a non-conservative behaviour of the terrOC.
- Results from analyses across the ESS suggest that the behaviour of BIT and R'_{soil} indices are controlled by different mechanisms; the BIT index is mainly controlled by substantial influx of the marine GDGT marker crenarchaeol, while the R'_{soil} is primarily governed by the removal of soil marker BHPs. Although both indices suggest a non-conservative behavior for the terrestrial derived OM, this leads todifferences in the estimations of the %terrOC present. A multi-proxy approach is suggested, since the use of single proxies can lead to over/underestimation of the outcome.
- Based on distinct trends observed in offshore and nearshore ESS sediments marked by the different behaviours of BIT and δ^{13}Csoc indices, it can be suggested, as soon by modelling, that the BIT index may reflect a predominantly fluvial input while δ^{13}Csoc represents both fluvial and coastal erosion input.
- The macromolecular terrOC compositions vary along the Eurasian Arctic climosequence and are mainly controlled by the river runoff and wetland coverage (sphagnum vs. higher plants) but are not governed by the presence/absence of continuous permafrost.

- Based on trends in phenols and pyridines along the Kolyma River-ESS transect, phenols/(phenols+pyridines) ratio was suggested as a proxy to trace terrestrial derived OC at the macromolecular level. The results indicate a non-conservative behaviour of the terrestrial macromolecular OC comparable to the bulk of the terrOC.
- Combined, all the molecular analyses/related proxies showed that they can be used to obtain valuable information about the relative amounts of terrOC transported to the Arctic shelves. All proxies showed decreasing trends in an offshore direction indicating that terrOC is not conserved but is actively removed potentially causing a positive feedback to global climate change.

6.2. Future work

Further work in this area should consider the following:

- A better understanding of terrestrial end-member values (by analysing wide range of terrestrial samples) to define the exact GDGT and BHP composition of material transported into the Arctic Ocean.
- Performing compound specific radiocarbon analysis on target soil and marine marker GDGTs and BHPs in sediment samples to make more robust estimation of the contribution of each end-member to the sediments.
- Analysing macromolecular compositions of terrestrial samples (from both the Kalix river and Kolyma watershed area) to better understand the composition of macromolecular terrestrial OM transported to the sub-Arctic marine environment.

- To distinguish between terrestrial and marine contributions to macromolecular OM, selected macromolecular moieties such as pyridines and furfurals should be analysed for their $\delta^{13}C$ values using py-GC/IRMS.

APPENDICES

Appendix A

Sample preparation methods

Sediments extraction-1

1. Freeze dry-homogenize sediments.
2. Add approximately 5 grams of sediments to 50 ml. centrifuge tubes.
3. The total lipid extract (TLEs) were obtained by ultrasonic extraction using monophasic dichloromethane (DCM), Methanol (MeOH) and bi distilled water mixture. Details are as follows;
4. Add 4 ml of Bi-water to the sediment sample in the centrifuge tubes
5. Add 15 ml of MeOH:DCM (2:1, v/v) mixture
6. Sonicate at 40C for 1 hour
7. Centrifugate at 1200 rpm for 15 minutes
8. Remove supernatant
9. Repeat the steps [2-8] twice more.
10. Remove supernatants into pear shaped flask
11. Wash remaining supernatant with 15ml DCM and 15ml bi-water and collect the DCM fraction.
12. Rotary evaporate the supernatant and evaporate the solvent to near dryness
13. Rinse pear shaped flask with warm DCM: MeOH (2:1 v/v)
14. Transfer the TLE to a 3.5 ml vial
15. Dry under a stream of N_2 to obtain the TLE.
16. Recover TLE by adding 2 ml of DCM (1ml for GDGTs and 1ml for BHPs analysis)

Fractionation

1. Pass one aliquot of TLE through a column packed with activated alumina
2. Elute with Hexane: DCM (1:1 v/v, 2ml) for apolar fraction
3. Elute with DCM:MeOH (1:1, 2ml) for GDGT fraction
4. Dry GDGT fraction under N_2 flow
5. Add 1 ml Hexane: Isopropanol solution
6. Filter over 0.45 um filter prior to analysis

Sediments extraction-2

1. Place 5 grams of freeze dried sediment into a 50 ml. centrifuge tube.
2. Add 4ml of phosphate buffer (0.05M phosphate buffer at pH 7.4) to sediment samples in the centrifuge tubes.
3. Add 15 ml of MeOH:DCM (2:1) solvent .
4. Sonicate samples for 10 min at 40°C.
5. Centrifuge them at 2,500 rpm for 5 minutes.
6. Transfer supernatant into a 100ml pear shape flask.
7. Add 5ml DCM and 5ml phosphate buffer to the supernatant to achieve ratio of MeOH:DCM:phosphate buffer 1:1:0.9 (v/v/v).
8. Mix and leave to settle out into two layers
9. Collect the DCM fractions from the bottom of the flask and transfer into another pear shape flask
10. Rinse the remaining supernatant with DCM
11. Collect all four DCM phases into one flask.
12. Repeat steps [2-11] twice more.
13. Rotary evaporate the DCM phase.
14. Dry completely under N_2 if needed.
15. Recover the TLE with 6 ml of DCM: MeOH (2:1 v/v) mixture.
16. Split it into 3 aliquots (for GDGTs, BHPs and as a backup).
17. Dry the TLE aliquot for GDGTs under a stream of N_2.

Fractionation

1. Redissolve the TLE aliquot it in DCM.
2. Pass the TLE through a column packed with activated silica.

3. Elute with 4 ml hexane:ethyl acetate (1:1) for core lipid fraction (includes GDGTs).
4. Elute with 8 ml MeOH to collect intact polar lipid fraction.
5. After separation, add 0.1 μg of a C_{46} GDGT standard to CL fraction.
6. Evaporate the CL fraction under N_2 gas to dryness.
7. Redissolve in hexane: isopropanol 99:1 (v/v).
8. Filter through a 0.45 μm PTFE filter.

Appendix B

Other publications and conference contributions

In addition to the first author papers/ manuscripts, presented in this thesis, the author co-authored following paper:

Schouten, S., Hopmans, E.C., Rosell-Melé, A., Pearson, A., Adam, P., Bauersachs, T., Bard, E., Bernasconi, S.M., Bianchi, T.S., Brocks, J.J., Carlson, L.T., Castañeda, I.S., Derenne, S., **Doğrul Selver, A.,** Dutta, K., Eglinton, T., Fosse, C., Galy, V., Grice, K., Hinrichs, K.-U., Huang, Y., Huguet, A., Huguet, C., Hurley, S., Ingalls, A., Jia, G., Keely, B., Knappy, C., Kondo, M., Krishnan, S., Lincoln, S., Lipp, J., Mangelsdorf, K., Martínez-García, A., Ménot, G., Mets, A., Mollenhauer, G., Ohkouchi, N., Ossebaar, J., Pagani, M., Pancost, R.D., Pearson, E.J., Peterse, F., Reichart, G.-J., Schaeffer, P., Schmitt, G., Schwark, L., Shah, S.R., Smith, R.W., Smittenberg, R.H., Summons, R.E., Takano, Y., Talbot, H.M., Taylor, K.W.R., Tarozo, R., Uchida, M., van Dongen, B.E., Van Mooy, B.A.S., Wang, J., Warren, C., Weijers, J.W.H., Werne, J.P., Woltering, M., Xie, S., Yamamoto, M., Yang, H., Zhang, C.L., Zhang, Y., Zhao, M., Sinninghe Damsté, J.S., 2013. An interlaboratory study of TEX_{86} and BIT analysis of sediments, extracts, and standard mixtures. Geochemistry, Geophysics, Geosystems 14, 5263-5285.

The following are the conference contributions during the course of this research:

2011

Doğrul Selver, A., Talbot, H. M., Gustafsson, Ö., Semiletov, I., Boult, S., van Dongen, B. E. Contrasting macromolecular organic matter compositions in surface sediments off the Eurasian Arctic rivers (July 2011). *British Organic Geochemistry Society meeting*. University of Swansea (Oral presentation).

Doğrul Selver, A., Varden, C., Semiletov, I., Gustafsson, Ö., Talbot, H. M., Boult, S., van Dongen, B. E. (September 2011). Contrasting macromolecular organic matter composition in surface sediments off the Eurasian Arctic rivers. *International Meeting on Organic Geochemistry*. Interlaken, Switzerland (Poster presentation).

Doğrul Selver, A., Talbot, H. M., Gustafsson, Ö., Boult, S., van Dongen, B. E. (December 2011). Tracking Soil Derived Organic Matter in the Arctic Region using Molecular Based Proxies. *School of Earth, Atmospheric and Environmental Sciences Postgraduate Research Conference*. Manchester, United Kingdom (Oral presentation).

2012

Doğrul Selver, A., Talbot, H.M., Gustafsson, Ö., Boult, S., van Dongen, B. E. (July 2012). Soil organic matter transport along a sub-Arctic river-sea transect. *British Organic Geochemical Society*. Leeds, UK (Poster presentation).

Doğrul Selver, A., Bischoff, J., Sparkes, R.B., Talbot, H. M., Gustafsson, Ö., Boult, S. and van Dongen, B. E. (December 2012). Tracking soil organic matter in the Arctic region using bacterial and archaeal membrane lipids. *School of Earth, Atmospheric and Environmental Sciences Postgraduate Research Conference.* Manchester, United Kingdom (Oral presentation).

2013

Doğrul Selver, A., Sparkes, R.B., Bischoff, J., Talbot, H. M., Gustafsson, Ö., Semiletov, I. P., Dudarev, O. V., Boult, S. and van Dongen, B. E. Tracing soil organic matter along the Kolyma paleo river transect using microbial membrane lipids (July 2013). *British Organic Geochemical Society*. Polymouth, UK (Oral presentation).

Doğrul Selver A., Sparkes,R.,Bischoff,J., Talbot, H. M., Gustafsson, Ö., Semiletov, I., Dudarev, O., Boult, S. and B. E. van Dongen. Tracing soil organic matter along an arctic river-sea transect using microbial membrane lipids (September 2013). *International Meeting on Organic Geochemistry.* Tenerife, Spain (Poster presentation)

Sparkes, R., **Doğrul Selver, A.**, Bischoff, J., Talbot, H. M., Gustafsson, Ö., Semiletov, I., Dudarev, O., Boult, S. and B. E. van Dongen (September 2013). Soil Biomarker Distribution across the East Siberian Shelf A Story of Carbon Liberation, Distribution and Degradation. *International Meeting on Organic Geochemistry.* Tenerife, Spain.

Bischoff, J., Sparkes, R., **Doğrul Selver A.**, Talbot, H. M., Gustafsson, Ö., Semiletov, I., Dudarev, O., Boult, S. and B. E. van Dongen. Bacteriohopanepolyols transport and degradation in the Buor-Khaya Bay, SE Laptev Sea and the East Siberian Arctic Shelf. *International Meeting on Organic Geochemistry.* Tenerife, Spain.

Doğrul Selver A., Sparkes,R., Bischoff, J., Talbot, H. M., Gustafsson, Ö., Semiletov, I., Dudarev, O., Boult, S. and B. E. van Dongen. The fate of soil organic carbon transported by the easternmost Great Russian Arctic rivers (December 2013). *School of Earth, Atmospheric and Environmental Sciences Postgraduate Research Conference.* Manchester, United Kingdom (Oral presentation).

Sparkes,R., **Doğrul Selver A.**, Bischoff, J., Talbot, H. M., Gustafsson, Ö., Semiletov, I., Dudarev, O., Boult, S. and B. E. van Dongen. Contrasting biomarker distributions on the Arctic Shelf give insights into organic carbon export from thawing Siberian permafrost (December 2013). *School of Earth, Atmospheric and Environmental Sciences Postgraduate Research Conference.* Manchester, United Kingdom.

2014

Sparkes, R.B., **Doğrul Selver, A**., Bischoff, J., Talbot, H. M., Gustafsson, Ö., Semiletov, I. P., Dudarev, O. V., Boult, S. and van Dongen, B. E. GDGT distribution across the East Siberian Shelf (April 2014). *Workshop on GDGT-based proxies at the Royal NIOZ*. Utrecht, The Netherlands.

Sparkes,R.B.,Doğrul Selver, A., Bischoff,J., Talbot, H. M., Gustafsson, Ö., Semiletov, I., Dudarev, O. and van Dongen, B. E.. Terrestrial organic carbon and biomarker export

from East Siberian Permafrost to the Arctic Ocean (June 2014). *Goldschmidt Conference*. California, US (Poster presentation)

Bischoff, J., Sparkes,R.B., **Doğrul Selver, A**., Gustafsson, Ö., Vonk, J., Spencer, R., Semiletov, I., Dudarev, O., van Dongen, B. E. and Talbot, H. M. Terrestrial Microbial Biomarkers Trace Organic Matter Transport to the Arctic Ocean (June 2014). *Goldschmidt Conference*. California, US (Poster presentation)

Sparkes, R.B., **Doğrul Selver, A**., Bischoff, J., Talbot, H. M., Gustafsson, Ö., Semiletov, I. P., Dudarev, O. V. and van Dongen, B. E. GDGT distribution across the East Siberian Shelf (July 2014). *British Organic Geochemical Society*. Liverpool, UK (Poster presentation)

Sparkes, R.B., **Doğrul Selver, A**., Bischoff, J., Talbot, H. M., Gustafsson, Ö., Semiletov, I. P., Dudarev, O. V. and van Dongen, B. E. GDGT distribution across the East Siberian Shelf (August 2014). *Gordon Research Conference - Organic Geochemistry*. Boston, MA, USA (Poster presentation)